



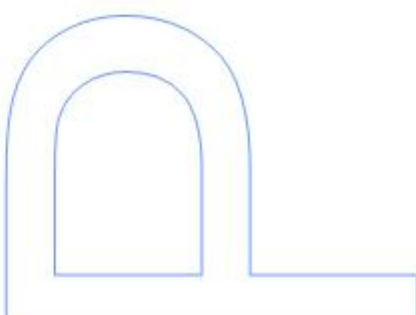
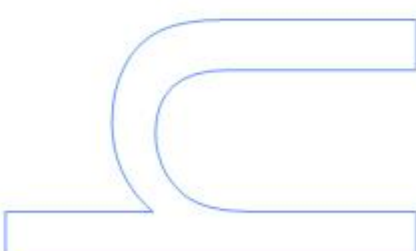
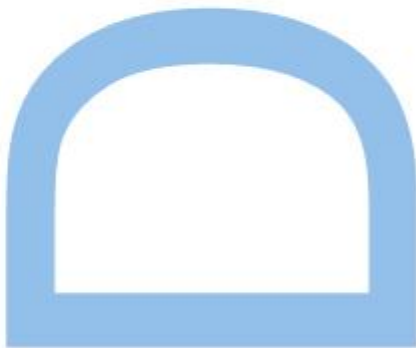
INOVAD-Development of new formulations based on polysaccharides to reduce the astringency of beverages

Elsa Judite Ferreira Azevedo Brandão

PhD in Sustainable Chemistry
Department of Chemistry and Biochemistry
2018

Supervisor

Victor Armando Pereira de Freitas, Professor Catedrático,
Faculty of Sciences, University of Porto



Acknowledgements

Em primeiro lugar gostava de agradecer à Fundação Para a Ciência e Tecnologia (FCT) pelo financiamento deste trabalho na forma de uma bolsa de Doutoramento (SFRH/BD/105295/2014) sem a qual a realização deste trabalho seria impossível.

Gostava de agradecer ao Departamento de Química e Bioquímica da Faculdade de Ciências da Universidade do Porto e à Linha de Investigação QUINOA/LAQV do REQUIMTE pelos diversos apoios logísticos e financeiros concedidos.

Gostava de agradecer ao meu orientador Professor Doutor Victor de Freitas sem o qual este trabalho não seria possível. Todo o interesse, disponibilidade, compreensão e paciência foram fundamentais. Sempre preocupado para que tudo corresse bem não só comigo em particular, mas com todos em geral. Agradeço o apoio, as discussões científicas e toda a confiança que depositou em mim. Mais do que um orientador foi também um bom conselheiro o que me permitiu crescer tanto a nível profissional como pessoal.

Gostava também de agradecer ao Professor Doutor Nuno Mateus por toda a paciência, descontração e humor característico. Sempre disponível e disposto a resolver qualquer problema no laboratório e fora dele.

Um agradecimento muito especial à Susana, que para além de mim, foi a pessoa que mais envolvida esteve neste projeto. Poderia fazer-lhe muitos elogios, mas primeiramente começaria por lhe agradecer a amizade. A sua perseverança, organização, dedicação e entusiasmo pelo trabalho são, sem dúvida, qualidades que tive oportunidade de partilhar e vivenciar e que muito contribuíram para o meu crescimento a todos os níveis. Todas as situações do dia-a-dia e os novos desafios que foram surgidos, só foi possível ultrapassá-los com sucesso devido à sua ajuda. Obrigada por todos os bons momentos passados, pelas gargalhadas, carinho e por toda a ciência que se foi fazendo tanto dentro do laboratório como fora dele.

Gostava de agradecer a alguns investigadores e professores do Departamento de Química e Bioquímica, nomeadamente à Dra. Zélia pela ajuda técnica nas análises de LC-MS e à Professora Paula Gameiro pela ajuda e esclarecimentos sobre fluorescência.

Gostava também de agradecer à Mariana Andrade pela ajuda técnica nas análises de STD-RMN, assim como pelos bons momentos passados no CEMUP durante as

análises. Um agradecimento especial à Sílvia Maia plea ajuda em algumas experiências, assim como pelo apoio constante e pelos bons momentos passados.

Agradeço ao Doutor Thierry Doco do INRA (Montpellier, França) pela oportunidade que me proporcionou de ir para o seu laboratório e aprender um pouco mais sobre polissacáridos. Uma pessoa sempre extremamente disponível, interessada e atenciosa. Gostaria de agradecer também à Pascale Williams pelo apoio técnico e toda a ajuda disponibilizada durante a minha estadia na França, assim como pela boa disposição e alegria todos os dias.

Aos meus colegas de laboratório que me acompanham ao longo de todos estes anos, sempre presentes para qualquer esclarecimento, ajuda e ensinamento. Agradeço profundamente todas as dádivas de saliva e reconheço o esforço e paciência para ficarem sem tomar café. Sem dúvida que sem vocês este trabalho também não seria possível. O vosso apoio e incentivo foram fundamentais durante todo este tempo. Agradeço ainda a todos os colegas de outros laboratórios com quem me fui cruzando nos corredores, pelos poucos minutos de conversa que por vezes suRG iam assim como pela boa disposição.

Um agradecimento especial aos “ex-elementos do grupo das proteínas”, Mafalda e Nacho. Foram sem dúvida um apoio e uma ajuda fundamental no desenvolver deste trabalho. Obrigada pelos bons momentos dentro e fora do laboratório, pelo entusiasmo, alegria, carinho, preocupação e incentivo. Trabalhar assim com pessoas como vocês tornou tudo mais fácil. Que saudades...

Aos meus amigos que, direta ou indiretamente, me ajudaram ao longo de tantos anos. Pelos bons momentos passados, pelos jantares, pelas gargalhadas, pelo apoio e por fazerem tudo parecer tão simples. Um agradecimento especial ao Diogo, à Cris, à Bárbara e à Filipa.

À minha família, em especial aos meus pais, irmãs, sobrinhos e avó por tudo o que me proporcionaram e proporcionam, pelo amor, apoio e motivação ao longo destes anos. Sem eles nada teria sido possível.

Finalmente, ao Rui. Por todo o apoio, incentivo e paciência em todos os momentos, pela compreensão e carinho e por ter estado sempre presente quando mais precisei ao longo destes anos. E por tudo aquilo que significa para mim.

Publications List

This work was performed in QUINOA-LAQV-REQUIMTE laboratory at Departamento de Química e Bioquímica da Faculdade de Ciências da Universidade do Porto with financial funding from FCT (Fundação para a Ciência e Tecnologia) by a PhD Grant (SFRH/BD/105295/2014).

This thesis includes results already published in international peer-reviewed scientific journals and scientific conferences through oral and poster communications.

Publications in international peer-reviewed scientific journals

Susana Soares; Mafalda Silva; Ignacio García-Estévez; Elsa Brandão; Fátima Fonseca; Frederico Ferreira-da-Silva; M. Teresa Escribano-Bailón; Nuno Mateus; Victor de Freitas. Effect of malvidin-3-glucoside and epicatechin interaction on their ability to interact with salivary proline-rich proteins, *Food Chemistry*, **2019**, 276:33-42.

doi: [10.1016/j.foodchem.2018.09.167](https://doi.org/10.1016/j.foodchem.2018.09.167)

Susana Soares, Mafalda Silva, Ignacio García-Estévez, Peggy Grobman, Natércia Brás; Elsa Brandão, Nuno Mateus; Victor de Freitas; Maik Behrens; Wolfgang, Meyerhof. Human bitter taste receptors are activated by different classes of polyphenols, *Journal of Agricultural and Food Chemistry*, **2018**, 66 (33), 8814-8823;

doi: [10.1021/acs.jafc.8b03569](https://doi.org/10.1021/acs.jafc.8b03569)

Susana Soares, Ignacio García-Estévez, Raúl Ferrer-Galego, Natércia F. Brás, Elsa Brandão, Mafalda Silva, Natércia Teixeira, Fátima Fonseca, SéRG Io F. Sousa, Frederico Ferreira-da-Silva, Nuno Mateus, Victor de Freitas. Study of human salivary proline-rich proteins interaction with food tannins, *Food Chemistry*, **2017**, 243, 175-185.

doi: [10.1016/j.foodchem.2017.09.063](https://doi.org/10.1016/j.foodchem.2017.09.063)

Elsa Brandão, Mafalda Santos Silva, Ignacio García-Estévez, Pascale William, Nuno Mateus, Thierry Doco, Victor de Freitas, Susana Soares. The role of wine polysaccharides on salivary protein-tannin interaction: a molecular approach, *Carbohydrates Polymers*, **2017**, 177, 77-85;

doi: [10.1016/j.carbpol.2017.08.075](https://doi.org/10.1016/j.carbpol.2017.08.075)

Mafalda Santos Silva, Ignacio García-Estévez, Elsa Brandão, Nuno Mateus, Victor de Freitas, Susana Soares. Study of salivary proteins and tannins interaction in the development of astringency, *Journal of Agricultural and Food Chemistry*, **2017**, 65 (31), 6415-6424;

doi: 10.1021/acs.jafc.7b01722

Elsa Brandão, Mafalda Silva, Ignacio García-Estévez, Nuno Mateus, Victor de Freitas, Susana Soares. Molecular study of mucin-procyanidin interaction by fluorescence quenching and Saturation Transfer Difference (STD)-NMR, *Food Chemistry* **2017**, 228, 427-434;

doi: 10.1016/j.foodchem.2017.02.27

Susana Soares, Elsa Brandão, Nuno Mateus, Victor de Freitas. Sensorial properties of red wine polyphenols: Astringency and Bitterness, *Critical Reviews in Food Science and Nutrition*, **2017**, 57 (5), 937-948;

doi: 10.1080/10408398.2014.946468

Susana Soares, Raul Ferrer-Gallego, Elsa Brandão, Mafalda Santos Silva, Nuno Mateus, Victor de Freitas. Contribution of human oral cells to astringency by binding salivary proteins/tannins complexes, *Journal of Agricultural and Food Chemistry*, **2016**, 64 (41), 7823-7828:

doi: 10.1021/acs.jafc.6b02659

Susana Soares, Elsa Brandão, Nuno Mateus, Victor de Freitas. Interaction between red wine procyandins and salivary proteins: effect of stomach digestion on the resulting complexes, *RSC Advances*, **2015**, 5, 12664–12670;

doi: 10.1039/c4ra13403f

Oral Communications

Elsa Brandão, Mafalda Santos Silva, Ignacio García-Estévez, Pascale Williams, Nuno Mateus, Thierry Doco, Victor de Freitas, Susana Soares. Are polysaccharides important to modulate protein-tannin interactions? XXIXth International Conference on Polyphenols & 9th Tannin Conference, 16-20th July 2018, Madison, EUA.

Elsa Brandão, Mafalda Santos Silva, Ignacio García-Estévez, Pascale Williams, Nuno Mateus, Thierry Doco, Victor de Freitas, Susana Soares. The role of wine polysaccharides on salivary protein-tannin interaction: a molecular approach. X IVAS, In Vino Analytica Scientia - Analytical Chemistry for Wine, Brandy and Spirits, 17-20th July 2017, Salamanca, Spain.

Elsa Brandão, Mafalda Santos Silva, Ignacio García-Estévez, Susana Soares, Nuno Mateus, Victor de Freitas. Binding of procyanidins to mucin protein: a molecular approach of astringency. XXII Encontro Luso-Galego Química, 9-11th November, 2016, Bragança, Portugal.

Elsa Brandão, Mafalda Santos Silva, Ignacio García-Estévez, Susana Soares, Nuno Mateus, Victor de Freitas. Molecular understanding of astringency: the role of salivary proteins, tannins and polysaccharides. 1st Meeting of Doctoral Programme in Sustainable Chemistry; 26th September 2016, Aveiro, Portugal.

Posters in conferences

Elsa Brandão, Mafalda Santos Silva, Ignacio García-Estévez, Ana Fernandes, Pascale Williams, Nuno Mateus, Thierry Doco, Victor de Freitas; Susana Soares. Have wine polysaccharides an important role on astringency modulation? 12^a Reunião do Grupo dos Glúcidos, 11-23rd September 2017, Aveiro, Portugal.

Elsa Brandão, Mafalda Santos Silva, Ignacio García-Estévez, Ana Fernandes, Pascale Williams, Nuno Mateus, Thierry Doco, Victor de Freitas and Susana Soares. Grape cell-wall polysaccharides: influence on the interaction between salivary proteins and tannins. X IVAS, In Vino Analytica Scientia - Analytical Chemistry for Wine, Brandy and Spirits, 17-20th July 2017, Salamanca, Spain.

Elsa Brandão, Mafalda Santos Silva, Ignacio García-Estévez, Susana Soares, Nuno Mateus, Victor de Freitas. Molecular understanding of astringency: The role of salivary

proteins, tannins and wine polysaccharides. XIII Encontro de Química dos Alimentos,
14-16th September 2016, Porto, Portugal

Elsa Brandão, Susana Soares, Nuno Mateus, Victor de Freitas. Study of the interaction
between procyanidins and mucin. IX IVAS, In Vino Analytica Scientia - Analytical
Chemistry for Wine, Brandy and Spirits, 14-17th July 2015, Trento, Italy

Resumo

Os polifenóis são metabolitos secundários das plantas e, por isso, estão presentes em diversos alimentos e bebidas de origem vegetal (e.g. vinho tinto, cerveja, chá, sumos de frutas, etc.). Estes compostos têm recebido especial atenção nos últimos anos devido às suas propriedades biológicas (antioxidantes, anticancerígena, etc.) e propriedades organoléticas dos alimentos como a cor e o sabor. Entre os polifenóis, os taninos são geralmente associados ao sabor e, em particular, à adstringência. A interação entre as proteínas salivares e os taninos é geralmente aceite, como um dos mecanismos responsáveis pela sensação de adstringência de certos alimentos. Das diversas proteínas salivares que interagem com os taninos, aquelas que se destacam são as proteínas ricas em prolina (PRPs), tais como as básicas (bPRPs), as glicosiladas (gPRPs) e as acídicas (aPRPs), a estaterina, o péptido P-B, as cistatinas e a mucina.

A adstringência é definida como um complexo grupo de sensações tácteis sentidas na cavidade oral que incluem secura, aspereza e constrição dos tecidos. No entanto, no caso de certas bebidas como o vinho, cerveja e café a adstringência é considerada um parâmetro de qualidade quando não se encontra em níveis elevados.

As interações proteínas salivares-taninos podem ser afetadas por diferentes fatores, tais como características estruturais do tanino e da proteína, o pH, a percentagem de etanol, a força iônica e a presença de polissacáridos. De uma forma geral, espera-se que os fatores que afetam a interação proteína-tanino afetem da mesma forma a adstringência. Por exemplo, os polissacáridos podem influenciar a interação das proteínas salivares com os taninos e, desta forma, podem conduzir à modulação da adstringência. Este trabalho teve como objetivo global a compreensão das propriedades sensoriais associadas aos taninos (adstringência) e, compreender de que modo, os polissacáridos naturalmente presentes na uva e que passam para o vinho podem influenciar estas interações.

Deste modo, este trabalho focou-se no: a) isolamento e síntese de taninos de diferentes classes, condensados e hidrolizáveis, assim como na obtenção de frações oligoméricas de procianidinas; b) determinação das principais famílias de proteínas salivares que possuem maior afinidade para interagir com os taninos; c) isolamento de diferentes polissacáridos a partir do vinho e da uva; d) isolamento das diferentes famílias de proteínas salivares a partir de saliva humana; e) caracterização da interação entre os referidos compostos através de diferentes técnicas, tais como Cromatografia Líquida de de Elevada Eficiência (HPLC), extinção de fluorescência, nefelometria, eletroforese em

gel de dodecilsulfato de sódio (SDS-PAGE) e Ressonância Magnética Nuclear de Diferença de Transferência de Saturação (STD-NMR).

Os resultados obtidos mostraram que: a) Os taninos hidrolizáveis possuem uma maior afinidade para interagir com as proteínas salivares do que os taninos condensados. Os taninos interagem primeiro com a estaterina/péptido P-B e as aPRPs e só depois com as restantes PRPs e cistatinas. No entanto, esta tendência depende se a interação ocorre com as proteínas salivares isoladas (purificadas) ou se estão numa mistura (diretamente na saliva), assim como do tipo de tanino usado. b) As procianidinas presentes nos alimentos interagem com a mucina e esta interação aumenta com o grau de polimerização médio das procianidinas. Para compostos puros, observou-se uma diminuição da afinidade da procianidina tetramérica em relação à procianidina dimérica B4, o que pode ser explicado pela baixa flexibilidade estrutural deste composto devido à sua complexa estrutura. c) O etanol e o dimetilsulfóxido (DMSO) podem afetar as principais forças de ligação destas interações - interações hidrofóbicas e pontes de hidrogénio - respetivamente, diminuindo significativamente as respetivas constantes de ligação.

Foi também estudado o efeito dos polissacáridos na interação entre taninos e proteínas salivares. A abordagem experimental consistiu no estudo da influência de dois polissacáridos do vinho (ramnogalacturonanas tipo II (RG II) e arabinogalactana-proteínas (AGPs)) na interação entre taninos (procianidina B2 e punicalagina) e proteínas isoladas da saliva (aPRPs e péptido P-B). De um modo geral, ambos os polissacáridos foram eficientes na inibição ou redução da interação e precipitação das proteínas salivares com os taninos. O efeito dos polissacáridos pode ser explicado por dois mecanismos (ternário e competitivo), dependendo do par tanino-proteína salivar. No caso do péptido P-B, as AGPs e o RG II parecem actuar através do mecanismo ternário, encapsulando o complexo proteína-tanino, aumentando a sua solubilidade. Considerando as aPRPs, os dois mecanismos foram observados, dependendo do tanino e do polissacárido envolvido. Assim, poderá existir a encapsulação do complexo tanino-proteína pelo polissacárido (ternário) ou a ligação do polissacárido ao tanino, impedindo que este se ligue à proteína (competitivo).

Foi desenvolvida uma abordagem experimental semelhante para os mesmos taninos e polissacáridos, mas usando as proteínas salivares presentes diretamente na saliva (meio competitivo). Também se estudou a influência da força iônica na interação das proteínas com os taninos e no efeito dos polissacáridos através da adição de sais (NaCl) à saliva. Os resultados indicaram que grande parte dos polissacáridos foram eficientes

na redução das interações das proteínas salivares e taninos. A combinação das diferenças técnicas (HPLC, nefelometria, extinção de fluorescência e SDS-APGE) demonstrou que há uma não agregação or (re)solubilização dos complexos proteína-tanino após a adição dos polissacáridos, através de um mecanismo competitivo ou formação do complexo ternário (proteína-tanino-polissacárido), respetivamente. A partir dos resultados obtidos, foi possível observar que o efeito dos polissacáridos é dependente tanto da amostra de saliva (na presença ou ausência de sais) como da estrutura do polissacárido e do tanino. O RG II que é um polissacárido acídico foi o mais eficiente na inibição da precipitação das proteínas salivares pelos taninos, especialmente para as aPRPs e estaterina/péptido P-B, do que as AGPs que possuem um carácter mais neutro.

Na parte final deste trabalho, que ainda se encontra em curso, estudou-se o efeito de duas frações de polissacáridos pécticos (polissacáridos pécticos solúveis em água (WSP) e solúveis num agente quelante como o oxalato (CSP)), isoladas a partir de película de uva, na interação dos taninos com as proteínas salivares. Estas frações foram caracterizadas em termos de composição de açúcares neutros e acídicos. Os resultados obtidos mostraram que ambas as frações foram capazes de reduzir as interações proteína-tanino, sendo que a fração de WSP foi mais eficiente quando comparada com a CSP. Na presença destas duas frações de polissacáridos parece existir o mecanismo de competição no qual os polissacáridos ligam-se aos taninos, diminuindo a sua disponibilidade para interagir com as proteínas salivares.

De uma forma global, este trabalho permitiu alargar o conhecimento acerca da capacidade dos polissacáridos em reduzir ou inibir as interações entre as proteínas salivares e os taninos e, desta forma, poderem ser usados para modular a percepção da adstringência. Esta informação pode ser de grande utilidade para as indústrias agro-alimentares que podem utilizar polissacáridos para modular a adstringência de bebidas. Por exemplo, a indústria vinícola poderia desenvolver métodos para aumentar a extração destes polissacáridos durante o processo de produção de vinho e assim modular a adstringência deste produto.

PALAVRAS-CHAVE: Adstringência; AGPs; extinção de fluorescência; interação tanino-proteínas salivares; HPLC; nefelometria; polissacáridos; polissacáridos pécticos; procianidinas; proteínas salivares; RG II; STD-RMN; taninos; taninos condensados; taninos hidrolisáveis.

Abstract

Polyphenols are secondary metabolites being present in several plant-based food and beverages (e.g. red wine, beer, tea, fruit juices, etc.). These compounds have received a great attention in the last years mainly due to their biological properties (antioxidants, anticancer, etc.) and because of their organoleptic properties (colour and flavor). Among polyphenols, tannins are usually associated with flavor, and particularly with astringency. Tannins have the ability to interact with proteins, particularly salivary proteins (SP). It is widely accepted that SP-tannin interaction and precipitation is at the origin of astringency sensation. Several SP are described to interact with tannins, namely proline-rich proteins (PRPs) such as basic (bPRPs), glycosylated (gPRPs) and acidic (aPRPs), statherin, P-B peptide, cystatins and mucin.

Astringency is defined as complex group of tactile sensations including dryness, puckering and tightening of the oral cavity. This sensation is often a non-pleasant sensation. However, in the case of red wine, astringency is a quality parameter and it is desired in balanced levels.

Tannin-protein interactions can be affected by different factors, such as tannin and protein structural features, pH, ethanol, ionic strength and the presence of polysaccharides, among others. In general, the factors that affect the binding affinity of tannins to SP are expected to affect astringency in the same way. For instance, polysaccharides can affect SP-tannin interactions and may hence lead to astringency modulation. The main goal of this work was to understand and have insights about the sensorial properties of tannins (astringency), and to study the influence of polysaccharides, naturally present in grapes and wine, on the interaction between SP and tannins.

So, this work was focused on: a) isolate and synthesize tannins from different classes, condensed and hydrolyzable as well as fractions containing a mixture of compounds; b) determine the main families of SP that have more affinity to interact with tannins; c) isolate different polysaccharides from grapes and wine; d) isolate SP from human saliva samples; e) characterize the interaction between the referred compounds by different techniques such as High Performance Liquid Chromatography (HPLC), fluorescence quenching, nephelometry measurements, sodium dodecylsulfate-polyacrylamide gel electrophoresis (SDS-PAGE) and Saturation Transfer Difference- Nuclear Magnetic Resonance (STD-NMR).

The results showed that hydrolyzable tannins have higher affinity to interact with SP in comparison with the condensed ones. Generally, tannins interact firstly with statherin/P-B peptide and aPRPs only then with the other PRPs and cystatins. However, this tendency is dependent if the interaction occurs with SP isolated (purified) or if they are present simultaneously in a competitive medium (saliva, as well as the tannin used). The results about mucin-procyanidin interaction provided evidences that food procyanidins interact with mucin. For fractions of oligomeric procyanidins, the mucin-procyanidin interaction increased with the mean degree of polymerization; however, for pure compounds, procyanidin TT has lower affinity than dimer B4 which could be due to a lower structural flexibility imposed by its complex structure. Furthermore, ethanol and dimethylsulfoxide (DMSO) can disrupt the main driving forces of these interactions, hydrophobic interactions and hydrogen bonds, respectively, lowering significantly the binding constants.

The effect of polysaccharides on tanins/proteins interaction was also studied. Firstly, the experimental approach consisted in study the influence of two wine polysaccharides (rhamnogalacturonan type II (RG II) and arabinogalactan-proteins (AGPs)) on the interaction between tannins (procyanidin B2 and punicalagin) and SP isolated from human saliva (aPRPs and P-B peptide). In general, both polysaccharides were effective to inhibit or reduce SP-tannin interaction and aggregation. They can act by two different mechanisms (ternary or competitive) depending on the SP-tannin pair. In the case of salivary P-B peptide, AGPs and RG II seem to act by a ternary mechanism, in which they surround this complex, enhancing its solubility. Concerning aPRPs, it was possible to observe both mechanisms, depending on the tannin and the polysaccharide involved.

A similar approach was conducted for the same tannins and polysaccharides, but using SP present directly in saliva (competitive assay). The influence of ionic strength (presence of salts) on the SP-tannin interaction and on the effect of polysaccharides was also studied. The results indicated that, in general, mostly polysaccharides were able to highly reduce the interactions between SP and tannins. All the techniques together (HPLC, nephelometry, fluorescence quenching and SDS-PAGE) clearly showed that there is a non-aggregation or (re)solubilization of SP-tannin aggregates upon the addition of polysaccharides, throughout a competitive mechanism or by the formation of a ternary complex (protein-tannin-polysaccharide), respectively. From the results obtained, it was possible to note that the effect of polysaccharides is dependent both on the saliva sample (the presence or absence of salts) as well as on the tannin and polysaccharide structures. RG II, an acidic polysaccharide, was more effective in the inhibition of

precipitation of SP, especially for aPRPs and statherin/P-B peptide, than AGPs which have a more neutral character.

In the final part of this work, which is still ongoing, it was studied the effect of two pectic polysaccharides fractions isolated from grape skin (water soluble pectic polysaccharides, (WSP) and chelate soluble pectic polysaccharides (CSP)) on SP-tannin interactions. These fractions were previously characterized in terms of neutral and acidic sugar composition. The results showed that these fractions are able to disrupt protein-tannin interactions, being WSP fraction more efficient than the CSP one. Both polysaccharides fractions seemed to act by a competition mechanism in which polysaccharides bind tannins, decreasing their availability to interact with SP.

In general, this work gave some insights about the ability of polysaccharides to reduce SP-tannin interactions and may hence lead to the modulation of astringency perception. This could be a valuable information for winemaking which can develop methods to increase these polysaccharides extraction during winemaking processes and, this way, modulate wine astringency.

KEYWORDS: Astringency; AGPs; fluorescence quenching; condensed tannins; HPLC; hydrolyzable tannins; nephelometry; pectic polysaccharides; polysaccharides; procyanidins; RG II; salivary proteins; STD-NMR; tannins; tannin-salivary protein interaction.

Outline of the thesis

This thesis is divided into four sections (I) Aim, (II) Introduction, (III) Research work and (IV) Final remarks and future work. Section III is divided into two chapters (chapter 1 and 2), which in turn, are divided into three parts each (parts A, B and C from chapter 1 and parts D, E and F from chapter 2). This is a formal organization and does not reflect the order of experimental work. This is an author's option in order to simplify the overall reading of this manuscript and to better present the works contained. A brief description of each part will be performed below.

A general approach regarding the global aim of this work is presented in section I. Following this section, section II consists in a bibliographic review of the most relevant literature that aims to elucidate the reader about the compounds used in this work (polyphenols, polysaccharides and proteins, in particular, salivary proteins), as well as the relevance of these compounds for the purpose of this study (influence of polysaccharides on salivary protein-tannin interactions).

Section III corresponds to research work which were divided into two chapters. The chapter 1 reports the molecular interaction between different salivary proteins families and food tannins, and it is divided into three parts (A, B and C). These parts were adapted from three publications in peer-reviewed scientific journals. In part A the ability of condensed tannins to interact with mucin by fluorescence quenching and STD-NMR is presented and the respective binding constants were determined. In part B, the interaction between PRPs and condensed tannins was studied by two complementary techniques, ITC and STD-NMR. Part C reports the interaction between some human salivary proteins (which are not PRPs) and condensed and hydrolyzable tannins. The relative affinity of these tannins towards salivary proteins was evaluated by fluorescence quenching and STD-NMR.

The content of chapter 2 concerns the influence of some polysaccharides on the salivary proteins-tannin interaction and it is also divided into three parts (D, E and F). In part A the ability of wine polysaccharides to reduce salivary proteins interaction with tannins was studied by different techniques, such as HPLC, nephelometry and STD-NMR. The content of this chapter was adapted from a published paper in a peer-reviewed journal. Part E reports the effect of wine polysaccharides on the interaction between tannins and salivary proteins, when the latter are present directly in saliva (competitive assay) as well as the inhibition mechanisms of these polysaccharides. Saliva samples in different

conditions were also tested. These results were adapted from a submitted manuscript in a peer-reviewed journal. Finally, in part F the role of pectic polysaccharides from grape skin on the interaction between salivary proteins present simultaneously in saliva and a mixture of procyanidins was also evaluated. This work is *in preparation* because it is not completely finished.

Section IV presents a general conclusion of the main results obtained concerning the global aim of this thesis. Final remarks and some indications for future work activities are also presented in this section.

The adaptation of these chapters from published, submitted and in preparation publications involved the standardization of the formatting and nomenclature. Some sentences and images were added in order to clarify some aspects.

Table of contents

Acknowledgements.....	3
Publications List.....	5
Resumo	9
Abstract	13
Outline of the thesis	17
Table of contents	19
List of Figures	25
List of Tables	31
List of Abbreviations and Symbols	33
I. Aims	37
II. Introduction.....	41
1. Phenolic compounds	43
1.1. Non-flavonoids	43
1.2. Flavonoids.....	44
1.2.1. Anthocyanins	46
1.2.2. Flavan-3-ols	48
2. Tannins	49
2.1. Condensed tannins (proanthocyanidins)	50
2.2. Hydrolyzable tannins	54
3. The importance of polyphenols in food	56
3.1. Sensorial aspects.....	56
3.2. Impact on food consumption	56
3.3. Impact on human health.....	57
4. Saliva	59
4.1. Salivary proteins (SP).....	61
4.1.1. Proline-rich proteins (PRPs).....	64
4.1.2. Statherin.....	66
4.1.3. P-B peptide	67
4.1.4. Cystatins	67
4.1.5. Mucins	68
4.1.6. Histatins	68
5. Protein-tannin interactions.....	69
5.1. Bonds Involved.....	69
5.2. Molecular models for protein-tannin interactions	71

5.3.	Astringency	74
5.3.1.	Mechanisms of astringency	75
5.4.	Factors that influence protein-tannin interactions	76
5.4.1.	Tannin structure	76
5.4.2.	Protein structure.....	77
5.4.1.	Presence of polysaccharides.....	78
5.4.2.	Other factors	84
III.	Research work	87
Chapter 1 - Molecular interaction between salivary proteins and food tannins		89
A.	Molecular study of mucin-procyanidin interaction by fluorescence quenching and Saturation Transfer Difference (STD)-NMR	93
A1.	Introduction	93
A2.	Material and methods.....	94
A2.1.	Reagents.....	94
A2.2.	Grape Seed Fraction (GSF) Isolation	95
A2.3.	Analysis and characterization of GSF.....	95
A2.4.	Synthesis and Purification of Procyanidins	96
A2.5.	Static Light Scattering	96
A2.6.	Fluorescence Quenching Measurements	97
A2.7.	STD-NMR Studies.....	98
A2.8.	Statistical Analysis	100
A3.	Results and discussion.....	100
A3.1.	Fluorescence Quenching Studies.....	101
A3.2.	STD-NMR studies	107
A4.	Conclusions	112
B.	Study of human salivary proline-rich proteins interaction with food tannins.....	113
B1.	Introduction	113
B2.	Material and methods.....	115
B2.1.	Isolation and identification of salivary proteins.....	115
B2.2.	Isolation of procyanidin dimer B2, procyanidin B2 3'-O-gallate (B2g) and procyanidin trimer	116
B2.3.	Saturation transfer difference (STD)-NMR.....	117
B2.4.	Isothermal Titration Microcalorimetry (ITC).....	118
B2.5.	Molecular Dynamics Simulation (MD).....	118
B3.	Results.....	118
B3.1.	Identification of the major salivary proteins.....	119

B3.2.	Interaction of the different salivary proteins with procyanidins by STD-NMR	120
B3.3.	Interaction of the different SP with procyanidins by ITC	123
B3.4.	Interaction of the different SP with procyanidins by MD	127
B4.	Discussion	129
B4.1.	Procyanidin epitopes of binding	129
B4.2.	Specificity of salivary protein-procyanidin interaction (binding constants)	130
B4.3.	Type of bonds involved in salivary protein-procyanidin interaction	132
B4.4.	Protein binding sites on salivary protein-procyanidin interaction	133
C.	Molecular interaction between salivary proteins and food tannins	137
C1.	Introduction	137
C2.	Material and Methods	140
C2.1.	Reagents	140
C2.2.	Salivary Proteins Isolation and Purification	140
C2.3.	Identification of Salivary Proteins	141
C2.4.	Ellagitannins Extraction and Isolation	141
C2.5.	Procyanidin Dimers B3 and B6 synthesis	142
C2.6.	Fluorescence quenching	142
C2.7.	Determination of Salivary Proteins Lifetime (τ_0)	144
C2.8.	Saturation Transference Difference-Nuclear Magnetic Resonance (STD-NMR)	144
C2.9.	Statistical Analysis	145
C3.	Results and Discussion	145
C3.1.	Binding constants of the interactions between salivary proteins and tannins by fluorescence quenching	146
C3.2.	STD-NMR Studies	152
C3.3.	Binding Constants of the Interaction between Salivary Proteins and Tannins by STD-NMR	153
Chapter 2 - Modulation of salivary protein-tannin interactions: the importance of polysaccharides		159
D.	The role of wine polysaccharides on salivary protein-tannin interaction: A molecular approach	163
D1.	Introduction	163
D2.	Material and methods	165
D2.1.	Isolation and characterization of SP	165

D2.2.	Isolation of procyanidin dimer B2 and PNG	165
D2.3.	Isolation and characterization of polysaccharide fractions	166
D2.4.	Tannin-protein interaction.....	167
D2.5.	Influence of polysaccharides on SP-tannin interaction.....	168
D2.6.	Statistical analysis.....	170
D3.	Results and Discussion	170
D3.1.	Salivary Proteins identification.....	170
D3.2.	Polysaccharide and oligosaccharide characterization.....	171
D3.3.	Interaction between SP and tannins.....	172
D3.4.	Effect of polysaccharides on the interaction between SP and tannins	
	173	
D4.	Conclusions	182
E.	Inhibition mechanisms of wine polysacharides on salivary protein precipitation	
	183	
E1.	Introduction	183
E2.	Matherial and Methods.....	185
E2.1.	Saliva isolation and saliva samples preparation in different conditions	
	185	
E2.2.	Isolation of procyanidin dimer B2 and punicalagin.....	186
E2.3.	Isolation and characterization of polysaccharide fractions	186
E2.4.	Influence of polysaccharides on saliva-tannin interactions	187
E3.	Results and Discussion	190
E3.1.	Salivary proteins identification and saliva samples	190
E3.2.	Polysaccharide and oligosaccharide characterization.....	191
E3.3.	Interaction between SP and tannins	191
E3.4.	Influence of polysaccharides on the interaction between SP and	
	tannins	
	192	
E4.	Conclusions	204
F.	The effect of pectic polysaccharides from grape skin on salivary protein-tannin	
	interactions.....	207
F1.	Introduction	207
F2.	Materials and Methods	209
F2.1.	Plant materials	209
F2.2.	Isolation of procyanidins.....	209
F2.3.	Isolation of human saliva.....	209
F2.4.	Isolation of pectic polysaccharides	209

F2.5.	Consecutive fractional extraction of AIR	210
F2.6.	The influence of pectic polysaccharides on salivary protein-procyanidin interaction.....	210
F2.7.	SDS-PAGE	211
F2.8.	Analytical methods.....	212
F2.9.	Polysaccharide analysis	213
F2.10.	Statistical analysis.....	213
F3.	Results and Discussion	213
F3.1.	Composition of the interaction species	214
F3.2.	Salivary proteins-procyanidins interaction	219
F3.3.	Effect of pectic polysaccharides on salivary proteins-procyanidins interactions.....	220
F3.4.	Interaction between pectic polysaccharides and procyanidins	225
F4.	Conclusions	228
IV.	Final Remarks and Future WorK	229
	References	235
	Supplementary Information	253

List of Figures

<i>Figure 1 – Chemical structures of the major classes of non-flavonoids and some examples of products-rich in these compounds.....</i>	44
<i>Figure 2 – Chemical structure of flavanic nucleous.....</i>	45
<i>Figure 3 - Chemical structures of the major classes of flavonoids and some examples of products-rich in these compounds.</i>	46
<i>Figure 4 - Chemical structure of different anthocyanidins and respective substituents.....</i>	47
<i>Figure 5 - Chemical structure of the most abundant flavan-3-ols in food.</i>	48
<i>Figure 6 - Proanthocyanidin decomposition reaction (Bate-Smith, 1954).....</i>	51
<i>Figure 7 - A-type dimeric PC – PC A2 (C4-C8 and C2-C7).</i>	51
<i>Figure 8 - Chemical structure of B-type dimeric PC and their substituents – (dimers C4-C8 and dimers C4-C6).....</i>	52
<i>Figure 9 - Trimeric PC – Trimer C1 composed by epicatechin-(4-8)-epicatechin-(4-8)-epicatechin.</i>	53
<i>Figure 10 - General structure of proanthocyanidin polymers.</i>	54
<i>Figure 11 - Structures of gallic and ellagic acid and examples of hydrolyzable tannins: Pentagalloylglucose (PGG, gallotannin) and Punicalagin (PNG, ellagitannin).....</i>	55
<i>Figure 12 - The absorption of dietary polyphenols in humans is schematically illustrated. The polyphenols are extensively modified during the absorption: the glycosides could be hydrolyzed in the small intestine or in the colon, and the released aglycones could be absorbed. Prior to the passage into the blood stream, the polyphenols undergo to other structural modifications due to the conjugation process, mainly in the liver. Adapted from Vissioli, F. et al. (2011).</i>	59
<i>Figure 13 - Representative scheme of the location of the major salivary glands.</i>	60
<i>Figure 14 - Approximate percentages of the major classes of SP and peptides found in saliva. aPRPs, acidic PRPs; bPRPs, basic PRPs; gPRPs, glycosylated PRPs; IgG, immunoglobulin G; sIgA, secretory immunoglobulin A. Adapted from Messana, I. et al. (2008).</i>	62
<i>Figure 15 - Scheme of the interaction between condensed tannins and proteins: main driving forces, hydrophobic interactions (yellow circles) and hydrogen bonds (blue dotted line) between phenolic rings (cross-linkers) of tannins and the amide groups and apolar side chains of amino acids such as proline. Adapted from Santos-Buelga, C. et al. (2008).</i>	70
<i>Figure 16 - Conceptual mechanism for protein-tannin interaction. Tannins are displayed as having two ends that can bind to protein. Proteins are displayed as having a fixed number of tannin binding sites. Adapted from Siebert, K. J. et al. (1996)....</i>	72

Figure 17 - Molecular mechanism proposed for the interaction between tannins and proteins. This represent a nephelometry curve for a fixed concentration of tannin and increasing concentrations of protein. Adapted from Hagerman, A. et al. (1987).....	73
Figure 18 - Molecular mechanism proposed for the interaction between PRPs and tannins. In the initial stage (first stage) proteins are compacted, due to multiple bonds with multidentate tannins. In the second stage a dimer is formed with another protein coated with tannins, rendering the complex insoluble. In the third stage, complexation and complex precipitation occurs. Adapted from Jobstl, E. et al. (2004).....	74
Figure 19 - Average time-intensity curves for astringency of red wines (10 mL wine sipped at 25-s intervals). Adapted from Lesschaeve, I. et al. (2005).....	75
Figure 20 - Schematic representation of (A) primary cell wall structure showing polysaccharides and the (B) degradation of cell wall during fruit ripening. Degradation of these polysaccharides reduces the integrity of cell walls, increasing fruit softening. Adapted from Wakabayashi, K. (2000).....	79
Figure 21 - Simplified schematic diagram of some pectin characteristics: HGs – Homogalacturonans; RG-I / II – Rhamnogalacturonans I / II; Kdo – 3-deoxy-D-manno-octulosonic acid; Dha – deoxy-D-lyxo-heptulosanic acid. RG I and RG II are thought to be linked HGs. Adapted from Willats, WGT. et al. (2001)	81
Figure 22 - Possible mechanisms (A, Ternary mechanism and B, Competition mechanism) involved on the inhibition of the aggregation of tannins and proteins by polysaccharides. P: Salivary proteins, T: tannin, PS: polysaccharide. Adapted from Mateus, N. et al. (2004)	82
Figure 23 - Fluorescence emission spectra (at λ_{ex} 282 nm) of mucin (0.25 μ M) in the presence of increasing concentrations of GSF 3. Each curve represents a triplicate assay after correction for procyanidin fluorescence.....	101
Figure 24 - Stern–Volmer plots describing tryptophan quenching of mucin (0.25 μ M) by increasing concentrations of GSF (GSF 1, GSF 2 and GSF 3) (0-25 μ M) in different acetate buffer solutions: (a) 0.1 M, pH= 5.0, (b) 0.1 M, 10% EtOH, pH= 5.0 and (c) 0.1M, 10% DMSO, pH= 5.0. The fluorescence emission intensity was recorded at λ_{ex} 282 nm.....	102
Figure 25 - Stern-Volmer (a and c) and modified Stern-Volmer (b) plots describing tryptophan quenching of mucin (0.25 μ M) by increasing concentrations of procyanidin B4 (0-60 μ M) in different acetate buffer solutions. The fluorescence emission intensity was recorded at λ_{ex} 282 nm.	105
Figure 26 - Stern-Volmer plots describing tryptophan quenching of mucin (0.25 μ M) by increasing concentrations of procyanidin TT (0-40 μ M) in different acetate buffer solutions (0.1 M, pH=5.0; 0.1M, 10% EtOH, pH=5.0; 0.1M, 10% DMSO, pH=5.0). The fluorescence emission intensity was recorded at λ_{ex} 282 nm.....	106

Figure 27 - Molecular structure (A) and proton spectrum of procyanidin B4 (B) showing the 8.0–2.5 ppm region where most protons resonate. Spectrum was recorded at 600 MHz and 281 K in D ₂ O.....	108
Figure 28 - (A) Proton spectrum of procyanidin B4 (1) and STD-NMR spectra of mixture between mucin (0.25 µM) and increasing concentrations of procyanidin B4, 0.10 mM (2), 0.20 mM (3), 0.40 mM (4) and 0.60 mM (5). (B) Proton spectrum of procyanidin TT (1) and STD-NMR spectra of mixture between mucin (1.25 µM) and increasing concentrations of procyanidin TT, 0.15 mM (2), 0.25 mM (3), 0.50 mM (4) and 0.60 mM (5). All of these spectra were recorded in D ₂ O.....	109
Figure 29 - Observed (symbols) and fitted (lines) integral intensities of B4 proton resonance and TT region resonance in the STD-NMR spectrum with increasing B4/TT concentration in three different conditions: D ₂ O, D ₂ O:EtOH-d ₆ (90:10) and D ₂ O:DMSO-d ₆ (90:10). Curves represent the best fit according to Eq. 4.....	110
Figure 30 - Molecular structure of the procyanidins used in this work.....	115
Figure 31 - RP-HPLC profile (214 nm) of the acidified saliva used to isolate the different fractions corresponding to the families of PRPs and P-B peptide (upper figure). The identity of the SP families eluted in the different fractions are indicated in the top of the chromatogram. In the bottom, the deconvolution of the mass spectrum outlining the main proteins identified for each HPLC fraction is displayed.....	119
Figure 32 - Proton spectra of procyanidin dimer B2 (up), procyanidin B2g (middle) and procyanidin trimer (bottom) showing the 7.5-2.0 ppm region where most protons resonate. Spectra were recorded at 600 MHz and 300 K in deuterium oxide (D ₂ O).....	120
Figure 33 - Right side: STD-NMR spectra for the interaction between aPRP (3.0 µM) and the different procyanidins (procyanidin dimer B2, procyanidin B2g and procyanidin trimer catechin-(4-8)-catechin-(4-8)-catechin) at different procyanidins molar ratios (indicated by numbers) (38-641) showing the 8.0-2.0 ppm region where most protons resonate. Spectra were recorded at 600 MHz and 300 K in deuterium oxide (D ₂ O). Left side: STD amplification factor (ASTD) for the interaction between aPRP (3.0 µM) and procyanidin dimer B2, procyanidin B2g and procyanidin trimer. Symbols represent experimental values and lines represent theoretical values by Eq. 1.....	122
Figure 34 - ITC interaction of aPRP (30 µM) (upper) and P-B peptide (lower) with procyanidin B2, procyanidin B2 g and procyanidin trimer: thermogram (left side) and binding isotherm (points) and fitting curve (line) (right side). The data for the interaction with procyanidin B2g and trimer are presented in Figures S4, S5 and S6 of Supplementary Information.....	124
Figure 35 - Illustration of representative geometries reflecting the maximum capacity of interaction for each PRP:(B2) ₄ and PRP:(B2-g) ₄ complex and information about the conformation changes (head-to-head distances) observed in the simulations with B2 and B2g.....	129

Figure 36 - Molecular structure of condensed tannins (procyanidin B3 and procyanidin B6) and ellagitannins (vescalagin, castalagin, and punicalagin, PNG). The hexahydroxydiphenyl (HHDP) moiety of PNG is identified.....	140
Figure 37 - Fluorescence spectra of P-B peptide (30.0 μ M) recorded at λ_{ex} 284 nm with increasing concentrations of PNG (0.0–30.0 μ M).....	146
Figure 38 - Stern–Volmer plots representative of the fluorescence quenching of (▲) statherin, (■) P-B peptide, and (●) cystatins in the presence of increasing concentrations of (A) procyanidin dimer B3 and (B) procyanidin B6.....	147
Figure 39 - Stern–Volmer (A) and modified Stern–Volmer plots (B) representative of the fluorescence quenching of (▲) statherin, (■) P-B peptide and (●) cystatins in the presence of increasing concentrations of ellagitannins: 1. Castalagin, 2. Vescalagin and 3. PNG.....	148
Figure 40 - STD-NMR spectra for the interaction with increasing concentrations of each tannin and proteins (3.0 μ M). It is presented in the 8.0–2.0 ppm region, where most protons resonate. Spectra were recorded at 600 MHz and 300 K in deuterium oxide (D_2O). Interaction between statherin with (A) procyanidin B3 and (B) procyanidin B6. Interaction between P-B peptide and (C) punicalagin, (D) castalagin, and (E) vescalagin.....	152
Figure 41 - STD amplification factor (A_{STD}) for the interaction between the three different SP (3 μ M) – statherin, P-B peptide and cystatins with increasing concentrations of procyanidin dimers (A) B3 and (B) B6. Symbols represent experimental values and lines represent theoretical values by Eq. 1.....	154
Figure 42 - STD amplification factor (ASTD) for the interaction between the three different SP (3 μ M) – statherin, P-B peptide and cystatins with increasing concentrations of ellagitannins (A) PNG, (B) castalagin and (C) vescalagin. Symbols represent experimental values and lines represent theoretical values by Eq. 1.....	154
Figure 43 - Structures of procyanidin B2 (A) and PNG (B) with the evidence of the HHDP moiety of PNG.....	165
Figure 44 - Purification by High Resolution Size-Exclusion Chromatography on Superdex-75 HR column of RG II fraction.....	166
Figure 45 - Typical HPLC profile of AS solution from human saliva detected at 214 nm in the absence (black line) and in the presence of tannins: PNG (60 μ M, black dashed line) and procyanidin B2 (540 μ M, red line). The vertical dotted lines show the ranges and the main SP families assigned to each HPLC peptide region.....	171
Figure 46 - Chromatogram showing the aPRPs' fraction (6 μ M) before and after the interaction with PNG (60 μ M), and in the presence of AGPs (1.2 g.L ⁻¹).	174
Figure 47 - Influence of increasing concentrations of polysaccharides (AGPs and RG II) on aPRPs (a) and P-B peptide (b) interaction with PNG (60 μ M and 40 μ M) and procyanidin B2 (540 μ M and 400 μ M) determined by HPLC. These results represent the average of three independent	

experiments. Values with different letters within each column are significantly different ($P \leq 0.05$).	175
Figure 48 - Influence of polysaccharide concentration on aggregate formation (%) between aPRPs/P-B peptide and tannins (procyanidin B2 and PNG) at 400 nm. Blue, AGPs; Green, RG II.	176
Figure 49 - Representative spectra region from STD experiments (4-8 ppm), considering a solution of aPRPs (15 μ M) and PNG (500 μ M) in the absence and in the presence of AGPs (0.8 g.L ⁻¹).	178
Figure 50 - Possible mechanisms involved in the inhibition of the aggregation of tannins and SP by polysaccharides. A, Competition mechanism where aPRPs and RG II compete to bind procyanidin B2. B, Ternary mechanism in which RG II encapsulates the aPRPs-PNG complex.	181
Figure 51 - Typical HPLC profile of human saliva detected at 214 nm in the absence (red line) and in the presence of tannins: PNG 130 μ M (black line) and procyanidin B2 1000 μ M (black dashed line). The vertical dotted lines show the ranges and the main SP families assigned to each HPLC peptide region.	192
Figure 52 - Influence of polysaccharides concentration (RG II and AGPs), on SP precipitation after interaction between saliva in the absence (DS ⁻ and MSP) or presence of salts (S and DS ⁺) and PNG (130 μ M). (A) S, (B) DS ⁺ , (C) DS ⁻ , and (D) MSP. These results represent the average of three independent experiments. Values with different letters within each column are significantly different ($P \leq 0.05$).	193
Figure 53 - Influence of RG II concentration on SP precipitation after interaction between saliva in the absence (DS ⁻ and MSP) or presence of salts (S and DS ⁺) and procyanidin B2 (1000 μ M). (A) S, (B) DS ⁺ , (C) DS ⁻ , and (D) MSP. These results represent the average of three independent experiments. Values with different letters within each column are significantly different ($P \leq 0.05$).	194
Figure 54 - Influence of AGPs concentration on SP precipitation after interaction between saliva in the absence (DS ⁻ and MSP) or presence of salts (S and DS ⁺) and procyanidin B2 (1000 μ M). (A) S, (B) DS ⁺ , (C) DS ⁻ , and (D) MSP. These results represent the average of three independent experiments. Values with different letters within each column are significantly different ($P \leq 0.05$).	195
Figure 55 - Variation (%) in fluorescence intensity at 260 nm of two saliva samples (S and DS ⁻) and PNG (4 μ M) and procyanidin B2 (40 μ M), with increasing concentrations of different polysaccharides – AGPs and RG II. These results represent the average of three independent experiments. Values with different letters within each column are significantly different ($P \leq 0.05$).	198

Figure 56 - Influence of AGPs and RG II concentration on aggregate formation (%) at 400 nm, between two saliva samples (Saliva, S and dialyzed saliva, DS) and tannins, PNG (60 μ M) and procyanidin B2 (540 μ M).	199
Figure 57 - SDS-PAGE of the pellets that resulted from the interaction between S/DS ⁻ and tannins (PNG and procyanidin B2) in the absence (Control) and presence of the several polysaccharides (RG II and AGPs, 1.2 g. L ⁻¹ and 2.4 g. L ⁻¹). The molecular weight markers are identified, and the molecular mass marked on the left side is expressed in kDa. The gels were stained with Imperial Protein Stain, a Coomassie R-250 dye-based reagent.....	201
Figure 58 - HPLC-DAD chromatogram detected a 280 nm of the mixture of PC used in this work and respective identification. ECG - epicatechin gallate; GD – galloylated dimer.....	218
Figure 59 - Influence of PC fraction (3.0 g. L ⁻¹) after interaction with several SP families (gPRPs, aPRPs, statherin/P-B petide and cystatins) determined by HPLC at 214 nm. Values with different letters within each SP are significantly different ($P<0.05$).	219
Figure 60 - PC fraction profile variation after interaction with SP determined by HPLC-DAD at 280 nm. Values with different letters within each procyanidin are significantly different ($P<0.05$)...220	
Figure 61 - Influence of increasing pectic polysaccharide concentration (A-WSP and B-CSP) on SP interaction with PC fraction (3.0 g.L ⁻¹) determined by HPLC at 214 nm. Values with different letters within each SP family are significantly different ($P<0.05$).	222
Figure 62 - Influence of SP and increasing pectic polysaccharide concentration (WSP) on 3.0 g.L ⁻¹ of PC fraction determined by HPLC-DAD. Values with different letters within each procyanidin are significantly different ($P<0.05$).	223
Figure 63 - Influence of SP and increasing pectic polysaccharide concentration (CSP) on 3.0 g.L-1 of PC fraction determined by HPLC-DAD. Values with different letters within each procyanidin are significantly different ($P<0.05$).	224
Figure 64 - SDS-PAGE of saliva (S) and of the precipitates that resulted from the interaction between SP and PC in the absence (S+PC, control) and presence of increasing concentrations of the polysaccharides fractions (CSP and WSP). The molecular weight markers were substituted by lines, and the molecular mass marked on the left side is expressed in kDa.The gel was stained with Imperial Protein Stain, a Coomassie R-250 dye-based reagent.	225
Figure 65 - PC fraction profile variation due to different polysaccharide concentration (WSP) determined by HPLC-DAD. Values with different letters within each procyanidin are significantly different ($P<0.05$).	226
Figure 66 - PC fraction profile variation due to different polysaccharide concentration (CSP) determined by HPLC-DAD. Values with different letters within each procyanidin are significantly different ($P<0.05$).	227

List of Tables

<i>Table 1 - Polyphenol's content of several plant-based products (Adapted from Scalbert and Williamson, 2000 and Macheix et al., 2005).....</i>	57
<i>Table 2 - Families of major SP: function, origin, genes, name of mature proteins, and main post-translational modifications (PTMs).....</i>	63
<i>Table 3 - Stern-Volmer quenching constants (K_{SV}) and Apparent Static Quenching Constant (K_{app})* for the interaction between mucin and procyanidins (0-60 μM) with increasing DP (dimer B4, tetramer TT and fractions GSF 1, GSF 2 and GSF 3 of oligomeric procyanidins). Values with equal letters (a-h) are not significantly different ($P<0.05$).</i>	102
<i>Table 4 – Bimolecular quenching constants (k_q) for the interaction between mucin (0.25 μM) and procyanidins with increasing DP (GSF of oligomeric procyanidins, B4 and TT) in different conditions. Values with equal letters (a-q) are not significantly different ($P< 0.05$).</i>	103
<i>Table 5- K_A for the interaction between mucin and procyanidins (B4 and TT) determined by STD-NMR.</i>	111
<i>Table 6 - Binding constant (K_A) values determined for the interaction between each protein family and the procyanidins dimer B2, B2g and trimer by STD-NMR.....</i>	123
<i>Table 7 - Binding constant (K_A) values determined for the interaction between each protein family and the procyanidins dimer B2, B2g and trimer by ITC. The number of binding sites (n) on the protein was also determined by ITC. Set (1,2 or 2,2) refers to the individual parameters for each set of sites.</i>	125
<i>Table 8 - Global thermodynamic parameters (ΔH, ΔG and $-T\Delta S$), number of protein binding sites (n) and global binding constants (K_A) for the interaction between procyanidins dimer B2, B2 gallate and trimer and SP (bPRPs, gPRPs, aPRPs and P-B).</i>	126
<i>Table 9 - Procyandins binding time (simultaneously bound to proteins) of B2 and B2g molecules to the various peptides (PRP1, PRP3, IB-8b and P-B peptide) for a PRP:(T)n model.</i>	127
<i>Table 10 - Stern-Volmer (K_{SV}) and apparent static quenching (K_{app}) constants for the interaction of statherin, P-B peptide and cystatins with the five studied tannins.</i>	149
<i>Table 11 - Proteins' lifetimes and biomolecular quenching constants (k_q) for the interaction of statherin, P-B peptide and cystatins with the five studied tannins.....</i>	151
<i>Table 12 - Association constant (K_A) values estimated for the interaction between each SP and the different tannins determined by Eq. 2 and 3.</i>	155
<i>Table 13 - Monosaccharides composition (% molar) of the RG II and AGPs fractions.</i>	172
<i>Table 14 - Integrals values (%) of ligand signals obtained by STD-NMR for the interaction between each SP (aPRPs and P-B peptide), different tannins (PNG and procyanidin B2) and polysaccharides (AGPs and RG II).</i>	178

<i>Table 15 - Different conditions of saliva samples used to study the influence of polysaccharides on the interaction between SP and tannins.....</i>	186
<i>Table 16 - The effectiveness of AGPs and RG II (2.4 g.L⁻¹) to inhibit SP precipitation by PNG (130 µM) and procyanidin B2 (1000 µM). These values represent the recovery (%) of each SP family.</i>	196
<i>Table 17 - Summary of the suggested mechanisms for the polysaccharides' effect on the interaction between SP and tannins used in this work.....</i>	202
<i>Table 18 - Consecutive fractional extraction of AIR and chemical characteristics of the extracted polysaccharides fractions. µg. mg⁻¹ dry weight (UA, uronic acids; NS, neutral sugars; TS, total sugars; SP, soluble proteins; P, polyphenols).</i>	216
<i>Table 19 - Neutral sugar composition of the extracted polysaccharide fractions (µg. mg⁻¹ dry weight)</i>	216

List of Abbreviations and Symbols

AGPs – Arabinogalactan-Proteins

AIR – Alcohol-insoluble residue

ANOVA – Analysis of Variance

aPRPs – Acidic proline-rich proteins

Ara – Arabinose

AS – Acidic saliva

B2g – B2 3'-O-gallate

bPRPs – Basic proline-rich proteins

BSA – Bovine serum albumin

BSAE – Bovine serum albumin equivalents

CSP – Chelate-soluble pectic polysaccharides

DAD – Diode Array Detector

Dha – Deoxy-D-lyxo-heptulosonic acid

DLS – Dynamic Light Scattering

DMSO – dimethylsulfoxide

DP – Degree of polymerization

ECG – Epicatechin gallate

EGCG – Epigallocatechin gallate

ESI – Electrospray Ionization

ESI-MS – Electrospray Ionization Mass Spectrometry

EtOH - Ethanol

FRET – Fluorescence Resonance Energy Transfer

Fuc – Fucose

GA – Gallic acid

GAE – Gallic acid equivalents

Gal – Galactose

Gal acid – Galacturonic acid

GC – Gas Chromatography

GCF – Gingival crevicular fluid

GD – Galloyated dimer

Glc – Glucose

Glc acid – Glucuronic acid

gPRPs – Glycosylated proline-rich proteins

GSF – Grape Seed Fraction

HGs – Homogalacturonans

HHDP – Hexahydroxydiphenic acid

HIV-1 – Human Immunodeficiency Virus type I

HPLC – High Performance Liquid Chromatography

IgG – Immunoglobulin G

ITC – Isothermal Titration Calorimetry

IS – Ionic strength

Kdo – 3-deoxy-D-*manno*-octulosonic acid

LC-MS – Liquid Chromatography Mass Spectrometry

Man – Mannose

MD – Molecular Dynamics Simulation

MPs – Mannoproteins

MS – Mass Spectrometry

MW – Molecular weight

NHTP – Nonahydroxytriphenoyl moiety

NMR – Nuclear Magnetic Resonance

NS – Neutral sugars

PC – Procyanidins

PD – Prodelfphinidins

PGG – Pentagalloylglucose

PNG – Punicalagin

pI – Isoelectric point

Pr – Parotid gland

PRAGs – Polysaccharides Rich in Arabinose and Galactose

PRP(s) – Proline-rich proteins

PTMs – Post-Translational Modifications

Rha – Rhamnose

RG I – Rhamnogalacturonan type I

RG II – Rhamnogalacturonan type II

ROS – Reactive Oxygen Species

S1 – Sublingual gland

SDS – Sodium Dodecylsulfate

SDS-PAGE – Sodium Dodecylsulfate-Polyacrylamide Gel Electrophoresis

SEM – Standard Error of Mean

sIgA – Secretory Immunoglobulin A

SLS – Static Light Scattering

Sm – Submandibular gland

SP – Salivary proteins

STD-NMR – Saturation Transfer Difference Nuclear Magnetic Resonance

TFA – Trifluoroacetic acid

TMS - Trimethylsilyl

TS – Total sugars

TT – Procyanidin tetramer

UA – Uronic acids

WSP – Water-soluble pectic polysaccharides

Xyl – Xylose

I. Aims

Nowadays, polyphenols have received special attention by the scientific community and general public mainly due to their sensorial characteristics and biological properties which are very important for different fields such as food industry and human health, respectively.

Polyphenols are present in several products, such as fruits, seeds, vegetables and beverages contributing for their organoleptic properties such as flavor (astringency and bitterness) and colour. Flavor is probably one of the most important parameters for consumer's choice. For instance, astringency can elicit negative consumer reactions when perceived at high intensities, leading to food rejection. The tactile sensation of astringency on the human palate has been defined as a complex group of sensations involving dryness of the oral surface and tightening and puckering sensations of the mucosa and muscles around the mouth. Astringency sensation has been described to arise from the interaction between dietary polyphenols and salivary proteins.

Therefore, in response to consumer's preference, it has been imperative for food industry to create or modulate the sensorial properties of some products in order to make them more appealing for consumers. Polysaccharides are frequently used in food industry as food colloids (gums) and are also naturally present in several food products, thereby affecting their astringent sensation. This way, the effect of polysaccharides on protein/tannin interaction has a great impact on the perception and choice of foodstuffs.

Bearing this, the overall objective of this thesis is to better understand taste, mainly astringency sensation. Despite of being seen very often as a negative attribute of tannin-rich products, astringency is also a quality parameter for some products such as red wine, tea, coffee and beer. For this reason, it was aimed to gain knowledge about the different ways to modulate astringency perception. Therefore, the effect of several polysaccharides naturally present in food and beverages on the interaction between salivary proteins and tannins was studied. Furthermore, it was also intended to understand the molecular mechanisms by which polysaccharides can modulate protein-tannin interactions.

In this context several objectives were defined for this work:

- Understand the molecular interaction of mucin protein with oligomeric fractions of procyandins isolated from grape seeds and with two pure procyandins [B2 and a tetramer (cat-(cat)₂-cat)]. The influence of different factors, such as pH, the

presence of solvents (EtOH and DMSO) and ionic strength was also evaluated (Part A).

- Study of the interaction between different salivary proteins with two classes of tannins – condensed and hydrolyzable. It was important to understand and characterize, at molecular level, how different salivary proteins interact with tannins when the latter are present alone (Parts B and C).
- Study of the influence of different wine polysaccharides on the interaction between two classes of tannins and salivary proteins alone (Part D).
- Comprehend how wine polysaccharides can act on tannin-protein interaction, when salivary proteins are present simultaneously in a competitive assay (whole saliva) and the inhibition mechanisms of these polysaccharides. It was also studied the influence of ionic strength of saliva (e.g. presence of salts) on those interactions (Part E).
- Study of the role of pectic polysaccharides fractions from grape skin on the interaction between saliva (competitive assay) and a mixture of procyanidins (Part F).

II. Introduction

1. Phenolic compounds

Phenolic compounds, often referred to as polyphenols, are secondary metabolites synthesized by plants both during normal development and in response to stress conditions. In plants, these compounds may act as antioxidants, antifeedants, attractants for pollinators, contributors to plant pigmentation, and protective agents against UV light, among others. These compounds are commonly found in both higher and edible plants and consequently they are abundant in our diet, particularly in plant-derived foods and beverages (e.g. wine, tea, beer, coffee, fruit juices) [1]. In these foodstuffs, polyphenols may contribute to their organoleptic properties such as flavor (bitterness and astringency), colour, aroma and oxidative stability [2]. Over the last years, dietary polyphenols have received special attention for their biologically properties [3-5].

Chemically, polyphenols present one or more aromatic rings with one or more hydroxyl groups, including a high structural diversity of compounds from small phenolic molecules until high molecular polymers. In addition to this diversity, polyphenols may be associated with various carbohydrates and organic acids [4]. To date, many structurally different polyphenols have been identified and it is believed that there are many others that remain unknown, especially those available in lower quantities or the ones with a high degree of structural complexity [6]. Plant polyphenols comprise a large diversity of structures being their composition highly variable both qualitatively and quantitatively; some of the compounds are ubiquitous, whereas others are restricted to specific families or species of plants (e.g. isoflavones can be found specially in soya) [6, 7]. Generally, polyphenols can be divided into two groups, non-flavonoids and flavonoids, being the latter the most abundant in food [6].

1.1. Non-flavonoids

The non-flavonoids have simple structures such as phenolic acids (benzoic and hydroxycinamic acids, based on C1-C6 and C3-C6 skeletons, respectively) and stilbenes. However, this group also includes complex molecules derived from those simple molecules, namely gallotannins, ellagitannins and lignins (Figure 1) [4]. One of the most common phenolic acids is caffeic acid, present in many fruits and vegetables, most often with quinic acid as in chlorogenic acid, which is the major phenolic compound in coffee [8]. Another common phenolic compound is ferulic acid, which is present in cereals and is esterified to hemicelluloses in the cell wall.

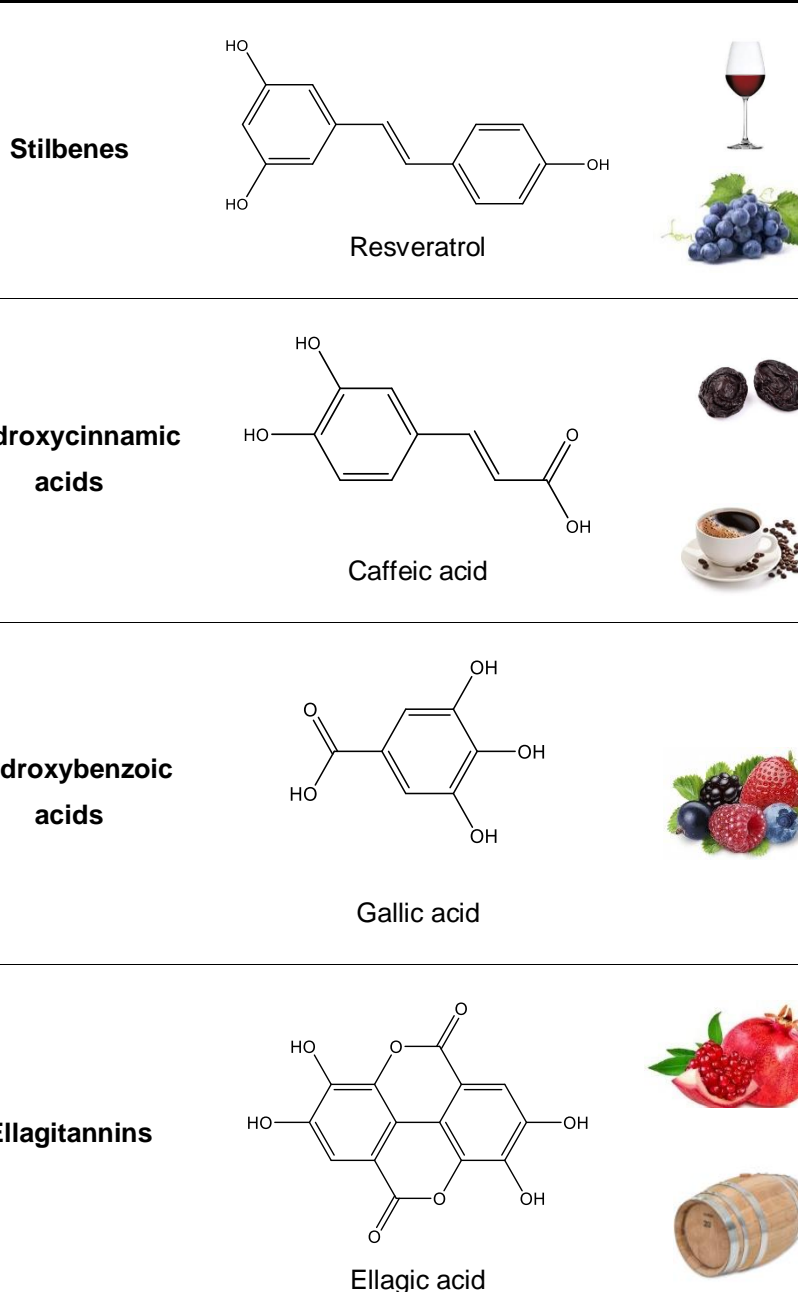


Figure 1 – Chemical structures of the major classes of non-flavonoids and some examples of products-rich in these compounds.

1.2. Flavonoids

In addition to being the most important class of phenolic compounds found in plant-based foodstuffs, the flavonoids group is also the most structurally diversified. At present, more than 4000 unique flavonoids have been identified and the number is still growing [7].

The flavonoids group share a common C6-C3-C6 skeleton, which is called flavanic nucleous, composed by two benzenic rings (A and B) and a heterocyclic pyran ring C, characteristic of flavonoids (Figure 2).

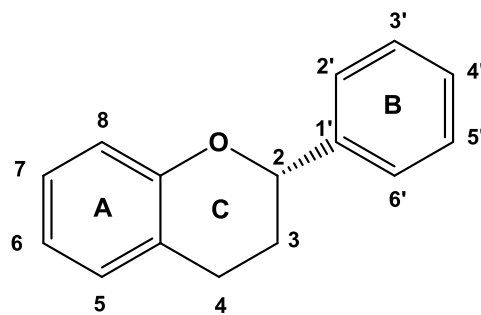
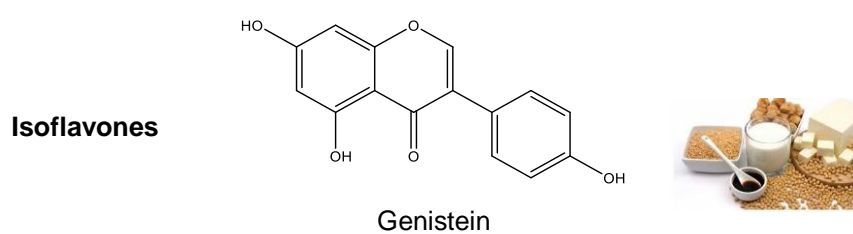


Figure 2 – Chemical structure of flavanic nucleous.

According to the oxidation degree and substitution pattern of the heterocyclic, the flavonoids group may be itself divided into several classes such as flavanones, flavones, flavonols, dihydroflavonols, isoflavonoids, anthocyanins, flavan-3,4-diols, flavan-4-ols and flavan-3-ols (Figure 3).

Within each class, as for example for flavan-3-ols, these compounds may differ from each other in the degree of hydroxylation of ring B as well as they may differ in the position and number of methoxyl and glycosyl groups. Some of the most common flavonoids are quercetin, a flavonol abundant in onion, tea, and apple; daidzein, the main isoflavone in soybean; cyanidin, an anthocyanin giving its colour to many red fruits (blackcurrant, raspberry, strawberry, etc.) and catechin, a flavanol found in tea and several fruits [8].

In the next sections the classes of flavonoids more relevant for food organoleptic properties will be presented.



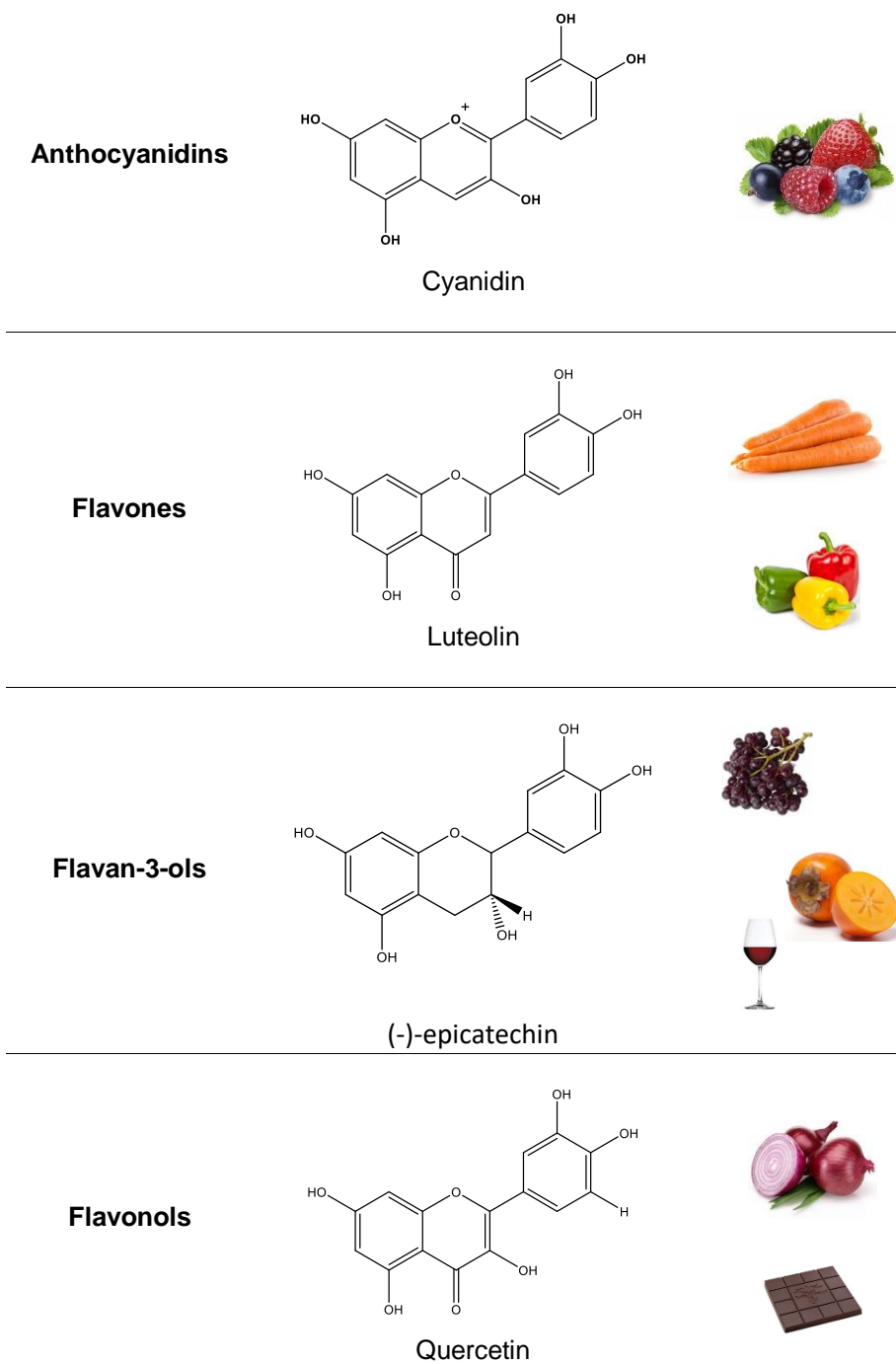


Figure 3 - Chemical structures of the major classes of flavonoids and some examples of products-rich in these compounds.

1.2.1. Anthocyanins

Anthocyanins are flavonoids commonly found in plant tissues, producing blue, red and purple colours [9]. Structurally, they are flavylium cation derivatives with different methylation and hydroxylation degrees in the ring B, which contributes for the different hue. Usually in fruits, anthocyanins are found in the glycosylated form, however they can also exist in the non-glycosylated form being denominated anthocyanidins (aglycones).

The mainly naturally occurring anthocyanidins are pelargonidin, cyanidin, peonidin, delphinidin, petunidin and malvidin [10]. The respective structures of these compounds are presented in Figure 4. The anthocyanins can also differ in the type, number and position of several sugar residues (glucose, rhamnose, galactose, xylose and arabinose) which are mostly linked at position 3-O, but they can also bind at other positions (5-O and 7-O), and by the esterification with various organic (citric and malic acids) and phenolic acids [4]. Due to all these possibilities of substitutions around 300 anthocyanins were already identified in nature [11].

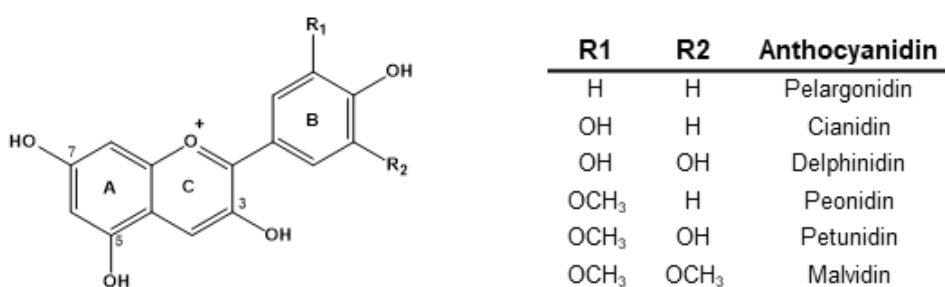


Figure 4 - Chemical structure of different anthocyanidins and respective substituents.

The main interest in these compounds arises from their role as water-soluble plant pigments with potential use as natural colourants in the food industry substituting synthetic colourants with toxic effects in human. However, anthocyanin's application in food matrices have been limited since their colour and stability are influenced by pH, light and temperature [12]. Regarding pH, anthocyanins can be found in different chemical forms which depend on the pH of the solution. For instance, at pH 1, the flavylium cation (red colour) is the predominant specie and contributes to purple and red colours. At pH values between 2 and 4, the quinoidal blue species are predominant. At pH values between 5 and 6 only two colourless species can be observed, which are a carbinol pseudobase and a chalcone, respectively. At pH values higher than 7, the anthocyanins are degraded depending on their substituent groups [12]. Furthermore, investigations about anthocyanins stability and the colour variation with pH conclude that the changes in the colour of these compounds are more significant in the alkaline region due to their instability [12].

Beyond the sensory properties, anthocyanins have also a high antioxidant activity [13]. Furthermore, several health-promoting benefits have been associated to anthocyanins such as inhibition of platelets aggregation, controlling diabetes, vaso-protective and anti-inflammatory properties, among others [14, 15].

Recently, it was suggested that, along with tannins, anthocyanins and pyranoanthocyanins could interact with salivary proteins (SP), namely proline-rich proteins (PRPs), contributing to red wine global astringency [16, 17].

1.2.2. Flavan-3-ols

Flavan-3-ols are the most abundant flavonoids in the plant kingdom. The basic structure of flavan-3-ols differ in the degree of hydroxylation of ring B, which can have one (afzlechin/epiafzlechin), two (catechin/epicatechin) or three (gallocatechin/epigallocatechin) hydroxyl groups, and the configuration of C3, yielding the natural (+)-afzelechin/(+)-catechin/(+)-gallocatechin and (-)-afzelechin/(-)-epicatechin/(-)-epigallocatechin compounds [6]. They have a basic monomeric unit of (+)-catechin or (-)-epicathecin and they can exist as monomers, oligomers or polymers (proanthocyanidins). In opposite to other classes of flavonoids (which exist mainly in the glycoside form), the flavanols can be found usually in the aglycone form. In certain positions, flavanol units may sometimes bear acyl or glycosyl substituents. The most common acyl substituent is gallic acid which forms an ester linkage with the hydroxyl group in the C3 position thus forming, by example, epigallocatechin and epigallocatechin gallate (Figure 5) [18].

Catechin and epicatechin are the main flavan-3-ols in fruits while gallocatechin, epigallocatechin and epigallocatechin gallate are found in certain seeds and leguminous plants and in tea [4, 19, 20].

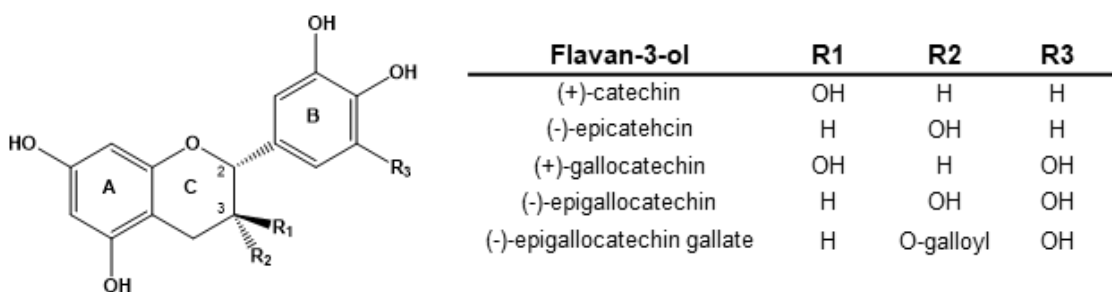


Figure 5 - Chemical structure of the most abundant flavan-3-ols in food.

As all the most polyphenols, several studies showed that flavanols have several antioxidant properties directly correlated with health promotion, mainly because they are involved in cardio- and neuroprotection, as well as in cancer prevention [21-23].

This is the most abundant class of flavonoids in food and it is normally associated with flavor, particularly with astringency and bitter taste. Some of the main sources of these compounds in diet are cocoa, red wine, green tea, red grapes and apples [4]. The importance of this class also relies in the fact that they are the structural unit of proanthocyanidins, commonly known as condensed tannins, which are very abundant in nature. A more detailed description of the tannin's chemistry will be presented below.

2. Tannins

Tannins are present in a wide variety of foodstuffs of plant origin such as fruits and grains, but also in several beverages such as wine, beer, coffee and tea [6]. Tannins constitute a complex group of naturally occurring polymers, very heterogeneous which difficult a rigorous chemical definition. The term was originally used to describe vegetable components that are responsible for converting animal hides into leather in the process of tanning by forming stable complexes with skin collagen [24]. Tannins were first defined by Bate-Smith and Swain (1962) as "water soluble phenolic compounds having molecular weights between 500 and 3000 (Da) and, besides giving the usual phenolic reactions, they have special properties such as the ability to precipitate alkaloids, gelatin and other proteins from solution" [25].

However, this definition underestimates the molecular weight of soluble tannins extract of plant sources. Over the years, several authors have determined the molecular weight of several tannins in the range of hundred to thousand Dalton. For instance, Haslam and co-workers described the existence of soluble proanthocyanidins and hydrolyzable tannins with molecular masses up to 20000 Da and 3000 Da, respectively [26]. Nowadays, it is believed that soluble tannins extracted from plant tissues may reach a molecular weight of several thousands, depending on their chemical structure and also on their colloidal behavior in aqueous solution [6, 27].

Plant tissues present not only soluble proanthocyanidins, but also insoluble forms that are resistant to all kinds of solubilisation. It was proposed that tannin polymers become insoluble because of their high molecular size, their involvement in noncovalent complexation and, more importantly, their covalent binding to an insoluble polysaccharide matrix within plant cells [60].

As mentioned previously, one of the main characteristics of tannins is the ability to complex and precipitate proteins. This property is doubly the origin of positive and

negative attributes of these compounds. On the one hand, it is precisely this capacity to precipitate proteins, particularly the SP in the oral cavity, which is believed to give them an astringent character easily recognized in tannin-rich food [3]. At a balanced level, astringency sensation which is characterized by dryness, constriction and perceived roughness in the oral cavity, can be a positive attribute of the quality of certain beverages (e.g. red wine, beer and tea) [28]. On the other hand, the interaction of tannins with digestive enzymes may inhibit them, causing some gastrointestinal problems related to nutrients absorption, which may lead to a decrease of body weight gain [29, 30].

Vegetable tannins are classically divided into two broad groups: condensed tannins (proanthocyanidins) and hydrolyzable tannins, according to their chemical structure. There are also other minor tannin classes such as phlorotannins and complex tannins [6].

2.1. Condensed tannins (proanthocyanidins)

Proanthocyanidins are more common in diet than hydrolyzable tannins, being present in significant amounts in chocolate, fruits (grapes, apples, among others) and beverages (wine, tea and beer) [3]. Proanthocyanidins are polymers of flavan-3-ol units and comprise a range of molecular forms from dimeric to oligomeric and various polymers. Flavan-3-ol units have the typical C6-C3-C6 skeleton and they are linked through C-C interflavanol bonds established between the C4 of one flavan-3-ol unit and the C8 or C6 of another unit. There are also tannins with an additional ether linkage between the C2 of the upper unit and the oxygen-bearing C7 or C5 of the lower unit in addition to the usual C4-C8 or C4-C6 interflavanol bond [6, 31].

Depending on the ring B hydroxylation degree of their units, proanthocyanidins can be classified as propelargonidins (mono-hydroxylated), procyanidins (PC) (di-hydroxylated) or prodelphinidins (PD) (tri-hydroxylated) [6]. PC are derived from catechin and epicatechin, while PD are derived from gallocatechin and epigallocatechin. The most common in food are PC or a mixture PC/PD, while propelargonidins are relatively rare in food sources [3]. The various subclasses are named based on the conversion of the monomeric units to the corresponding anthocyanidin during acid-catalyzed depolymerization; hence this broad class of polymers is named proanthocyanidins. Examples include conversion of (epi)catechin monomers to cyanidin (PC) and (epi)gallocatechin monomers to delphinidin (PD) (Figure 6) [32].

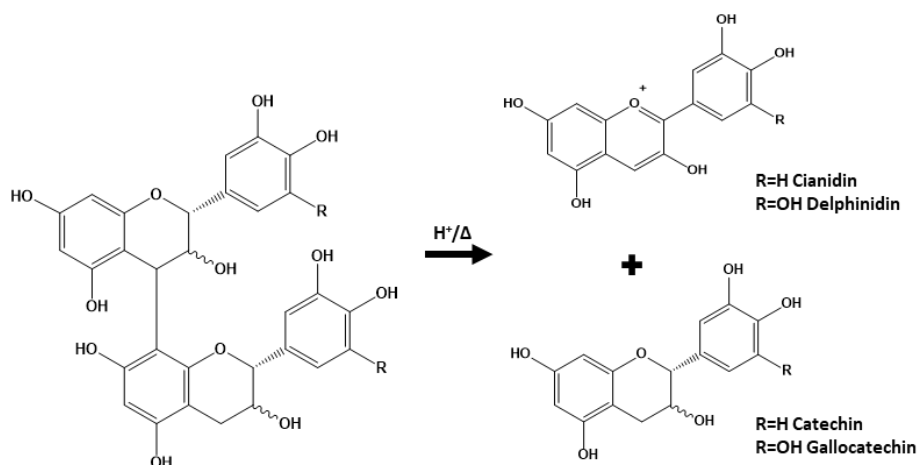


Figure 6 - Proanthocyanidin decomposition reaction (Bate-Smith, 1954) [33].

Dimeric PC are conventionally classified in A-type or B-type according to their interflavanic linkage. Both PC are classified numerically according to the stereochemistry of C3 of the ring C of each unit. The A-type PC have C4-C8 linkage with an extra ether bond between the hydroxyl group of C5 or C7 of the ring A of one unit and C2 of the pyran ring of the other unit (Figure 7).

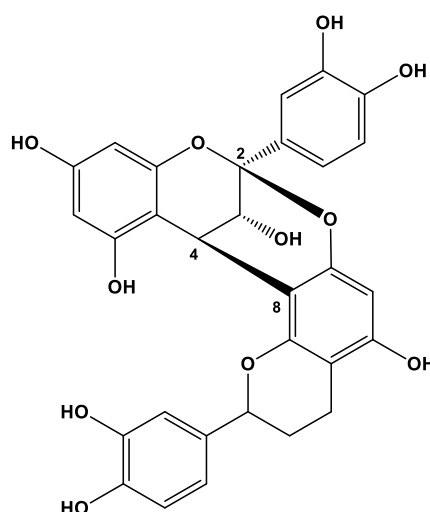
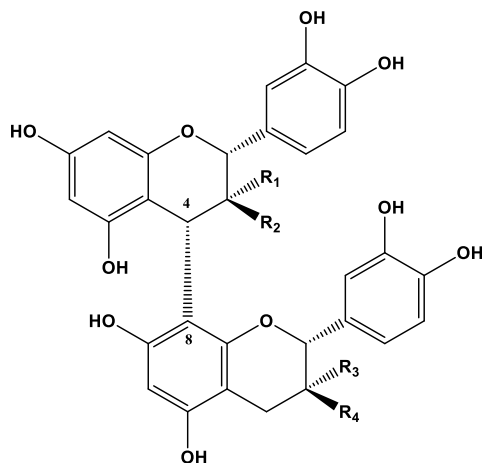


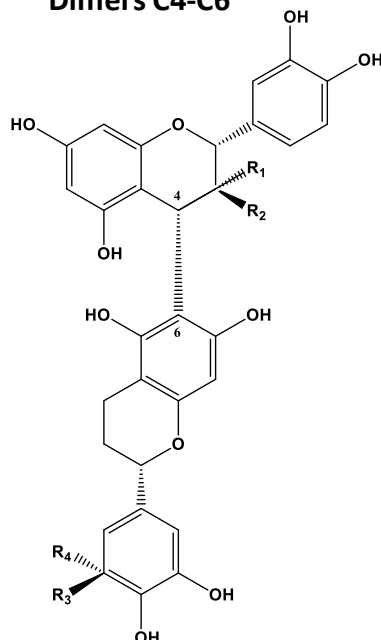
Figure 7 - A-type dimeric PC – PC A2 (C4-C8 and C2-C7).

The B-type dimeric PC has only interflavanic linkages between C4 of a flavan-3-ol unit and C8 or C6 of the other unit (Figure 8).

Dimers C4-C8



Dimers C4-C6



R1	R2	R3	R4	Dimers C4-C8	Dimers C4-C6
OH	H	H	OH	B1	B5
OH	H	OH	H	B2	B6
H	OH	H	OH	B3	B7
H	OH	OH	H	B4	B8

Figure 8 - Chemical structure of B-type dimeric PC and their substituents – (dimers C4-C8 and dimers C4-C6).

The trimeric PC are also divided into C-type (Figure 9) and D-type depending on the interflavanic linkage which can have two B-type linkages or one B-type and other A-type linkages, respectively.

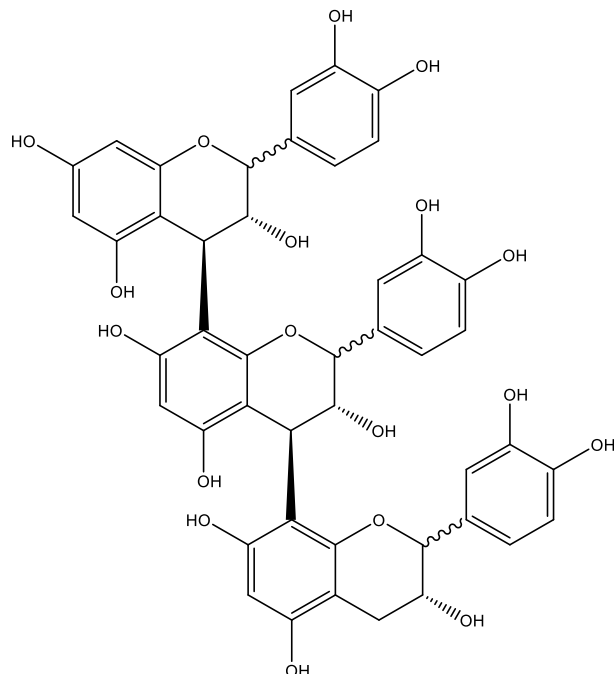


Figure 9 - Trimeric PC – Trimer C1 composed by epicatechin-(4-8)-epicatechin-(4-8)-epicatechin.

In addition to monomeric, dimeric and trimeric structures there are more polymerized structures - oligomers until 6 units of monomers and polymers composed of more than 6 units. Indeed, several polymers can have high degree of polymerization (DP) [34]. For instance, the DP of grape seeds can vary between 2 and 16 flavanol units, while in grape skin there are higher DP (3-83 units) (Figure 10) [27].

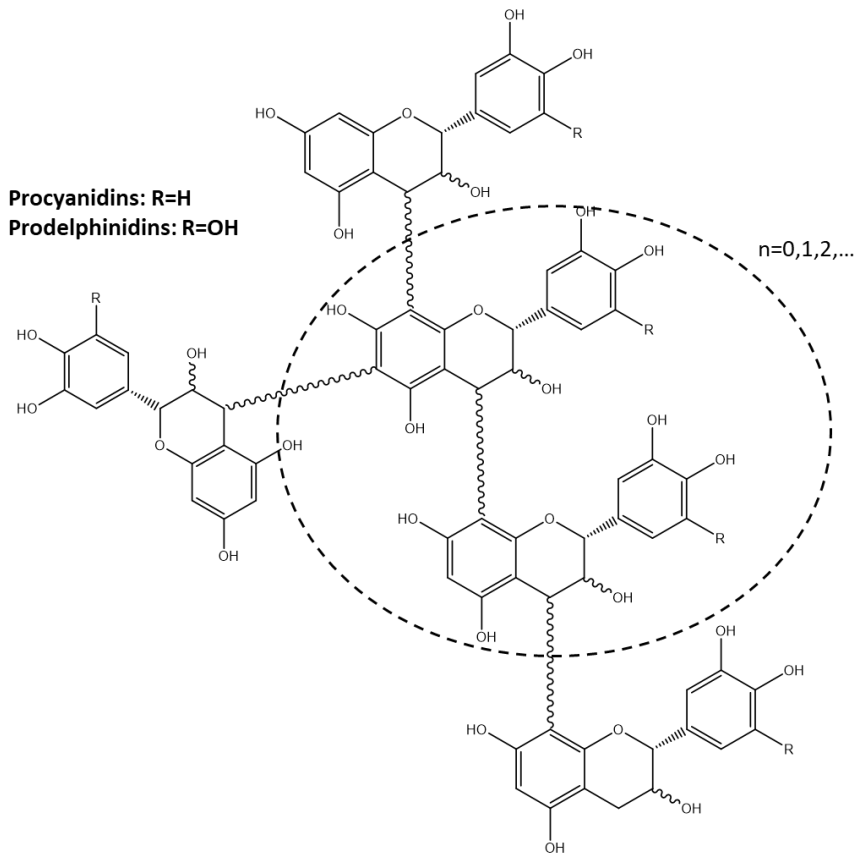


Figure 10 - General structure of proanthocyanidin polymers.

Therefore, condensed tannins can differ in the nature of their constitutive units (e.g. catechin and epicatechin in PC), their sequences, the positions of interflavanic linkages (C4-C6 or C4-C8 in the B-type series, with additional C2-O-C7 or C2-O-C5 bonds in A-type structures), their chain lengths, and the presence of substituents (e.g. galloyl or glucosyl groups) [7].

2.2. Hydrolyzable tannins

This group of tannins are found in some plant species, essentially in the non-edible parts of them such as wood, bark and galls [35, 36]. However, they can be also found in the berries, legumes, leafy vegetables, peanuts, walnuts, pecans, cashews, pomegranate, red apples, kiwi, etc. [36, 37].

Even though hydrolyzable tannins are essentially present in the non-edible portions of plants, these compounds can be introduced in the diet by technological operations. For instance, in wine, a small percentage of hydrolyzable tannins can be extracted from oak barrels or chips during ageing or can be added during winemaking by the addition of

enological tannins [38]. However, their intake from wine should be residual because most of wines are not matured in new oak wood in which there is a high content of ellagic tannins.

Chemically, hydrolyzable tannins are polyesters of a sugar moiety and organic acids. The term “hydrolyzable tannin” comes from the fact that these compounds undergo hydrolytic cleavage to the respective sugar and acid moiety upon treatment with diluted acids. Usually, the sugar component is glucose, but fructose, xylose, saccharose among other structures are also possible to be found [37]. The hydroxyl groups of the sugar are partially or totally esterified with phenolic groups such as gallic acid in gallotannins, or ellagic acid in ellagitannins (Figure 11). Most ellagitannins are mixed esters both with gallic acid and hexahydroxydiphenic acid (HHDP) [37, 39, 40]. Generally, these tannins are found in nature as multiple esters with sugars, mainly D-glucose, forming complex structures, as for example, β -1,2,3,4,6-pentagalloyl-O-D-glucopyranose (pentagalloylglucose, PGG) (Figure 11) [6, 41].

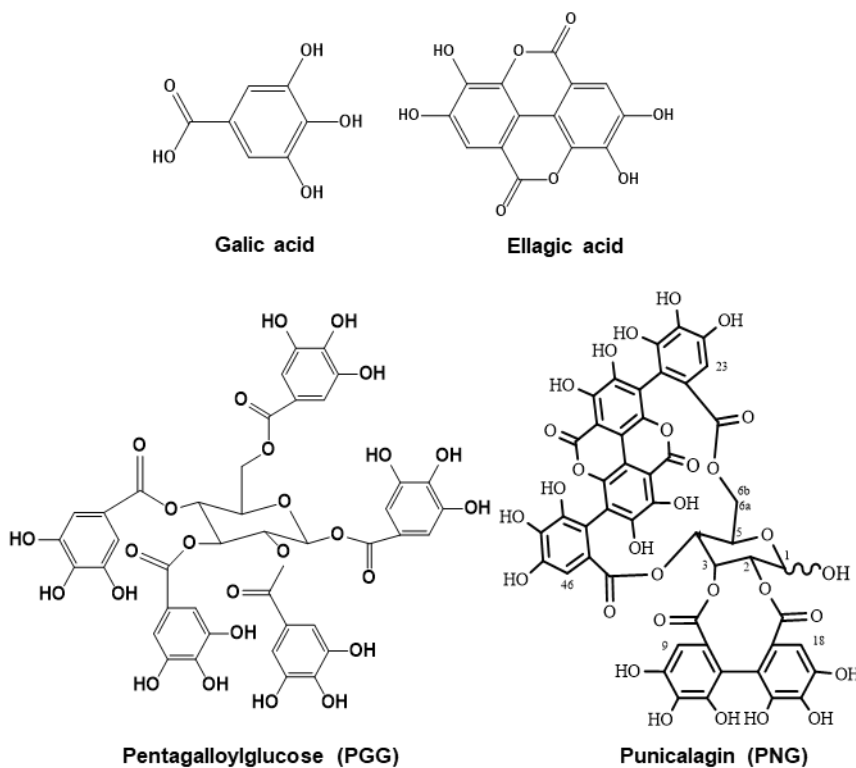


Figure 11 - Structures of gallic and ellagic acid and examples of hydrolyzable tannins: Pentagalloylglucose (PGG, gallotannin) and Punicalagin (PNG, ellagitannin).

3. The importance of polyphenols in food

3.1. Sensorial aspects

Phenolic compounds play an important role on the organoleptic characteristics of plant-based foods and beverages, namely in colour, flavor (astringency and bitterness), odor and oxidative stability [2].

As it was mentioned previously, anthocyanins are the main pigments of flowers and fruits and, depending on their structures, they can display various colours such as yellow, blue, red, orange and violet. The interest in dye substitution has increased natural dyes, using for example anthocyanins as red and violet foods. In certain foods, such as red wine, anthocyanins undergo structural changes during ageing affecting their properties. For instance, these changes can lead to the formation of compounds with different chromatic characteristics and, consequently, changing the wine colour [42, 43].

In some beverages like beer, fruit juices and wines, it is possible to observe some turbidity being the formation of protein-polyphenol aggregates one of the main causes of this phenomenon. This turbidity occurs over packaged products and may lead to rejection by the consumer. There are treatments that can be applied to these beverages (adsorption, ultrafiltration, collagens) in order to decrease the content of reactive polyphenols for a period than the expiry date of the product [44].

The sensorial aspect more relevant for this work is about taste, and particularly about astringency sensation which will be discussed on section 5.3.

3.2. Impact on food consumption

As it was referred previously, polyphenolic compounds are present in several plant-based products (Table 1) [2, 4]. They are not evenly distributed in plant tissues, and food fractionation during processing may result in a loss or enrichment of some phenolic compounds [45]. According to the diet, a person can eat daily from 100 mg to several grams of polyphenols, depending on the amount of fruits and vegetables ingested [46]. It is estimated that the total amount of polyphenols ingested every day is about 1/3 of phenolic acids and 2/3 of flavonoids according to the habits and food preferences [45, 47].

Table 1 - Polyphenol's content of several plant-based products (Adapted from Scalbert and Williamson, 2000 and Macheix *et al.*, 2005).

Product	Polyphenol's content (mg)
Orange juice (100 mL)	22 to 75
Red wine (125 mL)	100 to 225
Black tea (200 mL)	138 to 200
Dark chocolate (20 g)	100 to 200
Apple (unit – 150 g)	3 to 300
Peach (unit – 150 g)	15 to 200

In most cases, food presents a mixture of polyphenols which are still poorly characterized. The studies available about polyphenolic composition are focused only on monomers and oligomeric structures due to the absence of efficient techniques of separation of more complex structures. In this way, polymers have been neglected (although they are the major polyphenols of the plants) and the existing data only reflects a reduced information about polyphenol's food composition. However, although these limitations, it is important to note the work developed by Gu and colleagues [48] who determined the concentration and DP of condensed tannins from several products usually present in the human diet.

3.3. Impact on human health

Over the years polyphenols have been the subject of numerous epidemiological studies, having been assigned several benefic biological properties such as antimutagenic action [49], anticarcinogen [21], antioxidant [21, 50, 51], antiallergenic [52] and antibacterial [53, 54]. Indeed, polyphenols are the most abundant natural antioxidants in our diet and they are able to neutralize the reactive oxygen species (ROS) as a result of lipid peroxidation, preventing some cancers and diseases resulting from oxidative stress such as cardiovascular diseases, Alzheimer and Parkinson [3, 55-57].

The association of the Mediterranean diet with a low incidence of cardiovascular diseases is known and supported by several epidemiological studies. This diet is characterized by the low consumption of fat saturated-rich food and high caloric density, and for the high consumption of complex carbohydrates, fibers, vitamins, minerals and antioxidants, in particular, polyphenol-rich foods. In this kind of diet predominates cereals

and their derivatives as well as vegetables, fruits, and olive oil. The French Paradox is the first classic example of this association. According to this, drinking red wine has been correlated with the relatively low incidence of coronary disease in French population despite a high fat diet and tobacco habits [58].

However, to exert any biological effect, dietary polyphenols have to be available to some extent in the target tissues. This feature critically depends on their metabolism and absorption in the gut and of their final bioavailability. Indeed, phenolic compounds that are usually common in the human diet are not necessarily the most active within the body, either because they have a lower intrinsic activity or because they are poorly absorbed from the gastrointestinal tract, highly metabolized, or rapidly eliminated [4, 37].

Most of bioavailability studies about polyphenols is concerned on anthocyanins, and the absorption of some of these occurs at the small intestine but it can also occur at gastric level [59]. It has been accepted that absorption of anthocyanins occurs in the form of aglycones, after glycoside hydrolysis (Figure 12). Prior to passage into the blood stream, the polyphenols, that now are simple aglycones, undergo to other structural modifications due to the conjugation process that takes place in the small intestine and, mostly, in the liver. Although the process of conjugation on one hand produces active metabolites from some dietary polyphenols, on the other hand it reduces the total amount of polyphenols in the blood stream, increasing their excretion [13, 15]. Therefore, it is clear that the polyphenols are extensively modified, not only in the small intestine and in the colon as it has been discussed above, but also in the liver, where most of the conjugation takes place. Therefore, any single polyphenol generates several metabolites, as many as 20 in the case of quercetin glycosides, although two or three usually dominate [60]. All these modifications deeply affect the biological activity of polyphenols. Consequently, the compounds that reach cells and tissues are chemically, biologically and, in many instances, functionally different from the original dietary form.

Using both human and animal models, the absorption, bioavailability and metabolism of monomeric phenols have been widely studied [61, 62]. Nevertheless, there is few information about the bioavailability of polymeric tannins with the obtained results being controversial. Being quite unlikely that high-molecular-weight tannins are absorbed intact, it is supposed that the DP as well as the solubility of food tannins may have a major impact on their fate in the body. Therefore, highly polymerized tannins typically exhibit low bioaccessibility in the small intestine and low fermentability by colonic microflora [37, 63].

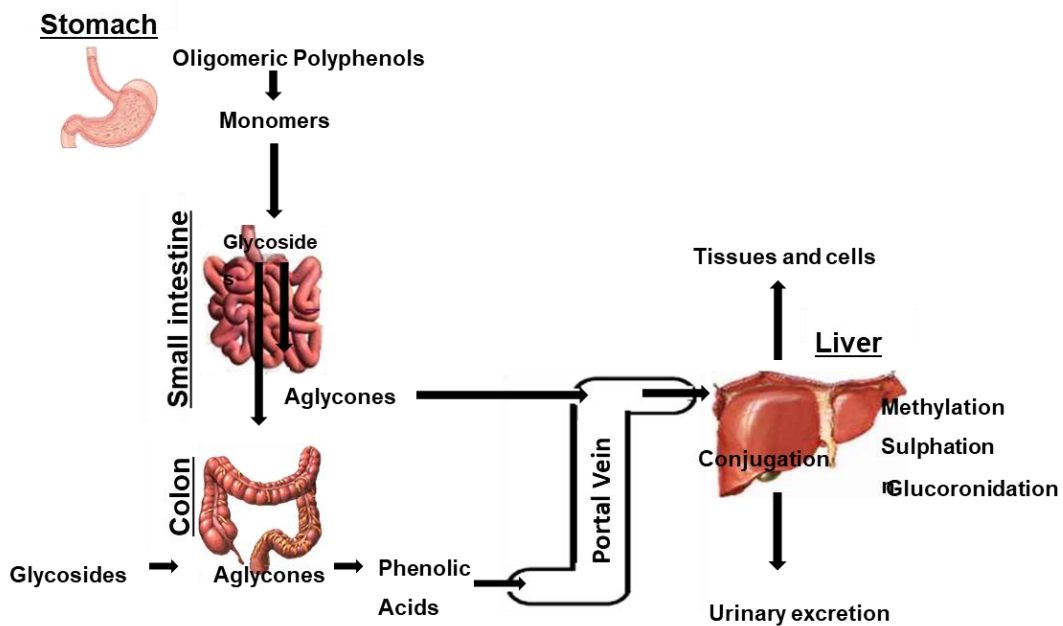


Figure 12 - The absorption of dietary polyphenols in humans is schematically illustrated. The polyphenols are extensively modified during the absorption: the glycosides could be hydrolyzed in the small intestine or in the colon, and the released aglycones could be absorbed. Prior to the passage into the blood stream, the polyphenols undergo to other structural modifications due to the conjugation process, mainly in the liver. Adapted from Vissioli, F. et al. (2011).

4. Saliva

Saliva is a body fluid with very relevant biological functions. Due to its lubricating capacity as well as antibacterial and buffering properties, saliva contributes to the maintenance of the integrity of the oral cavity [64, 65]. Furthermore, saliva also works as the first step of digestion as the result of the presence of some digestive enzymes such as α -amylase and lipase. Saliva is also very important in terms of flavor, particularly for taste and mouthfeel perception [64, 66].

In general, saliva consists in a complex mixture of proteins, electrolytes and small organic compounds. Saliva is predominantly composed by water (99%), but also composed of an organic and inorganic fraction. The first fraction includes a large number of compounds such as urea, ammonia, uric acid, glucose, cholesterol, fatty acids, mono-, di- and triglycerides, neutral and phosphorylated lipids, glycolipids, amino acids, steroid hormones and proteins, while the second one comprises numerous ions (Na^+ , Cl^- , Ca^{2+} , K^+ , HCO_3^- , H_2PO_4^- , F^- , I^- , Mg^{2+} and SCN^-) [67]. The normal pH of saliva varies between 6 and 7, however, this value can oscillate under different conditions such as the ingestion of food or beverages [65].

Whole saliva represents a mixture of the secretions of the major (submandibular, sublingual and parotid) and minor salivary glands, together with the crevicular fluid, bacteria and cellular debris (Figure 13). Saliva secretion is controlled by the autonomic nervous system via signal transduction systems that couple receptor stimulation to ion transport and protein secretory mechanisms [67].

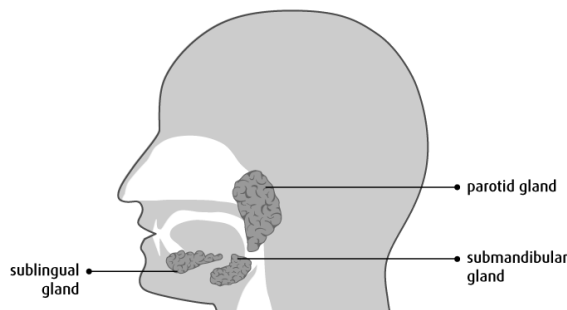


Figure 13 - Representative scheme of the location of the major salivary glands.

In general, saliva can be divided into stimulated and unstimulated. The saliva secreted at rest is often called unstimulated secretion, while saliva secreted in response to a strong stimulus is designated stimulated saliva. It has been reported that the contribution of the different salivary glands to whole saliva in resting and stimulated conditions is different [68]. The major contributor to unstimulated saliva is the submandibular gland, whereas parotid contribution increases dramatically during stimulation, producing a fluid with high PRPs concentration to protect against extrinsic agents [68-70]. For instance, in resting conditions (unstimulated saliva) the relative contributions of the major salivary glands generally correspond to 69% of submandibular, 26% of parotid and 5% of sublingual [66]. There are three types of triggers, or stimuli, for saliva production: mechanical (the act of chewing), gustatory (with acid the most stimulating trigger and sweet the least stimulating) and olfactory (a surprisingly poor stimulus) [65, 71].

It is estimated that in healthy humans, the daily production of whole saliva normally ranges from 500 to 1500 mL [72]. However, this value can vary considerably, since there is great individual variability in the salivary flow rate. On average, the flow rate of unstimulated saliva is $0.3 \text{ mL} \cdot \text{min}^{-1}$; for stimulated saliva, this value can reach a maximum of $7 \text{ mL} \cdot \text{min}^{-1}$ [65, 66].

The secretions from the different glands have been shown to differ considerably and to be affected by circadian rhythms, diet, age, gender, several disease states and pharmacological agents and different forms of stimulation [67, 73-75]. Circadian rhythms

are endogenous self-sustained oscillations with 24-hour periods that regulate diverse physiological and metabolic processes through complex gene regulation by “clock” transcription factors [76]. Fluctuations of several salivary variables throughout the day are influenced by these rhythms, namely flow rate, concentrations of total protein, various electrolytes and specific SP and peptides [74, 75]. For instance, it was reported elsewhere that saliva protein concentration follows a diurnal pattern that is higher in the afternoon than in the morning [70, 75, 77].

4.1. Salivary proteins (SP)

Saliva is a complex mixture rich in different SP and peptides. More than 2000 proteins and peptides were already identified in human saliva [24].

A common aspect of the major SP and peptides is the presence of genetic polymorphisms being the origin of the various families of SP which are related by function and structure. Many SP occur as families of isoforms, and it is characteristic that these isoforms may have more than one function. Moreover, the same function may be shared by different families of proteins, resulting in considerable functional redundancy. For instance, these general characteristics are well-represented by two families of SP, PRPs and histatins, which, among other activities, share the ability to precipitate tannins readily [24].

The protein composition of saliva has been of interest in recent years, and the knowledge of the salivary proteome has increased greatly, particularly in the last decade by the development of new and potent proteomics techniques. This technological advance allowed the identification of different classes of proteins and peptides, many of them specific of the oral cavity. They belong to the following major families: α -amylases, histatins, mucins, PRPs, further divided into acidic, basic, and basic glycosylated PRPs, statherin, P–B peptide, and salivary-type (S-type) cystatins (Figure 14)

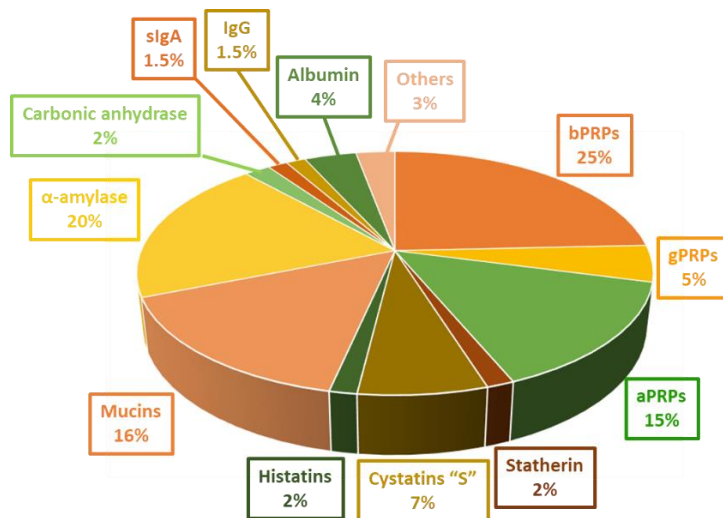


Figure 14 - Approximate percentages of the major classes of SP and peptides found in saliva. aPRPs, acidic PRPs; bPRPs, basic PRPs; gPRPs, glycosylated PRPs; IgG, immunoglobulin G; sIgA, secretory immunoglobulin A. Adapted from Messana, I. et al. (2008).

The function, origin, and encoding genes of the major SP are reported in Table 2, together with the name of mature proteins and the main post-translational modifications (PTMs) occurring before, during, and after secretion.

The most relevant SP families for this work will be presented in the following sections.

Table 2 - Families of major SP: function, origin, genes, name of mature proteins, and main post-translational modifications (PTMs).

Family	Function	Origin	Gene	Mature Proteins	Other PTMs
α -amylase	Antibacterial, digestion, tissue coating	Pr Sm/S1	AMY1A	α -Amylase 1	Disulfide bond, N-glycosylation, phosphorylation, proteolytic cleavages
Basic PRPs	Binding of tannins, tissue coating	Pr	PRB1, PRB2,	II-1, II-2, CD-IIg, IB-1, IB-6, IB-7, IB-8a (Con1- /+), P-D,	Disulfide bond (G1 8), further proteolytic cleavages, N- and
Glycosylated PRPs	Antiviral, lubrication		PRB3, PRB4	P-E, P-F, P-J, P- H, PRP GI 1-8, protein N1, salivary PRP Po	O-glycosylation, phosphorylation, protein network
Acidic PRPs	Lubrication, mineralization, tissue coating	Pr Sm/S1	PRH1, PRH2	Db-s, Pa, PIF-s, Pa 2-mer, Db-f, PIF-f, PRP-1, PRP- 2, PRP-3, PRP-4, P-C peptide	Disulfide bond, further proteolytic cleavages, phosphorylation, protein network
Cystatins	Antibacterial, antiviral, mineralization, tissue coating	Pr Sm/S1	CST1, CST2, CST3, CST4, CST5	Cystatin SN, cystatin SA, cystatin C, cystatin S, cystatin D	Disulfide bond, O-glycosylation, phosphorylation, sulfoxide, truncated forms
Histatins	Antifungal, antibacterial, mineralization, wound-healing	Pr Sm/S1	HTN1, HTN3	Histatin 1, histatin 2, histatin 3, histatin 5, histatin 6	Further proteolytic cleavages, phosphorylation, sulfation
Mucins	Antibacterial, antiviral, digestion, lubrication, tissue coating	All Salivary Glands	MUC5B, MUC19, MUC7	Mucin-5B, mucin- 19, mucin-7	Disulfide bond, N- and O- glycosylation, phosphorylation

Statherin	Inhibits crystal formation, lubrication, mineralization, tissue coating	Pr Sm/S1	STATH	Statherin, statherin SV2	Phosphorylation, proteolytic cleavages, protein network
P-B peptide	Not defined	Pr Sm/S1	SMR3B (PROL3)	Proline-rich peptide P-B	Proteolytic cleavages

Modified from Ekström, J. et al. (2012)

PRP-proline-rich protein; Pr-parotid; Sm-submandibular; S1-sublingual; GCF-gingival crevicular fluid

4.1.1. Proline-rich proteins (PRPs)

A large part of the human salivary secretions of the parotid and submandibular glands are composed of a family of proteins that have the ability to bind tannins - PRPs. These SP family is one of the most abundant in saliva contributing to almost two-thirds to the salivary proteome [68].

Approximately 25 to 42% of the amino acid residues of PRPs are proline. In addition to this residue, these proteins also have a high content in glutamine and glycine. Together, these three amino acid residues correspond to about 70 to 88% of the total residues of these proteins [78]. PRPs are highly polymorphic in their primary amino acid sequence, size and PTMs, which could be related with their functional diversity [68].

These proteins have been considered a class of intrinsically unstructured proteins, which are characterized by the absence of a tertiary structure. These proteins remain functional despite the absence of a well-defined structure [79]. It has been widely assumed that the high level of proline residues in PRPs is only important because it contributes to open and flexible structures in these proteins causing a higher capacity for complexation.

In humans, PRPs are expressed constitutively and each person expresses a number of different PRPs that vary in size and sequence. Indeed, considerable phenotypic variations of PRPs in different populations have already been documented [80].

Generally, salivary PRPs are classified into two major groups: acidic PRPs (aPRPs) and the basic ones (bPRPs). In addition, bPRPs are typically divided into glycosylated PRPs (gPRPs) and non-glycosylated PRPs. At the end this is also reflected in functional differences between the several classes.

In general, the PRPs family is encoded by six genes: two genes encode the aPRPs and four genes encode the bPRPs and the gPRPs. The genes that coding for these proteins are highly polymorphic, since only six genes allow to obtain a high number of PRPs [64, 81].

4.1.1.1. Basic (bPRPs) and glycosylated proline-rich proteins (gPRPs)

The bPRPs and gPRPs are the most complex groups of PRPs that are expressed by four different genes (PRB1-PRB4) that are grouped in the chromosome 12p13.2. The PRB1 and PRB2 genes originate non-glycosylated bPRPs and the PRB3 and PRB4 genes generate glycosylated bPRPs [82].

Unlike aPRPs, which are contemporaneously present in saliva as complete or truncated isoforms, all bPRPs are detected only in the form of multiple peptide fragments originating from larger proteins [83]. These peptides have very similar sequences and displaying repetitive patterns, in which some sequences of amino acids can be found several times in the same protein and in different proteins. However, is still missing to characterize more proteins or to deeply characterize some of them.

The bPRPs are composed of residues that are not charged at basic or neutral pH. Thus, its isoelectric point (pI) ($pI > 9$) is much higher than for the aPRPs. Although its function it is still not completely understood there are evidences that they can have protective function. Mehansho and his colleagues (1987) proposed that one of their functions would be to bind tannins, thereby preventing its toxic effects on the gastrointestinal tract [84]. Other authors have discovered that these proteins bind to viruses, particularly to HIV-1 protein, having an anti-viral action [85].

Regarding gPRPs, this class of proteins is characterized by the presence of glycosides in its structure. Recently, began to emerge the first studies about the sugar type and the position of glycosylation of these proteins [86]. In fact, this information is fundamental in the analysis of these proteins by Mass Spectrometry (MS), since only knowing its global structure is it possible to know its molecular weight.

The main functions assigned to gPRPs, together with mucins, is lubrication. In fact, gPRPs have a higher lubricant activity in comparison with the non-glycosylated forms [87]. However, this property is affected by the type of sugar as well as by the extension of glycosylation [88]. Typically, glycosylation of PRPs occurs by binding of sugars to the amino acid residues asparagine, threonine and serine, which allows to anticipate the

potential glycosylation sites [87, 89]. In addition to this function, it is also described that these proteins bind to bacteria from the oral cavity [90].

4.1.1.2. Acidic proline-rich proteins (aPRPs)

The aPRPs are encoded by the PRH1-2 genes (near the PRB1-4 genes) that are on the chromosome 12p13.2 and its expression results in proteins that have two distinct structural domains. The C-terminal region is structurally equivalent to bPRPs and comprises about 70-80% of the molecule. On the other hand, the N-terminal region contain strongly acidic residues (aspartic and glutamic acids) and few proline residues. The existence of this acidic region is responsible by its low pI (4-5). Moreover, at the structural level they may have some phosphate groups (Ser 8, 17 and 22) [91].

In human saliva 5 isoforms of aPRPs were identified. PRH1 produces aPRPs Db-s, PIF-s and Pa while PRH2 encodes for PRP1 and PRP2. All of them have a pyroglutamic N-terminal and are usually di-phosphorylated in Ser-7 and Ser-22, although smaller amounts of mono- and non-phosphorylated aPRPs were detected. Smaller percentages of tri-phosphorylated isoforms (Ser-17) were also found [68]. There are minor structural differences among the aPRPs and their predominant role is related to mineral homeostasis and tooth integrity preservation. Indeed, aPRPs have a high affinity for hydroxyapatite and are effective inhibitors of calcium phosphate crystal growth, participating in the formation of dental protein structure which protects the surface of the teeth (enamel). The activity and binding sites associated with maintenance of calcium levels is confined to the N-terminal acidic region of these proteins, since are negatively charged and have two phosphoserines which are fundamental for these properties and for mineral homeostasis [92-95].

4.1.2. Statherin

Statherin is a small salivary peptide of 43 amino acid residues, which is phosphorylated on Ser-2 and Ser-3 and it is very specific and multifunctional. This acidic peptide is secreted by several salivary glands and it has an unusual high content in tyrosine residues, proline and glutamine [96]. Its gene (STATH) is located on chromosome 4q13.3 [97].

This peptide contributes mainly to the balance of minerals on the surface of teeth. In fact, it has a high affinity for calcium, inhibiting its precipitation of supersaturated solutions

[96]. Thus, statherin maintains the supersaturation of human saliva in calcium, inhibiting the deposit of minerals on the surface of the teeth and contributing together with other SP, for the stabilization of the enamel [98]. In addition, statherin contributes to bacterial colonization and acts as a lubricant [99] [100]. The N-terminal region of the statherin is very negative, and the domain is responsible for the binding to calcium salts, but the level of phosphorylation of the protein is also crucial to this function [101].

4.1.3. P-B peptide

Although the P-B peptide is often included in the family of bPRPs because of its high proline content (almost 50% of its all sequence), it has more similarities with statherin [102]. Statherin and P-B peptide share some consensus sequences which means that they have a sequence of amino acids similar or identical between regions of homology in their protein sequence. Furthermore, P-B peptide is a product of PROL3 gene (PBI) clustered on chromosome 4q13.3 which is very close to the statherin gene and several characteristics of P-B peptide suggest a functional relationship with statherin [83, 103].

This peptide is also a mature protein and it is not a product resulting from the degradation of large proteins. It contains some hydrophobic amino acid residues such as phenylalanine, leucine and isoleucine residues, which could explain its low polarity. While the statherin role on modulation of oral calcium ion is recognized, no specific function of P-B peptide has been proposed to date [83].

4.1.4. Cystatins

Salivary cystatins are structured proteins comprising cystatin S, SN and SA which belong to family 2 of cystatins. The genes for all cystatins S are clustered on chromosome 20p11.21 and are named CST1-5. Cystatin S may be phosphorylated on Ser-3 (cystatin S1) or di-phosphorylated on Ser-1 and Ser-3 (cystatin S2). While cystatin SA seems to be specifically expressed in the oral cavity, cystatin S and SN have been detected also in other body fluids and organs [83].

Cystatins are inhibitors of cysteine proteinases and this property suggests its role in the protection of the oral cavity from pathogens and in the control of lysosomal cathepsins [83].

4.1.5. Mucins

Some of the more abundant proteins in saliva include mucins MUC5B and MUC7 that are produced by submandibular and sublingual glands [66]. These proteins are characterized as large, abundant and filamentous glycoproteins that are present at the interface between many epithelia and their extracellular environments. Both membrane bound mucins, and secreted mucins share many common features. They are both highly glycosylated consisting of 80% carbohydrates primarily N-acetylgalactosamine, N-acetylglucosamine, fucose, galactose, and sialic acid (N-acetylneuraminic acid) and traces of mannose and sulfate [104]. Their molecular weights range from 500 to 20000 kDa and it was reported that MUC5B, the highest molecular weight mucin, is composed of multiple highly glycosylated covalently linked subunits [66]. On the other hand, MUC7 has a lower molecular weight and is a single glycosylated peptide chain [104]. Mucin has been difficult to characterize, owing to its large molecular weight, polydispersity and high degree of glycosylation [104].

Mucins have received special attention in the recent years due to their biological properties and characteristics. Mucins can form a viscoelastic network that is important for hydration, pathogen exclusion, resistance to proteolytic digestion and lubrication of the oral cavity [105].

4.1.6. Histatins

Histatins are histidine-rich proteins with low molecular weight. Indeed, histidine constitutes about 18-29% of these proteins, which is unusual because histidine is, along with proline, one of the rarest amino acids to find in human biological proteins. To date, two genes responsible for the synthesis of histatins, HTN1 (HIS1) and HTN2 (HIS2), were identified and they are in the chromosome 4q13. It was already identified in saliva 12 histatins, among which, HRP1, 3 and 5 are the most abundant [106].

These proteins are considered as the main precursors of enamel. In addition, histatins have antibacterial and antifungal activity. Histatin 5 is especially effective against *C. albicans* and is also an inhibitor of metalloproteinases (MMP2 and MMP9) [106-108].

5. Protein-tannin interactions

One of the most important characteristics of tannins, as it was referred previously, is their ability to interact and precipitate proteins. This property has been extensively studied because is at the origin of several activities associated with these compounds, particularly with their biological and organoleptic activities, whether positive or negative. Due to its relevance, this ability has been the main aim of study of several research groups [6].

In the literature it was already reported the influence of many structural and environmental factors on the interaction between polyphenols and proteins such as their structures and molar ratio, concentrations, pH, ionic strength (IS) and temperature [6].

5.1. Bonds Involved

Initially, in the beginning of the last century, protein precipitation by tannins was described as a mutual colloidal electrolyte interaction between the positively charged collagen of skins and negatively charged tannin particles [6]. However, this physicochemical model was quickly replaced by a more consistent and realistic model. In fact, the interest in studying the molecular mechanisms (structure-activity relationships) involved in those interactions, and especially in foodstuffs and beverage astringency, has been increasing.

The polyphenolic nucleous has a molecular structure which favors the interactions with proteins, presenting two kinds of regions:

- Hydrophobic regions (apolar) due to the presence of benzenic ring which can interact with hydrophobic regions of proteins such as side chains of the amino acid residues alanine, leucine, isoleucine, proline, among others;
- Hydrophilic regions, such as hydroxyl groups, which can establish bonds with the carbonyl and amine groups of the proteins.

Based on many prominent research works, as well as a result of the large improvement of analytical techniques, tannins are now described to establish cross-links with proteins by different kinds of interaction or bonds (Figure 15) [6, 109-111]:

1. Hydrogen bonds between the hydroxyl groups of phenolic compounds and the carbonyl and –NH₂ groups of proteins;

2. Van der Waals interactions strengthened by the hydrophobic effect between the benzenic rings of phenolic compounds and the apolar amino acid side chains;
3. Ionic bonds between the phenolate anions and cationic sites of proteins;
4. Covalent bonds resulting from the reaction between the nucleophilic groups of proteins such as $-\text{NH}_2$ and $-\text{SH}$ and, on one side, quinone groups resulting from phenolic oxidation or, on the other side, carbocations resulting from acid-catalysed condensed tannins depolymerization.

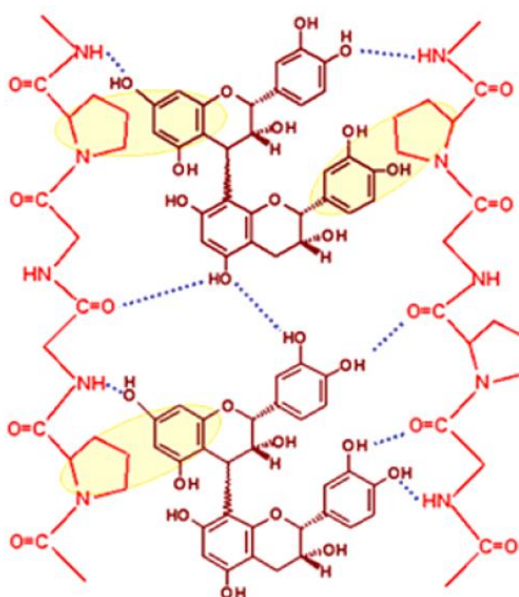


Figure 15 - Scheme of the interaction between condensed tannins and proteins: main driving forces, hydrophobic interactions (yellow circles) and hydrogen bonds (blue dotted line) between phenolic rings (cross-linkers) of tannins and the amide groups and apolar side chains of amino acids such as proline. Adapted from Santos-Buelga, C. et al. (2008).

Although the tannin structure allows the existence of different kinds of bonds, hydrophobic interactions [112, 113] and hydrogen bonds [114] have been described as the main driving forces involved on protein-tannin interactions. The possibility of ionic binding has been excluded at acidic and neutral pH because of the absence of charged groups at pH considerably below the pKa values of the phenolic groups (~9-10) [115].

Several authors observed the existence of hydrophobic interactions on protein-tannin complexes, particularly PRPs or other similar peptides, being hydrogen bonds also pointed out to be important on this interaction [116, 117].

In fact, some studies suggest that protein-tannin interactions are firstly governed by hydrophobic interactions and then, the complexes are stabilized by hydrogen bonds.

Indeed, hydrogen bonds are forces relatively weak individually, but together with other forces they are important for the stabilization of the tannin-protein complexes. [112, 118]. However, it is generally assumed that the polarity of the tannins used to interact with proteins can be significant for the type of bonds involved. For instance, more apolar compounds favor hydrophobic interactions, while more polar are important for hydrogen bonds [119].

5.2. Molecular models for protein-tannin interactions

Over the years several molecular models have emerged to describe protein-tannin interactions [120-122]. Several studies about the interaction between some proteins, such as bovine serum albumin (BSA), and tannins, suggested that tannins can act as multidentate ligands, that is, different phenolic rings of the same tannin can interact with protein. This allows tannins to establish cross-links between two or more protein molecules or to bind to more than one point of the same peptide chain of a protein [121, 123]. This way, it seems that stoichiometry and the size of the complexes are dependent on the relative concentrations of each species, which in turn, is dependent on protein/polyphenol ratios.

Hagerman and Robbins (1987) observed that the addition of increasing amounts of BSA to a fixed amount of tannin, would lead to an optimal protein/tannin ratio for which a maximum precipitation occurred (stoichiometric concentration). For higher or lower tannin/protein ratios, the amount of insoluble complexes would decrease [123].

Later, with the purpose to describe the turbidity process of beer, Siebert and colleagues proposed a molecular model to explain the previous observations [121] which is schematized in Figure 16.

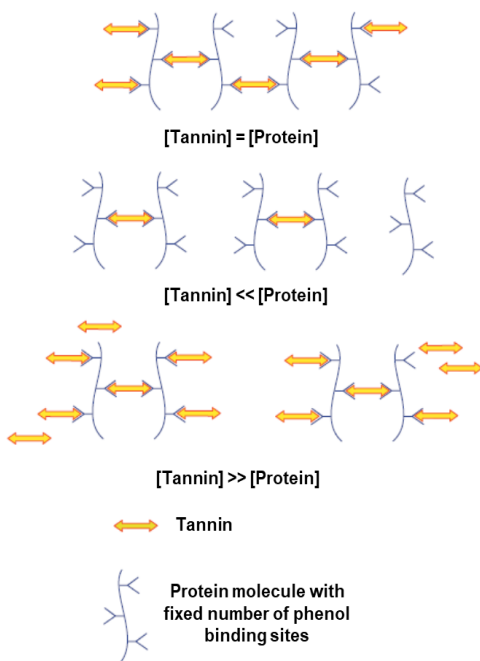


Figure 16 - Conceptual mechanism for protein-tannin interaction. Tannins are displayed as having two ends that can bind to protein. Proteins are displayed as having a fixed number of tannin binding sites. Adapted from Siebert, K. J. et al. (1996).

Considering that each molecule of tannin and protein have a fixed number of binding sites, what happens is that when the number of tannin binding sites is the same that the number of binding sites of the protein, there is the formation of bigger aggregates and a maximum of turbidity (plateau) (Figure 17). If there is an excess of protein relatively to tannin, each tannin will be able to establish bonds between two molecules of protein, but these proteins are unlikely to form more bonds with other proteins. This will result mainly in aggregates with two protein molecules. On the other hand, with an excess of tannin, all binding sites of the protein will be occupied, but the probability of forming bonds will be low because each free end of tannin will have little chance to find a binding site of a free protein. This will result in smaller aggregates.

Thus, in most cases, the aggregation is hyperbolically related to both protein and tannin concentration (Figure 17). The type of tannin-protein aggregates formed depends on their concentrations. At stoichiometric concentrations (plateau), tannins can act as multidentate ligands, establishing bonds between proteins or tannin-protein complexes, corresponding to a maximum aggregation forming large aggregates. For lower or higher tannin-protein ratios, smaller aggregates would be formed.

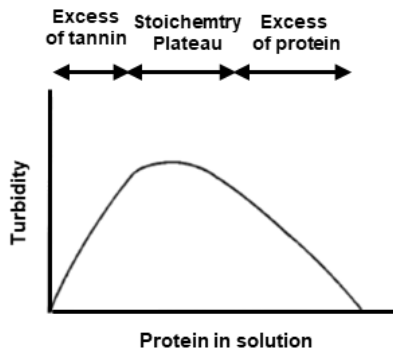


Figure 17 - Molecular mechanism proposed for the interaction between tannins and proteins. This represent a nephelometry curve for a fixed concentration of tannin and increasing concentrations of protein. Adapted from Hagerman, A. et al. (1987).

However, it seems that this model may not be applied to all proteins. For example, in the case of PRPs the behavior seems to be different. The addition of increasing amounts of a salivary PRP to a fixed amount of tannin led to the formation of insoluble protein-tannin complexes, which remained insoluble independently of the amount of protein added. In this way, an alternative molecular model for the interaction between tannins and PRPs was proposed (Figure 18).

The general principles of this mechanism are similar to the ones described in the other mechanism. The association of tannins with proteins is mainly a surface phenomenon. In a first stage and at low tannin concentration, the tannin associates onto the protein surface and generally several tannin molecules bind simultaneously and tightly to the same protein. This causes the protein, which originally exists in a loose randomly coiled conformation, to 'wrap' around the polyphenols hence experiencing a compaction of its structure. At the second stage tannin starts to cross-link different proteins leading to the recruitment of a second tannin-coated protein, which renders the complex insoluble, forming a colloidal solution. At the third and final stage, further cross-linking causes the aggregates growth and finally leading to precipitation [122, 124].

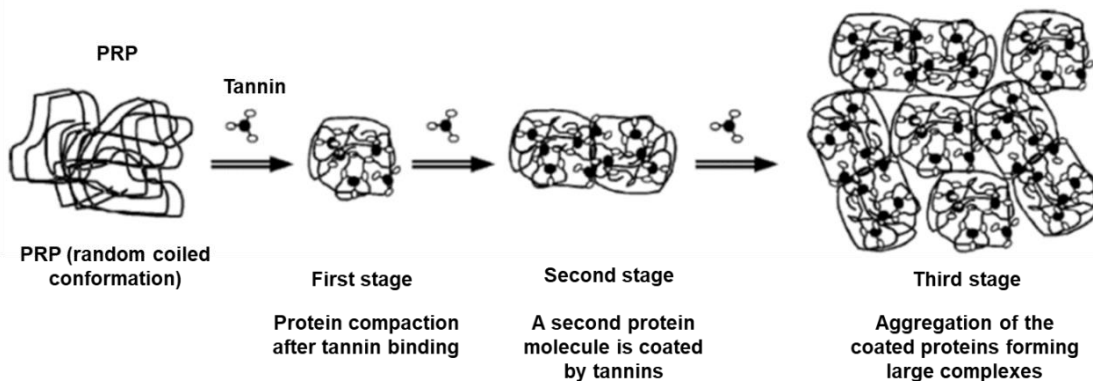


Figure 18 - Molecular mechanism proposed for the interaction between PRPs and tannins. In the initial stage (first stage) proteins are compacted, due to multiple bonds with multidentate tannins. In the second stage a dimer is formed with another protein coated with tannins, rendering the complex insoluble. In the third stage, complexation and complex precipitation occurs. Adapted from Jobstl, E. et al. (2004).

5.3. Astringency

The ingestion of polyphenol-rich foods and beverages is associated with a tactile sensation of dryness and roughness (lack of lubrication which causes friction in the oral cavity) and constriction (the sensation of tightness and contraction of the tissues felt in the mouth, lips and inner cheeks) perceived throughout the oral cavity called astringency [125-127]. Products such as wine, fruits, chocolate, tea and beer are rich in tannins that contribute to astringency sensation [127].

Astringency is often perceived as a negative attribute of these products, which sometimes leads to consumer rejection. Indeed, the astringency and bitterness of many vegetables and fruits containing phytonutrients are often cited as the reason for consumers rejecting the plant products, despite their known health benefits [126]. In the case of fruits, astringency is mainly due to the fact that they are not sufficiently ripe. However, there is like an adaptation of the consumer to astringency, eventually becoming accustomed to some products with this sensorial characteristic [47]. For instance, for red wine, one of the most consumed beverages worldwide, a balanced level of astringency is desirable for its quality [126].

In contrast to taste, astringency takes some time to develop and it seems to become more pronounced with continued exposure to these compounds (e.g. during several sips of wine) causing a cumulative effect (Figure 19) [126].

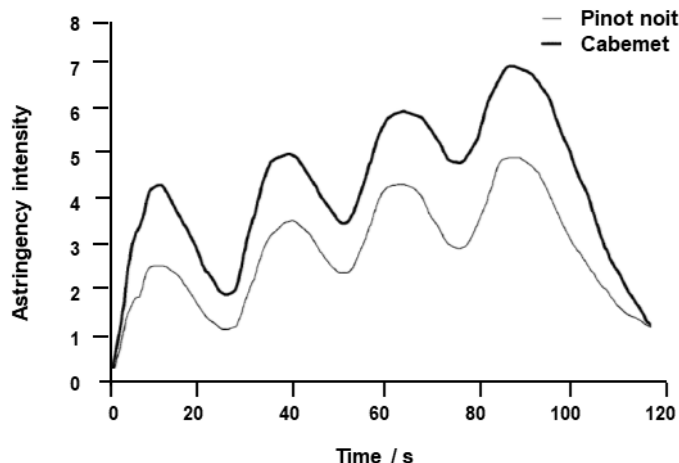


Figure 19 - Average time-intensity curves for astringency of red wines (10 mL wine sipped at 25-s intervals). Adapted from Lesschaeve, I. et al. (2005).

5.3.1. Mechanisms of astringency

Presently, the possible mechanisms for astringency development are controversially discussed by the scientific community with several mechanisms being proposed. The most established mechanism for astringency involves the interaction between tannins and proteins resulting in the formation of aggregates that will precipitate [127, 128].

However, other mechanisms have been proposed to explain astringency sensation. As astringency is considered to be a tactile sensation, some authors point that it could result from altered salivary lubrication [129, 130]. Nevertheless, Lee and Vickers (2012) [131] had provided evidences that the loss of salivary lubricity is not likely to be a central mechanism of astringency. Other authors suggest that astringency could be detected by increased activation of receptors located within the mucosa, like other primary tastes such as bitterness. However, astringency increases upon repeated exposure [132], in contrast to taste sensations, suggesting that it involves mechanical rather than chemosensory processes [133]. Moreover, astringency perception occurs on nongustatory mucosal surfaces and requires tissue movement to be perceived, in agreement with a tactile mechanism involving an increase of mouth friction. Another hypothesis suggest that astringency could be related to interactions between tannins and oral epithelial cells [134, 135]. In the past years, several research groups studied the molecular basis of astringency development using model bioassays with pure/isolated proteins, namely PRPs and tannins. However, there are some difficulties in correlating the perceived astringency to a single physical–chemical phenomenon.

5.4. Factors that influence protein-tannin interactions

Additionally, to the protein/polyphenol concentrations, these interactions seem to be affected by other factors. In that way, several structural and environmental variables known to drive these interactions have been extensively assayed and are still being presently studied by some research groups. Concerning the influence of the protein, the interaction can be affected by its size [147, 160], charge [147], presence and type of side chains [161, 162] and conformation [163]. In general, it has been found that proteins which are readily precipitated by tannins are large, have a high proline content, and lack of secondary or tertiary structure, although some of them may possess a polyproline helix [164]. For complexation to occur, both tannin and protein must have the appropriate steric structure and molecular weight.

5.4.1. Tannin structure

There are many works reported in the literature that have highlighted the strong influence of the tannin structure (hydroxylation degree, size, conformation, flexibility, type of interflavanic bond and others) on their interaction with proteins [136-139].

Overall, the affinity of tannins for proteins increases with the molecular weight (or DP) and the degree of galloylation apparently because the number of interaction sites increase with size. This behavior seems to be independent of the protein structure. The increase in size increases the apolar character (increase of aromatic rings) favoring the hydrophobic interactions with proteins. On the other hand, the increase of monomeric units allows an increase in the total number of hydroxyl groups involved in hydrogen bonding [140]. For instance, Sarni-Manchado and co-workers [141] studied the interaction between condensed tannins obtained from grape seeds and SP. They analyzed the supernatant and the precipitate resulting from this interaction by SDS-PAGE and acid thiolise. At the end, they observed that high-molecular weight PC (high DP) were selectively precipitated by SP, while dimeric and trimeric PC remained in solution (were not precipitated). However, some more polymerized tannins, despite the high number of binding sites can exhibit a more rigid conformation, presenting that way more restrictions in comparison with more flexible compounds [113, 142].

Concerning stereochemical, de Freitas and Mateus [136] observed that (+)-catechin was more reactive towards PRPs than (-)-epicatechin as well as dimers with C4-C8 interflavanic bonds were more reactive in comparison with the ones with C4-C6 interflavanic bonds. Probably, this is due to conformational constraints imposed by C4-

C6 bonds. As previously referred, more flexible tannins have better ability to bind proteins because they are more efficient cross linkers. Different results were obtained by Ricardo da Silva and co-workers [139] when measuring directly the PC dimers concentrations in a wine model solution of grape seed PC after fining treatment using various proteins. They have concluded that proteins bind more efficiently PC dimers C4-C6 than PC C4-C8. Recently, Nuclear Magnetic Resonance (NMR) determination of the dissociation constants of four C4-C8 PC dimers and a saliva 14 a.a. IB7 fragment has shown that the affinity for IB7 varies as follows: B2, B4 > B1 >> B3 [143]. The authors attributed these differences to the more extended conformation of dimers B2 and B4 that must facilitate the approach and/or fixation of the tannins to the peptide.

The presence of galloyl groups also affects the interaction of tannins with proteins because it induces an increase in tannin sites able to bind to the same protein or different proteins. Indeed, de Freitas and Mateus (2001) [136] observed that the presence of a galloyl group increased the reactivity compared to the non-galloylated counterparts. However, this increase of reactivity was higher in the case of monomers than in the case of dimers. This was explained by the closed structure of PC dimer B2 3'-O-gallate which presents as a result of a possible interaction π - π stacking between the benzenic rings of the galloyl group and catechol.

The effect of the presence of galloyl groups is also visible on hydrolyzable tannins. Kawamoto and colleagues (1995) [138] observed that the affinity of several galloylglucoses for interaction with BSA increases with the extension of the galloylation: monogalloylglucose <di- <tri- <tetra- <penta. In addition to the number of galloyl groups, their position in the hydrolyzable tannins also affects the interaction with proteins. Moreover, the hydrolyzable tannins seem to have a similar affinity as the condensed ones toward SP or, in some interactions, to be more reactive. This affinity may be correlated with their DP or the extension of their galloylation degree as well as by their more apolar character which favors the hydrophobic interactions between tannins and proteins [6, 144, 145].

5.4.2. Protein structure

The binding between proteins and tannins has been described by some authors to occur in a selective and specific manner. Concerning the influence of the protein, the interaction can be affected by its size, charge, presence and type of side chains, and

conformation [6]. For complexation to occur, both tannin and protein must have the appropriate steric structure and molecular weight.

Generally, tightly coiled globular proteins have much lower affinities for tannin than conformationally open and random coiled proteins, probably because of the increased accessibility of the backbone of the latter, which promotes a higher exposition of hydrophobic amino acids [110].

Regarding structure, it is known that protein-tannin interaction is influenced by the primary structure of the proteins, this is, the amino acid residue sequence. Wroblewski and colleagues (2001) [109] verified by NMR that the tannin binding to modified histatins (with the same primary structure, but in which the amino acid residues were arranged randomly in the chain peptide) was significantly decreased. In turn, the tertiary structure (which is related to the primary structure) also influences this interaction. Some proteins with a collagen type helix structure or a random winding and an open conformation showed high affinity for condensed tannins. The probable explanation is due to the high structural flexibility of these proteins, which establish a greater number of linkages with tannins (since the apolar amino acid residues become more accessible to establish hydrophobic bonds with the benzenic rings).

The composition in amino acids is also a factor that influences the interaction with the tannins. It is known that proteins and peptides with high affinity for tannins have a high content of proline residues. This amino acid residue provides specific structural features which represent very important binding sites (hydrophobic interactions and acceptor of hydrogen bonds). More precisely, its rigid planar conformation and its hydrophobic surface allow to establish stacking interactions with other hydrophobic surfaces such as the benzenic rings of phenolic compounds [110, 146]. Furthermore, the presence of proline residues promotes the extension and opening of the polypeptide structure, maximizing the binding surface of the proteins to the tannins [113].

Concerning glycosylation, it seems that PRPs glycosylation affect significantly their ability to aggregate tannins, similarly to what happens with the proline residues, providing a more open conformation and, consequently, a higher interaction [147].

5.4.1. Presence of polysaccharides

Protein-tannin interactions can be influenced by the presence of other compounds, namely polysaccharides. The first conceptions that the presence of polysaccharides

could inhibit this interaction appeared to understand the phenomenon of fruit ripening, which is closely related with the decrease of astringency sensation.

5.4.1.1. Ripening in fruits

During fruit ripening there are several physical-chemical and sensory changes. Two of the main changes are the decrease in astringency sensation and texture change, being fruits softer.

The texture change has been explained based on the enzymatic degradation of the cell wall polysaccharides (pectin, hemicellulose and cellulose) and of storage polysaccharides [148]. In this process pectins are of main importance since they are the main constituents of the cell wall, and practically the only constituents of the middle lamella (Figure 20A). Pectins appear to undergo enzyme-catalyzed depolymerization and deesterification during ripening, and the large insoluble molecules present before ripening are degraded, resulting in small soluble molecules (Figure 20B) [148].

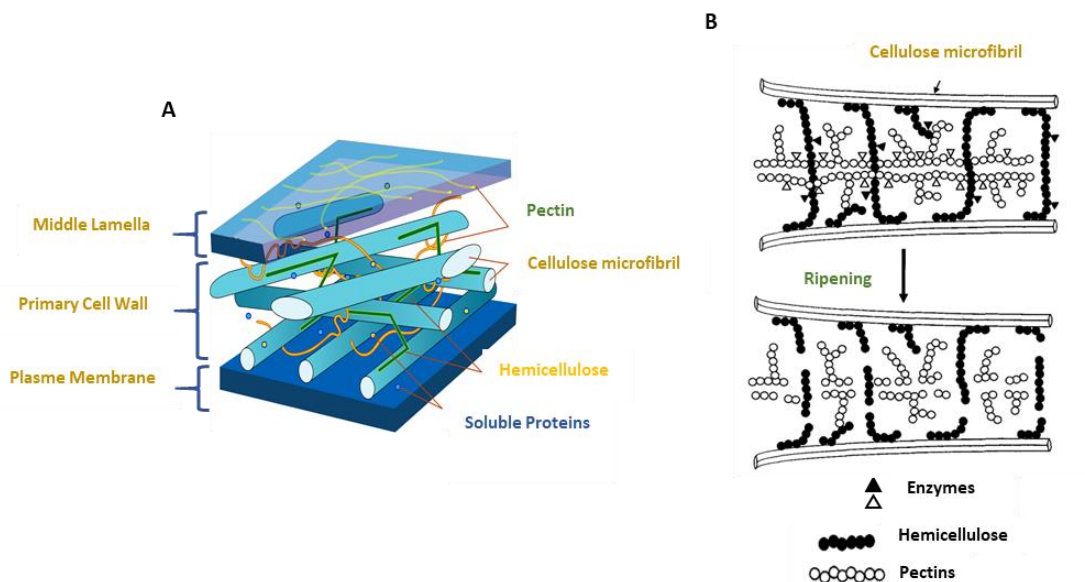


Figure 20 - Schematic representation of (A) primary cell wall structure showing polysaccharides and the (B) degradation of cell wall during fruit ripening. Degradation of these polysaccharides reduces the integrity of cell walls, increasing fruit softening. Adapted from Wakabayashi, K. (2000).

Besides the degradation of polysaccharides, fruit softening is accompanied by the reduction in cell adhesion, as a result of degradation of the middle lamella. Therefore, the degradation of polysaccharides leads to a decrease in the integrity of the cell wall, resulting at the end in the loss of firmness of the fruit tissues.

Concerning the decrease of astringency, two kind of hypotheses were proposed over the years to explain this phenomenon. One of the hypotheses is the modification of the polyphenolic composition throughout ripening, particularly the change of molecular weight/DP of tannins [149]. Some studies correlate the decrease in astringency with the amount of tannins in fruits. According to Goldstein and Swain (1963) [149] only the medium-sized polyphenols were effective in interacting with proteins, because the lower molecular weight ones were very small and those of high molecular weight were not sufficiently soluble or had a very large structure to fit into the matrix of SP. These authors also observed that during fruit ripening fruits there was a decline of these polyphenols [150].

However, although some studies support this theory, in some fruits there is no change in its polyphenolic composition and therefore the decrease of astringency may be explained differently.

Pectin is a very complex family of polysaccharides mostly present in middle lamella and primary cell wall, which exhibits significant heterogeneity both in chemical structure and molecular weight. Pectin is composed of as many as 17 different monosaccharides, organized into several structures that form the pectin constituent polysaccharides: homogalacturonan, xylogalacturonan, rhamnogalacturonan (I and II), arabinan and arabinogalactan (I and II) [151]. Although the structures of each of these constituents are known, it is not known exactly how they are organized in a macromolecular structure. The pectin composition depends on the source from which it was extracted, the extraction conditions and other factors [152].

Structurally, pectins comprise “smooth and hairy regions”. The “smooth regions”, also known as homogalacturonans (HGs), consisting in a long chain of (1→4) linked α-D-galacturonic acid (GalpA). Some of the carboxyl groups can be methyl-esterified and acethyl-esterified, depending on plant species. The linear units of HGs in which more than 50% of the GalpA are esterified with methyl (or methoxy) groups are conventionally called high methyl-esterified HGs; otherwise they are referred as to low methyl-esterified HGs [153]. The level of methylation also influences strongly the physiochemical properties of pectins. As it affects the hydrophobicity of the polymer, the degree of methylation of pectins can also modulate their interaction with other biomacromolecules [154].

The hairy regions, named rhamnogalacturonans (RGs) are of two types (I and II). RG I is formed by the repeating disaccharide →4)-α-D-GalpA-(1→2)-α-L-Rhap-(1→, with the

rhamnose residues of RG fractions being partially esterified by chains composed mainly of arabinose and galactose [155]. RG II, is a minor pectic component and as HGs possesses a backbone of (1→4) linked α -D-Galp with side chains containing rhamnose and a variety of rare monosaccharides [156]. Figure 21 shows a simplified representative scheme of the major pectin constituents.

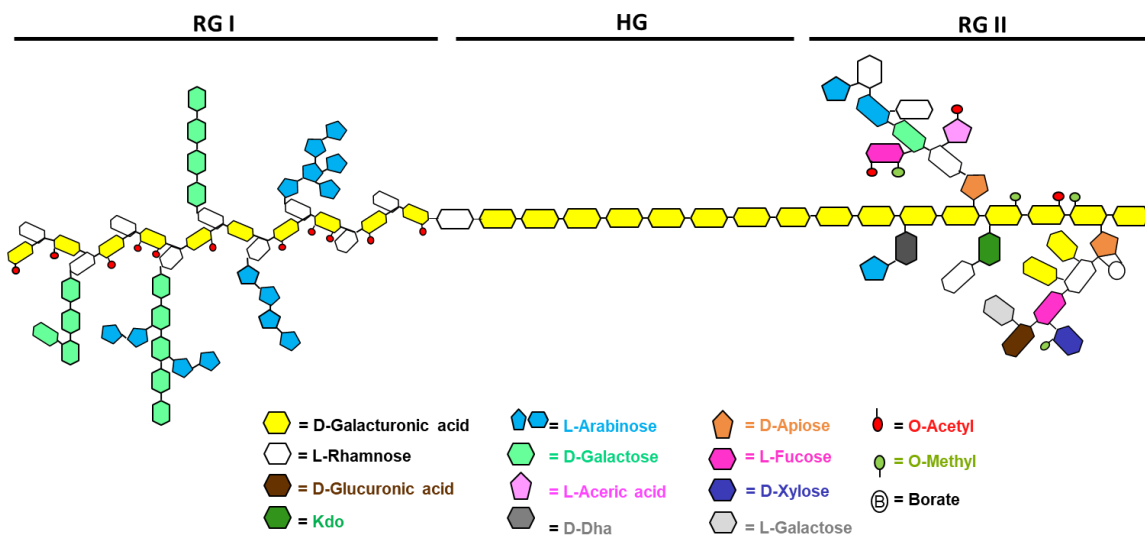


Figure 21 - Simplified schematic diagram of some pectin characteristics: HGs – Homogalacturonans; RG-I / II – Rhamnogalacturonans I / II; Kdo – 3-deoxy-D-manno-octulosonic acid; Dha – deoxy-D-lyxo-heptulosaric acid. RG I and RG II are thought to be linked HGs. Adapted from Willats, WGT. et al. (2001).

The observation that some polysaccharides were able to disrupt protein-tannin binding led to the suggestion of an alternative mechanism for the loss of astringency during ripening [124, 157]. Ozawa and co-workers [157] investigated the ability of polyphenols to inhibit β -glucosidase in the presence of other compounds, namely sodium polygalacturonate carbohydrates and cyclodextrins. This work demonstrated that these compounds were able to inhibit the interaction between polyphenols and this protein, recovering the enzymatic activity of β -glucosidase. The authors justified the action of these compounds by the ability of them to form hydrophobic pockets in solution which were able to encapsulate and complex with polyphenols, preventing them from interacting with the enzyme [157].

Indeed, it seems that some polysaccharides have the proper structure to compete with SP in complexing with tannins. The inhibition or reduction of SP-tannin aggregates in the mouth by polysaccharides could be at the origin of the decrease of astringency perception.

5.4.1.2. Inhibition mechanisms of SP-tannin interactions

After these first evidences about the ability of polysaccharides to inhibit or reduce protein-tannin interactions, two mechanisms were proposed (Figure 22) [124, 158]:

- (a) Ternary mechanism - Polysaccharides are generally polyelectrolytes (macromolecules which contain charged groups) and therefore can form complexes with the protein-tannin complex, increasing its solubility in aqueous medium;
- (b) Competition mechanism - Polysaccharides can encapsulate tannins, either total or partially and thus inhibit their interaction with proteins.

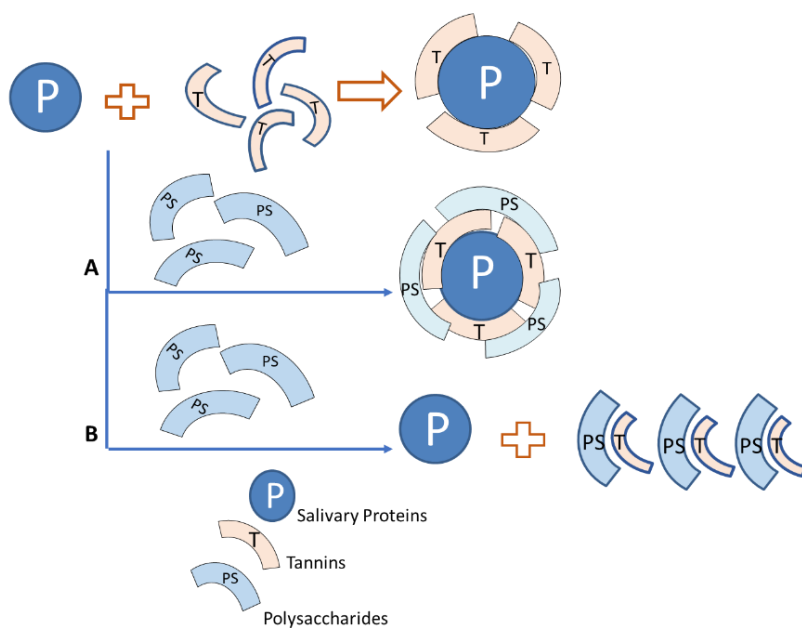


Figure 22 - Possible mechanisms (A, Ternary mechanism and B, Competition mechanism) involved on the inhibition of the aggregation of tannins and proteins by polysaccharides. P: Salivary proteins, T: tannin, PS: polysaccharide. Adapted from Mateus, N. et al. (2004).

For instance, consistent with the first mechanism, it was found that some of the most effective polysaccharides in inhibiting protein-tannin interactions are polyelectrolytes (gum arabic, polygalacturonic acid) [34].

5.4.1.3. Wine polysaccharides

As it was referred previously, in red wine a balanced level of astringency is desirable for its quality. In addition to polyphenols, polysaccharides are one of the most important macromolecules found in wine and have been widely isolated and characterized during the past decade [159-161]. They can be grouped into three major families: (i)

polysaccharides rich in arabinose and galactose (PRAGs), which include arabinans, arabinogalactans and arabinogalactan-proteins (AGPs) [160, 162], (ii) those rich in rhamnogalacturonans (RG I and RG II), which come from the pecto-cellulosic cell walls of grape berries, and (iii) the mannoproteins (MPs), another group of wine macromolecules, produced by yeasts (*S. cerevisiae*) during fermentation and during the aging of wines on lees [162, 163]. Vidal and colleagues [160] reported that the red wine was composed of 42% AGPs, 35% MPs, 19% RG II, and 4% RG I. Several authors have studied the properties of polysaccharides in wine, where they have been seen to act as protective colloids [161].

AGPs can be found both in red (100-200 mg. L⁻¹) and white wines (50-150 mg. L⁻¹) [160]. Structurally, AGPs are based on a ramified (1→3)-D-galactan inner core with (1→6)-linked D-galactan side chains highly substituted by arabinofuranosyl residues and minor amounts of arabinopyranose, rhamnose, xylose, glucuronic acid, and its 4-O-methyl ether. Typical AGPs commonly contain less than 10% protein and the polypeptide moiety typically contains hydroxyproline, glycine, serine and alanine as the major amino acids [164].

RG II is an acidic and complex polysaccharide. Its amount in red wines is about 100-150 mg. L⁻¹, while in white wines is about (20-50 mg. L⁻¹) [160]. As mentioned above, RG II has a main chain of galacturonic acid with different side chains which contains diverse residues such as glucuronic acid, rhamnose, galactose, arabinose and fucose, as well as various rare sugars, which are diagnostic of the presence of RG II, such as apiose, aceric acid (3-C-carboxy-5-deoxy-L-xylose), 2-O-methylfucose, 2-O-methylxylose, 3-deoxy-D-manno-octulosonic acid (Kdo) and 3-deoxy-D-/xyo-heptulosaric acid (Dha). These residues are linked together by more than twenty different glycosidic linkages. The RG II exists predominantly in wine in the form of a dimer, wherein two RG II molecules are attached covalently through borate ester linkages. The amount of RG II and AGPs can change during wine storage [165].

MPs are polysaccharides produced by yeast and are abundant in wines (150 mg. L⁻¹) [160]. However, the content of MPs in wine depends on the vinification processes [166] and the yeast strain used [167]. MPs are composed almost exclusively of mannose and protein fraction and their molecular weight range from 50 to 560 kDa [168]. Wine MPs have a very important role in the vinification process contributing, among others, to the inhibition of the crystallization of potassium tartrate salts, to the conservation of the aromatic characteristics, to phenolic stability and to decrease of protein turbidity [163].

Vidal and co-workers [169] had studied the mouthfeel properties of different wine polysaccharides, using one fraction containing a mixture of neutral polysaccharides, AGPs and MPs, and another fraction containing the acidic RG II. A trained sensory panel proved these polysaccharides which were dissolved in a model wine solution (13% aqueous ethanol solution, saturated with tartaric acid at pH 3.6) at concentrations normally found in wine. Both fractions were able to contribute to the “fullness” sensation (feeling of full, rounded sensation in the mouth) in wine in comparison with the reference solution (without polysaccharides), which was considered astringent by the panel. This sensation was detected by the panel, although the model solution did not have tannins, probably due to the effect of ethanol and acid. The fractions of polysaccharides decreased the attribute ratings associated with the astringency of the model wine, especially the fraction of RG II [169].

5.4.2. Other factors

External factors such as pH, IS, solvent composition (e.g. the presence of ethanol changes solvent polarity) and temperature also affect the complexation and precipitation of protein by vegetable tannins.

Carvalho and co-workers (2006) [170] observed an opposite effect of the IS to the interaction of two different proteins with a tannin. For aPRP, the increase of IS led to a large increase in interaction, while with α -amylase led to a slight decrease in the interaction with tannin. The suggested explanation was based on the pI of proteins; at the pH at which the experiments were carried out (pH 5), α -amylase probably would be less positively charged than PRP and therefore the IS did not cause any change. On the other hand, in the case of PRP there was probably a higher hydration of the ions with the increase of IS, which removed the water from the aggregate structure promoting protein-tannin interactions. However, studies about IS are quite controversial and apparently the effect of IS also depends on the protein and tannin features [112, 121, 171].

The pH of the medium is directly related to the protein-tannin interaction since it affects the degree of ionization of both components. In general, the interaction and precipitation decrease at low pH (<2) and high (> 8) and it is maximum at pH near to the protein pI, where the electrostatic repulsions are minimized [110, 172].

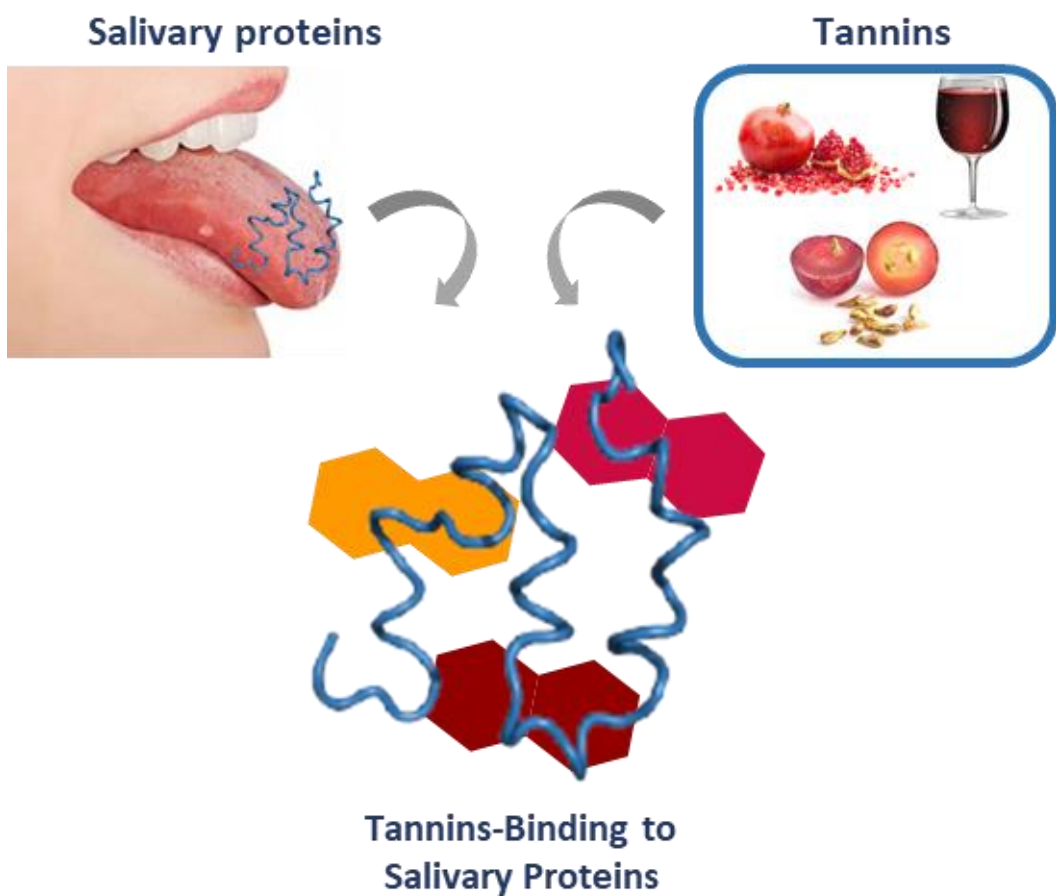
Regarding the effect of temperature, the information available in the literature is quite controversial. Hagerman and colleagues (1998) [119] observed that BSA precipitation

by PGG increases with temperature. On the other hand, Rawel and colleagues (2005) [171] showed that the binding of different tannins to BSA and human serum albumin decreased with increasing temperature. The effect of temperature seems to be dependent on the protein and tannins features.

Despite a few information available about this effect, it seems that the presence of ethanol can disrupt hydrophobic interactions or modify protein structure, resulting in a lower ability of proteins to bind tannins [173].

III. Research work

Chapter 1 - Molecular interaction between salivary proteins and food tannins



Synope

Part A – Molecular study of mucin-procyanidin interactions by fluorescence quenching and Saturation Transfer Difference (STD)-NMR

Adapted from:

Elsa Brandão, Mafalda Silva, Ignacio García-Estévez, Nuno Mateus, Victor de Freitas, Susana Soares, *Food Chemistry* **2017**, 228, 427-434. doi: 10.1016/j.foodchem.2017.02.27

With the exception of the grape seed isolation and the synthesis of procyanidin dimer B4 and tetramer, all the experimental work described in this part was carried out by the author, including molecular weight determination of mucin by SLS, fluorescence quenching studies and STD-NMR experiments.

Part B – Study of the interaction between human proline-rich proteins and food tannins

Adapted from:

Susana Soares, Ignacio García-Estévez, Raúl Ferrer-Galego, Natércia F. Brás, Elsa Brandão, Mafalda Silva, Natércia Teixeira, Fátima Fonseca, SéRG lo F. Sousa, Frederico Ferreira-da-Silva, Nuno Mateus, Victor de Freitas, *Food Chemistry*, **2017**, 243, 175-185.
doi: 10.1016/j.foodchem.2017.09.063

The STD-NMR experiments were carried out by the author.

Part C – Molecular interaction between salivary proteins and food tannins

Adapted from:

Mafalda Santos Silva, Ignacio García-Estévez, Elsa Brandão, Nuno Mateus, Victor de Freitas, Susana Soares, *Journal of Agricultural and Food Chemistry*, **2017**, 65 (31), 6415-6424. doi: 10.1021/acs.jafc.7b01722

The fluorescence quenching studies were carried out by the author.

A. Molecular study of mucin-procyanidin interaction by fluorescence quenching and Saturation Transfer Difference (STD)-NMR

Abstract

Astringency is closely related to the interaction between procyandins and salivary proteins (SP). The aim of this work was to study the interaction between mucin, a SP responsible for saliva lubricating properties, with different procyandins (B4 dimer, tetramer (TT) and fractions of oligomeric procyandins), and the influence of several conditions [pH, ionic strength (IS), procyandins' mean degree of polymerization (mDP) and different solvents (ethanol or dimethylsulfoxide)] on this interaction by fluorescence quenching and Saturation Transfer Difference-Nuclear Magnetic Resonance (STD-NMR). For fractions of oligomeric procyandins, the mucin-procyandin interaction increased with mDP; however, for pure compounds, procyandin TT has lower affinity than dimer B4 which could be due to a lower structural flexibility imposed by its complex structure. Furthermore, ethanol (EtOH) and dimethylsulfoxide (DMSO) can disrupt the main driving forces of these interactions, hydrophobic interactions and hydrogen bonds, respectively, lowering significantly the binding constants.

A1. Introduction

Condensed tannins, also known as procyandins, are plant secondary metabolites very common in fruits and vegetal-based beverages like tea, juice, red wine and coffee [6, 128]. They are polymeric ramified structures composed of flavan-3-ol units linked by C-C. In particular, dimeric procyandins are composed of catechin and/or epicatechin linked through C4-C8 and C4-C6 bonds [6].

Tannins have the ability to interact with SP which is important at sensory and health levels [6, 128]. Regarding the sensory level, tannins are directly related to astringency which is a tactile sensation in the oral cavity involving dryness of the oral surface and tightening and puckering sensations of the mucosa and muscles around the mouth during the ingestion of tannin-rich foods or beverages [174]. It is generally accepted that astringency is mainly due to tannins complexation with SP, resulting in their aggregation and/or precipitation and loss of their lubricating properties [175-177]. Hydrophobic

interactions and hydrogen bonds have been described as the main driving forces involved in this interaction [6].

Saliva presents a wide range of small proteins with various molecular weights [178]. It is possible to group the main SP into seven structurally related major classes namely: proline-rich proteins (basic, glycosylated and acidic), histatins, cystatins, statherin and mucins.

Mucins are abundant and filamentous glycoproteins that are present at the interface between many epithelia and their extracellular environments. They are characterized as large protein with molecular weights ranging from 500 to 20000 kDa. They are highly glycosylated consisting of 80% carbohydrates primarily N-acetylgalactosamine, N-acetylgalactosamine, fucose, galactose, and sialic acid (N-acetylneurameric acid) and traces of mannose and sulfate [104]. Due to their large size, these proteins have always been difficult to study, with much of their structure concealed by complex O-glycosylation. In recent years, mucins have received special attention due to their biological properties and characteristics because they can form a viscoelastic network that is important for hydration, pathogen exclusion, resistance to proteolytic digestion and lubrication of the oral cavity [105].

Since mucins are major SP and have a significant role in the lubrication of saliva, it is important to study the interaction of these proteins with tannins, and if this interaction can be directly connected to astringency sensation. It has already been reported that mucins form complexes with tannins [177, 179, 180]. However, most of the works done with mucins and tannins do not characterize the interaction at a molecular level.

Therefore, the goal of this work was to study, at a molecular level, mucin-procyanidin interaction. A “mucin model” (mucin from porcine stomach) and procyanidins with different molecular structures representative of wine/food tannins (grape seed fractions (GSF), B4 dimer and procyanidin tetramer (TT)) were used in this study. The interactions were characterized by two complementary techniques, fluorescence quenching and STD-NMR.

A2. Material and methods

A2.1. Reagents

All reagents used were of analytical grade or better. Mucin type III from porcine stomach, DMSO, sodium acetate trihydrate, (-)-epicatechin, (+)-catechin, deuterium oxide (D_2O)

and hexadeuteroethanol ($\text{EtOH-}d_6$) were purchased from Sigma Aldrich. Acetic acid was purchased from Carlo Erba Reagents. Ethanol (EtOH) was purchased from AGA, Álcool e Géneros Alimentares, SA. Hexadeuterodimethylsulfoxide ($\text{DMSO-}d_6$) was purchased from Euriso-top. Methanol was purchased from Chem-Lab. (+)-Taxifolin was purchased from Extrasynthese.

A2.2. Grape Seed Fraction (GSF) Isolation

Procyanidins were extracted from grape seeds (*Vitis vinifera*) with an ethanol/water/chloroform solution (1:1:2, v/v/v). The resulting solution was centrifuged and the chloroform phase, containing chlorophylls, lipids and other undesirable compounds was rejected. The hydroalcoholic phase was then extracted with ethyl acetate, and the organic phase was evaporated using a rotary evaporator (30 °C).

The resulting residue corresponding essentially to oligomeric procyandins was fractionated through a TSK Toyopearl HW-40(s) gel column (100 mm x 10 mm i.d., with 0.8 mL·min⁻¹, methanol as eluent), yielding five fractions according to the method described in the literature [181, 182].

The most important fractions were obtained after elution with 99.8 % methanol (v/v) (4h), with 5% acetic acid/methanol (v/v) (14h) and with 10% acetic acid/methanol (v/v) (8h), called GSF 1, GSF 2 and GSF 3, respectively. All fractions were mixed with deionized water, and the organic solvent was eliminated using a rotary evaporator under reduced pressure at 30 °C and then freeze-dried.

A2.3. Analysis and characterization of GSF

The procyandin composition of fractions was determined by direct analysis by Electrospray Ionization-Mass Spectrometry (ESI-MS) (Finnigan DECA XP PLUS) and subsequent analysis of the average full mass spectra. The mean DP was determined by acid-catalysis reaction in presence of phloroglucinol as described in the literature followed by Liquid Chromatography-Mass Spectrometry (LC-MS) (Finnigan DECA XP PLUS) and HPLC analysis [183]. Briefly, a solution of 0.1 N HCl in MeOH, containing 50.0 g. L⁻¹ and 10.0 g. L⁻¹ ascorbic acid was prepared. The GSF of interest was reacted in this solution (5.0 g. L⁻¹) at 50 °C for 20 min, and then it was added 5 volumes of 40 mM aqueous sodium acetate to stop the reaction. The resulting solutions were analyzed either by LC-MS to identify the flavan-3-ols monomers and the monomeric phloroglucinol

adducts as well as by HPLC to determine the moles of each monomer by a calibration curve obtained from (+)-catechin.

A2.4. Synthesis and Purification of Procyanidins

Procyanidin B4 was obtained according to the procedure described in the literature [184, 185], with slight modifications. Procyanidin B4 was obtained according to the procedure described in the literature, with slight modifications. Briefly, (+)-taxifolin and (-)-epicatechin (ratio 1:2) were dissolved in ethanol under argon atmosphere. The mixture was then treated by dropwise addition of sodium borohydride and left for 15 min under magnetic agitation. The pH was lowered to 4.5 by slowly adding acetic acid/water 50% (v/v) and the mixture was allowed to stand under argon atmosphere for 30 min. After this, the reaction mixture was extracted with ethyl acetate, evaporated and passed through C18 gel. Following extensive washing with water, procyanidins were recovered with methanol. The obtained fraction, after evaporation of methanol, was passed through a TSK Toyopearl HW-40(S) gel column (300 mm x 10 mm i.d., with 0.8 mL·min⁻¹ of methanol as eluent) coupled to a UV-Vis detector (Gilson 115) were several fractions were recovered and analyzed by ESI-MS (Finnigan DECA XP PLUS) yielding procyanidins with varying degrees of polymerization.

Procyanidin TT (catechin-(4-8)-catechin-(4-8)-catechin-(4-8)-catechin) was synthesized accordingly the procedure described above with some modifications. It was used, as initial reagents, (+)-taxifolin and (+)-catechin (ratio 2:1). The fractions containing procyanidin B4 ([M - H]⁻ at m/z = 577) and procyanidin TT ([M - H]⁻ at m/z = 1153) were isolated and freeze-dried. The purity of procyanidins was assessed by LC-MS and direct MS analysis, and was higher than 95%.

A2.5. Static Light Scattering

Mucin molecular weight determination was performed using a Malvern Zetasizer Nano ZS instrument running a Static Light Scattering (SLS) method which was adapted from one described in the literature [186]. The samples were studied in miliQ water at different mucin concentrations at 25 °C, and the average molecular weight of mucin was found to be about 1000 kDa.

A2.6. Fluorescence Quenching Measurements

In this work, the quenching of mucin intrinsic fluorescence by different procyanidins (procyanidin B4, procyanidin TT and oligomeric procyanidins GSF 1, 2 and 3) was assayed using a Perkin-Elmer LS 45 fluorimeter. Tryptophan residues were used as intrinsic fluorophore. The excitation wavelength was set to 282 nm and the emission spectrum was recorded from 300 to 500 nm. Both slits were 10 nm.

Since procyanidins absorb energy at the established emission wavelength [187], a blank was made for each procyanidin concentration, where the protein solution was replaced by distilled water. The respective spectrum of each procyanidin was then subtracted from the emission spectrum of the corresponding mixture [187, 188]. The possibility of fluorescence resonance energy transfer (FRET) between the mucin and procyanidins was discarded after analysis of both absorption and emission spectra [189]. Furthermore, to correct the inner filter effect, the optical density of each mixture was measured in order to use procyanidins concentrations with the lowest optical densities.

The experiments were performed in different acetate buffer solutions divided in 5 groups, according to IS, pH and the absence/presence of EtOH and DMSO. Therefore, the acetate buffer solutions were: (1) 0.05 M; pH= 5.0; (2) 0.1 M; pH= 5.0; (3) 0.1 M; pH= 5.0; 10% EtOH; (4) 0.1 M; pH= 5.0; 10% DMSO; (5) 0.1 M; pH= 2.6. All buffer solutions were filtered (polyethersulfone 0.20 µm). In several microtubes, increasing volumes of different procyanidins stock solutions were added to the mucin solution (0.25 µM), in order to give different final concentrations of procyanidin B4 (0-60 µM), procyanidin TT (0-40 µM) and GSF 1, 2 and 3 (0-25 µM). After this, the microtubes were shaken and the emission spectra were measured in the fluorimeter cell. Between each experiment, the cell was washed with distilled water.

Fluorescence quenching is described by the Stern-Volmer equation (Eq. 1), where F_0 and F are the fluorescence intensities in the absence and in the presence of quencher (procyanidin), respectively, k_q is the bimolecular quenching constant, τ_0 is the lifetime of the fluorophore in the absence of the quencher, [Q] is the concentration of the quencher, and K_{SV} is the Stern-Volmer quenching constant [190]. Eq. 1 is used to determine K_{SV} by linear regression of a plot of F_0/F against [Q].

$$\frac{F_0}{F} = 1 + k_q \tau_0 [Q] = 1 + K_{SV} [Q] \quad (1)$$

Linear Stern-Volmer plot is generally indicative of a single class of fluorophores in a protein, all equally accessible to the quencher, which means that only one mechanism (dynamic or static) of quenching occurs. In both cases, the bimolecular quenching constant, k_q , can be calculated by the ratio between K_{SV} and τ_0 .

However, positive deviations from the Stern-Volmer equation may occur if the extent of quenching is large. In these cases, the Stern-Volmer plot exhibits an upward curvature, concave toward the y axis at high [Q]. These positive deviations may be an indication that either the protein is being quenched by two mechanisms simultaneously or could mean the existence of a “sphere of action”. This last model assumes the existence of a sphere of volume around a fluorophore within which quenching occurs due to the quencher being adjacent to the fluorophore at the moment of excitation. Stern-Volmer equation which describes this situation is presented in Eq. 2 and allows the calculation of a quenching constant that is referred to as the apparent static quenching constant (K_{app}).

$$\frac{F_0}{F} = (1 + K_{app}[Q]) \exp([Q] VN/1000) \quad (2)$$

For mucin, τ_0 was measured at room temperature on a Fluoromax-4 spectrophotometer attached to a single photon counting controller (FluoroHub), both from Horiba Jobin-Yvon. The fluorescence excitation was performed with a Horiba Nano LED source of 290 nm, and fluorescence emission was recorded at the maximum wavelength for the protein solution (350 nm). The lamp profile was recorded by placing a scatter (dilute solution of LUDOX in water) in place of the sample [189, 191]. At the end, τ_0 of mucin was found to be 3.2×10^{-9} s.

A2.7. STD-NMR Studies

The interaction between mucin and procyanidins (B4 and TT) was studied by STD-NMR in different solvents: D₂O, D₂O/EtOH-d₆ (10% EtOH-d₆, v/v) and D₂O/DMSO-d₆ (10% DMSO-d₆, v/v). In order to quantify the affinity of the interactions, binding was followed by measuring the intensities of selected procyanidin protons observed in the STD spectra with increasing procyanidin concentrations [192]. In order to determine a binding constant, the amplification factor (A_{STD}) was calculated by Eq. 3, where I_0 and I_{SAT} are the intensity of the signals in the reference and saturated spectra, respectively, $[L]_T$ and $[P]$ are ligand and protein concentration. K_D was determined using Eq. 4 [193]:

$$A_{STD} = \frac{I_0 - I_{SAT}}{I_0} \times \frac{[L]_T}{[P]} = \frac{I_{STD}}{I_0} \times \frac{[L]_T}{[P]} \quad (3)$$

$$A_{STD} = \frac{\alpha_{STD} [L]}{K_D + [L]} \quad (4)$$

α_{STD} is the maximum amplification factor and $[L]$ is the ligand concentration. This expression is valid if $[L] = [L]_T$, which is usually the case in STD experiments since $[L]_T \gg [P]_T$. The differences in A_{STD} for the different ligands can be quantitatively expressed in function of ligand concentration and the experimental data can be fit using Solver utility from Microsoft Excel giving a K_D value. Then, a binding constant, K_A , can be determined by K_D , using the following equation:

$$K_D = \frac{1}{K_A} \quad (5)$$

The minimum procyanidin concentration used in the experiments was restricted by the detection limit for the STD resonances, while maximum concentrations tested were limited by procyanidins solubility. The different concentrations of procyanidin B4 (0-0.6 mM) and procyanidin TT (0-0.7 mM) were previously lyophilized and added as a powder.

Mucin samples containing 0.25 μ M and 1.25 μ M were prepared in the solvents previously referred, and divided into 5 mm NMR tubes, in which procyanidin B4 and procyanidin TT were added, respectively. The same NMR tube containing the reaction mixture was used for a maximum of three ligand concentrations, in order to avoid proton exchange since some ligand protons are labile and may change with D_2O .

NMR experiments were recorded on a Bruker Avance III 600 HD spectrometer, operating at 600.13 MHz, equipped with a 5 mm CryoProbe Prodigy and pulse gradient units capable of producing magnetic field pulsed gradients in the z direction of 50 G/cm. The measurements were made with standard Bruker pulse sequences at 300 K. 1H and STD spectra were recorded with a shaped pulse to suppress the water resonance [194] using the following parameters: spectral width, 16 ppm; nutation angle, 7.08 μ s and 90°; and shaped pulse duration, 2 ms. Selective saturation of the mucin off-resonance at 20 ppm and on-resonance at -1 ppm was performed using a pseudo-two-dimensional (2D) sequence for STD with a shaped pulse train alternating between the on and off resonances. STD-NMR spectra were acquired using Gauss 1.1000 pulses for selective saturation (50 ms), with a total saturation time of 2.5 s. The number of scans for procyanidin B4 (16) and for procyanidin TT (32), receptor gain value (2050), and relaxation delay (3.5 s) were kept constant. To subtract the unprocessed on- and off-

resonance spectra, to baseline correct the resulting difference spectrum and to integrate the areas, TopSpin 2.1 software from Bruker was used.

A2.8. Statistical Analysis

All assays, except STD-NMR studies, were performed in $n \geq 3$ repetitions. Values are expressed as the arithmetic means (SEM). Statistical significance of the difference between groups was evaluated by one-way analysis variance (ANOVA) followed by Tukey's test. Differences were considered significant when $P < 0.05$. Data were processed using GraphPad Prism 5.0 for Windows (GraphPad Software, San Diego, California, USA).

A3. Results and discussion

In this work, the interaction between mucin and procyanidins was studied by fluorescence quenching and STD-NMR. In the literature, the ability of mucin to interact and complex with procyanidins has been pointed out, indicating a possible involvement in astringency sensation. However, the molecular characterization of this interaction is still poor [179, 180].

Initially, the experiments were conducted using a GSF of oligomeric procyanidins, since they contain a mixture of several procyanidins with different mean degree of polymerization (mDP). These GSF are representative of the major tannin composition present in vegetal foods and beverages (red wine, coffee, chocolate, juice and tea). Next it was intended to study some pure compounds that have a DP near to that of GSF. For this purpose, procyanidin B4 and procyanidin TT were chosen. Procyanidin B4 is high abundant in the human diet and it has been described with a more extended conformation, comparatively to other procyanidin dimers [6, 143]. Regarding TT, it was chosen because it has a DP of 4 (double of procyanidin B4). Despite little information being available about the presence of TT in fruits and vegetables, it was already identified in apples [195].

This study was conducted using different conditions (pH, IS and the absence/presence of EtOH and DMSO) in order to evaluate the influence of several factors, namely protein charge, hydrophobic interactions and hydrogen bonds, etc.

A3.1. Fluorescence Quenching Studies

Fluorescence quenching measurements allow the identification of the kind of interactions that take place between the quencher (procyanidin) and the fluorophore (mucin) [190].

Figure 23 shows the fluorescence emission spectra obtained for mucin with the addition of increasing concentration of oligomeric procyanidins (GSF 3). The addition of increasing concentrations of oligomeric procyanidins (GSF 3) to mucin caused a gradual decrease in the protein fluorescence intensity. On the other hand, as it did not alter considerably λ_{em} , it was assumed that the interaction between mucin and procyanidins did not significantly change the environment of the tryptophan residues and, consequently, the protein structure [187]. Probably, this happens because mucin-procyanidin interaction is far from the tryptophan residue.

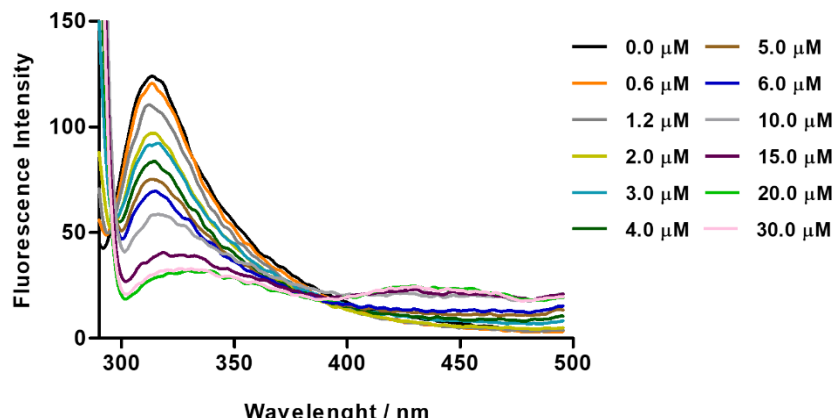


Figure 23 - Fluorescence emission spectra (at λ_{ex} 282 nm) of mucin (0.25 μ M) in the presence of increasing concentrations of GSF 3. Each curve represents a triplicate assay after correction for procyanidin fluorescence.

The Stern-Volmer plots presented in Figure 24 describe mucin quenching by increasing concentrations of GSF of oligomeric procyanidins in different conditions. It is possible to observe that Stern-Volmer plots were all linear using any fraction of oligomeric procyanidins, which means that only one type of quenching occurred, static or dynamic. The calculation of the Stern-Volmer constant (K_{sv}), which measures the affinity of the procyanidin to interact with mucin was achieved using Eq. 1 (Table 3).

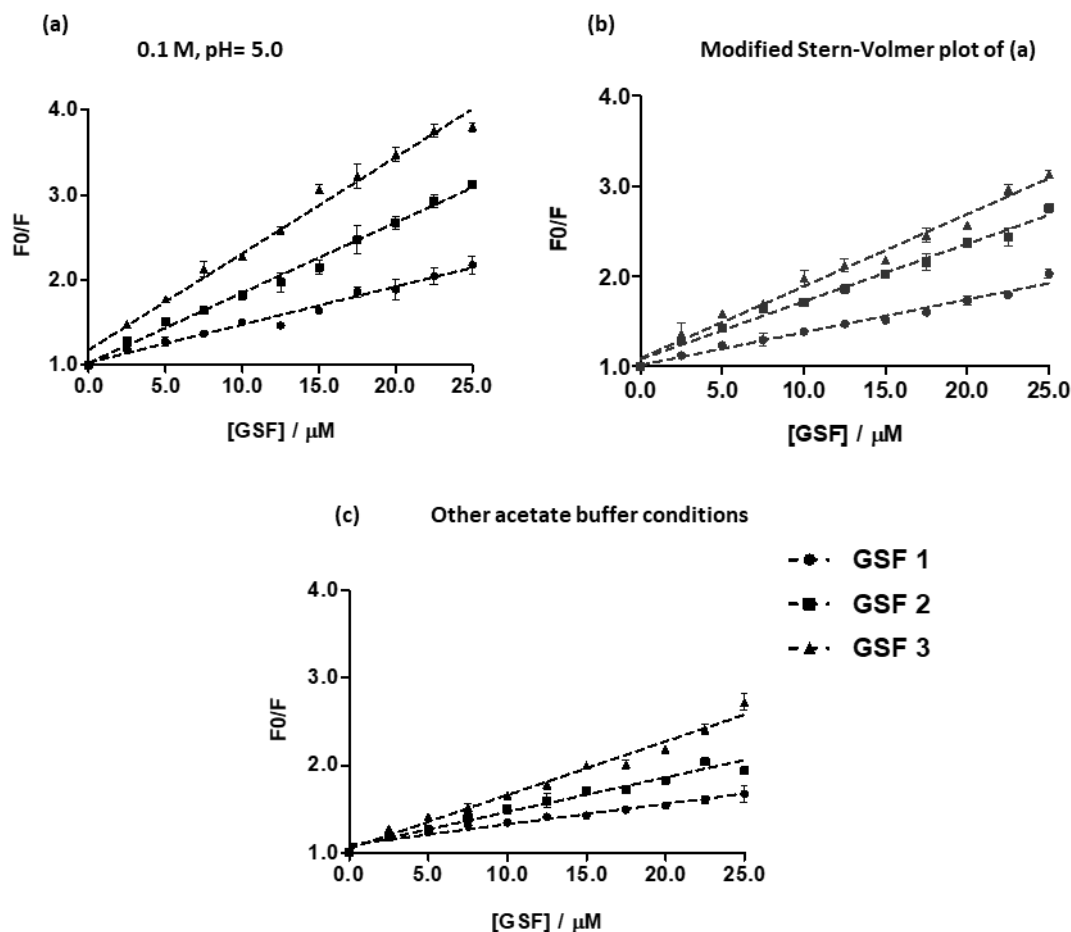


Figure 24 - Stern–Volmer plots describing tryptophan quenching of mucin (0.25 μM) by increasing concentrations of GSF (GSF 1, GSF 2 and GSF 3) (0–25 μM) in different acetate buffer solutions: (a) 0.1 M, pH= 5.0, (b) 0.1 M, 10% EtOH, pH= 5.0 and (c) 0.1M, 10% DMSO, pH= 5.0. The fluorescence emission intensity was recorded at λ_{ex} 282 nm.

Table 3 - Stern-Volmer quenching constants (K_{SV}) and Apparent Static Quenching Constant (K_{app})* for the interaction between mucin and procyanidins (0–60 μM) with increasing DP (dimer B4, tetramer TT and fractions GSF 1, GSF 2 and GSF 3 of oligomeric procyanidins). Values with equal letters (a–h) are not significantly different ($P<0.05$).

Procyanidin	$K_{\text{SV}} (\text{M}^{-1})$				
	0.1 M, pH=5.0	0.1 M, 10% EtOH, pH=5.0	0.1 M, 10% DMSO, pH=5.0	0.1 M, pH=2.6	0.05 M, pH=5.0
GSF 1	44780±2390 ^{a,b}	36350±1429 ^{a,b,d}	23340±1566 ^{b,d,e,f}	-	-
GSF 2	82700±2493 ^g	63890±1952 ^h	39580±1704 ^{a,b,d}	-	-
GSF 3	113500±3290	79810±2569 ^g	61260±2183 ^h	-	-
B4	38500±404 ^{*a}	32460±562 ^{*a,b}	7187±437 ^c	680±130 ^c	45620±1750 ^{a,b}
TT	29130±1256 ^{a,b,d}	21540±978 ^{b,d,e}	21450±908 ^{d,e,f}	-	-

*These values correspond to the apparent static quenching constant (K_{app}), which were calculated as previously described.

The obtained K_{sv} indicates that the affinity of mucin to interact with GSF is dependent on GSF mDP. An increase in K_{sv} values was observed as GSF mDP increased. GSF contains a mixture of several procyanidins with different structures. The number of catechin units and galloyl groups increases with the mDP procyanidins, resulting in a higher number of aromatic rings and hydroxyl groups that may be involved in hydrogen bonding and hydrophobic interactions with several protein binding sites. So, a stronger binding affinity was already anticipated for the high molecular weight procyanidin oligomers - GSF 3 – which was indeed observed.

Further important aspects should be taken into account such as the effect of EtOH and DMSO in this interaction. As seen from Table 3, the values for K_{sv} constants in the presence of these two solvents were significantly lower compared to those obtained in their absence. It has been described in the literature that solvents like EtOH and DMSO can disrupt hydrophobic interactions and hydrogen bonds, respectively [196, 197]. Since these kind of bonds are pointed as the main driving forces responsible for protein-tannin interactions, it is not surprising that their presence affects this interaction. In the case of mucin-GSF interactions K_{sv} constants with DMSO were always lower than the ones obtained with EtOH.

To verify if this quenching is due to a static or dynamic mechanism, it is essential to calculate k_q , according to Eq. 1. The obtained values for bimolecular quenching constants were higher than $10^{10} \text{ M}^{-1} \text{ s}^{-1}$ (Table 4), which is the maximum value possible for diffusion-limited quenching (dynamic mechanism).

Table 4 – Bimolecular quenching constants (k_q) for the interaction between mucin (0.25 μM) and procyanidins with increasing DP (GSF of oligomeric procyanidins, B4 and TT) in different conditions. Values with equal letters (a-q) are not significantly different ($P < 0.05$).

$$k_q (10^{13})/\text{M}^{-1} \text{ s}^{-1}$$

$\tau_0 (\text{s})$	Condition	GSF 1	GSF 2	GSF 3	B4	TT
Mucin 3.2×10^{-9}	0.1 M, pH=5.0	$1.41 \pm 0.08^{\text{a}}$	$2.60 \pm 0.08^{\text{d}}$	$3.56 \pm 0.10^{\text{g}}$	$1.21 \pm 0.01^{\text{*b,f,j}}$	$0.92 \pm 0.04^{\text{c,k,o}}$
	0.1 M, 10% EtOH, pH=5.0	$1.14 \pm 0.04^{\text{b}}$	$2.01 \pm 0.06^{\text{e}}$	$2.51 \pm 0.08^{\text{h}}$	$1.02 \pm 0.02^{\text{*b,k}}$	$0.68 \pm 0.03^{\text{c,k,p}}$
	0.1 M, 10% DMSO, pH=5.0	$0.73 \pm 0.05^{\text{c}}$	$1.24 \pm 0.05^{\text{b,f}}$	$1.92 \pm 0.07^{\text{i}}$	$0.23 \pm 0.02^{\text{l}}$	$0.67 \pm 0.03^{\text{c,k,p,q}}$
	0.1 M, pH 2.6	-	-	-	$0.02 \pm 0.01^{\text{m}}$	-
	0.05 M, pH=5.0	-	-	-	$1.43 \pm 0.06^{\text{a,n}}$	-

*These values refer to the apparent bimolecular quenching constant (K_q^{app}).

Thus, these results suggest that all GSF interact with mucin by a static type, involving the formation of a stable ground-state complex between the two compounds, independently of the DP and solvent polarity [198].

After studying the interaction between mucin and a mixture of oligomeric procyanidins, it was also intended to study the same interaction with pure compounds (procyanidin B4 and procyanidin TT). The Stern-Volmer and modified Stern-Volmer plots presented in Figure 25 describe mucin quenching by increasing concentrations of procyanidin B4 in different conditions.

It is possible to note two different behaviors for procyanidin B4 according to the used conditions: a linear Stern-Volmer plots in presence of 10% DMSO, at IS 0.05 M and at pH 2.6 (Figure 25c) (similar to the behavior observed for GSF); and an upward-curving Stern-Volmer plots which are concave toward the y axis at high procyanidin concentration in the absence of EtOH/DMSO and with 10% EtOH (Figure 25a). Positive deviations from the Stern-Volmer equation (upward-curving plots) are frequently detected when the extent of quenching is large. For these cases, a modified form of Stern-Volmer equation is required (Eq. 2). Through the resulting $\ln(F_0/F) = f([quencher])$ plot (Figure 25b) it is possible to calculate the apparent static quenching constant (K_{app}) [187, 199]. This modified form of Stern-Volmer plot allows, as previously, to determine the apparent bimolecular quenching constant (K_q^{app}) dividing the K_{app} by the lifetime of mucin. However, these positive deviations may be an indication that either the protein is being quenched by two mechanisms simultaneously or could mean the existence of a “sphere of action”. After measuring the lifetime of mucin with increasing B4 concentrations in the absence/presence of 10% EtOH, the values obtained were not compatible with quenching by the two mechanisms simultaneously. Thus, the most probable explanation for these positive deviations is the “sphere of action” model. This last model assumes the existence of a sphere around the fluorophore within which quenching occurs due to the quencher being adjacent to the fluorophore at the moment of excitation, without the formation of a ground-state complex [190].

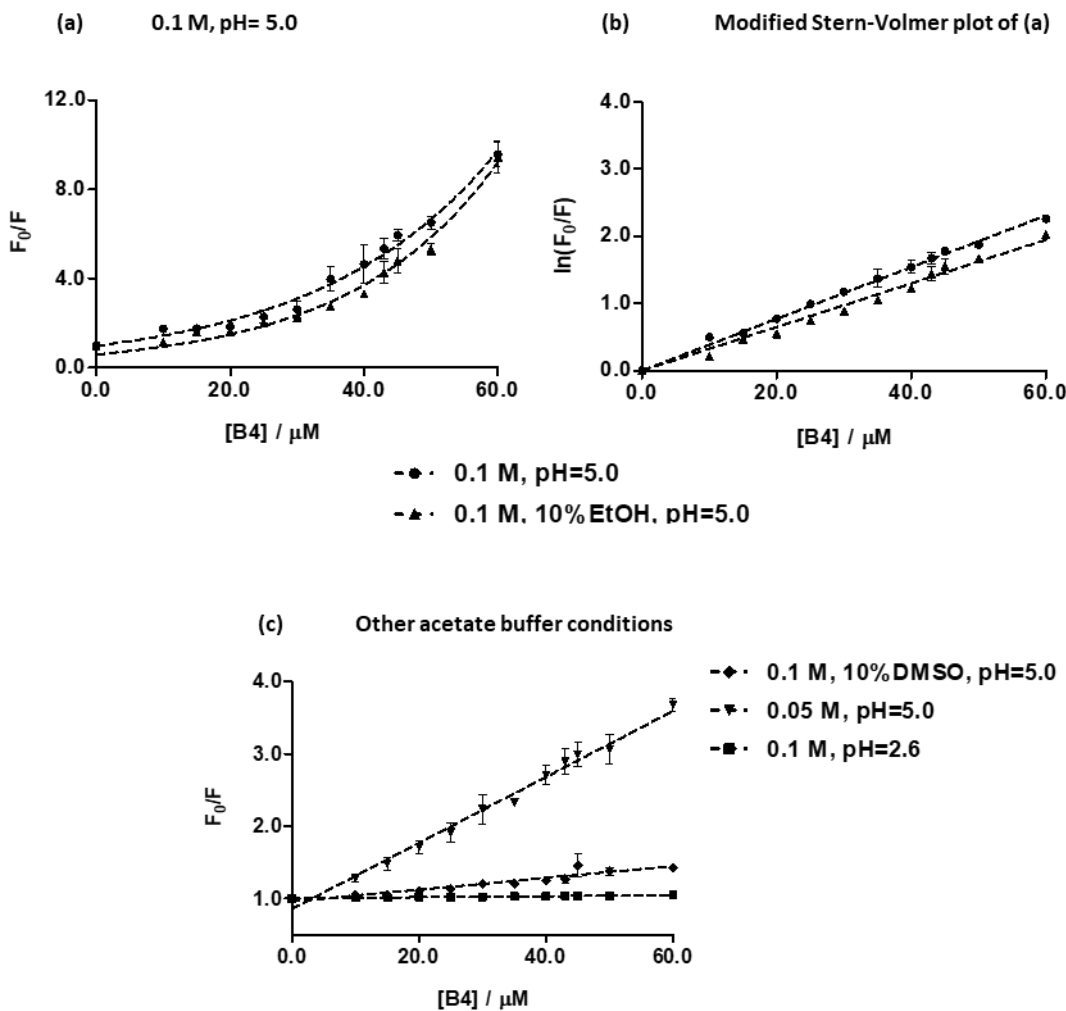


Figure 25 - Stern-Volmer (a and c) and modified Stern-Volmer (b) plots describing tryptophan quenching of mucin ($0.25 \mu\text{M}$) by increasing concentrations of procyanidin B4 ($0-60 \mu\text{M}$) in different acetate buffer solutions. The fluorescence emission intensity was recorded at $\lambda_{\text{ex}} 282 \text{ nm}$.

The other observed behavior for procyanidin B4 (linear plot, Figure 25c) means that only one type of quenching occurred. In this case, the K_q values presented in Table 4 suggest that the mechanism in these conditions is of static type. Concerning the influence of EtOH and DMSO in this interaction it is possible to note that it was similar to that observed for GSF. A higher decrease was observed in K_{SV} by DMSO rather than EtOH.

The influence of other factors that affect the charge/structure of the protein were also studied, namely pH and IS (Figure 25c). The influence of IS on the interaction was studied using a lower concentration of acetate buffer solution (0.05 M). The respective K_{SV} and K_q values (Tables 3 and 4) for this interaction indicate that decreasing the IS increases K_{SV} constants, which means a stronger mucin-procyanidin binding. pH is known to affect the overall charge of proteins. It is known that proteins have an isoelectric

point (pl) that corresponds to the pH at which no net electrical charge is observed. Since the pH of red wine is near 3, it was planned to study this interaction at a lower pH (pH=2.6). The pH seems to affect greatly this interaction, since K_{SV} value at this pH is too low comparatively to the one at pH 5.0. This is not surprising since the pl of mucin lies between 2 and 3 [104], and so at pH 2.6 its net charge could be nearly zero. This data points out to the importance of pH in the protein structure and, consequently, in the significance of residues side chains charge, which influence the ability of mucin to interact with procyanidin B4.

Figure 26 shows the mucin quenching by increasing concentrations of procyanidin TT. For the three studied conditions the obtained Stern-Volmer plots were all linear, and according to the K_q values of Table 4, the responsible quenching mechanism is of static type. In the same way, it is important to take into account the effect of EtOH and DMSO in this interaction. Both solvents seem to influence mucin-TT interaction since lower K_{SV} values were obtained in their presence. However, these K_{SV} values are very close to each other.

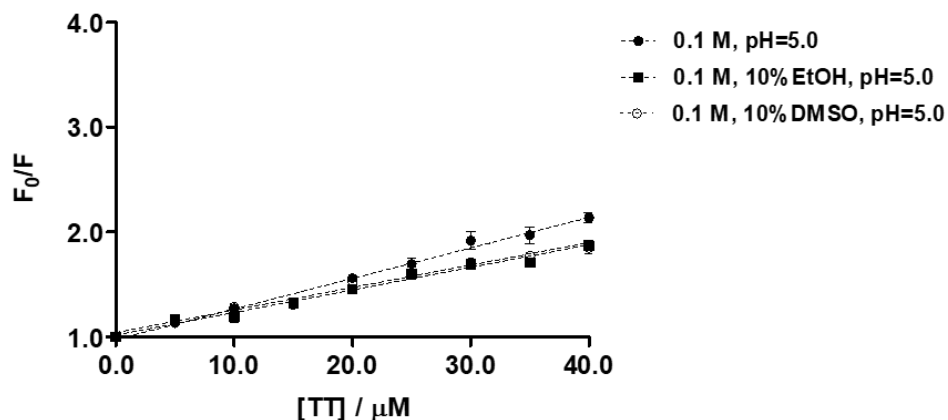


Figure 26 - Stern-Volmer plots describing tryptophan quenching of mucin ($0.25 \mu\text{M}$) by increasing concentrations of procyanidin TT ($0-40 \mu\text{M}$) in different acetate buffer solutions (0.1 M , pH=5.0; 0.1 M , 10% EtOH, pH=5.0; 0.1 M , 10% DMSO, pH=5.0). The fluorescence emission intensity was recorded at λ_{ex} 282 nm

The overall results show that whatever the used tannin (quencher), their addition induced a quenching in the fluorescence intensity of mucin. For most mucin-tannin interactions, the experimental data determined a static mechanism of quenching. In these cases this means that there was a formation of a stable complex between mucin and tannins. For only two conditions using procyanidin B4 (highest IS and presence of EtOH), a “sphere

of action" quenching was observed, which is considered a type of apparent static quenching, but with no complex formation.

Comparing K_{SV} values for all the tannins at 0.1 M and in the absence of both solvents, the lowest K_{SV} values were observed for procyanidin TT. Although an increase in the interaction is expected as the procyanidins mDP increases, this was only valid for GSF, which are a complex mixture of procyanidins where it is possible to find different structures with different DP. In the case of procyanidin TT, although the number of binding groups increases with an increase in procyanidin units, other factors, such as structure flexibility can influence the interaction with proteins. The lack of structural flexibility of TT and, consequently steric constrains, may explain its lower affinity for mucin [149, 200].

Regarding K_{SV} values determined in the presence of EtOH and DMSO, it was possible to verify a decrease in K_{SV} values obtained for all tannins, meaning a decrease on mucin-tannin interactions. Concerning DMSO, the results suggest that DMSO affects mainly mucin interaction with GSFs and procyanidin B4 rather than with procyanidin TT. This fact suggests a higher contribution of hydrogen bonds than hydrophobic interactions, in comparison with mucin-procyanidin TT interaction.

A3.2. STD-NMR studies

STD-NMR has been receiving much attention for the study of protein-tannin interaction mostly because a great deal of structural information about the interaction may be obtained [201]. Briefly, ligand protons that are in close contact with the receptor ($\leq 5 \text{ \AA}$) receive saturation transfer from the receptor (via spin diffusion, through the nuclear Overhauser effect), and as a result, STD-NMR signals can be observed. Protons that are not involved in the binding process reveal no STD-NMR signals [202]. Once there is little information at a molecular level about the mucin-procyanidin interaction, this technique was chosen to complement the study of the mucin interaction with procyanidin B4 and procyanidin TT.

A3.2.1. Mucin-procyanidin binding studies by STD-NMR

First, to ensure the specificity of STD eliciting resonances and to validate the functionality of the STD pulse sequence chosen, control STD-NMR experiments were performed for procyanidins alone at the highest concentration studied. It was observed that the signals

corresponding to these procyanidins are not present in the STD spectrum, appearing only in the regular ^1H spectrum (Figure 27).

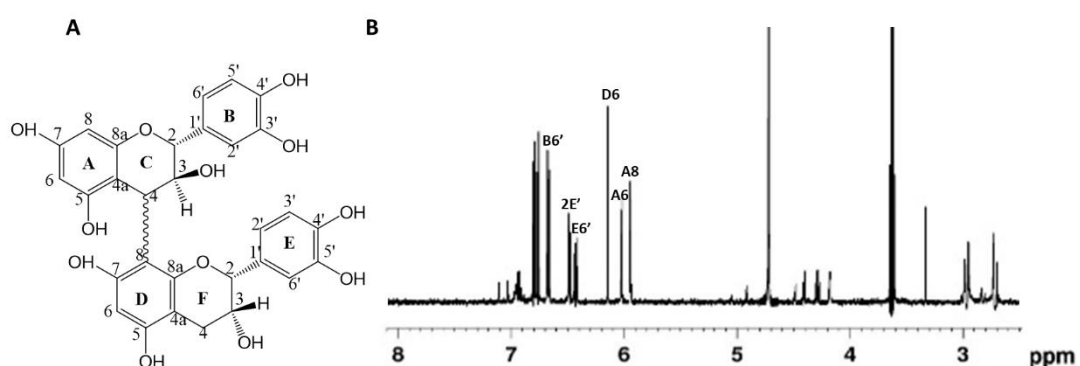


Figure 27 - Molecular structure (A) and proton spectrum of procyanidin B4 (B) showing the 8.0–2.5 ppm region where most protons resonate. Spectrum was recorded at 600 MHz and 281 K in D_2O .

As an example, part of the STD-NMR titration experiment conducted at a fixed mucin concentration (0.25 μM or 1.25 μM , according to the procyanidin used) is presented in Figure 28. The concentrations of procyanidin B4 ranging from 0.10 mM to 0.60 mM (corresponding to mucin/procyanidin ratio of 1:2400) (Figure 28A) while the concentrations of procyanidin TT ranging from 0.15 mM to 0.70 mM (corresponding to mucin/procyanidin ratio of 1:560) (Figure 28B).

From Figure 28, it is possible to perceive, especially for the highest concentrations, strong elicited resonances in specific regions for each ligand. Based on STD spectra, it was chosen from each ligand the proton or the proton set with the highest intensity to calculate binding constants.

From Figure 28A, strong elicited procyanidin B4 resonances were observed in a main region – 7.0–6.0 ppm. These STD signals increase systematically with increasing procyanidin B4 concentration, indicate that there is a strong interaction between mucin and this ligand. The proton signal at 6.10 ppm (corresponding to proton H6 of ring D) was chosen, since it was the proton with the highest signal.

Figure 28B shows part of the STD-NMR titration experiment conducted with mucin and increasing TT concentration. From these results, a similar behavior was noted to that observed for procyanidin B4, in which STD signal of the main proton signal region increases systematically with increasing procyanidin TT concentration. However, due to the structural complexity of procyanidin TT and presence of rotamers in solution, it was

not possible to appoint a specific proton signal, and in this way, a main proton signal region was selected, comprised at 7.1-6.5 ppm, called hereafter TT region.

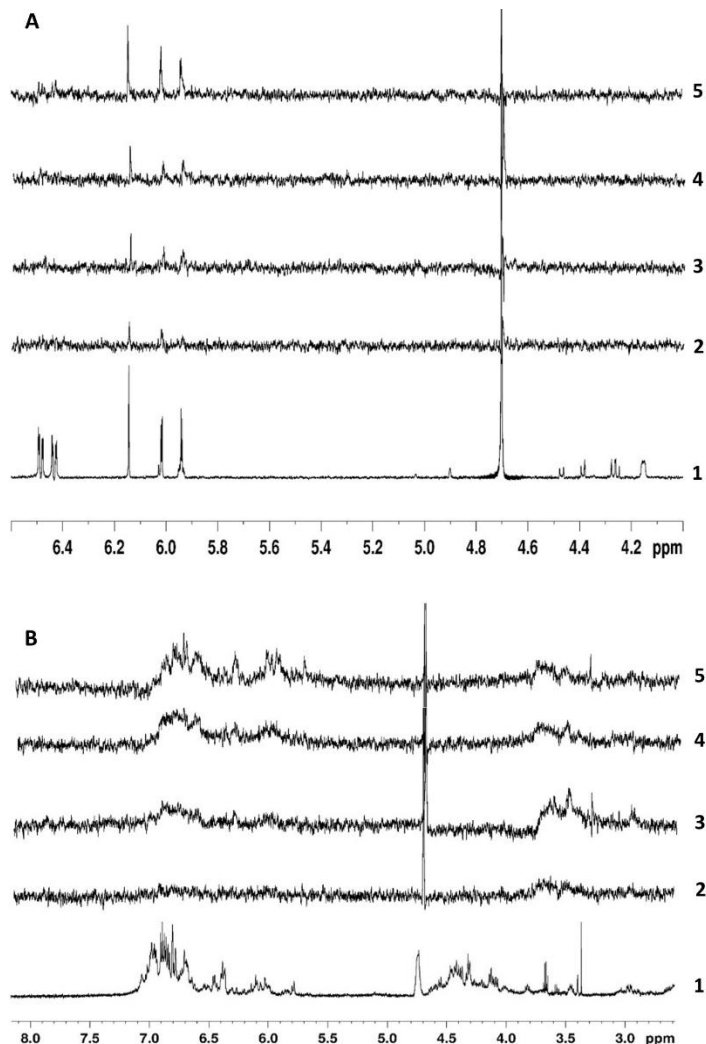


Figure 28 - (A) Proton spectrum of procyanidin B4 (1) and STD-NMR spectra of mixture between mucin (0.25 µM) and increasing concentrations of procyanidin B4, 0.10 mM (2), 0.20 mM (3), 0.40 mM (4) and 0.60 mM (5). (B) Proton spectrum of procyanidin TT (1) and STD-NMR spectra of mixture between mucin (1.25 µM) and increasing concentrations of procyanidin TT, 0.15 mM (2), 0.25 mM (3), 0.50 mM (4) and 0.60 mM (5). All of these spectra were recorded in D₂O.

A3.2.2. Binding Constant Calculation (K_A)

The strength of the interaction between mucin and procyanidins was assessed by determination of the binding constant (K_A) (Table 5). Firstly, K_D was calculated by measuring the intensities of procyanidin B4 proton and TT region observed in the STD spectra with increasing procyanidin concentration (Figure 28). Then a binding constant was determined using Eq. 5.

Figure 29 shows the plot of the intensity of the integral for procyanoindin B4 and procyanoindin TT titrations as a function of ligand concentration at a fixed mucin concentration (0.25 μ M or 1.25 μ M, according to the procyanoindin used) in three different conditions, and the respective fitting by Eq. 4.

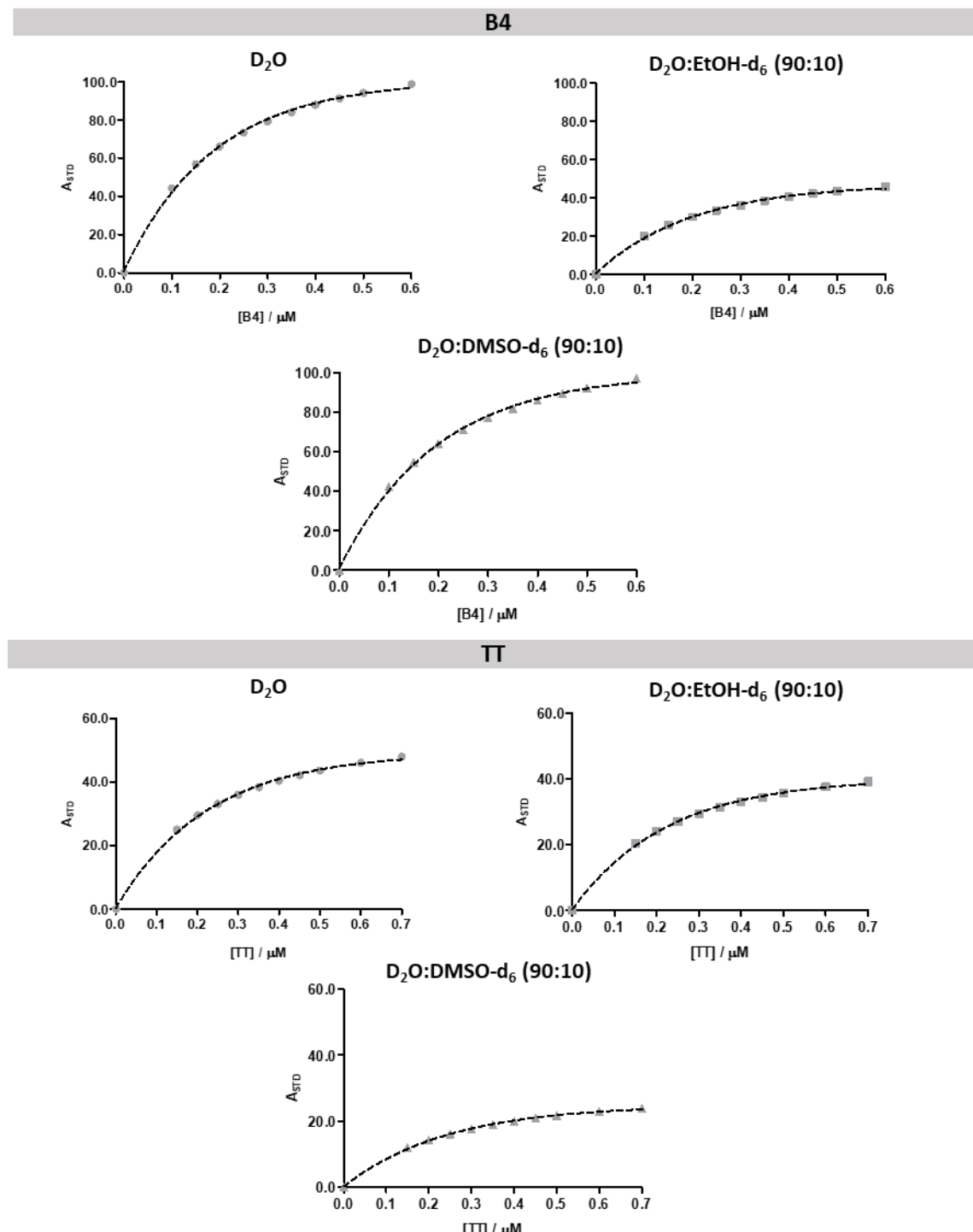


Figure 29 - Observed (symbols) and fitted (lines) integral intensities of B4 proton resonance and TT region resonance in the STD-NMR spectrum with increasing B4/TT concentration in three different conditions: D₂O, D₂O:EtOH-d₆ (90:10) and D₂O:DMSO-d₆ (90:10). Curves represent the best fit according to Eq. 4.

The titrations were conducted at high protein-ligand ratios ranging from 1:400 to approximately 1:2400 for procyanidin B4 and ranging from 1:120 to 1:560 for procyanidin TT. The selected procyanidin concentration ranges were chosen due to restrictions of the detection limit in the STD experiments.

From Figure 29, for all conditions, it was observed a hyperbolic curve with increasing procyanidin concentration. In Table 6 are reported the values of K_A obtained from the K_D values determined by fitting the experimental points. In general, the K_A values obtained for both tannins were quite similar. So, the major goal of STD experiments was the identification of procyanidin B4 structural epitope mainly responsible for the interaction with mucin – the ring D.

Due to differences in the sensitivity and detection limit of the two techniques employed, the range of procyanidin concentrations used was different. STD-NMR enabled this interaction to be studied at high ratios SP/procyanidin (high procyanidin concentrations) working with procyanidins concentrations at millimolar range. At these high ratios, it is probable that we have been focused only onto non-specific interactions which could explain why there are no major differences between the constants obtained when compared to the ones obtained by fluorescence quenching, where the interaction was studied at micromolar range of concentrations.

Table 5- K_A for the interaction between mucin and procyanidins (B4 and TT) determined by STD-NMR.

Procyanidin	Condition	K_A (M⁻¹)
B4	D ₂ O	5300*
	EtOH-d ₆	4820**
	DMSO-d ₆	4810**
TT	D ₂ O	4450*
	EtOH-d ₆	4430*
	DMSO-d ₆	3800**

*The confidence level is ≥87%.

**The confidence level is ≥90%.

A4. Conclusions

For the first time the study of the interaction between mucin and different procyanidins was evaluated by STD-NMR and fluorescence quenching. In general, both techniques allowed to evaluate the binding/affinity between those elements, giving different details about the interaction. Fluorescence quenching and STD-NMR were shown to be two complementary techniques, in which the first one gives information about the modification of protein structure induced by binding and allowed evaluation of the binding mechanism underlying to the interaction; from the second one, it is possible to know which structural features of the ligand are involved in the interaction.

The overall fluorescence quenching results demonstrated that the size and structural features of the procyanidins are related to their quenching ability. However, this is not always a linear relationship, since sometimes complex structures of procyanidins, as procyanidin TT, can present steric constraints that could be due to a lack of structural flexibility. Mucin-tannin interaction were affected by pH and IS, but also by the presence of solvents like EtOH and DMSO. When comparing the effect of solvents on the binding constants, hydrogen bonds seem to be more relevant for mucin interaction with GSF and procyanidin B4, than for mucin-TT interaction.

STD-NMR allowed information to be obtained about the affinity of the ligands for the protein and which structural features of the ligand are involved in the interaction. Both tannins, procyanidin B4 and procyanidin TT, demonstrated a great affinity towards mucin (high K_A). In the case of procyanidin B4 it was also possible to identify the proton H6 of ring D as the one with more affinity to interact with mucin.

Concerning the astringency sensation, the results herein provide unequivocally evidences that food procyanidins interact with mucins at molecular level and this interaction can compromise mucins lubricating functions.

B. Study of human salivary proline-rich proteins interaction with food tannins

Abstract

In this work, saturation transfer difference-NMR, isothermal microcalorimetry (ITC) and molecular dynamics (MD) simulations have been used to study the individual interactions between basic, glycosylated and acidic proline-rich proteins (bPRPs, gPRPs, aPRPs) and P-B peptide with some representative food tannins [procyanidin B2, procyanidin B2 3'-O-gallate (B2g) and procyanidin trimer (catechin-4–8-catechin-4–8-catechin)]. Results showed that P-B peptide was in general the salivary protein (SP) with higher affinity whereas aPRPs showed lower affinity to the studied procyanidins. Moreover, B2g was the procyanidin with higher affinity for all SP. Hydrophobic and hydrogen bonds were present in all interactions but the major driving force depended on the procyanidin-SP pair. Furthermore, proline clusters or residues in their vicinity were identified as the probable sites of proteins for interaction with procyanidins. For bPRP and aPRP a significant change to less extended conformations was observed, while P-B peptide did not display any structural rearrangement upon procyanidins binding.

B1. Introduction

Condensed tannins are polymers of flavan-3-ol units, namely (epi)catechin or (epi)gallocatechin, which are among the most abundant flavonoids in the human diet (e.g. red grapes, chocolate, red wine). These compounds have received high attention due to their health benefits, e.g. antioxidant and anticancer properties, neurodegenerative and cardiovascular protection [203]. Furthermore, these compounds are also related to the sensory properties of vegetable-derived food such as astringency and bitterness [204].

Astringency is usually a non-pleasant sensation mainly when perceived with high intensity. However, in some foodstuffs like red wine it is a quality parameter and desired in balanced levels. Astringency has been described as dryness, tightening and puckering sensations perceived in the oral cavity during the ingestion of foodstuffs rich in tannins [205]. Several mechanisms have been proposed for the astringency onset but the most accepted one relies on the interaction/precipitation of salivary proteins (SP), mainly proline-rich proteins (PRPs), by tannins [6].

SP are usually divided into several major classes including PRPs, statherin (stat), cystatins (cyst), P-B peptide and histatins that account for almost 50% of all SP [83]. PRPs, as the name suggests, are characterized by a high content in proline residues (25-42%). This family is divided in basic (bPRPs), acidic (aPRPs) and glycosylated (gPRPs) classes [206]. The differences between these classes depend on their charge and presence or absence of carbohydrates. aPRPs are characterized by a highly acidic N-terminal region, rich in aspartic and glutamic acid residues whilst its C-terminal is similar to bPRPs. They also present some phosphate groups throughout their structure (Ser 24, 33 and 38). Regarding gPRPs, they are bPRPs N- and O-glycosylated that present carbohydrates in 50% of their structure. These carbohydrates are composed of highly fucosylated N-linked saccharides; the major structure is a biantennary asialosaccharide containing 2 fucose residues on one antenna and an unsubstituted terminal lactosamine sequence on the other [207]. Salivary P-B peptide is usually included in the PRPs family due to high content in proline residues (near 50% of its sequence) but it shows higher similarities with salivary statherin [102]. P-B peptide structure is not similar to the PRPs structure as it shows the presence of several hydrophobic amino acid residues (such as Phe, Leu and Ile) and three tyrosine residues. Furthermore, P-B peptide is the product of a specific gene very close to STATH gene and is secreted as a mature protein not a degradation product of larger proteins. Besides this genetic correlation between the P-B and statherin, these two peptides show other highly significant correlations in whole saliva, such as a concentration dependence, as well as both being secreted by the same salivary glands (parotid and submandibular/sublingual glands). On the other hand, none of the two peptides shows a significant correlation with other PRPs. In this work P-B peptide is examined independently of bPRPs.

Most of astringency studies with SP are focused in bPRPs, which has been referred along the years as the one with the highest affinity for food tannins [208]. In fact, the major biological function attributed to bPRPs is the precipitation of food tannins impeding the subsequent deleterious effects of these compounds in the digestive system, whereas other PRPs have been described to mainly accomplish other functions, such as maintaining oral homeostasis in the case of aPRPs (Shimada, *et al.*, 2006). However, it seems that despite the main function attributed to the different families of the PRPs, most of them are able to precipitate tannins. In fact, some works (*in vitro* and *in vivo*) have shown that other SP different than bPRPs are highly reactive toward polyphenols, namely aPRPs and P-B peptide [209, 210]. Both works studied the protein precipitation in the presence of different tannins in a competitive assay when SP are present

simultaneously (saliva). Therefore, the aim of this work was to study the interactions between the fractions of bPRPs, gPRPs, aPRPs and P-B peptide separately with selected representative food tannins [procyanidin B2, procyanidin B2 3'-O-gallate (B2g) and a procyanidin trimer (catechin-4-8-catechin-4-8-catechin) (Figure 30)]. These tannins are present in a wide range of vegetables, fruits and derived products, namely, red wine, tea and beer [211].

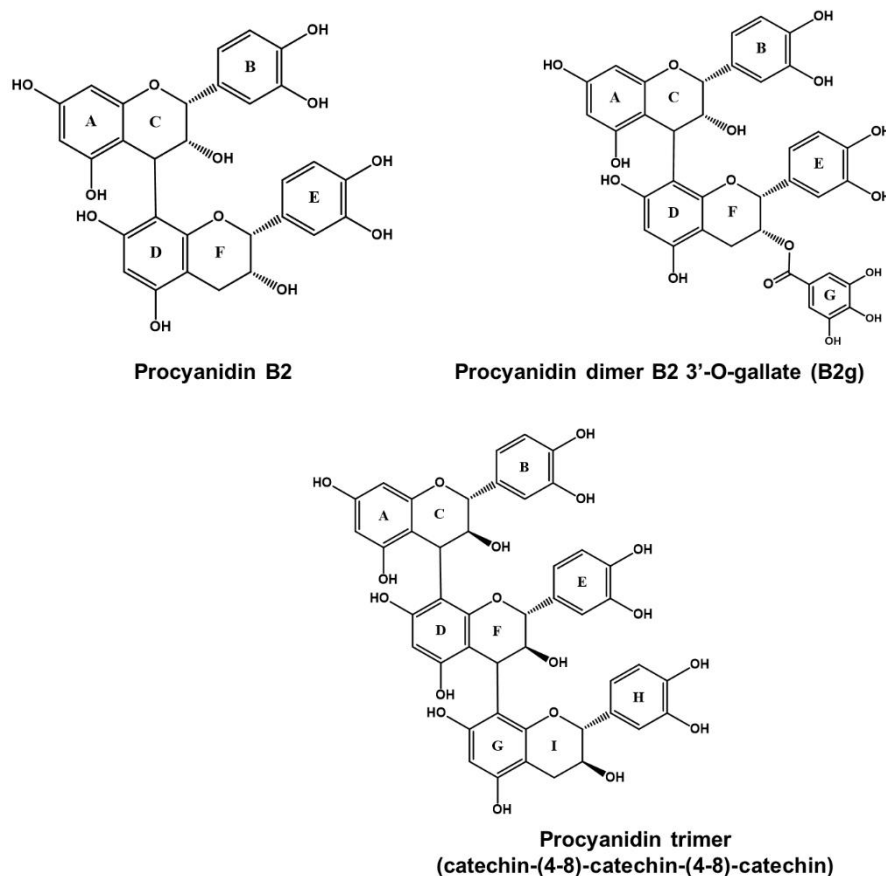


Figure 30 - Molecular structure of the procyanidins used in this work.

B2. Material and methods

B2.1. Isolation and identification of salivary proteins

Large volumes of unstimulated saliva were isolated from eighteen healthy volunteers and treated as reported previously [212]. After this treatment, saliva was dialyzed for 24h (cellulose membrane, MWCT 3.5 kDa) against water at 4°C with stirring. Water was replaced several times. Then, saliva was centrifuged, and the supernatant was freeze-dried. The resulting powdered saliva was solubilized in the minimal possible volume of water and filtered. The resulting solution was used to isolate the different families of

PRPs and P-B peptide by semi-preparative HPLC: HPLC equipped with reversed-phase C8 column (150 × 2.1 mm, 5µm), solvents were 0.2% aqueous TFA (A) and 0.2% TFA in ACN/water 80/20 (v/v) (B) and gradient applied was 10 to 45% of B in 40 min, at a flow rate of 0.60 mL·min⁻¹ and detection at 214 nm.

The several fractions of PRPs and P-B peptide were freeze-dried and the major proteins present in each fraction were identified by Electrospray Ionization-Mass Spectrometry (ESI-MS) by flow injection analysis into an LTQ Orbitrap XL mass spectrometer (Thermo Fischer Scientific, Bremen, Germany) controlled by LTQ Tune Plus 2.5.5 and Xcalibur 2.1.0. The capillary voltage of the Electrospray Ionization (ESI) was set to 3100 V. The capillary temperature was 275°C. The sheath gas flow rate (nitrogen) was set to 5 (arbitrary unit as provided by the software settings). The capillary voltage was 36 V and the tube lens voltage 110 V. Samples were diluted into a methanol/acetonitrile/TFA 0.01% (5:5:90 v/v) mixture 1:10 prior to analysis. After Mass Spectrometry analysis, deconvolution of mass spectra was done using the MagTran 1.03 software.

gPRPs molecular weight determination was performed by static light scattering (SLS) measurement with modifications [213]. Different concentrations of gPRPs were prepared in miliQ water and were measured at 25 °C. The average molecular weight was found to be about 16 kDa.

The study was conducted according to the Declaration of Helsinki and was submitted to Ethics Committee.

B2.2. Isolation of procyanidin dimer B2, procyanidin B2 3'-O-gallate (B2g) and procyanidin trimer

Procyanidin dimer B2 and procyanidin B2 3'-O-gallate (B2g) were isolated by preparative HPLC from a procyanidin fraction extracted from grape seeds (*Vitis vinifera*). Grape seeds were extracted as described previously yielding four fractions. Procyanidin B2g was isolated from fraction I and isolated according to the procedure described elsewhere [214].

Procyanidin trimer (catechin-(4-8)-catechin-(4-8)-catechin) was obtained by chemical synthesis between taxifolin and (+)-catechin as described in the literature [215]. After the reaction, the mixture was fractionated through a TSK Toyopearl HW-40(s) gel column (300 mm × 10 mm i.d., 0.8 mL·min⁻¹, methanol as eluent) and the fraction corresponding to the trimer fraction was recovered and analyzed by ESI-MS (Finnigan DECA XP PLUS). Spectroscopical data were in accordance with literature [216].

B2.3. Saturation transfer difference (STD)-NMR

Protein samples were prepared in D₂O containing 3 µM of each protein and the procyanidins were progressively added to the protein samples in the 0.1 to 3.5 mM ranges. To maintain protein concentration constant throughout the experiments, the procyanidins were lyophilized and added as a powder.

STD-NMR experiments were recorded on a Bruker Avance III 600 HD spectrometer, operating at 600.13 MHz, equipped with a 5 mm PATXI 1H/D-13C/15N and pulse gradient units capable of producing magnetic field pulsed gradients in the z direction of 50 G.cm⁻¹. The measurements were made with standard Bruker pulse sequences at 300 K. ¹H and STD spectra were recorded with a shaped pulse to suppress the water resonance using the following parameters: spectral width, 16 ppm; nutation angle, 7.08 µs and 90°; and shaped pulse duration, 2 ms. Selective saturation of the peptide off-resonance at 20 ppm and on-resonance at -1 ppm was performed using a pseudo-two-dimensional (2D) sequence for STD with a shaped pulse train alternating between the on and off resonances. STD-NMR spectra were acquired using Gauss 1.1000 pulses for selective saturation (50 ms), with a total saturation time of 2.5 s. The number of scans (16), receptor gain value (2030), and relaxation delay (3.5 s) were kept constants.

To process all the spectra, to baseline and phase corrections and to integrate the areas, TopSpin 2.1 software from Bruker was used. The binding constants (K_A) were determined using the following equations [193]:

$$A_{STD} = \frac{I_0 - I_{Sat}}{I_0} \times L/P \text{ molar ratio} = \frac{I_{STD}}{I_0} \times L/P \text{ molar ratio} = \frac{\alpha_{STD} \times [L]}{K_D + [L]} \quad (1)$$

$$K_A = \frac{1}{K_D} \quad (2)$$

where I₀ and I_{Sat} are the signal intensities off-resonance and on-resonance, respectively; and α_{STD} is the maximum amplification.

B2.4. Isothermal Titration Microcalorimetry (ITC)

ITC experiments were conducted at 298 K using a V-P MicroCalorimeter controlled by Origin VPViewer software. Aqueous solutions of each protein (between 20 to 30 μ M) and of procyanidins (titrant, between 1 to 10 mM) were prepared and degassed before titration. The sample cell was loaded with 1.4 mL of protein solution and titrant was loaded into the injection syringe. After baseline stability was achieved, procyanidin solution was injected (4 to 12 μ L/injection) into the sample cell 15 to 35 times until reaching stabilization. Spacing between injections was equal or higher than 350 s. Samples were stirred constantly at 307 rpm to ensure thorough mixing. Raw data obtained from a plot of heat flow vs. injection number were transformed using the AFFINIMETER software to construct a plot of enthalpy change vs. molar ratio. The resulting data were fitted in order to obtain the binding constant (K_A), the binding sites (n) and the thermodynamic parameters change for all the studied SP-procyanidins interaction.

B2.5. Molecular Dynamics Simulation (MD)

Several molecular systems composed by some human salivary proline-rich peptides and B2 and B2g molecules were built to evaluate the interaction between these compounds (detailed experimental conditions in Supplementary Information). In brief, an explicit solvation model (TIP3P water molecules) was used, filling a truncated rectangular box with a minimum distance of 15 Å until any atom of each system. Three different simulations were performed for each system: 1) with one peptide (IB-8b, PRP1, PRP3 or P-B peptide); 2) with one peptide and one molecule of B2 or B2g; and 3) with four B2 or B2g molecules randomly positioned near the peptide (to reproduce the experimental conditions). The temperature was maintained at 303.15 K using a Langevin dynamics thermostat [217]. All MD simulations were performed using the AMBER 12.0 simulations package [218]. In literature, similar protocols using MD simulations were successfully applied to study the interaction of tannins and catechin to SP [219-221]

B3. Results

The interaction between different families of SP (bPRPs, gPRPs, aPRPs and P-B peptide) and some representative tannins [procyanidin dimer B2, procyanidin B2g and procyanidin trimer (catechin-(4-8)-catechin-(4-8)-catechin)] was studied by two

molecular and complementary techniques, STD-NMR and ITC, as well as by MD simulations.

B3.1. Identification of the major salivary proteins

The identification of the major SP present in the fractions isolated from human saliva was obtained by Mass Spectrometry using a proteomic approach. The HPLC semi-preparative chromatogram displaying the different SP families and the deconvoluted mass spectra of each PRPs family is presented in Figure 31 [222].

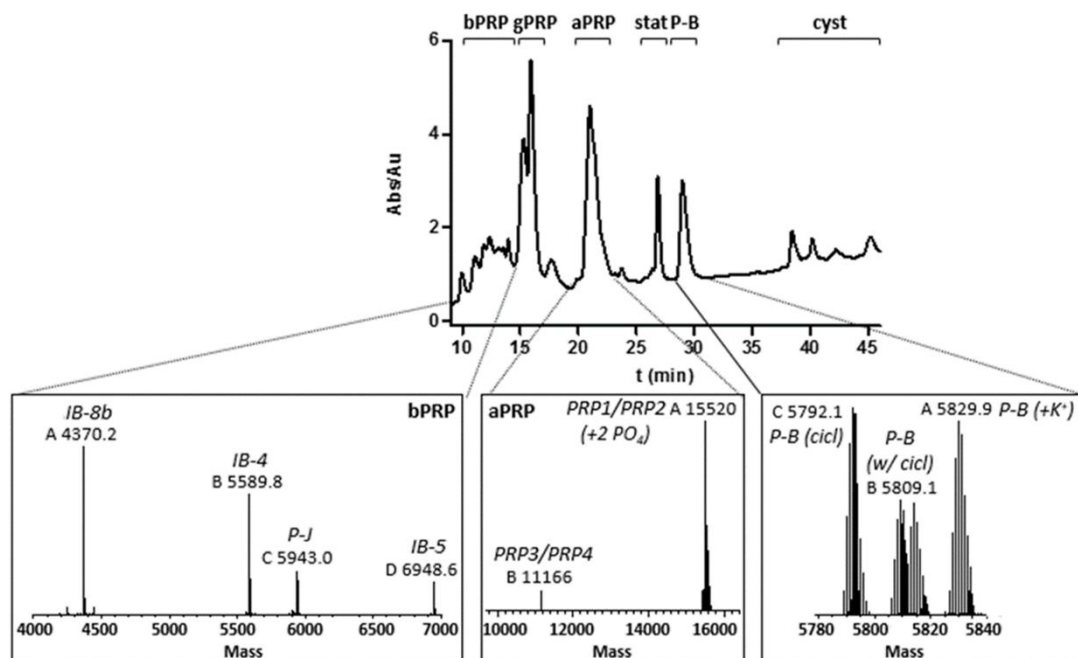


Figure 31 - RP-HPLC profile (214 nm) of the acidified saliva used to isolate the different fractions corresponding to the families of PRPs and P-B peptide (upper figure). The identity of the SP families eluted in the different fractions are indicated in the top of the chromatogram. In the bottom, the deconvolution of the mass spectrum outlining the main proteins identified for each HPLC fraction is displayed.

From mass analysis, IB-8b and IB-4 were identified as the major proteins of bPRPs fraction which also contains P-J and IB-5 proteins. aPRPs fraction contains PRP1 and PRP3. Regarding P-B peptide fraction, the presence of two isoforms was identified, one with the cyclization of the N-terminal glutamine residue that spontaneously cyclize to pyroglutamate and one without this cyclization. Regarding gPRP, due to the existence of carbohydrates in their structure the direct analysis by Mass Spectrometry is highly complex. So, in order to identify the proteins present, this fraction was digested with

trypsin and the hydrolysis product was analyzed by Mass Spectrometry and identified by MASCOT protein database which has parotid salivary glycoprotein G1.

After identification of the major proteins, the average molecular weight of each fraction was estimated based on ESI-MS signals intensity: bPRP (5388 Da), aPRP (14643 Da) and P-B peptide (5792 Da). gPRP average molecular weight was determined to be 16000 Da by SLS.

B3.2. Interaction of the different salivary proteins with procyanidins by STD-NMR

The ^1H chemical shifts for procyanidin B2, procyanidin B2g and procyanidin trimer (catechin-(4-8)-catechin-(4-8)-catechin) were identified based on the literature (Figure 32) [216, 223]

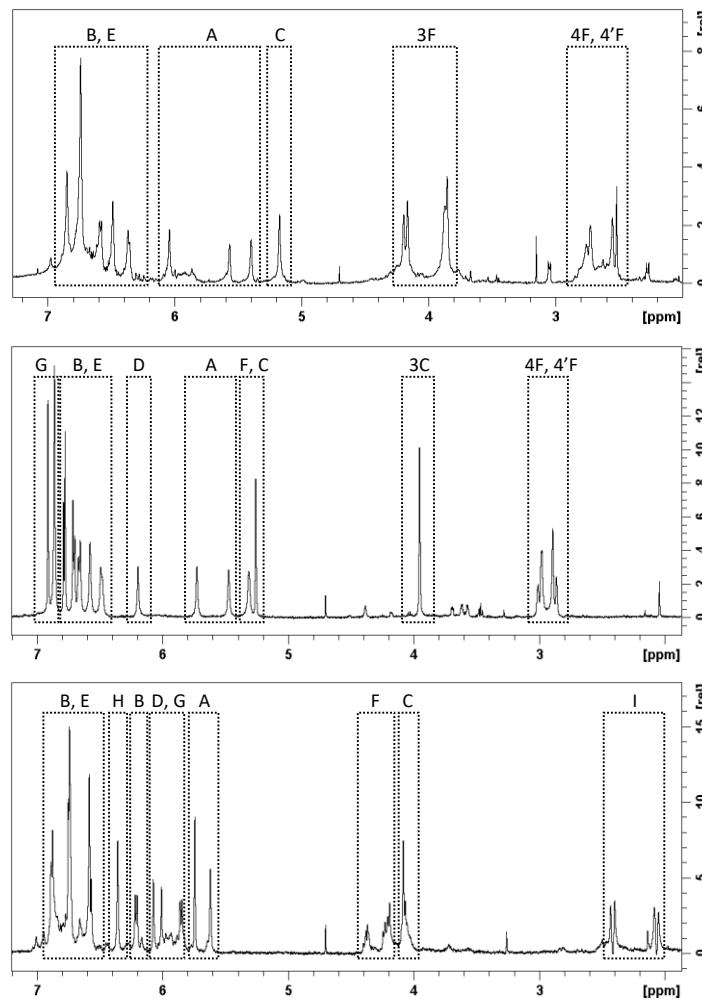


Figure 32 - Proton spectra of procyanidin dimer B2 (up), procyanidin B2g (middle) and procyanidin trimer (bottom) showing the 7.5-2.0 ppm region where most protons resonate. Spectra were recorded at 600 MHz and 300 K in deuterium oxide (D_2O).

The STD-NMR technique allows procyanidin binding epitopes to be identified, as well as to estimate binding constants (K_A) [17, 224, 225]. Primary control STD-NMR experiments at high procyanidin concentrations were made in order to confirm that the on-resonance irradiation frequency did not affect the procyanidin protons and that each protein was saturated by the on-resonance irradiation. The procyanidins aromatic protons resonances were not visible at these control conditions.

Figure 33 (left side) presents STD-NMR spectra titration obtained for the interaction between aPRP and increasing concentrations of procyanidins. After establishing the experimental parameters and testing several concentrations of protein and ligand, it was only possible to obtain STD-NMR signals on the [tannin]/[protein] molar ratio range from 30 to 1000. For dimers B2 and B2g, it is possible to observe that at low concentrations (i.e. ratios of 38 – 288) only appear signals of protons from rings B, E and G (at 6.8 ppm region). When the concentration increased, signals due to other protons appeared, namely protons at 2.8 ppm for procyanidin B2 (ring F) and protons at 6.6 – 5.0 and at 4.0 ppm for procyanidin B2g. For procyanidin trimer most protons signals' (7.0 – 5.0 ppm) appear at the lowest concentrations.

This behavior was also observed for the interaction with the other proteins bPRPs, gPRPs and P-B peptide (Supplementary Information, Figures S1 to S3).

The protons that presented the highest intensities in the STD spectrum were used to perform a STD-NMR titration for each protein/tannin pair. The STD amplification factor (A_{STD}) was calculated from the differences between on-resonance and off-resonance spectra with increasing procyanidins concentration, according to Eq. 1 (Experimental Section). The respective STD titration graphs obtained for the interaction between aPRPs with increasing concentrations of each studied procyanidin are shown in Figure 33 (right side). Similar graphics were obtained for the other SP studied (see Figures S1, S2 and S3 in supplementary information).

It is possible to observe that the STD signal increases systematically with concentration until it reaches a plateau of maximum interaction. This plateau is dependent on the procyanidin:protein system.

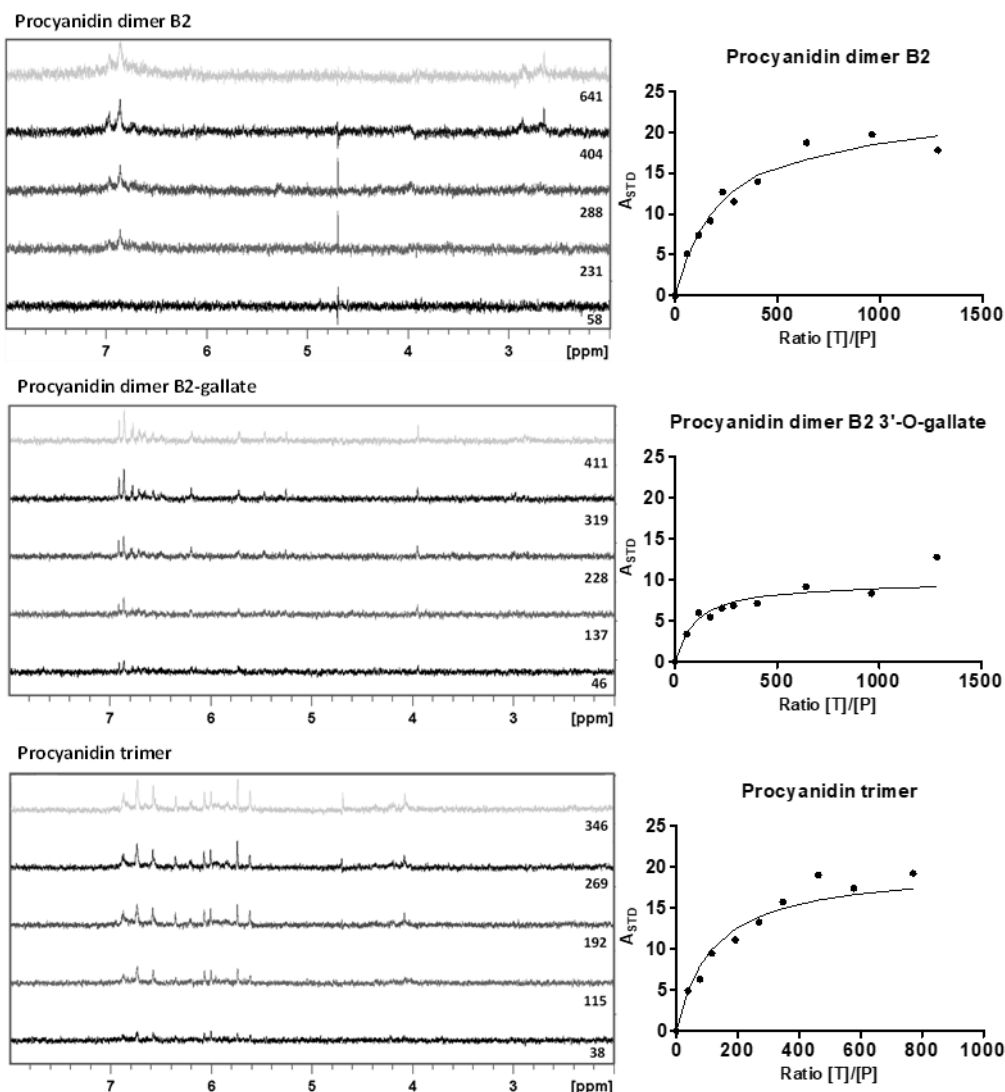


Figure 33 - Right side: STD-NMR spectra for the interaction between aPRP (3.0 μ M) and the different procyanidins (procyanidin dimer B2, procyanidin B2g and procyanidin trimer catechin-(4-8)-catechin-(4-8)-catechin) at different procyanidins molar ratios (indicated by numbers) (38-641) showing the 8.0-2.0 ppm region where most protons resonate. Spectra were recorded at 600 MHz and 300 K in deuterium oxide (D_2O). Left side: STD amplification factor (ASTD) for the interaction between aPRP (3.0 μ M) and procyanidin dimer B2, procyanidin B2g and procyanidin trimer. Symbols represent experimental values and lines represent theoretical values by Eq. 1.

The K_A for each interaction was estimated according to Eq. 2 (Experimental Section). The K_A obtained range from 910 to 5561 M⁻¹ (Table 6) and, in general, have similar magnitude. However, procyanidin trimer tend to have a K_A higher than the procyanidin dimer. This is evident for bPRPs, aPRPs and P-B peptide but not for gPRPs which presents a similar K_A for all procyanidins.

Such a tendency was not observed for procyanidin B2g. For bPRP, procyanidin B2g had the lowest K_A while for gPRPs and aPRPs procyanidin B2g had the highest K_A . Comparing the interaction of the different SP with the same procyanidin, in general, there

are no important differences. P-B peptide and bPRPs were the proteins with lowest K_A ($< 1000 \text{ M}^{-1}$) for the interaction with procyanidin B2 and B2g, respectively. In fact, bPRPs were the SP that presented both the lowest and the highest K_A depending on the tannin, procyanidin B2g and trimer, respectively. Regarding procyanidin trimer the K_A was quite similar for all SP.

Table 6 - Binding constant (K_A) values determined for the interaction between each protein family and the procyanidins dimer B2, B2g and trimer by STD-NMR.

Protein	$K_A (\text{M}^{-1})$		
	Procyanidin B2 (MW = 578)	Procyanidin B2g (MW = 730)	Procyanidin Trimer (MW = 866)
bPRP	2560**	910*	5561*
gPRP	5000*	4005*	3850*
aPRP	1390*	3330*	2861**
P-B	930*	3030*	4170*

*The confidence level is $\geq 85\%$.

**The confidence level is $\geq 73\%$.

B3.3. Interaction of the different SP with procyanidins by ITC

ITC is a more sensitive technique comparatively to STD-NMR and allows the interaction between protein and tannin to be studied at lower molar ratios ([T]/[P] 0 to 60). Figure 34 presents the ITC titration of aPRP with the three procyanidins studied. The peak areas were plotted against the procyanidin-to-protein molar ratio and the resulting curve was fitted with the AFFINIMETER software using the independent sites model.

Figure 34 shows that the interaction of aPRP with all the procyanidins (upper graphics) has two phases resulting in an “inverted bell” curve. This could point out that, the binding sites occupied at the beginning of the interaction are mainly binding sites with a less exothermic behavior, whereas after a few injections, the occupation of more exothermic binding sites becomes more important, which implies more energy generated. In fact during the first ten injections there was energy generated that increased reaching a plateau at -2 kJ/mol for B2, -5.0 kJ/mol for B2g and -3.5 kJ/mol for procyanidin trimer. Then, the energy generated decreased, corresponding to saturation of protein binding sites at tannin:protein molar ratios in excess. A similar behavior was observed for bPRP and gPRP interaction with all the procyanidins (Supplementary Information, Figures S4

and S5). As in previous reported studies, data were best fitted as independent sites model with two set of sites, each with different binding strengths [226, 227].

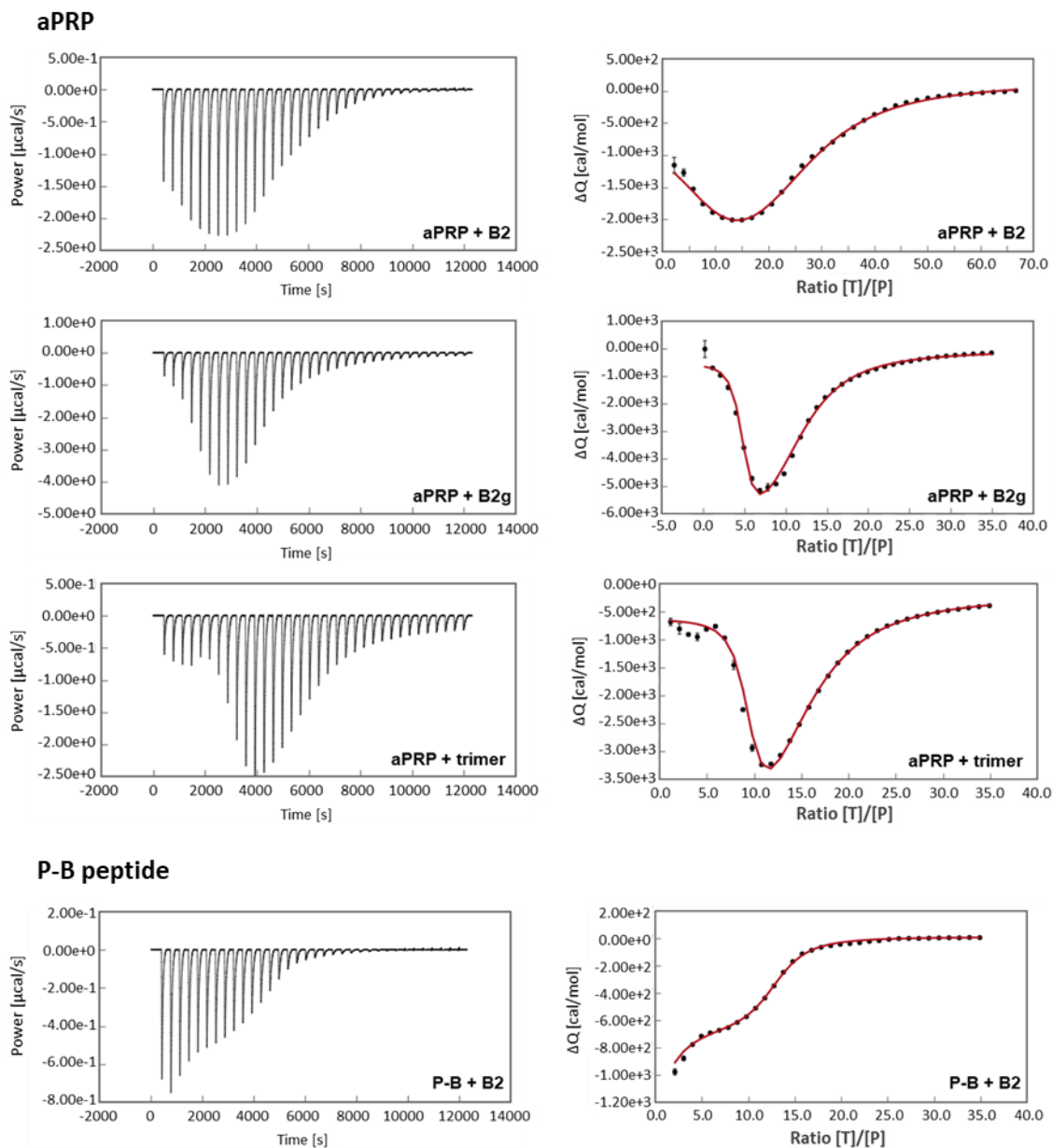


Figure 34 - ITC interaction of aPRP ($30 \mu\text{M}$) (upper) and P-B peptide (lower) with procyanidin B2, procyanidin B2g and procyanidin trimer: thermogram (left side) and binding isotherm (points) and fitting curve (line) (right side). The data for the interaction with procyanidin B2g and trimer are presented in Figures S4, S5 and S6 of Supplementary Information.

For the P-B peptide a different behavior was observed for the interaction with all procyanidins (Figure 34 and Figure S6 of Supplementary Information). In each case a two-phase sigmoidal curve was observed with a plateau around 5 to 10 molar ratio.

The K_A and number of binding sites in protein for each interaction are summarized in Table 7.

Table 7 - Binding constant (K_A) values determined for the interaction between each protein family and the procyanidins dimer B2, B2g and trimer by ITC. The number of binding sites (n) on the protein was also determined by ITC. Set (1,2 or 2,2) refers to the individual parameters for each set of sites.

Protein	Set	B2		B2g		Trimer	
		n	$K_A (10^6 M^{-1})$	n	$K_A (10^6 M^{-1})$	n	$K_A (10^6 M^{-1})$
bPRP	(1,2)	3.2±0.1	0.88±0.4	3.7±0.1	12.0±5.0	11.1±10.4	4.5±1.4
	(2,2)	7.1±0.2	0.080±0.001	5.1±0.2	0.8±0.3	10.2±9.6	0.020±0.005
gPRP	(1,2)	9.1±0.2	1.3±0.3	10.8±0.2	11.2±2.2	19.6±2.1	1.6±0.1
	(2,2)	10.2±0.3	0.02±0.01	6.7±0.2	0.27±0.03	10.1±1.0	0.030±0.001
aPRP	(1,2)	11.9±0.8	0.006±0.001	4.6±0.1	1.45±0.03	7.1±0.1	1.270±0.002
	(2,2)	21.2±1.7	0.009±0.003	7.4±0.4	0.020±0.001	4.8±0.1	0.010±0.001
P-B	(1,2)	1.0±0.1	0.99±0.02	5.9±0.1	83.5±8.6	1.0±0.1	0.27±0.01
	(2,2)	12.0±0.1	0.15±0.01	10.6±0.1	1.4±0.2	14.9±0.02	0.400±0.001

The values obtained for the K_A present a wide range from 0.009 to $83.5 \times 10^6 M^{-1}$. It was observed for all interactions that the first set of sites (1,2) had always higher K_A than the second set of sites (2,2). In general, it was also observed that B2g was the compound with the highest K_A for all the SP studied, followed by procyanidin trimer. Procyanidin dimer B2 was the compound with lowest K_A .

An overall trend could not be observed regarding the protein number of binding sites (n). From these results, it might be ascertained that, for bPRPs and gPRPs, procyanidin trimer could be the procyanidin that interact with the protein through the highest number of binding sites onto the proteins (21 and 30 sites, respectively). For aPRP, procyanidin dimer B2 showed the highest value of n (33 sites) whereas for P-B peptide the number of binding sites would be similar for all tannins. Comparing the procyanidins it was observed for procyanidin B2 and B2g that n of set (1,2) was always lower than of set (2,2), with the exception of B2g-gPRP interaction.

Beside these parameters, the ITC results also yielded thermodynamic parameters to characterize the interaction between SP and the studied ligands (Supplementary Information, Table S1). From these individual parameters the global thermodynamic values for each interaction were determined (Table 8).

Table 8 - Global thermodynamic parameters (ΔH , ΔG and $-T\Delta S$), number of protein binding sites (n) and global binding constants (K_A) for the interaction between procyanidins dimer B2, B2 gallate and trimer and SP (bPRPs, gPRPs, aPRPs and P-B).

Protein	n	B2				B2g				Trimer					
		ΔH [cal.mol $^{-1}$]	ΔG [kcal.mol $^{-1}$]	$-T\Delta S$ [kcal.mol $^{-1}$]	K_A (10 11 M $^{-2}$)	n	ΔH [cal.mol $^{-1}$]	ΔG [kcal.mol $^{-1}$]	$-T\Delta S$ [kcal.mol $^{-1}$]	K_A (10 11 M $^{-2}$)	n	ΔH [cal.mol $^{-1}$]	ΔG [kcal.mol $^{-1}$]	$-T\Delta S$ [kcal.mol $^{-1}$]	K_A (10 11 M $^{-2}$)
bPRP	10.3	-271.9	-14.8	-14.5	0.70	8.8	175.4	-17.8	-17.9	96.00	21.3	-4286.0	-15.0	-10.7	0.903
gPRP	19.3	-393.7	-14.3	-13.9	0.26	17.5	335.9	-17.9	-17.3	30.24	29.7	-362.7	-14.6	-14.2	0.49
aPRP	33.1	-4555.3	-11.9	-7.3	0.00054	12.0	-8483.3	-14.3	-5.8	0.29	11.9	-6852.5	-13.8	-6.9	0.13
P-B	13.0	-3547.0	-15.2	-15.2	1.49	16.5	-3053.3	-19.2	-16.1	11161.07	15.9	-3134.3	-15.0	-11.9	1.08

ΔH – enthalpy, ΔG – free Gibbs energy, ΔS – entropy, T – temperature.

The global Gibbs free energy (ΔG) is negative for all interactions, which is a requirement for a spontaneous biological interaction. The entropy change was highly positive for most interactions which means that they are entropically driven interactions. Enthalpy change was highly negative for most cases.

B3.4. Interaction of the different SP with procyanidins by MD

To further characterize the interaction between procyanidin B2 and B2g molecules with some representative human SP, computational studies were additionally carried out. These will help to understand at an atomistic level the different steps that drive their recognition and binding processes. MD simulations with only one tannin molecule [PRP:(B2)₁] and four tannin molecules [PRP:(B2)₄] were done to evaluate the specificity of the interaction and avoid the auto-association of procyanidin molecules [228, 229]. It was observed in the interaction of PRP:(B2)₁ for all four proteins (PRP1, PRP3, IB-8b and P-B) a different time of binding: starting at 0.78 ns, 1.04 ns, 14.6 ns and 0.82 ns for PRP1, PRP3, IB-8b and P-B, respectively. A similar scenario was observed for B2g molecules.

In general, the results of MD simulations with model systems showed a very dynamic interaction with procyanidin molecules binding and unbinding the PRPs during the simulation. At the same time, the results of MD simulations confirm the formation of stable complexes involving the B2 molecules and residues of these SP. So, in order to compare the interaction of PRP-B2 and PRP-B2g complexes, different time indicators (total binding time: sum of each time procyanidins were bound to protein) were obtained for each MD simulation (Table 9).

Table 9 - Procyanidins binding time (simultaneously bound to proteins) of B2 and B2g molecules to the various peptides (PRP1, PRP3, IB-8b and P-B peptide) for a PRP:(T)_n model.

B2	PRP1:(B2) _n	PRP3:(B2) _n	IB-8b:(B2) _n	P-B:(B2) _n
total binding time of n procyanidins (ns) (n = 2)	1.8	1.2	8.2	22.2
total binding time of n procyanidins (ns) (n = 3)	12.9	8.8	11.7	24.6
total binding time of n procyanidins (ns) (n = 4)	32.8	39.4	29.6	2.1
B2g	PRP1:(B2g) _n	PRP3:(B2g) _n	IB-8b:(B2g) _n	P-B:(B2g) _n
total binding time of n procyanidins (ns) (n = 2)	7.4	8.9	5.5	1.5
total binding time of n procyanidins (ns) (n = 3)	38.8	40.3	9.0	5.4
total binding time of n procyanidins (ns) (n = 4)	1.4	0.0	34.3	39.3

For procyanidin B2, the total binding time of four molecules was higher for PRP3:(B2)₄, followed by PRP1:(B2)₄, and IB-8b:(B2)₄. P-B:(B2)₄ presented significantly smaller binding time of four B2 molecules. However, it is noteworthy that for two or three B2 molecules the total binding time of P-B was the highest (22.2 and 24.6 ns, respectively).

For procyanidin B2g, the total binding time of four molecules was significantly higher for IB-8b:(B2g)₄ and P-B:(B2g)₄, with 34.3 and 39.3 ns respectively. PRP3:(B2g)₄ and PRP1:(B2g)₄ showed almost negligible ability to bind to four B2g molecules (< 1.5 ns), although they showed high total binding times in the case of three molecules of procyanidin (40.3 and 38.8 ns, respectively).

Significant conformational changes of PRP1, PRP3 and IB-8b peptides, from extended forms to a coiled one, were observed along the simulations for both B2 and B2g (Figure 35). For PRP1 these changes were slightly greater for B2 than for B2g while for PRP3 this decrease was equivalent for B2 and B2g (ca. 36-37% in length). For IB-8b the decrease in length was much stronger for B2g (from ca. 68.2 Å to 12.3 Å), representing an 82% decrease in length.

Moreover, MD simulation allowed the identification of the amino acid residues mainly involved in hydrogen bonds (H-bonds) (Supplementary Information, Tables S2 and S3) whilst it was not possible to identify the hydrophobic spots. The short length of the H-bonds reported demonstrates the importance of these bonds in the stabilization of B2 and B2g complexes with PRPs. For all the proteins studied, it has to be noted the importance of backbone Pro resides in the establishment of these bonds. For aPRPs and IB-8b, residues from the backbone and the side chains are involved in H-bonds, mainly through the carbonyl groups of Pro, Asp, Gln, Gly, Ser and Leu. For P-B, the main amino acid residues involved in H-bonds are Pro, Tyr and Gly. Some of these residues (Pro, Gln and Gly) have been already identified to be involved in similar interactions [219]

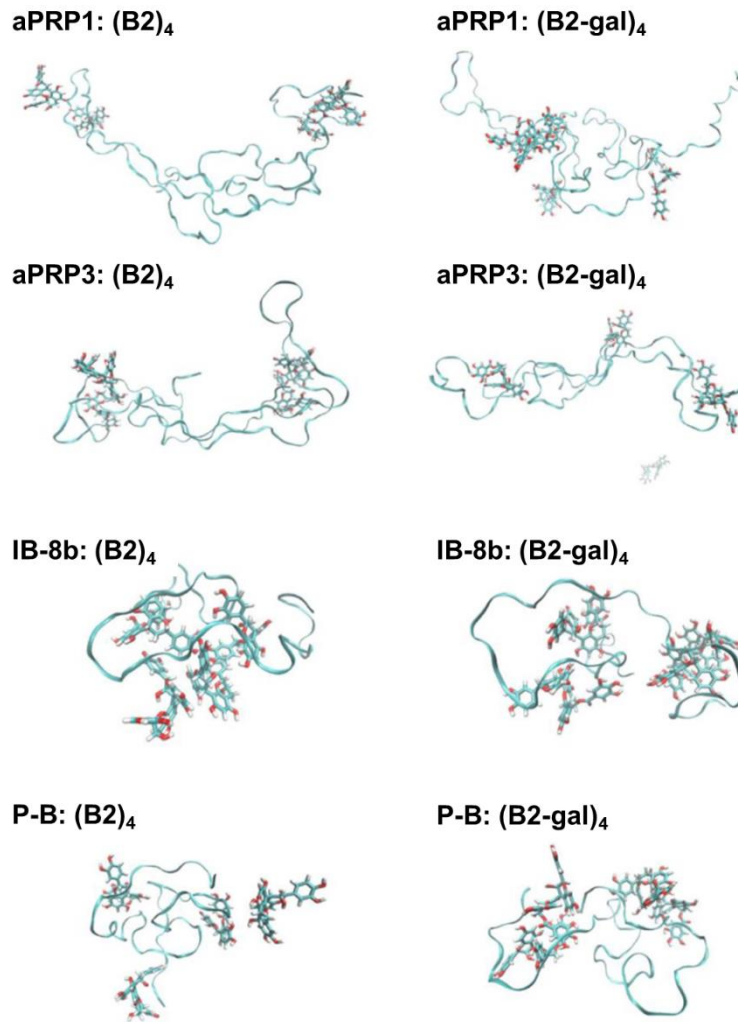


Figure 35 - Illustration of representative geometries reflecting the maximum capacity of interaction for each PRP:(B2)₄ and PRP:(B2-gal)₄ complex and information about the conformation changes (head-to-head distances) observed in the simulations with B2 and B2g.

B4. Discussion

B4.1. Procyanidin epitopes of binding

STD-NMR experiments have been proved useful to characterize ligand-protein complexes allowing determination of the ligand binding epitopes. From the results, it was observed that for low concentrations of procyanidin B2 the first epitopes involved in the interaction are rings B and E. The engagement of these two rings was already observed for other procyanidin systems involving B3 interaction with trypsin enzyme and with small PRP peptides (IB₉₃₇ and IB₇₁₄) [215, 219, 221]. For low concentrations of procyanidin B2g the first epitopes involved in the interaction were the ring G followed by rings B and E. When concentration increases, it was observed that ring F of procyanidin B2 and rings A, C and F of procyanidin B2g also seem to be involved in these interactions. On the

contrary, for procyanidin trimer it seems that all the structure is involved in the interactions in all concentration ranges. These results indicated that tannins could act as multidentate ligands, with one region of the molecule being favored for the initial interaction and the other parts of the procyanidin participating in the interaction when concentration increases. This is not exactly what happens for procyanidin trimer which seems to be less selective.

B4.2. Specificity of salivary protein-procyanidin interaction (binding constants)

STD-NMR technique also allows to estimate the magnitude of binding constant (K_A) of protein-ligand interactions [17, 224, 225]. So, besides gathering insights about the procyanidins epitopes involved in the interaction, STD-NMR spectroscopy was also used to estimate the affinity of the interaction between procyanidins and each PRPs family. The values obtained are in the same magnitude as the ones reported in the literature for similar interactions (proline-rich peptide IB7₁₄ interaction with procyanidin dimers B1 to B4 and trimer) [219]. From the yielded data, it was possible to observe that the structure/molecular weight of procyanidins affects the interaction with aPRPs, bPRPs and P-B peptide. For gPRP, it seems that the structure of the studied procyanidins has only a small effect on the interaction. This lack of selectivity has been previously observed by Lu and Bennick who compared the ability of gPRPs to precipitate condensed tannins (quebracho extract) and tannic acid [208] and attributed this similar reactivity to the presence of a sugar moiety in the protein structure. The same authors observed that deglycosylation of gPRPs led to an increase of the interaction as well as in selectivity. For aPRP and P-B peptide it is clear that the interaction increases with tannin molecular weight. This was also observed for bPRP interaction with procyanidin B2 and procyanidin trimer.

STD experiments only cover the interaction for high ratios of procyanidin/salivary protein ([T]/[P], 38-1000) (high procyanidin concentrations). It is well known that the interaction between tannins and proteins depends partially on the concentration and molar ratio of both. This has been previously reported for the interaction with a similar procyanidin, procyanidin B3 [215]. It is possible that the molar ratios studied correspond to the non-specific part of the mechanism, when tannin acts as multidentate ligand. In fact, tannins could occur as aggregated forms at higher tannin concentrations (even below their critical micellar concentration) which could be accounted for nonspecific interaction to occur with proteins [221].

In order to get more insights about the affinities at low [T]/[P] ratios, ITC experiments were performed and focused on low ratios procyanidin/salivary protein. ITC technique was used to study the thermodynamic parameters of protein-ligand interaction and allows determination of K_A' . This technique has already been applied to study the interaction between procyanidins and proteins [226, 230].

In order to compare all the interactions, the global affinity was calculated by the product of the individual values (Table 8). The magnitude of the constants estimated by STD-NMR and ITC are comparatively different which is probably related to the different concentrations and [T]/[P] ratios used for each technique.

Regarding the influence of procyanidin structure, it was observed an important increase in K_A' from procyanidin dimer B2 to procyanidin B2g for all SP studied. However, galloylation of procyanidin B2 increases much more the interaction with P-B and aPRP rather than with bPRP and gPRP. Regarding the trimer, it showed a K_A' similar or slightly higher for all salivary proteins tested comparing to procyanidin B2. This seems to indicate that galloylation superpose the influence of molecular weight from dimer to trimer in the interaction with proteins. There are few works that study the influence of galloylation on these interactions. Canon *et al.* have observed that the complexes between IB5 and B2g have a higher stability to the complexes obtained with B2 [231]. Latter, these authors have attributed this to the more compact conformation of B2g predominant in solution when compared to the more extended procyanidin B2 [232]. This allows B2g to establish a higher number of hydrogen bonds which, herein, could explain the higher K_A' observed when compared to procyanidin trimer. In fact, the contribution of hydrogen bonds in the interaction between B2g with aPRPs and P-B is higher than in the case of bPRPs and gPRPs, as can be observed both by the enthalpy changes and the MD simulations results discussed ahead.

Also, the lower affinity of trimer could be related to stereochemical restraints related to the size and to a more extended conformation of the several trimer rotamers present in solution [233].

In brief, the MD results suggest that proanthocyanidin B2 and B2g molecules interact highly and stably with the four SP studied. In the case of B2, the total binding time of complexes with less than four procyanidin molecules were higher for IB-8b (bPRP) and P-B, despite the highest total binding time to bind simultaneously four molecules was observed for aPRPs (PRP1 and PRP3). This could be related to the size of the proteins

since aPRPs are bigger proteins while bPRPs and P-B peptide are much smaller proteins.

Regarding B2g, IB-8b (bPRP) and P-B proteins were the proteins that interacted with four molecules through more time which could be related to the strength of the interaction. In fact, on the basis of ITC results, it seems that the interaction of B2g with both bPRPs and P-B is stronger than with aPRPs.

In general, MD simulations observed that once established, the interaction of procyanidins with the peptides remained well formed along the rest of the simulation, indicating the higher stability of these interactions.

B4.3. Type of bonds involved in salivary protein-procyanidin interaction

All classes of PRPs (bPRPs, gPRPs and aPRPs) presented a similar ITC behavior for the interaction with all procyanidins (“inverted bell” curve) while P-B peptide presented a different behavior (two-sigmoidal phase curve). This is highly related to changes in entropy or enthalpy energy terms which can be related to the type of bonds involved in the interaction. The ITC “inverted bell” curve observed for most interactions, has been previously observed for the interaction of a proline-rich peptide (poly-L-proline) with procyanidins [226, 234]. In addition, all the ITC curves show that the process reaches a plateau in the second phase (saturation) [229].

All the experimental data were fitted by “two independent set of sites model”. This treatment has been previously reported for similar interactions [200, 235].

The interaction between these macromolecules is highly complex, and therefore the interpretation of thermodynamic changes will be necessarily generalized. The thermodynamic parameters allowed the type of bonds involved in each interaction to be investigated. Enthalpy (ΔH) indicates changes in hydrogen bonds, while entropy ($-T\Delta S$) indicates changes in hydrophobic interaction and conformational changes. In this case, since PRP are unstructured proteins, the changes in entropy could be mainly associated with the displacement of structured water molecules on the tannin as a result of hydrophobic interactions with protein apolar residues. This dislocates the structured water that has a higher heat capacity than the bulk water. As hydrophobic interaction takes place, structured water is displaced leading to an enthalpy increase.

The global thermodynamic parameters were determined by adding the individual enthalpy or free energy terms and calculating the global $-\Delta TS$ term through the equation $\Delta G = \Delta H - T\Delta S$ (Table 8).

In general, the interaction of SP with procyanidins was shown to be due to both hydrophobic interactions and hydrogen bonding, as already observed in other works [234]. The balance of entropy and enthalpy terms give an idea about the relative contribution of each type of bonding. This contribution was different for each case. The global entropy term was always positive, although with lower magnitude for aPRP interaction with B2g, trimer and B2. The global enthalpy term was negative for most interactions, except for bPRP and gPRP interaction with B2g. The balance of entropy and enthalpy terms means that hydrophobic interactions are favored as main driving forces of the whole interaction for bPRPs interaction with B2 and B2g as well as for gPRPs interaction with all procyanidins. This has already been observed in other works [226]. Regarding bPRPs interaction with procyanidin trimer it seems that both type of bonds contribute to the interaction.

For aPRPs interaction with all procyanidins it was observed a dominance of hydrogen bonds mainly for the interaction with B2g and trimer. It is interesting that this happens only for aPRPs which present an N-terminal with acidic residues which could be more prone to establish hydrogen bonds. So, this region could be actively involved in the second phase of the interaction with procyanidins. In fact, the MD results show that 70% of the aPRPs residues that establish hydrogen bonds with B2g are located in this acidic N-terminal.

Some researchers have considered that interactions might be either specific if they are driven by hydrogen bonding or nonspecific if they are ruled by π - π stacking [219, 236]. The present work gathered evidences that the situation is not so well dichotomized and that both hydrophobic and hydrophilic interactions can play complementary roles in the network formation depending on the protein and procyanidin structures.

B4.4. Protein binding sites on salivary protein-procyanidin interaction

The thermodynamic parameters allowed the total number of protein binding sites to be determined for each interaction (Table 8). It could be worth to mention that the observation of binding sites with different affinity could be due to different affinity between the proteins present in the same fraction. However, attending that the interactions were studied for mixtures of SP that present a high similarity among them, the number of

binding sites will be considered as a mean for each family of SP. It was observed that bPRP and gPRP have a lower number of binding sites for B2 than for trimer. The opposite tendency was observed for aPRP. For P-B it was observed a small increase in the number of binding sites for procyanidin B2g and trimer, which is interesting since P-B was the only SP studied that did not present a significant structural rearrangement upon procyanidins binding. This could mean that the interacting residues are available in a similar way upon binding, being able to interact with more procyanidin molecules. Furthermore, from MD results it was observed an increase on the P-B number of binding sites from B2 to B2g. Oppositely, IB-8b (bPRPs) and aPRPs, showed significant conformational changes from an extended conformation to a coiled one. Similar conformational rearrangements were previously described for the interaction between tannins and PRPs [221, 237, 238].

It is noteworthy that looking at the two set of protein binding sites ($[n(1,2)$ and $n(2,2)$]), they do not participate in the interaction in a sequence manner: the processes described by each set of protein binding sites $n(1,2)$ and $n(2,2)$ may occur simultaneously. However, the processes described by the first set of sites $n(1,2)$ seem to be predominant at lower tannin-to-protein ratios and present a higher K_A . It is also known from the literature and in agreement with STD-NMR results that at higher tannin-to-protein ratio, tannin can act as mono- and/or multidentate ligand. This ability allows procyanidins to have an extensive occupation of more sites into protein molecules, which is in accordance with higher $n(2,2)$ binding sites (Table S1, Supplementary Information).

Regarding the different SP, a similar behavior was observed for $n(1,2)$ of bPRPs and gPRPs for which the number of protein binding sites increased with procyanidins molecular weight. This similar behavior is interesting because these families of proteins are highly structurally related.

It has to be noted that looking at the sequence of each bPRP identified in bPRPs fraction (Uniprot database), the number of regions with two or more proline residues (proline clusters) (4 to 8 clusters/protein) are in the same range as the number of protein binding sites. IB-8b has one cluster with six proline residues, one with three and five clusters with two proline residues. IB-5 has one cluster with five proline residues, one with four, one with three and two clusters with two proline residues. IB-4 has one cluster with one and six clusters with two proline residues.

This could indicate that proline clusters could be the favored binding site and the first spot [$n(1,2)$] of specific interaction between procyanidin and bPRPs. In fact, of all the

residues of IB-8b that establish H bonds with B2 and B2g (five and nine, respectively) identified by MD simulations, three proline residues were located on these clusters and the other residues were in the near of a proline residue.

As it was observed for bPRP, the regions of aPRPs responsible for the interaction seem to be the clusters of proline residues. PRP1 has eleven and PRP3 has seven proline clusters and the first set of binding sites [n(1,2)], which can be considered as predominant at the first stage of interaction, is between 4 and 11. From MD simulations it were identified eight residues from PRP1 that establish hydrogen bonds with B2 and B2g, four of which are in the referred clusters or in the vicinity. A similar trend was observed for PRP3. Regarding the effect of the procyanidin structure, the number of binding sites in aPRPs was higher for B2 than for the other procyanidins. The opposite was observed for bPRPs. This could be related to the fact that these aPRPs are three times larger than bPRP and so are able to accommodate more procyanidin B2 molecules, which is in agreement with MD simulations results.

For P-B peptide it was observed that the number of binding sites of the first stage was in the same magnitude for all ligands (1 or 6 sites) while it was higher for the second stage of interaction (around 10 sites). This protein has one cluster with seven proline and two clusters with five and two proline. Altogether these clusters give five potentially sites for interaction. Additionally, P-B peptide has more nine proline residues along its sequence which could justify the n increase observed in the second stage of interaction. From MD simulations three residues from P-B that establish hydrogen bonds with B2 were identified with all of them located on proline clusters. For the interaction with B2g seven residues were identified, five of which are in these clusters or in the vicinity.

The importance of proline residues in this type of interactions had already been proposed by others including with IB-5 protein, a bPRP, and herein its importance has also been observed by MD simulations for all the studied proteins [221, 239]. However, it is worth mentioning that MD simulations also identified other residues as binding residues of B2 and B2g, namely glycine, glutamine and serine, which is in accordance with other works [221].

Besides, it seems that the aPRPs have a higher ability to accommodate more procyanidin B2 molecules than bPRP (IB-8b) or P-B, which is in accordance with the number of binding sites determined by ITC. This could be related to the higher size of aPRPs ($\approx 3x$ higher) in comparison with bPRPs or P-B peptide.

Overall, the combination of these techniques allowed the characterization of the interaction from low procyanidin/salivary protein ratios (low procyanidin concentrations) to high ratios. Both techniques (STD-NMR and ITC) are in agreement that P-B peptide was in the major part of the cases one of the salivary proteins with higher affinity for all procyanidins and, oppositely aPRPs, were the salivary proteins with less affinity to the studied procyanidins. To our knowledge, only one work have studied the interaction of each family of PRPs with condensed tannins individually [208]. These authors found that bPRPs were the ones with highest interaction while gPRPs and aPRPs did not interact with a mixture of condensed tannins. Besides, they have focused on the ability to form insoluble complexes while the present work has been directly focused on the interaction leading or not to insoluble complexes.

Furthermore, the results support that some procyanidins could be multidentate ligands and the first epitopes of interaction for each procyanidin were identified (rings B and E for B2 and galloyl ring for B2g).

The results are somehow different from previous works focused essentially on the reactivity of the different families of salivary proteins directly in saliva toward tannins [240]. There are strong evidences that the interaction of PRPs with tannins is quite different when the proteins are present alone or simultaneously. In this later case, a co-protein interaction with tannins would be expected. So, these differences in the interaction remain to be clarified in future works.

C. Molecular interaction between salivary proteins and food tannins

Abstract

Polyphenols interaction with salivary proteins (SP) has been related with organoleptic features such as astringency. The aim of this work was to study the interaction between some human SP and tannins through two spectroscopic techniques, fluorescence quenching, and saturation transfer difference-nuclear magnetic resonance (STD-NMR). Generally, the results showed a significant interaction between SP and both condensed tannins and ellagitannins. Herein, STD-NMR proved to be a useful tool to map tannins' epitopes of binding, while fluorescence quenching allowed one to discriminate binding affinities. Ellagitannins showed the greatest binding constants values (K_{SV} from 20090 to 94080 M⁻¹; K_A from 725 to 8310 M⁻¹) in comparison with procyanidins (K_{SV} from 5415 to 42250 M⁻¹; K_A from 1120 to 2700 M⁻¹). In fact, punicalagin was the tannin that demonstrated the highest affinity for all three SP. Regarding SP, P-B peptide was the one with higher affinity for ellagitannins. On the other hand, cystatins showed in general the lower K_{SV} and K_A values. In the case of condensed tannins, statherin was the SP with the highest affinity, contrasting with the other two SP. Altogether, these results are evidence that the distinct SP present in the oral cavity have different abilities to interact with food tannins class.

C1. Introduction

Polyphenols are natural phenolic compounds that result from plant secondary metabolism and have associated innumerable health benefits mostly owing to their antioxidant properties [6]. Besides its useful effects in many health disorders [189], its application is also wide known in the food, beverages and cosmetics fields [241, 242]. Therefore, polyphenols have been drawing a lot of attention from all-around researchers to expand their applicability. Among this complex group, there are many classes, each with different functions and characteristics. Tannins are one of them and they can be further divided into condensed (proanthocyanidins) and hydrolysable tannins according to their structure [6]. The second ones, that include ellagitannins, are found in fruits especially berries and nuts, such as pomegranate or raspberry, but can also be found in red wine due to migration from oak wood to wine during ageing [243, 244].

Ellagitannins differ from gallotannins in that some gallic acid moieties or galloyl groups are biaryl coupled to each other through carbon–carbon bond to form a hexahydroxydiphenyl (HHDP) moiety [245]. Ellagitannins contain numerous HHDP units as well as galloyl and/or sanguisorboyl units bound to a sugar moiety. Castalagin and vescalagin are the most representative structures of ellagitannins and are the major ones found in oak wood [243]. Condensed tannins are naturally found in cereals, vegetables, fruits, and also in some beverages. However, condensed tannins are much more available in the diet comparing to hydrolyzable tannins, being the most abundant polyphenols in plants after lignins [246]. They are composed of flavan-3-ol units, forming dimers, oligomers, and polymers with different substitution patterns (hydroxylation and galloylation). Procyanidins are a subclass of condensed tannins composed by (+)-catechin and/or (-)-epicatechin subunits linked through C4-C8 (dimers from B1 to B4) or C4-C6 (dimers from B5 to B8) interflavanic linkage. These compounds in solution present different conformers, specially resulting from the rotation of the interflavanic bond. This behavior in solution can also result in an equilibrium of different isomer forms [247].

In a sensorial point of view, tannins are associated with the consumer's perception of astringency. Astringency has been defined as a complex group of tactile sensations involving dryness, puckering, and tightening of the oral cavity, typically experienced during the ingestion of tannin-rich food and beverages. It has been generally accepted that astringency results from the tannin-induced interaction and/or precipitation of salivary proteins (SP) in the mouth [174]. Tannins interact with proteins through multiple binding sites, and this association is mediated by hydrophobic and hydrogen bonds, depending on the protein size, charge, and structure as well as on tannins molecular weight [6].

Among SP, the most important families include proline-rich proteins (PRPs), statherin, P-B peptide, cystatins, and mucin. Statherin (5232 Da) is known to contain a highly acidic N-terminal and for being phosphorylated at two residues (Ser2 and Ser3) [248]. This protein is produced by the parotid and submandibular glands and has several isoforms [249]. Among the 43 amino acid residues of statherin, tyrosine residues are very abundant. Salivary P-B peptide (5792 Da) is usually included into the bPRPs family due to its high content in proline residues (near 50% of its sequence) but it shows higher similarities with salivary statherin [103, 250]. Statherin and P-B peptide have in common convertase consensus sequences, but their structures differ as P-B peptide presents several hydrophobic amino acid residues (such as Phe, Leu, and Ile) and three tyrosine residues. Besides, P-B peptide is the product of a specific gene very close to the STATH

gene, unlike other bPRPs which are encoded by the four genes PRB1-4. Cystatins are a group of endogenous cysteine proteinase inhibitors. They are structured proteins with molecular masses ranging from 13 to 14 kDa and two disulfide bridges [251].

Most of astringency studies are focused on condensed tannins, due to its considerable amount in the diet. Further, among SP, PRPs and especially basic PRPs have been referred to as the most reactive SP toward tannins [80, 116]. However, previous *in vitro* and *in vivo* studies have gathered evidence that statherin and P-B peptide are highly reactive and precipitated by tannin, while cystatins are slightly precipitated by tannins [210, 240].

Some works point out that hydrolyzable tannins tend to be more reactive toward proteins when compared with condensed tannins [252, 253]. However, in general, these works were done with model proteins [244, 254]. Therefore, the aim of this work was to study the interaction between three important SP (statherin, P-B peptide, and cystatins) and five common tannins (castalagin, vescalagin, punicalagin (PNG), and procyanidins B3 and B6). Tannin compounds were chosen due to particular structural features. Concerning ellagitannins, the major difference between castalagin/vescalagin (stereoisomers) and PNG is in the glucose moiety, acyclic for the firsts and cyclic for the last one (Figure 36). Procyanidin dimer B3 and B6 are isomers with different positions of the interflavonoid linkage, C4-C8 and C4C6, respectively. The interaction between these compounds was studied by two molecular techniques: fluorescence quenching and STD-NMR.

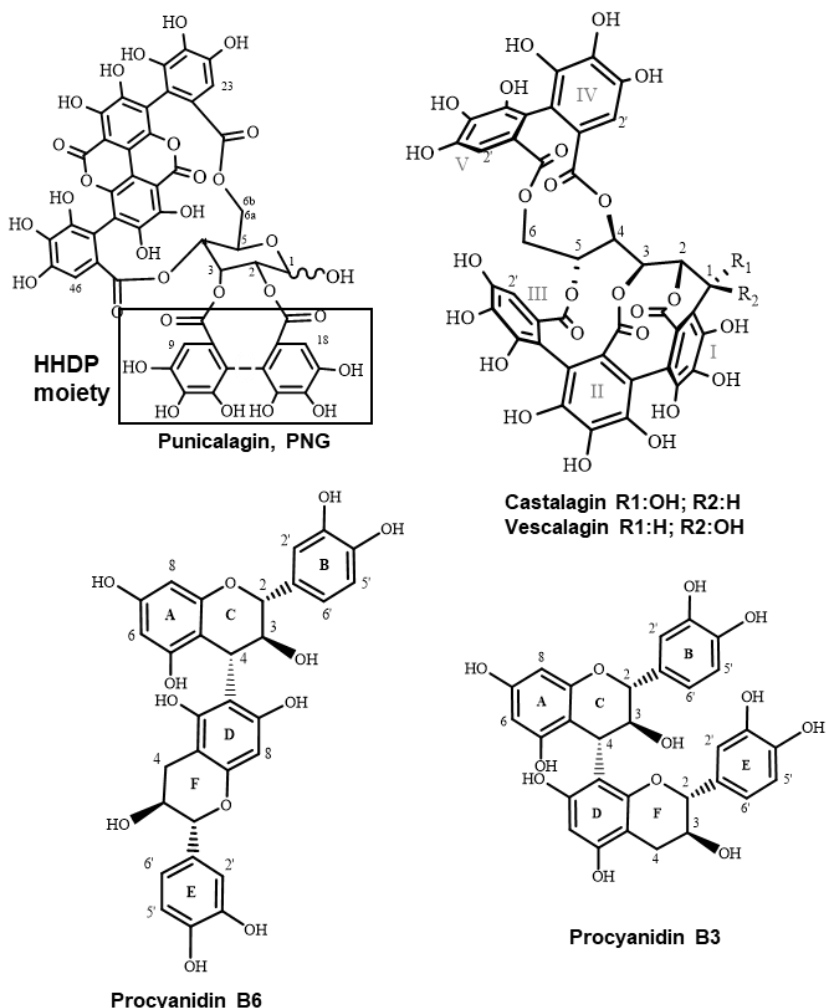


Figure 36 - Molecular structure of condensed tannins (procyanidin B3 and procyanidin B6) and ellagitannins (vescalagin, castalagin, and punicalagin, PNG). The hexahydroxydiphenyl (HHDP) moiety of PNG is identified.

C2. Material and Methods

C2.1. Reagents

All reagents used were of analytical grade or better. Acetonitrile was purchased from Chem-Lab, Trifluoroacetic acid (TFA) from Sigma-Aldrich and etanol was acquired from AGA, Álcool e Gêneros Alimentares, SA.

C2.2. Salivary Proteins Isolation and Purification

The procedure of saliva collection and treatment was already described in the literature [103, 255]. Whole saliva was collected from healthy nonsmoking volunteers at 2 p.m. after at least 1 h without food or beverage ingestion. Then, it was treated with 10% TFA

solution (final concentration 0.1%) and centrifuged at 8000 g for 5 min. The supernatant (acidic saliva, AS) was dialyzed (cellulose membrane, MWCO, 3.5 kDa) for 24 h at 4 °C under constant stirring and with at least three water changes. Then, the sample was centrifuged, freeze-dried, resuspended in water, and injected into semipreparative-HPLC in order to isolate the human SP families of interest (statherin, P-B peptide, and cystatins). For this, a HPLC Lachrom Merck Hitachi system (L-7100) was used equipped with a Vydac C8 column (Grace Davison Discovery Sciences, 5 µm particle, 150 mm × 2.1 mm); detection at 214 nm; eluent A, 0.2% aqueous TFA in water; eluent B, 0.2% TFA in ACN/water 80/20 (v/v); linear gradient from 10 to 55% (eluent B) in 45 min, at a flow rate of 0.60 mL·min⁻¹. After this program, the column was washed with 100% eluent B for 10 min to elute other late-eluting proteins. After washing, the column was stabilized with the initial conditions (90% eluent A and 10% eluent B).

C2.3. Identification of Salivary Proteins

The three SP families were freeze-dried and identified by Electrospray Ionization-Mass Spectrometry (ESI-MS) by flow injection analysis into an LTQ Orbitrap XL mass spectrometer (Thermo Fischer Scientific, Bremen, Germany) controller by LTQ Tune Plus 2.5.5 and Xcalibur 2.1.0. The capillary voltage of the Electrospray Ionization was set at 3100 V. The capillary temperature was 275 °C. The sheath gas flow rate (nitrogen) was set to 5 (arbitrary unit as provided by the software settings). The capillary voltage was 36 V and the tube lens voltage 110 V. Samples were diluted in a methanol/CAN/TDA 0.01% (5:5:90 v/v) mixture 1:10 prior analysis. After Mass Spectrometry analysis, deconvolution of mass spectra was done using the MagTran 1.03 software.

C2.4. Ellagitannins Extraction and Isolation

Castalagin and vescalagin were obtained from *Quercus petraea* (Matt.) Liebl wood (medium-toasted oak chips) as referred in the literature [243]. It was used a Sephadex LH-20 column and methanol:acidified water for elution to obtain different fractions which contained major ellagitannins. Its composition was determined by HPLC-DAD-MS as well as the ellagitannins purity after they were isolated by semi-preparative HPLC.

PNG was isolated from pomegranate as previously reported [256]. Briefly, 1g of dried husk powder was extracted ultrasonically with 30 mL of 40% ethanol for 30 minutes twice. After ethanol evaporation, the extract was lyophilized and analyzed by Liquid

Chromatography-Mass Spectrometry (LC-MS) in order to confirm PNG presence. PNG purification was performed by semi-preparative HPLC and its purity was determined by LC-MS and ^1H NMR.

C2.5. Procyanidin Dimers B3 and B6 synthesis

The synthesis of procyanidin dimers B3 (catechin-(4-8)-catechin) and B6 (catechin-(4-6)-catechin) followed the procedure described in the literature [257]. Briefly, a taxifolin and (+)-catechin mixture (ratio 1:3) was dissolved in ethanol under argon atmosphere and treated with sodium borohydride (in ethanol). Using $\text{CH}_3\text{COOH}/\text{H}_2\text{O}$ 50% (v/v), the pH was adjusted to 4.5 and the mixture was kept under argon atmosphere for 30 min. The reaction mixture was extracted with ethyl acetate. After evaporation of the solvent, water was added, and the mixture was passed through C18 gel, washed again and recovered with methanol. After evaporation of methanol, this fraction was separated through a TSK Toyopearl HW-40(s) gel column (300 mm × 10 mm i.d., 0.8 mL·min $^{-1}$, methanol as eluent) coupled to a UV-Vis detector. From this separation, several fractions were recovered and analyzed by ESI-MS (Finnigan DECA XP PLUS). The fractions yielding procyanidin dimers B3 and B6 were analyzed by HPLC-MS and its purity by ^1H NMR analysis. Spectroscopical data were in accordance with literature [216].

C2.6. Fluorescence quenching

In all experiments, proteins and polyphenols stocks were prepared in distilled water. The mixtures were prepared using 30 or 60 μM concentration of each protein and tannins were added at increasing concentrations (0–50 μM). Statherin, P-B peptide, and cystatins exhibit intrinsic fluorescence due to their content in aromatic residues, such as tryptophan and tyrosine. Herein, tryptophan was used as intrinsic fluorophore. The excitation wavelength (λ_{ex}) was 284 nm. After mixing, the samples were transferred to the fluorimeter cell and the emission spectra (from 290 to 500 nm) were measured in a PerkinElmer LS 45 luminescence spectrometer. After each measurement, the cell was washed with ethanol and distilled water. Fluorescence intensity was always registered at the wavelength of maximum fluorescence signal concerning each SP. These wavelengths were 314, 313, and 355 nm for statherin, P-B peptide, and cystatins, respectively. To evaluate the possibility of fluorescence resonance energy transfer (FRET) between the proteins and the procyanidins, the absorption spectra of both were analyzed: the proteins studied herein presents an absorption spectrum at 200–290 nm.

At this wavelength, the procyanidins do not emit light (maximum at 330 nm). Procyanidins have an absorption maximum at 270 nm, and their spectrum decreases reaching residual values close to 310 nm. The protein emission spectrum starts at 320 nm, and at this λ the polyphenol absorbance is small. FRET seems highly unlikely at the experimental conditions used. However, it was made a blank measurement for each concentration for these tannins at the λ_{ex} , where the protein was replaced by distilled water [215]. These blank signals were then subtracted to the corresponding measurements of the complexes SP-dimer. Castalagin, vescalagin, and PNG did not display fluorescence in these conditions.

Fluorescence quenching data was addressed considering the Stern-Volmer equation (Eq. 1):

$$\frac{F_0}{F} = 1 + k_q \tau_0 [Q] = 1 + K_{SV} [Q] \quad (1)$$

Where F_0 and F represent the fluorescence intensities before and after the addition of the quencher (tannin), respectively; k_q is the bimolecular quenching constant; τ_0 is the lifetime of the fluorophore (salivary protein) in the absence of the quencher; $[Q]$ concern the quencher concentration; and K_{SV} is the Stern-Volmer quenching constant. Taking this into account, the results obtained from the fluorimeter were represented in plots of F_0/F versus $[Q]$ in order to determine K_{SV} by linear regression.

A linear Stern-Volmer plot generally indicates that only one kind of mechanism occurs: static, which implies the formation of a stable complex, or dynamic, which is related to collisional encounters between the fluorophore (protein) and quencher (tannin). On the other hand, a positive deviation toward the x-axis appears when the extent of quenching is large and in two situations: both mechanisms are present simultaneously or a sphere of action exists, which means that the quencher is adjacent to the fluorophore at the moment of excitation. In this circumstance a different term arises, the so-called “apparent static quenching”, and the Stern-Volmer equation (Eq. 1) is modified to (Eq. 2):

$$\frac{F_0}{F} = (1 + K_{app} [Q]) \exp([Q]VN/1000) \quad (2)$$

The apparent static constant (K_{app}) resembles K_{SV} and can also be determined by linear regression with the difference that in this case the plot represents $\ln(F_0/F)$ as a function of $[Q]$.

For static or dynamic quenching to occur, regardless the mechanism, the fluorophore and quencher must be in contact [258]. Based on the k_q , it is possible to predict which type of fluorescence mechanism (static or dynamic) is present, since it demonstrates if the quenching was efficient or not. This constant can be calculated by the ratio between K_{SV} or K_{app} and τ_0 .

C2.7. Determination of Salivary Proteins Lifetime (τ_0)

τ_0 was measured on a Fluoromax-4 spectrophotometer attached to a single photon counting controller (FluoroHub), both from Horiba Jobin-Yvon, at room temperature. The fluorescence excitation was performed with a Horiba Nano LED source of 290 nm, and fluorescence emission was recorded at the maximum wavelength for the protein solution (313, 314, and 355 nm). The lamp profile was recorded by placing a scatter (dilute solution of LUDOX in water) in place of the sample [189, 191].

C2.8. Saturation Transference Difference-Nuclear Magnetic Resonance (STD-NMR)

A solution of each SP was prepared in D₂O (3 μ M) and the ligands were added in increasing concentrations (0.1 to 3.5 μ M) as a lyophilized powder. The amplification factor (A_{STD}) and the dissociation constant (K_D) were acquired considering Eq. 3 and 4, respectively [259]:

NMR experiments were recorded on a Bruker Avance III 600 HD spectrometer, operating at 600.13 MHz, equipped with a 5 mm CryoProbe Prodigy and pulse gradient units capable of producing magnetic field pulsed gradients in the z direction of 50 G/cm. The measurements were made with standard Bruker pulse sequences at 300 K. ¹H and STD spectra were recorded with a shaped pulse to suppress the water resonance using the following parameters: spectral width, 16 ppm; nutation angle, 7.08 μ s and 90°; and shaped pulse duration, 2 ms. Selective saturation of the SP off-resonance at 20 ppm and on-resonance at -1 ppm was performed using a pseudo-two-dimensional (2D) sequence for STD with a shaped pulse train alternating between the on and off resonances. STD-NMR spectra were acquired using Gaus 1.1000 pulses for selective saturation (50 ms), with a total saturation time of 2.5 s. The number of scans for tannins (4), receptor gain value (250), and relaxation delay (2.5) were kept constant. To process the STD-NMR spectra, TopSpin 2.1 software from Bruker was used.

The amplification factor (A_{STD}) and the association constant (K_A) were determined by Eq. 3 and 4, respectively [193]:

$$A_{STD} = \frac{I_0 - I_{Sat}}{I_0} \times L/P \text{ molar ratio} = \frac{I_{STD}}{I_0} \times L/P \text{ molar ratio} = \frac{\alpha_{STD} \times [L]}{K_D + [L]} \quad (3)$$

$$K_A = \frac{1}{K_D} \quad (4)$$

where I_{SAT} is the signal intensity of the selectively saturated protein spectrum (on-resonance), I_0 represents the signal intensity of the spectrum recorded without protein saturation (off-resonance), $[L]$ is the concentration of the ligand (tannin), $[P]$ is the protein concentration, and α_{STD} is the maximum amplification factor. After the determination of A_{STD} values from the experimental results (Eq. 3), a plot of A_{STD} in the function of $[L]$ was done, and K_D values were determined by Solver Supplement of Microsoft Excel Office.

C2.9. Statistical Analysis

All assays, except STD-NMR analysis, were performed at least in $n = 3$ repetitions. Values are expressed as the arithmetic means (SEM). Statistical significance of the difference between various groups was evaluated by one-way analysis variance (ANOVA) followed by the Tukey test. Differences were considered significant when $P < 0.05$. All statistical data were processed using the GraphPad Prism 5.0 for Windows (GraphPad Software, San Diego, USA).

C3. Results and Discussion

In this work, the interaction between statherin, P-B peptide, and cystatins and some representative food tannins (ellagitannins PNG, vescalagin and castalagin; condensed tannins procyanidin B3 and B6) were studied by two complementary techniques, STD-NMR and fluorescence quenching, thus allowing the study of differences in protein–tannin interaction related both with proteins and tannin structures.

Tannin compounds were chosen due to its particular structural features and to gather insights about how these features affect the interaction with proteins. Ellagitannins are more apolar compounds when compared to condensed tannins [6]. Castalagin and vescalagin are diastereoisomers which differ in the stereochemistry at the C1 position of glucose moiety, with one HHDP unit in their structure. PNG also presents a HHDP group, but opposite to castalagin and vescalagin, its glucose moiety is cyclic. Procyanidins

dimers B3 and B6 are isomers composed by two catechin units that differ only in the interflavonoid linkage, C4-C8 and C4-C6, respectively. SP were chosen based on previous studies that statherin and P-B peptide are also highly precipitated by tannins, opposed to cystatins [210, 240].

C3.1. Binding constants of the interactions between salivary proteins and tannins by fluorescence quenching

Fluorescence quenching is a spectroscopic method described as a reduction in the fluorescence intensity of a sample due to molecular interactions with a quencher [190]. In this process, the fluorescence intensity of the fluorophore (intrinsic fluorescence of statherin, P-B peptide, and cystatins) decreases when it is associated with tannins. This technique has been widely used to study polyphenols interactions, providing binding affinities information on the complexes formed [187, 188, 257]. Because of its high sensitivity, this technique allowed one to study the interaction with low tannins concentration. The fluorescence quenching assays permitted one to establish a relation between the decrease of protein fluorescence intensity and the increase of tannins concentrations. This is observed in the spectrum presented in Figure 37 for the interaction between P-B peptide and PNG. Similar fluorescence spectra were obtained for all the other interactions.

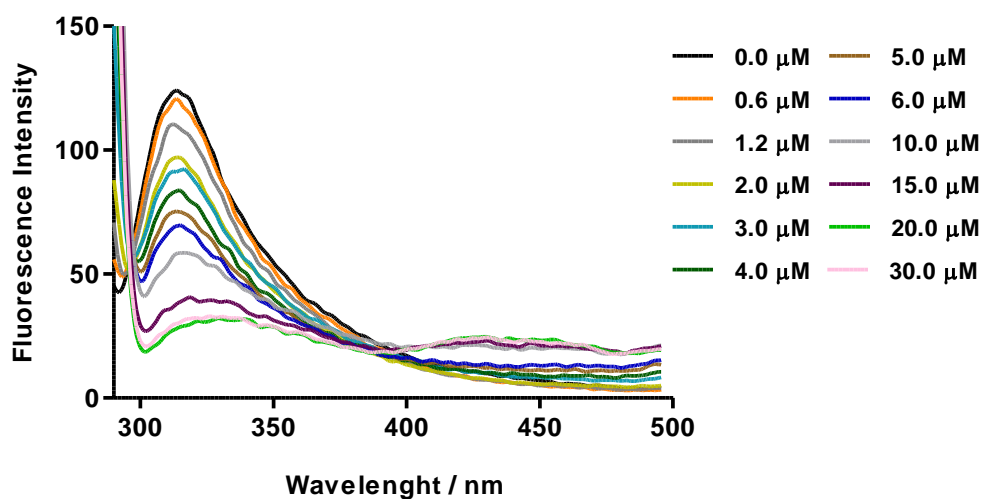


Figure 37 - Fluorescence spectra of P-B peptide (30.0 μM) recorded at λ_{ex} 284 nm with increasing concentrations of PNG (0.0–30.0 μM).

From these fluorescence spectra, the maximum fluorescence signals were acquired and Stern–Volmer plots obtained. From Figure 38 it is possible to note that the interaction of procyanidin dimers B3 (Figure 38A) and B6 (Figure 38B) with all SP exhibited a linear behavior.

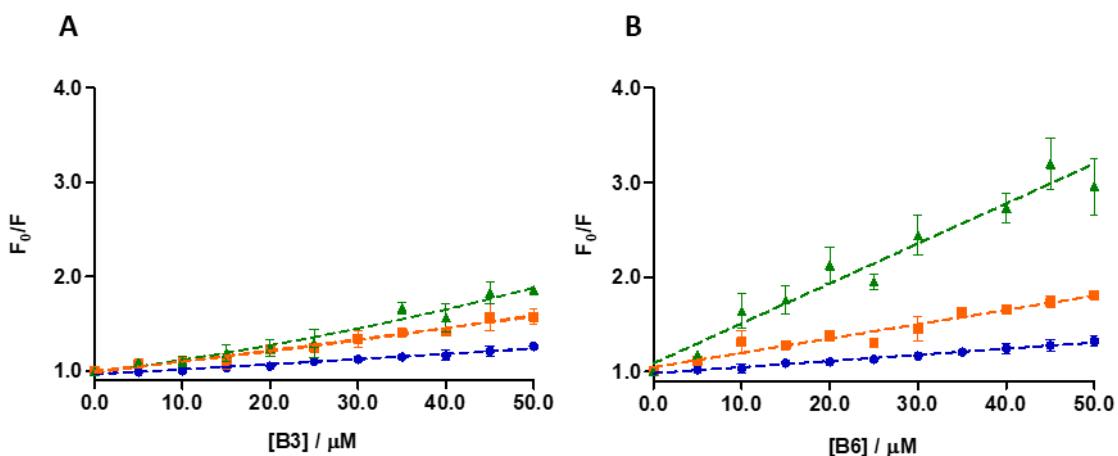


Figure 38 - Stern–Volmer plots representative of the fluorescence quenching of (▲) statherin, (■) P-B peptide, and (●) cystatins in the presence of increasing concentrations of (A) procyanidin dimer B3 and (B) procyanidin B6.

A different behavior was observed for ellagitannins, since castalagin, vescalagin, and punicalagin interaction with most proteins presented a nonlinear behavior (Figure 39). Only the interaction of punicalagin with P-B peptide and statherin exhibited a linear behavior (Figure 39-3A).

From a linear Stern–Volmer plot and considering Eq. 1, the Stern–Volmer quenching constant (K_{SV}) can be directly determined (Table 10). K_{SV} constants were mainly obtained for the interactions with condensed tannins. In the situations where an upward-curving Stern–Volmer plot is observed, a modified form of these plots was represented based on Eq. 2, to determine the corresponding apparent static constant (K_{app}), which was mainly obtained for ellagitannins (Table 10). Both constants are a measure of the interaction affinity. The different form of calculation for each constant is related to the quenching mechanism.

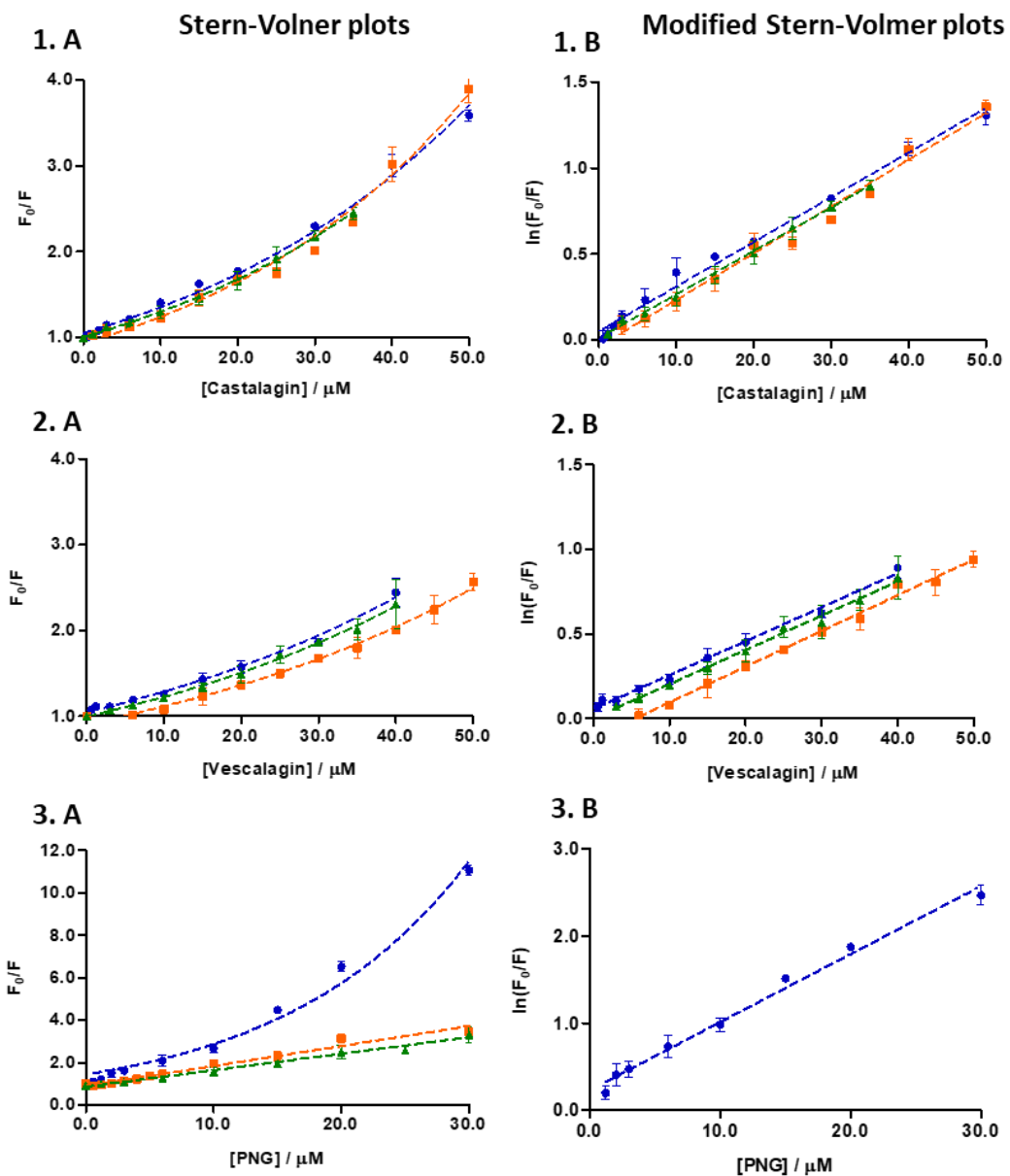


Figure 39 - Stern-Volmer (A) and modified Stern-Volmer plots (B) representative of the fluorescence quenching of (\blacktriangle) statherin, (\blacksquare) P-B peptide and (\bullet) cystatins in the presence of increasing concentrations of ellagitannins: 1. Castalagin, 2. Vescalagin and 3. PNG.

Table 10 - Stern-Volmer (K_{sv}) and apparent static quenching (K_{app}) constants for the interaction of statherin, P-B peptide and cystatins with the five studied tannins.

Condensed Tannins							
Protein	Procyanidin B3			Procyanidin B6			Cystatins
	Statherin	P-B	Cystatins	Statherin	P-B	Cystatins	
K_{sv}/ M^{-1}	17760±1205 ^{f,g}	11810±711 ^h	5415±306 ⁱ	42250±4108 ^c	15120±812 ^g	6497±207 ⁱ	
Ellagitannins							
Protein	Castalagin			Vescalagin			PNG
	Statherin	P-B	Cystatins	Statherin	P-B	Cystatins	Statherin
K_{sv}/ M^{-1}	-	-	-	-	-	-	77900±430 ^b
K_{app}/M^{-1}	25330±701 ^d	27200±805 ^d	25990±622 ^d	20250±918 ^{e,f}	21150±632 ^e	20090±625 ^{e,f}	94080±300 ^a
*Values with the different letter are significantly different (P< 0.01)							

*Values with the different letter are significantly different (P< 0.01)

The lowest affinity constants were obtained for the interaction of cystatins with condensed tannins, procyanidin B3 (5415 M^{-1}) and B6 (6497 M^{-1}). On the other hand, it is also evident that the affinity constants obtained for procyanidin B6 are always higher than the ones for procyanidin B3. Another tendency observed by comparing the different SP was that statherin showed the highest affinities for the interaction with procyanidins B3 and B6, 17760 , and 42250 M^{-1} , respectively. In general, the highest affinity constants were obtained for the interaction with hydrolyzable tannins, in particular for PNG. This latter presents the highest constant (94080 M^{-1}) for the interaction with P-B peptide. Indeed, hydrolyzable tannins have been referred in other studies as the ones with higher interaction when compared with condensed tannins [144-146, 253]. This higher interaction could be related with the fact that hydrolyzable tannins present in general much more complex structures than the oligomeric procyanidins studied. The affinity constants obtained for the interactions with castalagin and vescalagin were significantly lower than for the ones with PNG. On the other hand, castalagin presented similar constants to those of vescalagin for the different proteins studied.

In general, P-B peptide was the protein with highest interaction for ellagitannins, while for condensed tannins it was statherin. This high binding affinity of P-B peptide is somehow expected if we consider the high content in proline residues of this protein. The presence of proline residues induces more rigid and open structures and therefore more exposure of hydrophobic residues able to form hydrophobic bonds [80, 221, 239].

In the case of statherin, the high affinity toward condensed tannins could be owed to the presence of two polar serine residues (phosphorylated amino acids) which are assumed to establish hydrophilic bonds, strengthening the interaction with those more polar tannins.

A linear Stern–Volmer plot generally indicates that only one kind of mechanism occurs: static, which implies the formation of a stable complex, or dynamic, which is related to collisional encounters between the fluorophore (protein) and quencher (tannin). To discriminate the type of mechanism involved, the calculation of the bimolecular quenching constant (k_q) (Eq. 1) is required. For this, it was also necessary to determine proteins' lifetimes (Table 11).

Table 11 - Proteins' lifetimes and biomolecular quenching constants (k_q) for the interaction of statherin, P-B peptide and cystatins with the five studied tannins.

Protein	τ_0 (s)	B3	B6	Castalagin	Vescalagin	PNG
Statherin	1.73	1.03±0.07	2.32±0.02	*	*	4.51±0.25
P-B	2.55	0.46±0.03	0.59±0.03	*	*	3.69±0.12
Cystatins	4.0	0.14±0.01	0.16±0.01	*	*	*

*These compounds presented a nonlinear Stern-Volmer plot.

The k_q values higher than the diffusion-controlled limited value ($1 \times 10^{10} \text{ M}^{-1} \text{ s}^{-1}$) are usually associated with higher affinities and stronger interactions, which was observed for all linear Stern–Volmer plots. In fact, the interactions of PNG with statherin and P-B peptide presented the highest k_q values. These high values, about 100-fold larger than the diffusion-controlled limited value, suggests that a static mechanism is more probable to occur, where a stable complex is formed between each protein and tannin. Therefore, the results suggest the formation of a stable complex for procyanidins B3 and B6 with statherin, P-B peptide, and cystatins as well as PNG with statherin and P-B peptide.

A positive deviation toward the x-axis observed for castalagin and vescalagin appears when the extent of quenching is large (Figure 39-1A and 2A) and this could mean one of two situations: both mechanisms (static and dynamic) are present or a sphere of action exists, which means that the quencher (tannin) is adjacent to the fluorophore at the moment of excitation. In these situations, the deduction referred above (magnitude of k_q) cannot be directly applied to determine the mechanism responsible for the quenching. Therefore, it becomes necessary to verify whether the protein is being quenched by both mechanisms simultaneously or if a sphere of action exists. For this, the proteins' lifetime was measured as a function of tannin concentration and the subsequent data gathered evidence that fluorescence quenching could be due to the sphere of action mechanism. This mechanism assumes the existence of a sphere of volume within which the quenching only occurs if a quencher is immediately adjacent to the fluorophore when it is excited. In other words, if a tannin is adjacent to a protein at the moment of excitation, the SP will not fluoresce and the quenching is experienced [257]. The presence of a sphere of action was observed for the interaction between cystatins and PNG as well as for all the interactions of castalagin and vescalagin. It is interesting that these two last compounds, which are stereoisomers, present a similar mechanism of interaction for the several proteins studied.

C3.2. STD-NMR Studies

The STD technique was used to determine the tannins binding epitopes as well as to estimate association constants (K_A). The structure of castalagin, vescalagin, punicalagin, and procyanidins B3 and B6 were clarified by NMR ^1H chemical shifts described in the literature [228, 246, 260, 261].

In STD experiments, primary control assays with high tannins concentrations were made to confirm that the on-resonance irradiation frequency did not affect the tannins aromatic protons and that each protein was saturated by the on-resonance irradiation. The tannins' aromatic protons resonances were not visible with these control conditions.

Figure 40 presents a STD-NMR spectra titration obtained for the interaction between the three SP studied and increasing concentrations of tannin. After establishing the experimental parameters and test several protein and ligand concentrations, it was only possible to obtain STD-NMR signals in the tannin's concentration range from 0.1 mM to 3.5 mM, depending on the tannin.

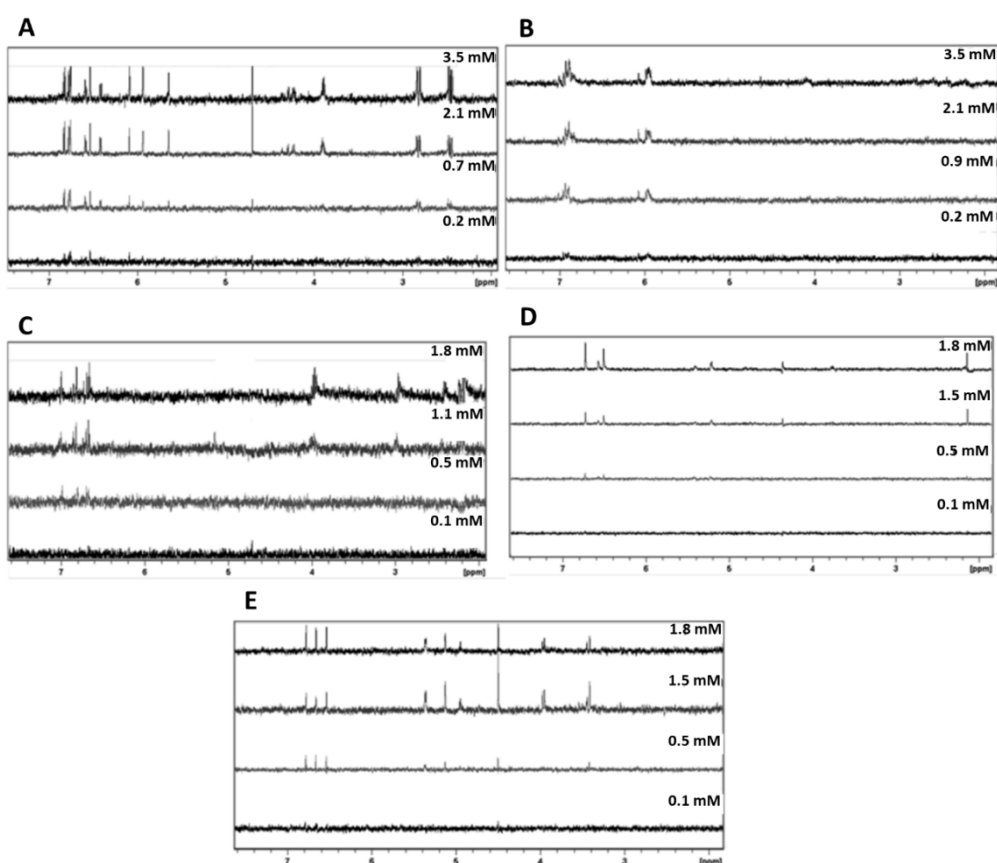


Figure 40 - STD-NMR spectra for the interaction with increasing concentrations of each tannin and proteins (3.0 μM). It is presented in the 8.0–2.0 ppm region, where most protons resonate. Spectra were recorded at 600 MHz and 300 K in deuterium oxide (D_2O). Interaction between statherin with (A) procyanidin B3 and (B) procyanidin B6. Interaction between P-B peptide and (C) punicalagin, (D) castalagin, and (E) vescalagin.

From the results presented in Figure 40, it is possible to observe that at low concentrations (0.1–0.5 mM) the signals of protons that appear first are near 7.0 ppm, which correspond to the HHDP and nonahydroxytriphenoyl (NHTP) moieties' protons. When concentration increases, other protons signals emerge, namely, in 4.0 and 3.0 ppm regions, which correspond to glucose moiety protons. This was observed for the interaction between all hydrolyzable tannins and the proteins studied.

Regarding condensed tannins, it was also observed a similar tendency. For procyanidin B3, at low concentrations the first sites of interaction are rings B and E while other regions of the molecule interact only at higher concentrations (rings A and D). Interestingly, the same tendency was not observed for procyanidin B6. In this case, the only molecular regions that interacted were rings B and E even for the highest concentrations.

The engagement of procyanidin B3 rings B and E was already observed for the interaction with other proteins, namely, trypsin enzyme and small PRP peptides (IB9₃₇ and IB7₁₄) [143, 215, 221]. When concentration increases, it was observed that rings A, D, and F also seem to be involved in these interactions. To our knowledge, there is no data in the literature about the involvement of procyanidin dimer B6 (C4-C6 linkage) epitopes in the interaction with proteins.

From these results, evidence that tannins could act as multidentate ligands were gathered, wherein one region of the molecule is favored for the initial interaction and the other parts participate in the interaction when concentration increases. The same does not exactly happens for procyanidin B6, which seems to be more selective. This could be related to a more elongated and flexible structure of C4-C6 dimers.

C3.3. Binding Constants of the Interaction between Salivary Proteins and Tannins by STD-NMR

The protons that presented the highest intensities on the STD spectrum were used to perform a STD-NMR titration for each protein/ tannin pair. The STD amplification factor (A_{STD}) was calculated from the differences between the off-resonance and the on-resonance spectra with increasing procyanidins concentration, according to Eq. 1 (Materials and Methods). The plots of each tannin titration regarding A_{STD} values as a function of ligand concentration at a fixed SP concentration (3 μ M) are represented in Figures 41 and 42.

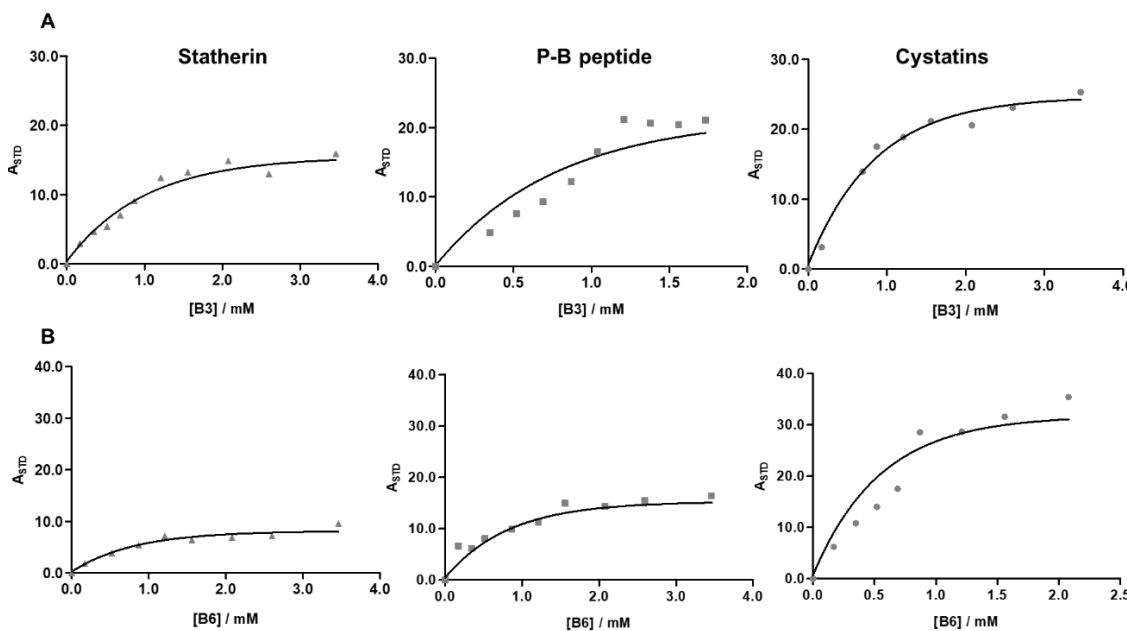


Figure 41 - STD amplification factor (A_{STD}) for the interaction between the three different SP (3 μ M) – statherin, P-B peptide and cystatins with increasing concentrations of procyanidin dimers (A) B3 and (B) B6. Symbols represent experimental values and lines represent theoretical values by Eq. 1.

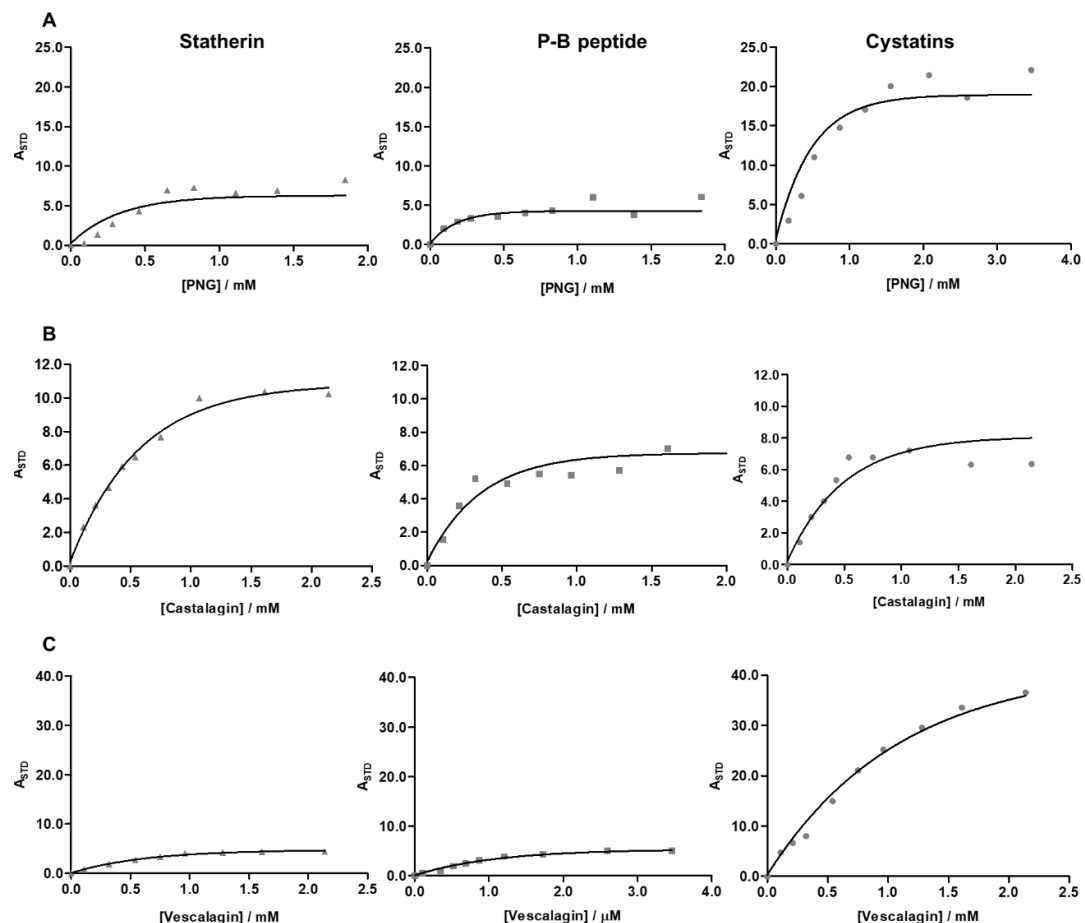


Figure 42 - STD amplification factor (A_{STD}) for the interaction between the three different SP (3 μ M) – statherin, P-B peptide and cystatins with increasing concentrations of ellagitannins (A) PNG, (B) castalagin and (C) vescalagin. Symbols represent experimental values and lines represent theoretical values by Eq. 1.

On the basis of these graphics, the STD signal increases systematically with concentration until reaching a plateau of maximum interaction, which depends on the protein. Each corresponding K_A was estimated according to Eq. 3 and 4 (Materials and Methods), using the Solver tool of Microsoft Excel software. The K_A values obtained range from 0.7 to 8.3 mM (Table 12).

In general, and although the K_A values have the same magnitude, there is an increase of K_A in the order procyanidin B3 < procyanidin B6 and vescalagin < castalagin < punicalagin. Overall, hydrolyzable tannins present higher K_A than procyanidins. The highest K_A value was obtained for punicalagin interaction with P-B peptide (8.3 mM), while procyanidins maximum value was only 2.7 mM (for interaction with statherin).

The K_A values obtained by STD-NMR are lower than the values obtained by fluorescence quenching assays. However, it must be noted that the concentrations imposed by each technique were different. Fluorescence quenching allowed the use of low tannins concentrations (up to 50 μ M), while STD-NMR focused on higher concentrations (up to 3.5 mM). The interaction between tannins (T) and proteins (P) are highly dependent on the T and P concentration and molar ratio T/ P [6].

Table 12 - Association constant (K_A) values estimated for the interaction between each SP and the different tannins determined by Eq. 2 and 3.

Protein	B3	B6	PNG	Castalagin	Vescalagin
Statherin	1700 ^c	2700 ^a	3300 ^a	1700 ^c	1625 ^c
P-B peptide	1120 ^b	1830 ^a	8310 ^a	3300 ^a	1410 ^a
Cystatins	1200 ^b	1650 ^b	2640 ^a	2240 ^b	725 ^b

^aConfidence of the fitting $\geq 97\%$.

^bConfidence of the fitting $\geq 93\%$.

^cConfidence of the fitting $\geq 80\%$.

The K_A values obtained for procyanidins are similar to the ones reported in the literature for similar interactions using STD-NMR (proline-rich peptide IB7₁₄ interaction with procyanidin dimers B1 to B4 and trimers) [143]. To the best of our knowledge, with exception of procyanidin B3 [221], there is no data in the literature about the affinity toward SP or similar proteins. Thus, this is the first time that the affinity of statherin, P-B peptide, and cystatins toward different food tannins have been studied.

In summary, regarding the influence of each SP, P-B peptide presents K_A values higher than the other proteins for the interactions with ellagitannins, except vescalagin. In fact, this ellagitannin showed very similar K_A values for the three SP. Cystatins are the SP with the lowest K_A values for almost all tannins, except for the interaction with procyanidin B3 and castalagin. On the other hand, statherin was the SP with higher K_A when the interaction involved procyanidins. This is in agreement with previous studies in which statherin has been reported as one of the SP with higher interaction for condensed tannins [178]. Overall, the combination of fluorescence quenching and STD-NMR techniques allowed the characterization of the tannin–SP interaction. It was observed that ellagitannins (vescalagin, castalagin, and punicalagin) interact better with the three SP than procyanidins. This could be explained since ellagitannins are globally more apolar molecules than condensed tannins, being probably more able to establish hydrophobic interactions [6], which have been described as the main driving forces involved in tannin–protein interaction [240].

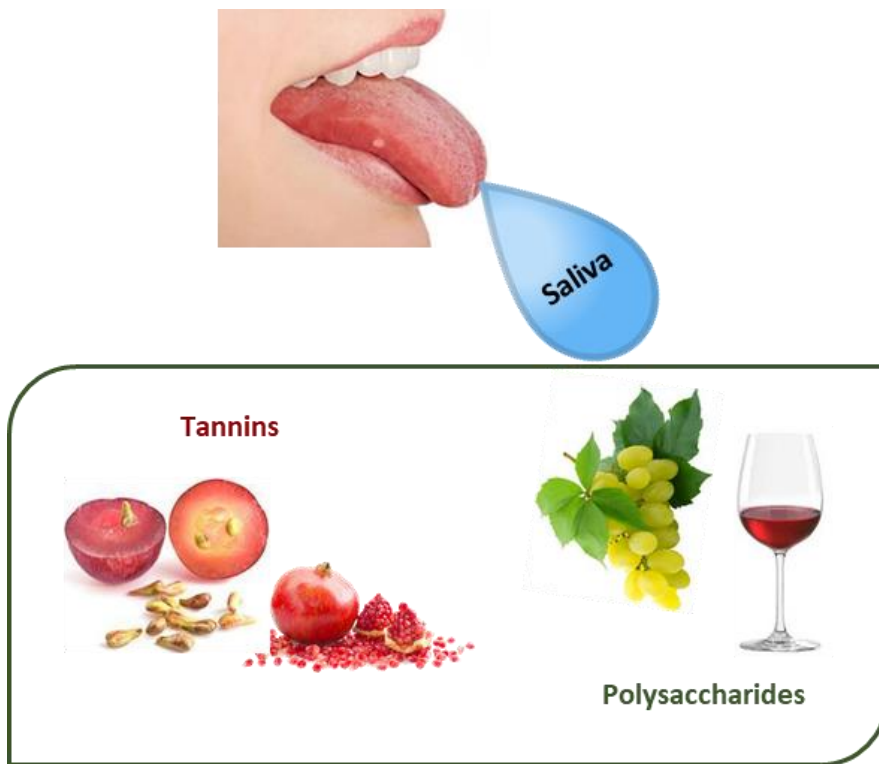
Their higher interaction was observed for P-B peptide, which is the only one rich in proline residues among the studied proteins [103]. These amino acids have been pointed as crucial for interaction with tannins and are able to establish hydrophobic stacking [6]. Thus, the results point out that hydrophobic bonds may be more significant for hydrolyzable tannins interaction than for condensed tannins, as it was already proposed by other authors [6, 236]. However, in the case of vescalagin, the affinity is significantly lower than in the case of the other ellagitannins and close to that shown by B3 and statherin. Since vescalagin is more hydrophilic than its stereoisomer castalagin [245], the hydrophobic interactions with protein could be less important, which may explain the lower affinity of vescalagin regarding the other ellagitannins.

The high affinity of procyanidin B6 toward tannins compared to procyanidin B3 was also observed. This could be related to a more extended structure of procyanidin B6 than procyanidin B3. Molecular mechanistic studies have shown that the C4-C6 linkage presents a large number of conformers and a more extended structure, which results in a higher flexibility of these structures compared to the C4-C8 isomers [56, 139].

Moreover, it seems that protein structure could play an important role in the interaction with tannins. It has been observed that proteins with structure have low affinity toward tannins, probably because the interaction is thought to involve only surface exposed residues [113, 200]. This could explain the lowest affinity for tannins of cystatins, since they are the only structured proteins here studied.

On the basis of the results herein, it seems that the ability of tannins to interact with SP is highly related with tannin structure, which in turn is related to the hydrophobicity of these compounds. Moreover, the existence of more extended tannin structures may favor the interaction with SP. Regarding proteins, the abundance of some specific amino acids such as proline in the structure and the fact that they are structured proteins are the main factors affecting the interaction with tannins. Further studies must be done in order to explore the interaction between other proteins and tannins and also to try to establish a relationship with sensorial properties.

Chapter 2 - Modulation of salivary protein-tannin interactions: the importance of polysaccharides



Synopse

Part D – The role of wine polysaccharides on salivary protein-tannin interaction: A molecular approach

Adapted from:

Elsa Brandão, Mafalda Silva, Ignacio García-Estévez, Pascale Williams, Nuno Mateus, Thierry Doco, Victor de Freitas, Susana Soares, *Carbohydrates Polymers*, **2017**, 177, 77-85. doi: 10.1016/j.carbpol.2017.08.075.

With the exception of tannin's isolation as well as polysaccharides isolation, all the experimental work described in this part, including polysaccharides purification, HPLC analysis, nephelometry measurements, STD-NMR experiments, was carried out by the author.

Part E – Inhibition mechanisms of wine polysaccharides on salivary protein precipitation

Adapted from:

Elsa Brandão, Mafalda Silva, Ignacio García-Estévez, Pascale Williams, Nuno Mateus, Thierry Doco, Victor de Freitas, Susana Soares, *Journal of Agricultural and Food Chemistry*, (submitted)

With the exception of tannin's isolation as well as polysaccharides isolation, all the experimental work described in this part, including including polysaccharides purification, HPLC analysis, nephelometry measurements, fluorescence studies and SDS-PAGE, was carried out by the author.

Part F – The effect of pectic polysaccharides from grape skin on salivary protein-tannin interactions

In preparation for submission.

With the exception of polyphenols and proteins quantification as well as procyanidins isolation, all the experimental work described in this part, including HPLC analysis and SDS-PAGE, was carried out by the author.

D. The role of wine polysaccharides on salivary protein-tannin interaction: A molecular approach

Abstract

Polysaccharides are described to inhibit aggregation between food polyphenols and salivary proteins (SP) and may hence lead to astringency modulation. In this work, the effect of two wine polysaccharides (arabinogalactan-proteins (AGPs) and rhamnogalacturonan type II (RG II)) on SP-polyphenol interaction was evaluated. In general, both polysaccharides were effective to inhibit or reduce SP-polyphenol interaction and aggregation. They can act by two different mechanisms (ternary or competitive) depending on the SP-tannin pair. In the case of salivary P-B peptide, AGPs and RG II seem to act by a ternary mechanism, in which they surround this complex, enhancing its solubility. Concerning acidic proline-rich proteins (aPRPs), it was possible to observe both mechanisms, depending on the tannin and the polysaccharide involved. Overall, this work point out for a specific property of wine polysaccharides important to modulate this and other beverages and food astringency perception.

D1. Introduction

Astringency is usually defined as the array of tactile sensations felt in the mouth including shrinking, puckering and tightening of the oral surface [6, 188]. Although the physicochemical mechanism of astringency is not completely understood, it is generally accepted that it is directly correlated with the capacity of food and beverages tannins to interact with SP, resulting in the formation of protein-tannin aggregates in the mouth [6].

Tannins are divided into two major classes according to their structure: condensed tannins (also known as proanthocyanidins) which are polymers of catechins, and hydrolyzable tannins which are composed of a polyol such as glucose, connected by ester linkage to at least one gallic acid (gallotannins) or hexahydroxydiphenic acid (HHDP) (ellagitannins) [6].

Over the years, condensed tannins have been the compounds mostly associated with astringency. Although some human sensory experiments revealed that ellagitannins can have an impact on astringency, there is not much information about the interaction of hydrolyzable tannins and SP [262-264].

SP include very structurally diverse proteins that are divided into different families. The major SP families include proline-rich proteins (PRPs), histatins, statherin, P-B peptide, cystatins and mucins [83]. PRPs are one of the most studied families due to their high ability to interact with tannins [253, 265]. They are characterized by a high content in proline residues (25-42%) [266] and are usually divided in three classes according to their acidic/basic characteristics: basic PRPs (bPRPs) have mainly basic residues, glycosylated PRPs (gPRPs) are bPRPs with carbohydrates in their structure, and finally acidic PRPs (aPRPs) that are rich in aspartic and glutamic acid residues [266]. Despite of its high amount in proline residues, salivary P-B peptide is not usually included into the PRP family, due to its similarities with statherin [102]. This peptide has been recently described to strongly interact with tannins [267].

It has been known that astringency is affected by several factors. Polysaccharides have been shown to inhibit tannin-protein aggregation and may hence lead to astringency modulation [268-271]. Two mechanisms have been proposed to explain this inhibitory effect: (I) competition between polysaccharides and SP toward tannins; or, (II) formation of a ternary complex protein-polyphenol-polysaccharides, with enhanced solubility in an aqueous medium [272]. Polysaccharides are also present in red wine being the major high-molecular weight components of wines. In the last years, they have been associated to the mouthfeel perception, modifying the sensory properties of wine [169, 273]. The main polysaccharides found in wine can derive from grapes and yeasts, including rhamnogalacturonan type II (RG II) and Polysaccharides Rich in Arabinose and Galactose (PRAGs) consisting of arabinogalactan-proteins (AGPs) from grape cell walls, and mannoproteins from yeast cell walls [160].

In this study, the effect of two wine polysaccharides (AGPs and RG II) on the interaction between hydrolyzable and condensed tannins toward two SP families (aPRPs and P-B peptide) was investigated. PNG and procyanidin dimer B2 (Figure 43) were chosen as model tannins, since the first one is commonly used as a hydrolyzable tannin model and is easily found in pomegranate [274], while procyanidin B2 is one of the most abundant procyanidin dimers in red wine [6]. On the other hand, aPRPs and P-B peptide have been previously reported as the SP that most interact with tannins both *in vitro* and *in vivo* studies [253, 265, 267].

With this purpose, High Performance Liquid Chromatography (HPLC) analysis and nephelometry measurements were used as the main techniques, complemented with Saturation Transfer Difference (STD)-NMR.

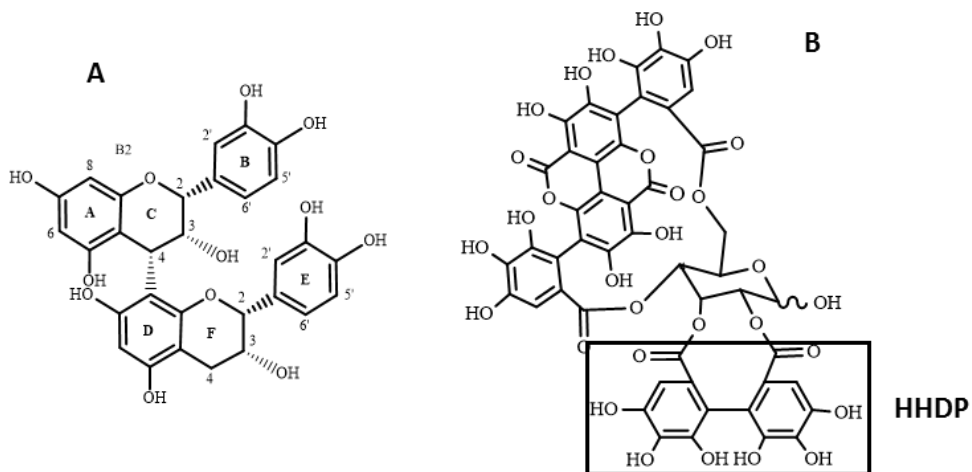


Figure 43 - Structures of procyanidin B2 (A) and PNG (B) with the evidence of the HHDP moiety of PNG.

D2. Material and methods

D2.1. Isolation and characterization of SP

A large pool of saliva was collected from several healthy volunteers and treated as described in the literature [70]. In order to reduce concentration variability connected to circadian rhythms, a collection time at 2 p.m. was standardized. After acidic treatment with trifluoroacetic acid (TFA), peptides and proteins like histatins, PRPs, statherin, P-B peptide and cystatins remained in saliva. This acidic saliva (AS) was dialyzed in a cellulose dialysis membrane (MWCO: 3.5 kDa) for 24 h at 4°C with stirring against deionized water. After dialysis, saliva was centrifuged, and the supernatant was freeze-dried. The lyophilized saliva was solubilized in a minimum volume of water as possible in order to concentrate total protein composition. The resulting solution was purified by semi-preparative HPLC in which different families of SP were collected, according to their retention time [178]. The fractions of PRPs and P-B peptide were freeze-dried, and the major proteins present in each fraction were identified by Electrospray Ionization-Mass Spectrometry (ESI-MS) as described in the literature [178]. This study was conducted according to the Declaration of Helsinki and was approved by the Ethics Committee of Medical School of University of Porto (EK84032011).

D2.2. Isolation of procyanidin dimer B2 and PNG

Four fractions of grape seeds (*Vitis vinifera*) were obtained as previously described [182]. Procyanidin dimer B2 was isolated from these fractions by preparative HPLC. PNG was isolated from pomegranate following several steps described in the literature [274].

Briefly, 1g of dried husk powder was extracted ultrasonically with 30 mL, 40% ethanol, for 30 minutes twice. After ethanol evaporation, the extract was lyophilized and analyzed by LC-MS in order to confirm the presence of PNG which was then purified by semi-preparative HPLC and its purity determined by LC-MS and ^1H NMR.

D2.3. Isolation and characterization of polysaccharide fractions

D2.3.1. Isolation of RG II and AGPs

RG II fraction was isolated from wine, following the procedure reported elsewhere [275]. Briefly, wine samples were de-alcoholized and fractionated by adsorption chromatography (polystyrene/divinyl benzene resin), obtaining two different fractions. The first fraction (A) was not retained on the column and was eluted with water, while the second one (B) was eluted with 20% ethanol. Then, size exclusion chromatography was conducted to purify fraction B. Elution was performed on a Superdex-75 HR column (60 x 1.6 cm, Pharmacia, Sweden) with a precolumn (0.6 x 4.0 cm) (equilibrated at 1 mL min $^{-1}$ with 30 mM ammonium formate, pH= 5.8), an Intelligent pump 301 (FLOM, France) and a rheodyne injector with a 2 mL loop. Elution of complex polysaccharides were followed using a refractive index detector (RI 101 (Shodex Showa Denko, Japan)). RG II fraction was eluted between 65 and 75 min (Figure 44), and then was freeze-dried, redissolved in water and freeze dried again for three times to remove the ammonium salt.

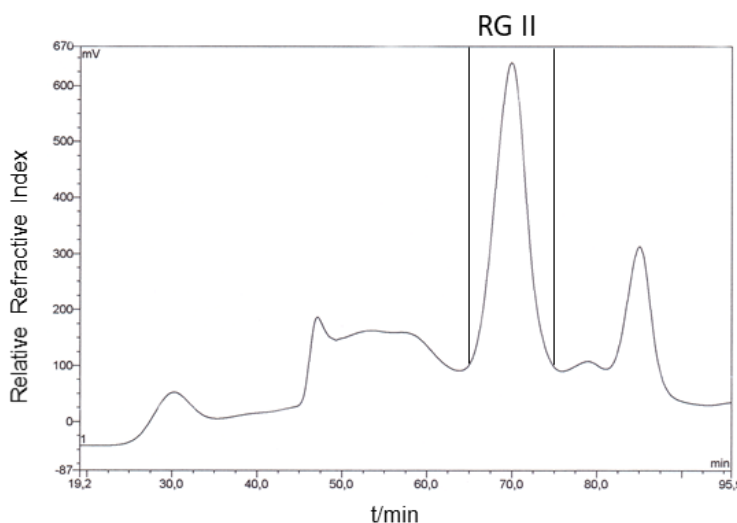


Figure 44 - Purification by High Resolution Size-Exclusion Chromatography on Superdex-75 HR column of RG II fraction.

AGPs fraction was isolated from wine sample fractions after anion-exchange and/or size-exclusion chromatographic steps. A final fraction containing a mixture of AGPs and MPs was purified by affinity chromatography, using mannoproteins' ability to bind to Concanavalin A lectin [160]. This mixture was loaded (40 mg.mL^{-1}) on a Concanavalin A-Sepharose (Pharmacia XH 26/40) column equilibrated with 50 mM sodium acetate buffer pH 5.6 containing 150 mM NaCl, 1 mM CaCl₂, 1 mM MgCl₂ and 1 mM MnCl₂. AGPs were the first fraction to be eluted with the same buffer. The desorption of the MPs (second fraction) was carried out using two bed volumes of the previous buffer containing 100 mM of methyl- α -D-mannopyranoside. AGPs fraction was dialyzed extensively against water to remove all salts and freeze-dried. Both RG II and AGPs fractions were then analyzed in terms of their neutral and acidic sugar composition.

D2.3.2. Neutral and acidic sugar composition

Neutral sugar composition was determined as alditol acetates after TFA hydrolysis (75 min at 120 °C), reduction and acetylation, as described in the literature [161, 276]. The resulting alditol acetate derivatives were quantified by gas chromatography (GC) analysis using a fused silica DB-225 (210 °C) capillary column (30 m × 0.25 mm i.d., 0.25 µm film), with hydrogen as the carrier gas, on a Shimadzu GC-2010 Plus gas chromatograph. The different alditol acetates were identified from their retention time by comparison with that of standard monosaccharides. Neutral sugar amounts were calculated relatively to the internal standards (allose and myo-inositol).

Neutral and acidic sugar composition was determined after solvolysis with anhydrous MeOH containing 0.5 M HCl (16h, 80°C) by GC-MS of their per-O-trimethylsilylated methyl glycoside derivatives. The resulting trimethylsilyl (TMS) derivatives were separated on a DB-1 (temperature programming 120–145 °C at $1.5 \text{ }^{\circ}\text{C min}^{-1}$, 145–180 °C at $0.9 \text{ }^{\circ}\text{C min}^{-1}$, and 180–230 °C at $50 \text{ }^{\circ}\text{C min}^{-1}$ and hold time 4 min) capillary columns (30 m × 0.25 mm i.d., 0.25 µm film), coupled to a single injector inlet, with hydrogen as the carrier gas, on a Shimadzu GCMS-QP 2010 Plus gas chromatograph [277]. Myo-inositol was used as internal standard.

D2.4. Tannin-protein interaction

In order to assess the minimal tannin concentration that leads to a significant precipitation of SP, preliminary experiments were made. The two SP families with the highest affinity toward tannins were chosen (aPRPs and P-B peptide). SP concentration

was chosen in order to be as close as possible to the physiological values found in saliva. After analysis of saliva chromatogram and using a calibration curve, the concentrations of aPRPs (6 µM) and P-B peptide (4 µM) were achieved. After this, samples were analyzed by HPLC before and after the interaction with PNG and procyanidin B2. It was chosen the minimal tannin concentration with the concentration range previously referred that precipitates more than 50 % of these SP families. Thereby, for aPRPs were selected the concentrations of 60 µM PNG and 540 µM of procyanidin B2, while for P-B peptide were selected the concentrations of 40 µM PNG and 400 µM procyanidin B2.

D2.5. Influence of polysaccharides on SP-tannin interaction

D2.5.1. HPLC analysis

The control condition was a mixture of the two SP families and each tannins' class ((final volume, 120 µL). Protein-tannin mixture was shaken and kept to react for 10 min, centrifuged (8000 g, 5 min) and the supernatant was analyzed by HPLC, according to the procedure described in the literature [265, 269].

After establishing the concentration of SP and tannins, tannins firstly react with increasing concentrations of polysaccharides (0.0-1.2 g.L⁻¹) for 30 min. After this time, SP were added to this mixture and kept to react for more 10 min. The resulting solution was centrifuged and 100 µL of the supernatant were analyzed by HPLC, following the method reported elsewhere [267].

D2.5.2. Nephelometry measurements

Polysaccharides, tannins and SP were prepared in water at the same concentrations used in HPLC in order to compare the results from these two techniques. Therefore, polysaccharides react with tannins (30 min), and then SP were added and kept to react for 10 min. Nephelometry experiments were conducted on a Horiba Jobin Yvon Fluoromax-4 Spectrofluorometer, which was used as a 90° light scattering photometer. The excitation and the emission wavelengths were set at 400 nm because at this wavelength proteins, tannins and polysaccharides do not absorb the incident light [268, 278]. Since polysaccharides can interact with tannins and/or proteins, a blank was made used a fixed concentration of tannins or proteins and each polysaccharide concentration. Only for the blank between tannins and polysaccharides the aggregation value increased with the increase of polysaccharide concentration. For this reason, the respective blank

was subtracted to the aggregation value obtained for each experiment. Then a relative aggregation value (%) was calculated for each experiment considering the ratio between the scatter intensity of the measured sample and the most turbid sample (100 %) containing protein and tannins without polysaccharides.

D2.5.3. STD-NMR Studies

For STD-NMR experiments, samples concentration needed to be adapted due to a different sensitivity of this technique in comparison with HPLC and nephelometry. Thus, aPRPs and P-B peptide were prepared at 15 μM and 30 μM , respectively, in D_2O . In order to maintain the protein concentration constant throughout the experiments, tannins and polysaccharides samples were lyophilized and added as a powder to the protein solution. As explained previously, tannins (PNG, at 500 μM and procyanidin B2, at 1000 μM) were mixed with polysaccharides and kept to react for 30 min. Then the protein solution was added and the mixture was kept to react for 10 min. Both AGPs and RG II were used at a concentration of 0.8 $\text{g}\cdot\text{L}^{-1}$, since it is within the polysaccharide concentrations range used in the other two techniques.

The final solution was transferred to 5 nm NMR tubes and STD-NMR experiments were recorded on a Bruker AVANCE III 400 spectrometer equipped with a 5 mm PABBI 1H/D-BB Z-GRD probe. A shaped pulse to suppress the water resonance was used to obtain ^1H and STD spectra, selecting as parameters: spectral width, 16 ppm; 90° shaped pulse duration, 2 ms; and nutation angle (90°), 7.8 μs . The measurements were made with standard Bruker pulse sequences at 300 K. Selective saturation of protein off-resonance at 8000 Hz and on-resonance at 200 Hz was performed using a pseudo-two-dimensional (2D) sequence for STD. The number of scans (64 for aPRPs-PNG and aPRPs-procyanidin B2; 104 for P-B peptide-procyanidin B2; 154 for P-B peptide-PNG), the receptor gain value (2050), and the relaxation delay (3.5 s) were kept constant during the experiment.

As control, an experiment of each tannin alone was done in order to ensure that the tannin concentration was correctly chosen, since no signal should appear in the STD spectrum. Furthermore, a solution containing polysaccharides and tannins was also tested as a control. Software (TopSpin 2.1; Bruker, Newark, DE) was used to subtract the unprocessed on- and off-resonance spectra, to baseline correction of the resulting difference spectrum, and to integrate the areas of tannins' peaks.

D2.6. Statistical analysis

All assays, except STD-NMR experiments, were performed in $n \geq 3$ repetitions. Values are expressed as the arithmetic mean \pm SEM. Statistical significance of the different HPLC values was evaluated by two-way analysis variance (ANOVA) followed by Bonferroni test. Differences were considered significant when $P \leq 0.05$. Data were processed using GraphPad Prism 5.0 for Windows (GraphPad Software, San Diego, California, USA).

D3. Results and Discussion

The influence of wine polysaccharides on the interaction between two SP families and condensed/hydrolyzable tannins was assessed by some complementary techniques, namely HPLC, nephelometry and STD-NMR. Several studies reported the higher affinity of PRPs towards tannins, especially aPRPs. Previous works allowed not only to confirm the higher affinity of aPRPs, but also the great affinity of P-B peptide to interact with similar tannins [265, 267, 269]. Concerning tannins, one compound representative of each tannins' class was chosen. Therefore, procyanidin B2 and PNG were chosen to represent the condensed and hydrolyzable tannins, respectively.

Experiments were then conducted using two cell wall polysaccharides with different chemical properties: AGPs, a neutral polysaccharide and RG II, an acidic polysaccharide.

D3.1. Salivary Proteins identification

The identification of the major SP present in the chromatogram of human AS has been previously done (Figure 45). Figure 45 presents the typical HPLC chromatogram of the AS solution at 214 nm, which can be divided into six regions: bPRPs, gPRPs, aPRPs, statherin, P-B peptide and cystatins. bPRPs region contains IB-8b, IB-4, IB-5 and P-J proteins. The second region comprises mainly gPRPs, and the next region corresponds entirely to aPRPs, namely PRP1 and PRP3. The fourth and fifth regions contain phosphorylated and non-phosphorylated forms of statherin and P-B peptide. The last region is mostly composed by cystatins. According to this chromatogram, the proteins of interest, aPRPs and P-B peptide were isolated by HPLC semi-preparative and characterized by Mass Spectrometry [178]. These proteins are described to be the ones which mostly interact with tannins [265, 267]. The average molecular weight was

estimated for each fraction based on ESI-MS signals intensity: aPRPs (14643 Da) and P-B peptide (5792 Da).

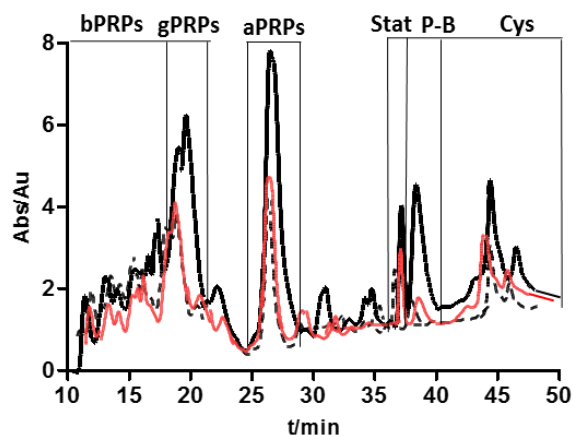


Figure 45 - Typical HPLC profile of AS solution from human saliva detected at 214 nm in the absence (black line) and in the presence of tannins: PNG (60 μ M, black dashed line) and procyanidin B2 (540 μ M, red line). The vertical dotted lines show the ranges and the main SP families assigned to each HPLC region.

D3.2. Polysaccharide and oligosaccharide characterization

AGPs consist in a ramified (1 \rightarrow 3)-D-galactan inner core with (1 \rightarrow 6)-linked galactan side chains that are highly substituted with arabinose linked in 3 and 4 position and with few amounts of rhamnose and glucuronic acid [164]. The analysis of the sugar composition showed the higher content of arabinose and galactose, allowing to characterize this fraction as AGP (Table 13).

RG II has a backbone of at least eight residues of galacturonic acid with four different secondary side chains. RG II contains twelve different glycosyl residues, including galacturonic and glucuronic acids, fucose, arabinose, rhamnose, galactose, and several rare and diagnostic sugars of RG II presence, such as apiose, aceric acid, 2-O-methylfucose, 2-O-methylxylose, 3-deoxy-D-manno-octulosonic acid (Kdo) and deoxy-D-lyxo-heptulosaric acid (Dha) [159, 279]. The analysis of the sugar composition allowed to classify this fraction as RG II (Table 13).

Table 13 – Neutral monosaccharides composition (% molar) of the RG II and AGPs fractions.

	RG II	AGPs
Ara	15.8	38.5
Gal	25.8	50.8
Man	3.3	8.9
Rha	28.6	-
Xyl	-	-
Glc	2.5	1.9
Fuc	4.2	-
2-O-methyl-fucose	5.7	-
2-O-methyl-xylose	5.1	-
Apiose	9.3	-

Ara – arabinose; Gal – galactose; Man – mannose; Rha – rhamnose; Xyl – xylose; Glc – glucose; Fuc – fucose.

It is important to refer that the analysis of sugar composition had more relevance in a qualitative way in order to confirm the presence of these two fractions of polysaccharides.

D3.3. Interaction between SP and tannins

Preliminary experiments were made in order to achieve the minimal tannin concentration that leads to a significant precipitation of SP. It is essential to establish this concentration since a small amount of tannins could be insufficient to lead to a significant precipitation, while an excess of tannins could lead to a total depletion of proteins or also to free molecules of PNG and procyanidin B2. With this purpose, saliva was analyzed by HPLC before and after the interaction with increasing concentrations of each tannins' class. The control condition was a mixture of saliva (70 µL) and water (50 µL) (final volume, 120 µL). Different volumes of tannins' solution were added to saliva to obtain several concentrations (0-400 µM), being the final volume adjusted with water. The mixture was shaken and kept for 10 min at room temperature, then centrifuged (8000 g, 5 min) and finally, the supernatant was injected into the HPLC.

It can be seen from Figure 45 that the addition of 60 µM of PNG and 540 µM of procyanidin B2 reduced the amount of several SP, with the two most reduced being aPRPs and P-B peptide. Furthermore, it is important to note that PNG seem to have a higher affinity to interact with SP than procyanidin B2, since procyanidin B2 concentration was almost 10-fold higher than PNG concentration to cause approximately the same % SP precipitation. In fact, aPRPs and P-B peptide were reduced ca. 60-70 %, while gPRPs

and cystatins were only reduced ca. 40 % and 20 %, respectively. Therefore, the effect of polysaccharides on the interaction between SP and tannins was focused on aPRPs and P-B peptide.

For this study, the concentration of aPRPs and P-B peptide was chosen in order to be as close as possible to the physiological values found in saliva, which is in agreement with the values reported in the literature [266]. For this purpose, 6 μM and 4 μM were estimated as concentrations of aPRPs and P-B peptide, respectively.

PNG and procyanidin B2 concentrations were then adjusted in order to produce approximately the same interaction of the two SP families. Therefore, 60 μM of PNG and 540 μM of procyanidin B2 were used to interact with aPRPs, while 40 μM of PNG and 400 μM of procyanidin B2 were selected to interact with P-B peptide. For the nephelometry measurements it was possible to use the same concentrations of proteins and tannins used in the HPLC assays. However, for STD-NMR experiments the concentrations needed to be adapted due to a different sensitivity of this technique in comparison with the other two techniques.

D3.4. Effect of polysaccharides on the interaction between SP and tannins

D3.4.1. HPLC analysis

The experimental approach described herein intended to mimic the phenomenon during ingestion, where polysaccharides and tannins are present together in food and beverages and enter simultaneously in contact with SP. For this purpose, a solution of tannins-polysaccharides was prepared to which the different SP fractions (P-B peptide and aPRPs) were subsequently added. The control condition was made with isolated SP before and after interaction with tannins in the referred concentration. Figure 46 shows part of the chromatogram of aPRPs before, after the interaction with PNG 60 μM , and in the presence of AGPs (1.2 g.L⁻¹). It can be observed a recovering of the aPRPs' chromatographic peak in the presence of this polysaccharide. Similar chromatograms were obtained with other interactions.

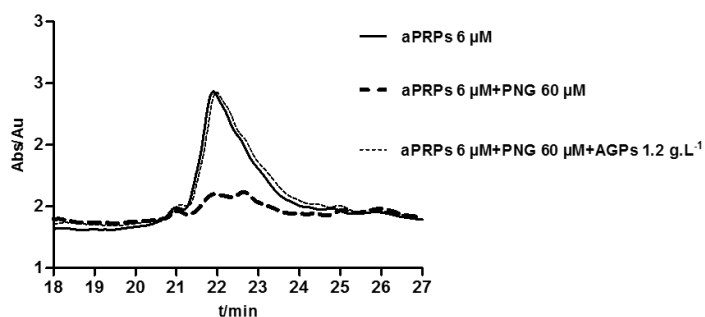


Figure 46 - Chromatogram showing the aPRPs' fraction (6 μM) before and after the interaction with PNG (60 μM), and in the presence of AGPs (1.2 $\text{g} \cdot \text{L}^{-1}$).

Figure 47 shows the variation of the chromatographic peaks area (% area) of aPRPs and P-B peptide with the increase of polysaccharide concentration, expressed relatively to the respective area of the control condition (SP in the absence of tannins). In general, all polysaccharides in solution enhanced the chromatographic peaks of these SP families, with the exception of P-B peptide-PNG interaction with RG II (Figure 47b). For most cases there was a recovery of SP concomitantly with polysaccharides' concentration. The observed changes may be interpreted as the inhibition of SP precipitation by tannins in the presence of these polysaccharides. However, the effect of polysaccharide depends on the SP-tannin pair.

Concerning the influence of polysaccharides on the aPRPs-tannin interaction, it is possible to observe that RG II was the most efficient polysaccharide in preventing aPRPs precipitation by tannins (Figure 47a). For the same concentration of AGPs and RG II, a highest recovery of the chromatographic peak area of aPRPs was noted in the presence of RG II, regardless of the tannin present (PNG or procyanidin B2).

As for P-B peptide-tannin interaction (Figure 47b), the polysaccharides seem to have different influence depending on the tannin (condensed or hydrolyzable). For the interaction with procyanidin B2, RG II and AGPs lead to a similar recovery of the P-B peptide chromatographic peak area. On the other hand, for the interaction with PNG, the presence of RG II did not alter significantly its chromatographic peak area, while in the presence of AGPs there was a recovery at the highest AGPs' concentration.

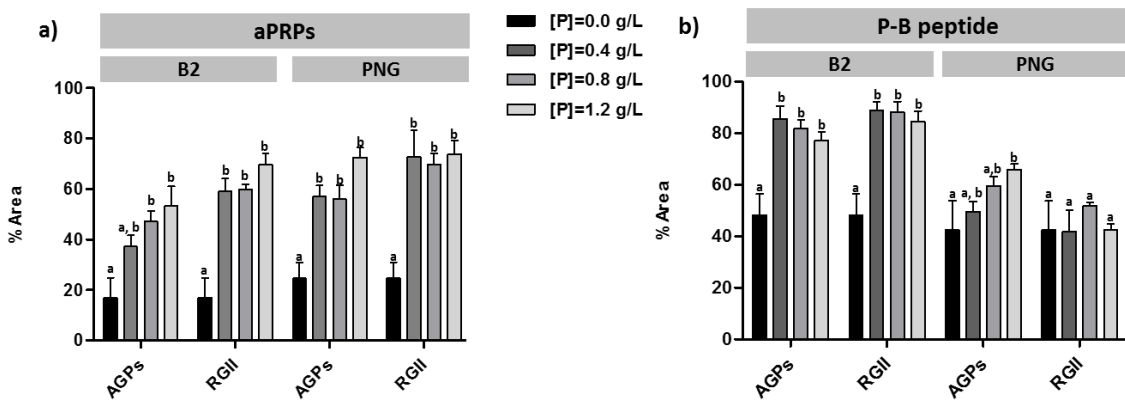


Figure 47 - Influence of increasing concentrations of polysaccharides (AGPs and RG II) on aPRPs (a) and P-B peptide (b) interaction with PNG (60 μ M and 40 μ M) and procyanidin B2 (540 μ M and 400 μ M) determined by HPLC. These results represent the average of three independent experiments. Values with different letters within each column are significantly different ($P \leq 0.05$).

D3.4.2. Nephelometry measurements

The inhibitory effect of different polysaccharides against SP precipitation by tannins was evaluated by measuring the decrease of the aggregates in solution by nephelometry. A blank was made using tannins or proteins and increasing polysaccharide concentrations. For the blank between tannins and polysaccharides, the aggregation value increased with the increase of polysaccharide concentration. On the other hand, the aggregation value of the interaction between proteins and polysaccharides remained practically constant as polysaccharide concentration increased. For this reason, the blank of polysaccharides and tannins was subtracted to the aggregation value obtained for each experiment. In this assay, increasing concentrations of polysaccharide were used until practically no changes in the amount of (in)soluble SP-tannin complexes were observed (Figure 48). A relative aggregation value (%) was then calculated as the ratio between the scatter intensity of each sample and the control condition (SP with tannin in the absence of polysaccharide, 100%). Values lower than 100% indicate less scattered light, which may be due to smaller or less aggregates.

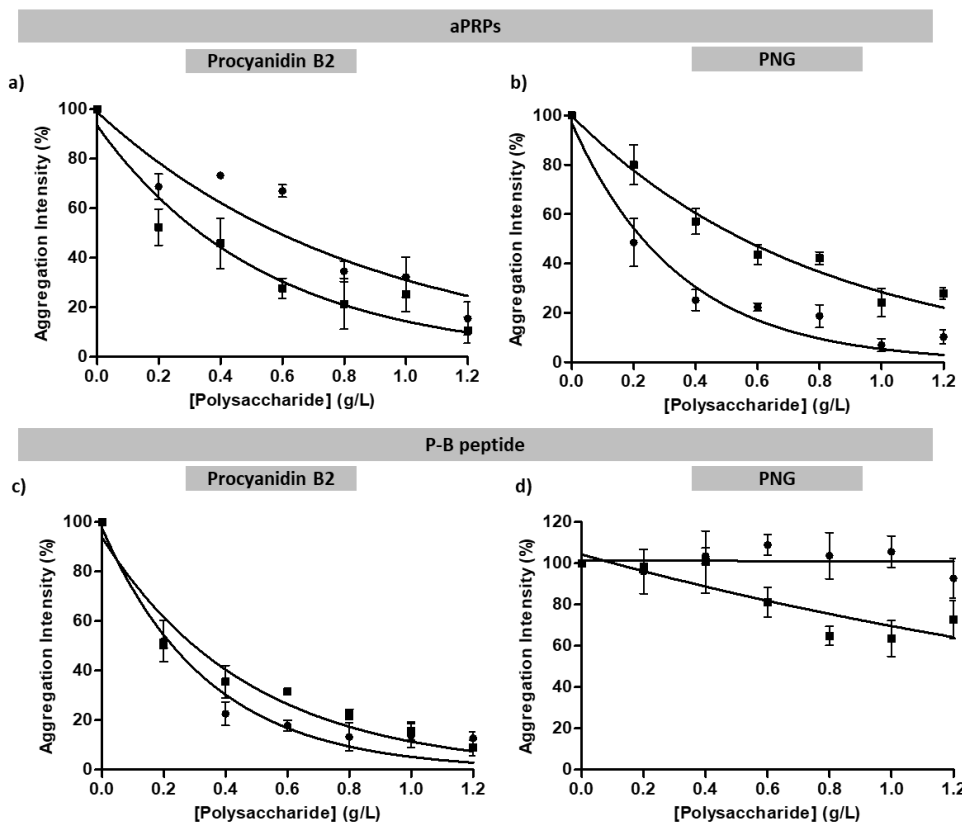


Figure 48 - Influence of polysaccharide concentration on aggregate formation (%) between aPRPs/P-B peptide and tannins (procyanidin B2 and PNG) at 400 nm. Blue, AGPs; Green, RG II.

In general, the presence of polysaccharides in solution can inhibit the formation of (in)soluble aggregates, which can be observed by a decrease of aggregation (Figure 48). This may be due to either the solubilization of SP-tannin aggregates by the formation of a ternary complex (protein-tannin-polysaccharide) or to the inhibition of their formation. The only exception was noted on the interaction between P-B peptide and PNG in the presence of RG II, for which the amount of aggregates precipitated remained practically constant (Figure 48d). The curves obtained for aPRPs and P-B peptide-procyanidin B2 interactions (Figure 48a, 48b and 48c) show an initial stage of aggregation reduction that tends to stabilize with the increase of polysaccharide concentration. Strong dissociation or solubilization of aggregates ($\geq 80\%$ of initial aggregation) was observed for most cases.

RG II has shown different behaviors with aPRPs and P-B peptide: it has been relatively effective for the interaction between aPRPs and PNG, however it did not have any effect in the P-B peptide-PNG complex formation. These results are in agreement with those obtained by HPLC. Even the non-effect of RG II on P-B peptide-PNG interaction was also observed previously by HPLC.

D3.4.3. STD-NMR studies

STD technique is widely used to study the interaction of proteins with ligands [193, 280]. This technique is based on the ligand resonance signals in which ligand protons that are in close contact with the protein receive saturation transfer from the protein. Briefly, an STD experiment involves subtracting a spectrum in which the protein was selectively saturated (on-resonance spectrum obtained by irradiating at a region of the spectrum that contains only resonances of the protein) from one recorded without protein saturation (off-resonance spectrum). Consequently, a difference spectrum called STD-NMR is obtained, where only the signals of the ligand(s) that received saturation transfer from the protein are observed. Protons that are not involved in the binding process reveal no STD-NMR signals [193].

Herein, STD was used as a complementary technique to try to gather information about the mechanism by which AGPs and RG II affect the interaction between SP and tannins. A primary control assay at high tannin concentrations was done in order to ensure the specificity of STD eliciting resonances and to validate the functionality of the STD. Then, a control STD-NMR experiment was performed on a solution containing each SP family (aPRPs, 15 µM; P-B, 30 µM) and each tannin (PNG, 500 µM; procyanidin B2, 1000 µM). After these preliminary controls, the experiments with polysaccharides were made, keeping the order of addition previously referred: tannins react with polysaccharides (30 min), and each SP family was then added and to (10 min).

Figure 49 shows the STD-NMR spectrum of the interaction between aPRPs with PNG and procyanidin B2 in the absence and in the presence of AGPs. For most interactions, it was observed a decrease in tannin proton intensity in the presence of polysaccharides as the result of the decrease of protein-tannin interaction. The signals that appear in the STD spectra of PNG belong to HHDP moiety (6.74-6.60 ppm) that are the first ones to interact with proteins. For procyanidin B2 the signals that appear in the STD spectra (7.04-6.73 ppm) belong to the rings B and E that are responsible for the interaction with proteins.

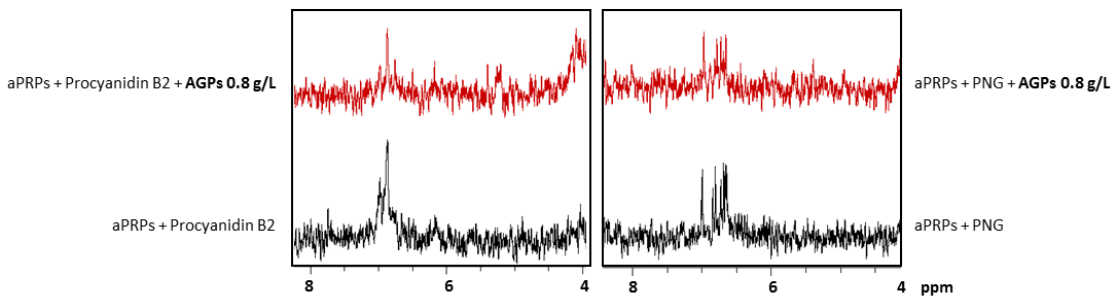


Figure 49 - Representative spectra region from STD experiments (4-8 ppm), considering a solution of aPRPs (15 μ M) and PNG (500 μ M) in the absence and in the presence of AGPs (0.8 g.L $^{-1}$).

These changes in proton intensity were used to determine the % of protein-tannin-polysaccharide interaction based on the integral value of protons on the protein-tannin interaction (100%) (table 14).

Table 14 - Integrals values (%) of ligand signals obtained by STD-NMR for the interaction between each SP (aPRPs and P-B peptide), different tannins (PNG and procyanidin B2) and polysaccharides (AGPs and RG II).

	B2		PNG	
	AGPs	RG II	AGPs	RG II
aPRPs	65.4	42.9	57.7	89.1
P-B peptide	83.0	87.6	86.3	99.8

In general, the values suggest that the presence of polysaccharides decrease the interaction between proteins and tannins, especially for aPRPs' interaction. In the case of aPRPs-procyanidin B2 interaction with both polysaccharides and aPRPs-PNG interaction with AGPs, it was observed a high decrease of the integral values (approximately half of the initial integral value, table 14). This could indicate that polysaccharides compete with proteins to bind tannins, reducing the STD tannin signal since tannin does not receive saturation transfer from the protein. Conversely, this feature was not observed for the aPRPs-PNG interaction in the presence of RG II and for P-B peptide-tannin interaction in the presence of both polysaccharides. Indeed, the small decrease observed ($\leq 17\%$ of the initial integral value) may indicate the formation of soluble ternary complexes where the tannin remains bound to proteins. The presence of RG II does not seem to affect P-B peptide-PNG interaction, which is corroborated with the other two techniques, where no effect was observed. In this case, RG II does not seem to influence the P-B peptide-PNG complex.

STD-NMR is a powerful tool to give informations at a molecular level on protein-ligand interactions, which cannot be obtained by HPLC and nephelometry. The overall results

of the three techniques indicate that all polysaccharides were able to highly reduce the interactions between SP and tannins. HPLC and nephelometry were used as the main techniques and clearly show that there is a non-association or (re)solubilization of SP-tannin aggregates upon the addition of polysaccharides, throughout a competitive mechanism or by the formation of a ternary complex (protein-tannin-polysaccharide), respectively. These results taken together with STD-NMR results make possible to suggest which mechanism is responsible for each interaction.

Several studies reported that the interaction between proteins and tannins is mainly driven by hydrophobic interactions and hydrogen bonds, being the first one more important to the formation of protein-tannin complex and the latter more related to its stabilization [6].

Concerning the effect of polysaccharides on the protein-tannin interaction, it was possible to observe different mechanisms, which can be mainly explained based on the differences of polarity of the molecules involved, which, in turn, would affect the main forces involved in the interactions. Thus, it has to be taken into account that P-B peptide is more apolar than aPRPs as well as PNG is more apolar than procyanidin B2, being these molecules probably more able to establish hydrophobic interactions.

When P-B peptide interacts with tannins, the equilibrium of this interaction seems to be orientated to the formation of the protein-tannin complex. Thus, for most interactions with P-B peptide, there is firstly the formation of P-B peptide-tannin complex, probably ruled by hydrophobic interactions and stabilized by hydrogen bonds, and then the polysaccharides can act by a ternary mechanism through the encapsulation of this complex, increasing its solubility. Through the results obtained with HPLC (no significant recovery of proteins), nephelometry (no decrease of aggregation) and STD-NMR (no decrease of the ligand proton intensity) it was possible to observe the exception of RG II on the P-B peptide-PNG interaction. This can be explained by the polarity of their components. P-B peptide and PNG are more apolar molecules, being their interaction mainly governed by hydrophobic interactions. Consequently, RG II, an acidic polysaccharide, does not have any effect on this interaction.

Concerning the influence of polysaccharides on aPRPs-tannin interaction, it was possible to observe the presence of the two mechanisms: the ternary mechanism and the competition one (Figure 50). For aPRPs interaction with procyanidin B2, the ability of this protein to interact with the procyanidin does not seem to be as strong as in the case of P-B peptide which might be due to a less extent of hydrophobic interactions since

aPRPs are more polar than P-B peptide. Indeed, the addition of procyanidin B2 to saliva caused a higher decrease of the chromatographic peak area of P-B peptide in comparison with aPRPs. According to this mechanism, AGPs and RG II can compete with protein to binding procyanidin B2. As for the interaction of PNG with aPRPs a similar trend seems to occur in the presence of AGPs. Since PNG and AGPs are the less polar molecules present in this interaction, there is also a kind of competition having PNG and AGPs a higher affinity to interact between them, instead of interacting with aPRPs. For the referred interactions, it was observed a recovery of aPRPs' protein (HPLC analysis), a decrease in aggregation (nephelometry) and a high reduction of tannin interaction with protein (STD-NMR).

On the other hand, RG II, which is a more polar polysaccharide, has a lower affinity towards PNG and, in this case, protein-tannin interaction is more important than polysaccharide-tannin interaction and RG II act by a ternary mechanism. In this case, the recovery of aPRPs' protein (HPLC analysis) and a decrease in aggregation (nephelometry) could indicate a competition mechanism. However, when these results are taken together with STD-NMR studies and after analyzing the blank between polysaccharides and tannins, the global results point to the ternary mechanism. Indeed, the aggregation values acquired by nephelometry for the interaction between PNG with AGPs and RG II revealed that in the first case the values of aggregation are higher with the increase of polysaccharides' concentration when compared with the ones obtained for PNG-RG II interaction. This could confirm the great affinity of PNG towards AGPs.

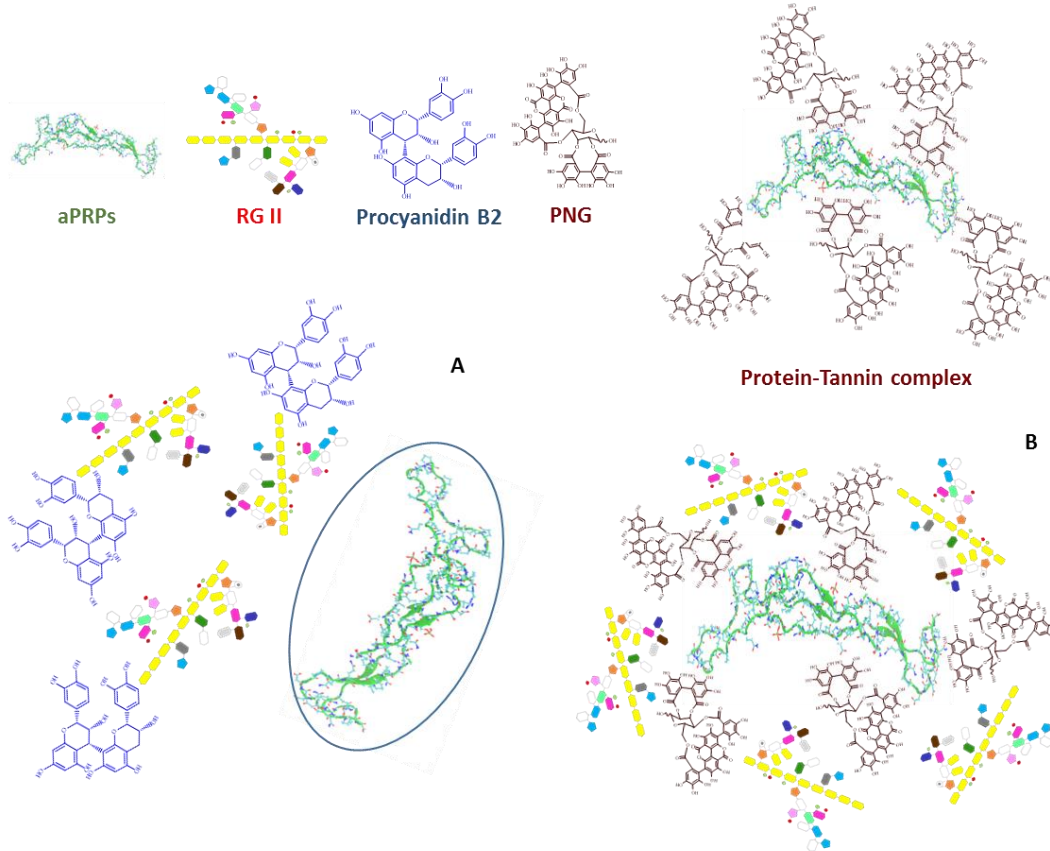


Figure 50 - Possible mechanisms involved in the inhibition of the aggregation of tannins and SP by polysaccharides. A, Competition mechanism where aPRPs and RG II compete to bind procyanidin B2. B, Ternary mechanism in which RG II encapsulates the aPRPs-PNG complex.

Therefore, the results confirm the role of polysaccharides on the SP-tannins interaction. As described in the literature, polysaccharides have influence on the mouthfeel properties of wines such as mellow ness, fullness and roughness [169, 281]. Therefore, they can be connected with the modulation of tannin astringency. However, to be able to complex with tannins or with SP-tannin complex, polysaccharides must have a suitable structure and composition (ionic character), as well a sufficient size and flexibility.

In summary, it was observed that in general RG II, an acidic polysaccharide, can be more effective to disrupt SP-tannin interaction than AGPs, a neutral polysaccharide. This is in agreement with some works reporting the high ability of RG II to reduce protein-tannin interactions [268, 282, 283].

Nevertheless, the results presented herein also showed that this is dependent on the SP family and the class of tannins used. For instance, RG II did not have any influence on P-B peptide-PNG interaction but it can disrupt considerably aPRPs-procyanidin B2 interaction. Furthermore, both polysaccharides have more influence on aPRPs-tannins

interaction than on P-B peptide-tannins interaction due, probably, to the higher affinity of these tannins to interact with aPRPs.

D4. Conclusions

This work clearly demonstrated the ability of polysaccharides to disrupt SP-tannin interaction. Some beverages such as wines, have a considerable level of structural polysaccharides, such as RG II, AGPs and mannoproteins, which probably leads to a corresponding decrease in the perception of astringency.

In conclusion, most polysaccharides tested were able to disrupt aggregates formed between SP and tannins by either a competition mechanism or formation of a ternary complex. This could mean that wines with high levels of these polysaccharides would present lower astringency, even if they have a high polyphenolic content. From a food sensorial perspective, these effects may be relevant since food tannins are usually ingested together with food polysaccharides. Thus, the presence of polysaccharides in food products can modulate their astringency.

E. Inhibition mechanisms of wine polysaccharides on salivary protein precipitation

Abstract

In this work the influence of polysaccharides naturally present in wine (arabinogalactan proteins (AGPs) and rhamnogalacturonan II (RG II)) on the interaction between salivary proteins (SP) directly present in saliva (competitive assay) and tannins (punicalagin (PNG) and procyanidin B2) was evaluated by High Performance Liquid Chromatography (HPLC), fluorescence quenching, nephelometry and sodium dodecylsulfate-polyacrylamide gel electrophoresis (SDS-PAGE). It was also studied the influence of ionic strength (IS) (e.g. presence of salts) on the interaction between SP and tannins as well as the effect of polysaccharides in this condition. In general, RG II, an acidic polysaccharide, was more efficient in the inhibition of SP precipitation by tannins, especially for acidic proline-rich proteins (aPRPs) and statherin/P-B peptide, than AGPs which is a neutral polysaccharide. RG II can act mainly by a competition mechanism in which polysaccharides compete by tannin binding. However, the presence of Na^+ ions can attract the negative charges on the surface of RG II and neutralize it, thereby reducing its ionic character and no polysaccharides' effect in these interactions was observed. On the other hand, AGPs can act by both mechanisms – competition and ternary – depending on the the saliva sample as well as the tannin studied. According to the ternary mechanism, AGPs can form a ternary complex with SP-tannin aggregates enhancing their solubility.

E1. Introduction

Wine creates mouthfeel sensations of astringency, body, burning, balance, pricking, warmth and viscosity [284]. These mouthfeel sensations are recognized as important for wine appearance, aroma or taste [285, 286]. Although astringency is often perceived as negative attribute of tannin-rich products, a balanced level of astringency is desirable for their quality. Astringency is a tactile sensation involving dryness, puckering and tightening of the oral surface [128]. Its onset has been associated with the interaction between SP) and tannins, leading to aggregate formation and, consequently, to precipitation [127, 176, 287]. Tannins are a group of polyphenols structurally very diverse that share the ability to interact with proteins, namely SP. They are usually divided in condensed and hydrolysable tannins, with the first ones, being oligomers of catechins

and the last ones esters of monosaccharides with gallic acid or oligomers of gallic/ellagic acids [127].

Red wine tannins include mainly condensed tannins extracted from grapes and subsequently structurally modified during winemaking and ageing [127]. On the other hand, hydrolysable tannins can be found in wine due to migration from oak wood to wine during ageing or by the addition of enological tannins during winemaking [38]. However, due to their lower amounts in red wine, they have not been associated as the major contributors of astringency sensation. Nevertheless, in the recent years, some studies revealed that ellagitannins can bind SP and may hence be attributed to the perceived astringency [244, 262, 264, 288].

Whole saliva is a complex mixture of proteins, electrolytes and small organic compounds as the result of the secretions of the major and minor salivary glands, gingival crevicular fluid, oral bacteria and food debris [83, 289]. Saliva has a diverse range of SP families and peptides that can be grouped according to their structures and characteristics [290]. These include mucins, histatins, statherin, P-B peptide, cystatins and proline-rich proteins (PRPs), which are in turn divided into basic (bPRPs), glycosylated (gPRPs) and acidic (aPRPs) [290]. PRPs are one of the most abundant families of SP present in saliva and they have been extensively studied due to their high ability to interact with tannins [128, 291, 292]. Statherin and P-B peptide have also been described to interact strongly with tannins [102, 293].

Tannin-protein interactions can be affected by different factors, such as tannin and protein structural features, pH, ethanol, IS and the presence of polysaccharides, among others [127]. In general, the factors that affect the binding affinity of tannins to proteins are expected to affect astringency in the same way [6]. Polysaccharides are one of the major classes of macromolecules found in wine, together with polyphenols and proteins. They are also known to modify wine processing and wine organoleptic properties, since they can stabilize other molecules in solution [294]. Several studies using different approaches showed that polysaccharides can affect protein-tannin interactions and may hence lead to astringency modulation [28, 269, 270, 295, 296]. Two mechanisms have been proposed to explain this effect: (I) competition between polysaccharides and SP toward tannins; or, (II) formation of a ternary complex protein-polyphenol-polysaccharides, with enhanced solubility in an aqueous medium [272].

The main polysaccharides in wine are grape-derived RG-II and polysaccharides rich in arabinose and galactose (PRAGs), consisting of AGPs, and yeast-derived mannoproteins [160]. It has been reported that acidic polysaccharides have a great impact on the reduction of astringency perception, such as the case of RG-II, the main acidic polysaccharide present in wines. Other studies revealed that neutral polysaccharides, such as AGPs, have a higher impact on reducing bitterness than on reducing the intensity of the astringency attributes [169, 282]. There are some works studying the influence of polysaccharides on SP-tannin interactions where SP isolated were used. Moreover, other authors studied the effect of commercial polysaccharides on the interaction between SP and tannins [268-270, 272, 297]. However, there are no studies focused on the influence of polysaccharides naturally present in fruits or beverages on the interaction between SP directly present in saliva (competitive assay) and tannins.

So, the aim of this work was to go deeper into the knowledge, at a molecular level, of the influence of polysaccharides on the interaction between SP and tannins. This way, polysaccharides naturally present in wine with different charges and structures (AGPs and RG II) were chosen. Additionally, PNG and procyanidin dimer B2 were chosen as model tannins, since the first one is commonly used as a hydrolyzable tannin model, while the second one is an abundant procyanidin dimer in red wine [6].

E2. Matherial and Methods

E2.1. Saliva isolation and saliva samples preparation in different conditions

Saliva was collected from several healthy volunteers and treated as described in the literature [178]. After acidic treatment with trifluoroacetic acid (TFA), peptides and proteins like histatins, PRPs, statherin, P-B peptide and cystatins remained in acidic saliva (**S**).

Saliva was then dialyzed in a cellulose dialysis membrane (MWCO: 3.5 kDa) for 24 h at 4°C with stirring against deionized water and centrifuged, which was called dialyzed saliva (DS). This supernatant was then divided into two aliquots: one containing salts (NaCl, final concentration 200 mM) (**DS⁺**), and the other one without salts (**DS⁻**).

Part of DS⁻ sample was also freeze-dried and the lyophilized saliva was solubilized in a minimum volume of water to concentrate total protein composition. The resulting solution

was purified by semi-preparative HPLC in which different SP families were collected, according to their retention time [267]. Then, they were freeze-dried, and the major peptides present in each fraction were identified by Electrospray Ionization-Mass Spectrometry (ESI-MS) as described in the literature [178]. These isolated SP families were then mixed (without salts) at concentrations similar to the physiological values reported in the literature forming the last saliva sample (Mixture of SP, **MSP**) [266]. The four saliva samples are summarized in Table 15 and they were used for the interactions with tannins and polysaccharides, as it will be explained in the next sections.

This study was conducted according to the Declaration of Helsinki and was approved by the Ethics Committee of Medical School of University of Porto (EK84032011).

Table 15 - Different conditions of saliva samples used to study the influence of polysaccharides on the interaction between SP and tannins.

Saliva sample	Characteristics
S	Non-dialyzed saliva (standard saliva)
DS-	Dialyzed saliva in the absence of salts,
DS⁺	DS- with salts (NaCl, 200 mM)
MSP	Mixture of different SP families, previously purified, in the absence of salts

E2.2. Isolation of procyanidin dimer B2 and punicalagin

Four fractions of grape seeds (*Vitis vinifera*) were obtained and characterized as described somewhere [182]. Procyanidin dimer B2 was isolated from these fractions by preparative HPLC. PNG was isolated from pomegranate following several steps described in the literature [274].

E2.3. Isolation and characterization of polysaccharide fractions

E2.3.1. Isolation of AGPs and RG II

RG II fraction was isolated from wine, following the procedure reported elsewhere [275, 298]. AGPs fraction was also isolated from wine sample fractions after anion-exchange and/or size-exclusion chromatographic steps. A final fraction containing a mixture of AGPs and mannoproteins was purified by affinity chromatography, using mannoproteins' ability to bind to Concanavalin A lectin as it was reported in the literature [160, 298]. Both

RG II and AGPs fractions were then analyzed in terms of their neutral and acidic sugar composition.

E2.3.2. Neutral and acidic sugar composition

Neutral sugar composition was determined as alditol acetates after TFA hydrolysis (75 min at 120 °C), reduction and acetylation, as described in the literature [161, 276]. The resulting alditol acetate derivatives were quantified by gas chromatography (GC) analysis using a fused silica DB-225 (210 °C) capillary column (30 m × 0.25 mm i.d., 0.25 µm film), with hydrogen as the carrier gas, on a Shimadzu GC-2010 Plus gas chromatograph. The different alditol acetates were identified from their retention time by comparison with that of standard monosaccharides. Neutral sugar amounts were calculated relatively to the internal standards (allose and myo-inositol).

Neutral and acidic sugar composition was determined after solvolysis with anhydrous MeOH containing 0.5 M HCl (16h, 80°C) by GC-MS of their per-O-trimethylsilylated methyl glycoside derivatives. The resulting TMS derivatives were separated on a DB-1 (temperature programming 120–145 °C at 1.5 °C min⁻¹, 145–180 °C at 0.9 °C min⁻¹, and 180–230 °C at 50 °C min⁻¹ and hold time 4 min) capillary columns (30 m x 0.25 mm i.d., 0.25 µm film), coupled to a single injector inlet, with hydrogen as the carrier gas, on a Shimadzu GCMS-QP 2010 Plus gas chromatograph [277]. Myo-inositol was used as internal standard.

E2.4. Influence of polysaccharides on saliva-tannin interactions

The influence of two wine polysaccharides (AGPs and RG II) on saliva-tannin interactions was assessed by different techniques namely HPLC, nephelometry and fluorescence quenching and SDS-PAGE. After establishing the tannin concentration for each technique, the procedure was always the same: polysaccharides react first with tannins (30 min) and after this time saliva was added (10 min). The final mixture was then analyzed by the different techniques.

E2.4.1. HPLC analysis

Preliminary experiments were made to access the minimal tannin concentration that precipitate most of the SP families. For this, S sample was analyzed by HPLC before and after increasing concentrations of PNG and procyanidin B2. The control condition was a mixture of S (70 µL) and water (50 µL) (final volume, 120 µL). Different volumes of tannins' stock solution were added to S in order to obtain the desired final concentrations, being the final volume adjusted with water. The mixture was shaken and kept reacting for 10 min at room temperature, centrifuged (8000 g, 5 min) and finally, the supernatant was injected into the HPLC. The tannin concentration chosen for HPLC was 130 µM (PNG) and 1000 µM (procyanidin B2) because at these concentrations a partial reduction of the chromatographic peaks area of the most SP families was observed. For the other techniques, the tannin's concentration needed to be adjusted according to their sensitivity. This way, for fluorescence studies the PNG and procyanidin B2 concentrations were 4 µM and 40 µM, respectively; whereas for nephelometry measurements the concentrations were 60 µM for PNG and 540 uM for procyanidin B2. For the experiments with polysaccharides, increasing concentrations of AGPs and RG II (0.0-2.4 g.L⁻¹) reacted with tannins. After this time, the four saliva samples were added, the mixture was then centrifuged and the supernatant (100 µL) was analyzed by HPLC using the method previously reported [298].

E2.4.2. Fluorescence quenching

The presence of increasing concentrations of different polysaccharides (0.0-1.2 g.L⁻¹) was assayed by alterations of the quenching effect of PNG and procyanidin B2 on the saliva fluorescence. These assays were done in Horiba Jobin Yvon Fluoromax-4 Spectrofluorometer. Since procyanidins are known to possess intrinsic fluorescence (λ_{ex} max=282 nm) the λ_{ex} was set to 260 nm, and the emission spectrum was recorded from 300 to 500 nm. This λ_{ex} was established since allowed to minimize the maximum absorption of procyanidin B2 (282 nm) and at the same time it was possible to obtain a saliva fluorescence spectrum. Even in these conditions, a residual procyanidin B2 fluorescence was observed. So, a blank of procyanidin B2 was performed and subtracted in all fluorescence experiments with this tannin. Considering polysaccharides at this wavelength no significant polysaccharide fluorescence was noted. The possibility of fluorescence resonance energy transfer (FRET) between SP from saliva and procyanidin B2 was discarded after analysis of both absorption and emission spectra [192].

Due to a higher sensitivity of this technique, PNG and procyanidin B2 concentrations were the lowest used for all techniques (4 μM and 40 μM , respectively). In these experiments, saliva samples (S and DS⁻) were added to a mixture tannin-polysaccharide. For each experiment, a relative fluorescence value (%) was calculated as the ratio between the fluorescence of the measured sample (F) and that of the unquenched saliva (F_0 , 100%).

E2.4.3. Nephelometry measurements

Nephelometry experiments were conducted in a Horiba Jobin Yvon Fluoromax-4 Spectro Fluorometer which was used as a 90° light scattering photometer. The excitation and the emission wavelengths were set at 400 nm because at this wavelength proteins, tannins and polysaccharides do not absorb the incident light [268, 278]. In these experiments, PNG (60 μM) and procyanidin B2 (540 μM) react firstly with increasing concentrations of AGPs and RG II (0.0-1.2 g.L⁻¹). After this time, S and DS⁻ samples were added reacting for 10 min, and the resulting solution was analyzed before centrifugation. A blank was made for each polysaccharide concentration, using a fixed concentration of tannins or saliva. A relative aggregation value (%) was then calculated as the ratio between the scatter intensity of each sample and the control condition (saliva with tannin in the absence of polysaccharide, 100%).

E2.4.4. SDS-PAGE

For some interactions such as the interactions between S/DS⁻ samples and tannins (PNG and procyanidin B2) it was necessary carried out more experiments to give evidences about the mechanism by which RG II or AGPs were acting. This way, the precipitates that resulted from the interaction between these saliva samples and tannins in absence and presence of the two highest polysaccharide concentrations (1.2 g.L⁻¹ and 2.4 g.L⁻¹) were analyzed by SDS-PAGE. This method is based on a separation of proteins according to their sizes using a 16% acrylamide resolving gel. The precipitates were resolubilized in 25 μL of electrophoresis buffer (125 mM Tris-HCl pH 6.8, 20 % v/v glycerol, 4 % SDS, 10 % v/v β -mercaptoethanol, and 0.004 % bromophenol blue) and heated at 90 °C for 20 min.

The running buffer was 0.2 M Tris-HCl pH 8.3, 1.9 M glycine and 0.1 % SDS. Molecular weight markers were broad ranged (Precision Plus ProteinTM Unstained Standards, Bio-Rad). The separation was performed on a Bio-Rad MiniProtean Cell electrophoresis

apparatus (Bio-Rad) at constant amperage (0.3 A). After electrophoresis, the gels were stained with Imperial Protein Stain - a Coomassie R-250 dye-based reagent - for 30 min. The destaining step was done by washing the gels overnight with water:methanol:acetic acid (70:20:10 v/v/v).

E2.4.5. Statistical analysis

Statistical significance of the different HPLC values was evaluated by test *t*. Statistical significance of fluorescence quenching values and nephelometry values were evaluated by two-way analysis variance (ANOVA), followed by the Bonferroni test. Differences were considered to be statistically significant when P< 0.05. All of the experiments were performed in n = 3 repetitions.

E3. Results and Discussion

The aim of this work was to understand the influence of wine polysaccharides on the interaction between SP and tannins. The influence of two wine polysaccharides, AGPs and RG II, on the interaction between two representative tannins (PNG and procyanidin B2) and different saliva samples was studied by HPLC, fluorescence quenching, nephelometry measurements and SDS-PAGE. The experimental approach described herein intended to mimic the phenomenon during ingestion, where polysaccharides and tannins are present together in food or beverages and enter simultaneously in contact with SP. For this purpose, a solution of tannins-polysaccharides was previously prepared to which different saliva samples were subsequently added.

E3.1. Salivary proteins identification and saliva samples

Saliva is a very complex body fluid mainly composed by water, proteins, electrolytes and small organic compounds. The major SP families from human saliva detected on the HPLC chromatogram were already identified in previous works [178, 299]. Briefly, HPLC chromatogram of human saliva at 214 nm can be divided into five regions: bPRPs, gPRPs, aPRPs, statherin/P-B peptide and, finally cystatins (Figure 51). After identification of the major proteins, the average molecular weight of each fraction was estimated based on ESI-MS signals intensity: bPRPs (5388 Da), aPRPs (14643 Da), statherin (5232 Da), P-B peptide (5792 Da) and cystatins (14300 Da). gPRPs average

molecular weight was determined to be 16000 Da by static light scattering [299]. Saliva is rich in different salts which contribute to its high IS (50 mM) [300]. It was already described that IS can affect the interaction between tannins and proteins [268]. On the other hand, we hypothesize that salts may also affect the influence of polysaccharides on the interaction between proteins and tannins [119, 270]. Through dialysis is possible to remove small molecules which contributes to decrease the IS of saliva. So, four saliva samples were prepared: S (Standard saliva) and DS⁺ (Dialyzed saliva with NaCl) which correspond to samples with a higher amount of salts (high IS), and DS⁻ (Dialyzed saliva) and MSP (mix of SP families) samples which correspond to saliva with a less amount of salts (low IS). Indeed, the MSP sample was composed by several SP families at concentrations similar to the physiological values found in saliva, based in the values reported in the literature but in the absence of salts [266]. For this purpose, the PRPs concentrations were 35 µM, 16 µM and 30 µM for bPRPs, gPRPs and aPRPs, respectively. For the other SP families, such as statherin/P-B peptide and cystatins the concentrations estimated were 24 µM and 26 µM, respectively.

E3.2. Polysaccharide and oligosaccharide characterization

Both polysaccharides fractions AGPs and RG II were characterized previously in terms of sugar composition [298]. AGPs consist in a ramified (1→3)-D-galactan inner core with (1→6)-linked galactan side chains that are highly substituted with arabinose and with few amounts of rhamnose, xylose, and glucuronic acid [164]. RG II has a backbone of at least eight residues of galacturonic acid with four different secondary side chains. RG II contains twelve different glycosyl residues, including galacturonic and glucuronic acids, fucose, arabinose, rhamnose, galactose, and several rare and diagnostic sugars of RG II presence, such as apiose, aceric acid, 2-O-methyl fucose, 2-O-methylxylose, Kdo (3-deoxy-D-manno-octulosonic acid) and Dha (3-deoxy-D-lyxo-heptulosaric acid) [159, 279].

E3.3. Interaction between SP and tannins

Firstly, it was necessary to establish tannin concentration that causes the precipitation of the several SP families. A small concentration of tannins could be insufficient to lead to SP precipitation, while an excess of tannins could lead to a total depletion of proteins and also to free molecules of PNG and procyanidin B2. These concentrations were optimized with S sample.

It can be seen from Figure 51 that the addition of PNG (130 μ M) or procyanoindin B2 (1000 μ M) to S sample reduced the amount of several SP families, with the two most reduced being aPRPs and statherin/P-B peptide. Furthermore, it is important to note that PNG seem to have a higher affinity to interact with SP in comparison with procyanoindin B2, since procyanoindin B2 concentration was almost 10-fold higher than PNG concentration to cause approximately the same % SP reduction. In fact, aPRPs and statherin/P-B peptide reduced *ca.* 60-80 % of their initial chromatographic peaks area, while gPRPs and cystatins reduced *ca.* 20 % and 30 %, respectively.

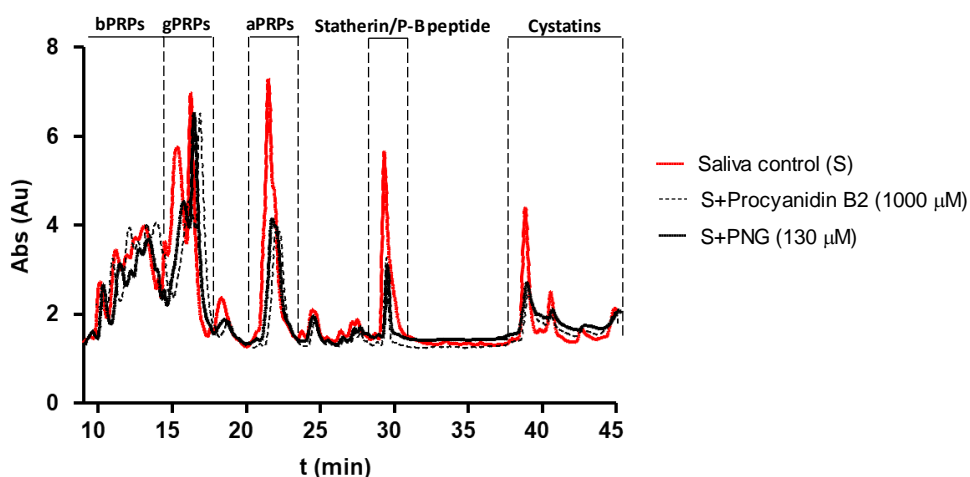


Figure 51 - Typical HPLC profile of human saliva detected at 214 nm in the absence (red line) and in the presence of tannins: PNG 130 μ M (black line) and procyanoindin B2 1000 μ M (black dashed line). The vertical dotted lines show the ranges and the main SP families assigned to each HPLC peptide region.

E3.4. Influence of polysaccharides on the interaction between SP and tannins

E3.4.1. HPLC analysis

The ability of AGPs and RG II to inhibit the precipitation of SP from different samples (S, DS⁺, DS⁻ and MSP) was firstly evaluated by HPLC. As an example, Figure 52 shows the variation of the chromatographic peaks area of the different SP families concerning the four saliva samples studied, after interaction with PNG and with increasing concentrations of polysaccharides (RG II and AGPs). These results are expressed as percentage of the area of these proteins relatively to the respective area in saliva without tannin.

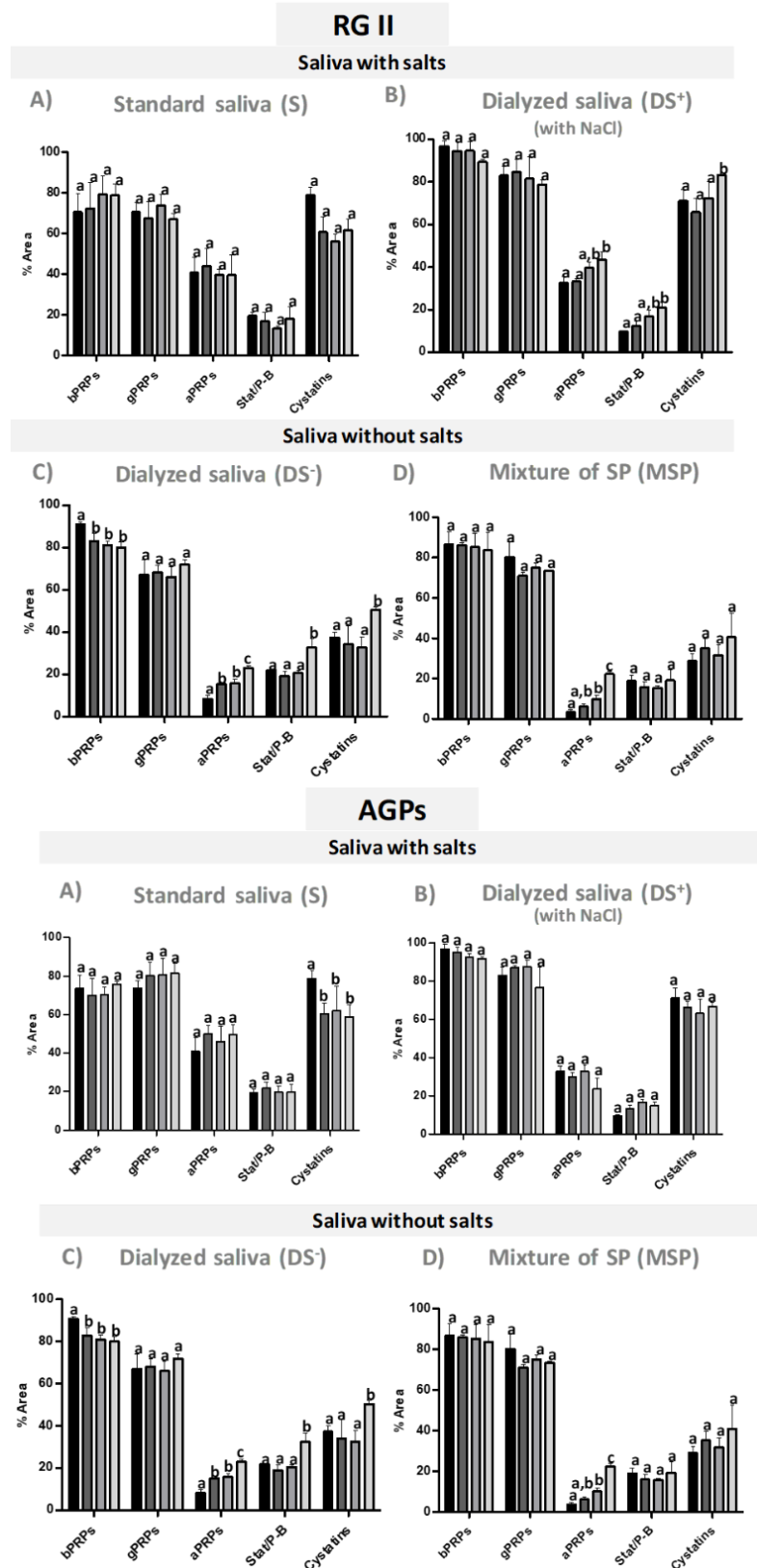


Figure 52 - Influence of polysaccharides concentration (RG II and AGPs), on SP precipitation after interaction between saliva in the absence (DS⁻ and MSP) or presence of salts (S and DS⁺) and PNG (130 μ M). (A) S, (B) DS⁺, (C) DS⁻, and (D) MSP. These results represent the average of three independent experiments. Values with different letters within each column are significantly different ($P \leq 0.05$).

Concerning the influence of polysaccharides on SP-tannin interaction, it is possible to observe that their effect is more evident on dialyzed saliva (DS^-) as well as on the mixture of SP (MSP) (absence of salts), independently of the tannin used. In general, RG II was the most efficient polysaccharide in preventing SP precipitation, independently of the saliva sample and the tannin used. However, the effect of RG II is dependent both on the saliva sample used as well as on the SP family. Similar results were obtained for the interaction with procyanidin B2 (Figure 53 and 54).

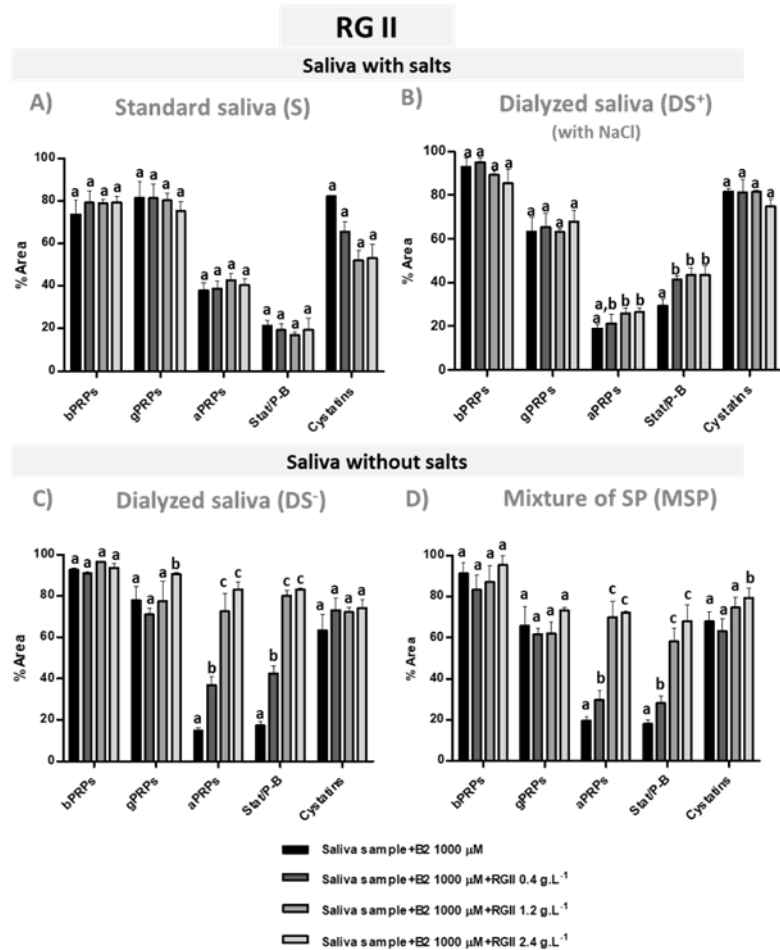


Figure 53 - Influence of RG II concentration on SP precipitation after interaction between saliva in the absence (DS^-) and MSP) or presence of salts (S and DS^+) and procyanidin B2 (1000 μ M). (A) S, (B) DS^+ , (C) DS^- , and (D) MSP. These results represent the average of three independent experiments. Values with different letters within each column are significantly different ($P \leq 0.05$).

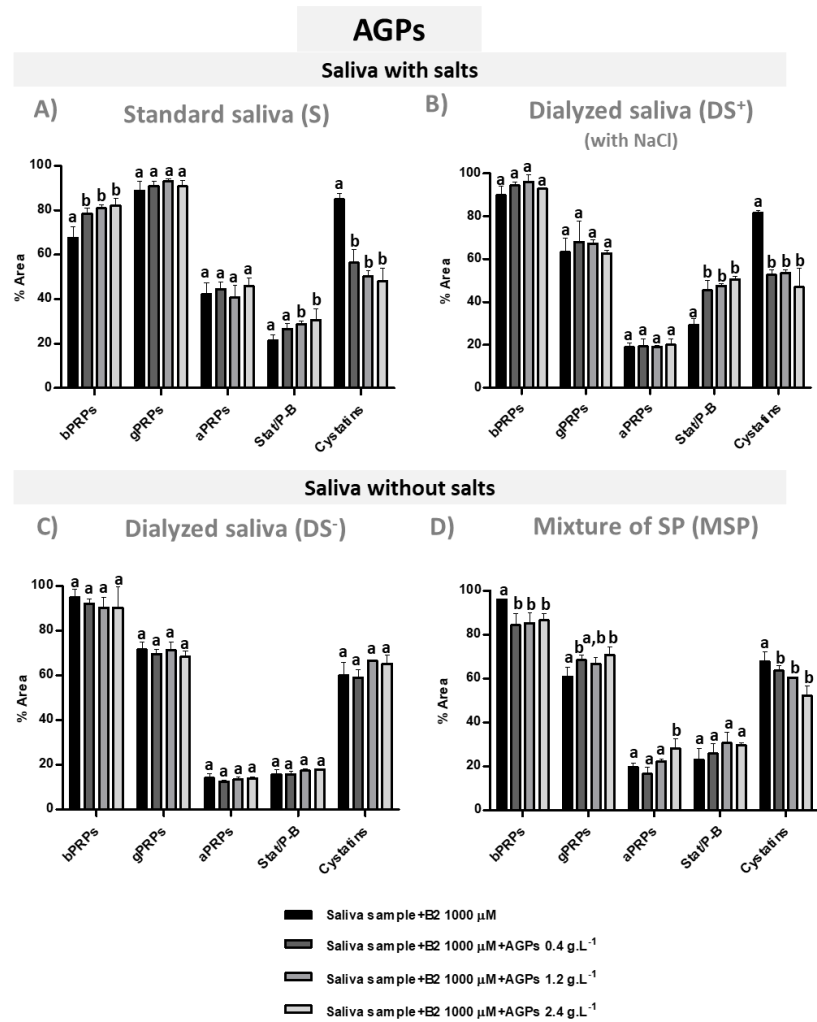


Figure 54 - Influence of AGPs concentration on SP precipitation after interaction between saliva in the absence (DS⁻ and MSP) or presence of salts (S and DS⁺) and procyanidin B2 (1000 μM). (A) S, (B) DS⁺, (C) DS⁻, and (D) MSP. These results represent the average of three independent experiments. Values with different letters within each column are significantly different ($P \leq 0.05$).

To easily compare the effectiveness of polysaccharides in preventing SP precipitation by tannins, through the HPLC results, the recovery of each SP family (%) in the presence of polysaccharides is presented on Table 16. These values were calculated as the difference between the maximum value of the chromatographic peaks area of each SP family (saliva with tannins and the highest polysaccharide concentration – 2.4 g.L^{-1}) and the minimum value of these chromatographic peaks (saliva with tannins in the absence of polysaccharides). Only the values of the different SP families which significantly recovered in the presence of polysaccharides are presented in this table.

Table 16 - The effectiveness of AGPs and RG II (2.4 g.L^{-1}) to inhibit SP precipitation by PNG (130 μM) and procyanoindin B2 (1000 μM). These values represent the recovery (%) of each SP family.

Saliva sample	Tannin-Polysaccharide pair	bPRPs	gPRPs	aPRPs	Statherin/P-B peptide	Cystatins
Standard saliva (S)	PNG-AGPs	-	14.7 \pm 5.3	15.6 \pm 4.5	7.2 \pm 2.6	-
	B2-AGPs	14.5 \pm 5.8	-	-	9.1 \pm 3.8	-
Dialyzed saliva with NaCl (DS⁺)	PNG-RG II	-	-	-	6.4 \pm 1.8	12.2 \pm 3.8
	PNG-AGPs	-	-	-	6.2 \pm 1.1	-
	B2-RG II	-	-	7.5 \pm 2.1	14.2 \pm 5.0	-
Dialyzed saliva without NaCl (DS⁻)	B2-AGPs	-	-	-	21.4 \pm 4.1	-
	PNG-RG II	-	-	69.9 \pm 3.2	57.2 \pm 2.7	31.0 \pm 8.2
	PNG-AGPs	-	-	14.8 \pm 2.5	7.7 \pm 2.8	13.2 \pm 3.1
Mixture of SP (MSP)	B2-RG II	-	12.8 \pm 5.3	68.1 \pm 3.3	65.9 \pm 2.5	-
	PNG-RG II	-	22.8 \pm 6.1	60.9 \pm 6.0	53.5 \pm 6.2	44.2 \pm 7.0
	PNG-AGPs	-	-	16.2 \pm 1.9	-	16.8 \pm 7.4
	B2-AGPs	-	9.9 \pm 3.7	8.6 \pm 3.8	-	-

From Figures 52, 53 and 54 and the values presented on table 16 it is possible to observe that RG II was significantly effective in inhibiting SP precipitation, mainly for the interactions between DS⁻/MSP samples and PNG/procyanoindin B2 (higher % recovery, 40-70%), which is interesting because these were the saliva samples with lower amount of salts and, consequently, lower IS. This effect was more pronounced for some SP families, such as aPRPs, statherin/P-B peptide and cystatins leading to a higher recovery of the chromatographic peaks area of these proteins, regardless of the tannin present (PNG or procyanoindin B2). Although not so important, RG II also causes the recovery of some SP families on the interaction of DS⁺ with PNG. The influence of AGPs was also significant for the interaction between DS⁻ and MSP samples with tannins, however with a lower recovery of the chromatographic peaks area of SP (10-20 %).

Therefore, the behavior of polysaccharides was quite similar for the interaction between saliva S and DS⁺ and tannins, as well as, for the interaction between of DS⁻ and MSP samples toward tannins. For this reason, for fluorescence quenching studies, nephelometry measurements and SDS-PAGE only saliva samples S and DS⁻ were used.

E3.4.2. Fluorescence quenching

To supplement the information obtained by HPLC, fluorescence quenching studies were conducted. The most common chromophore in proteins is tryptophan. As previously reported, the addition of quenchers to a fluorophore can cause a fluorescence quenching effect reducing the intensity of the fluorophores' emission maximum [288]. Some experiments concerning only tannins and polysaccharides were performed in order to study if there is any interaction between these two compounds. This study was also performed in the presence or absence of salts (NaCl). Depending on the tannin-polysaccharide pair, the fluorophore was the tannin or the polysaccharide, and the quencher was the other compound. RG II was used as fluorophore on the interaction with procyanidin B2 and PNG (quenchers). On the other hand, procyanidin B2 was used as fluorophore with AGPs (quencher). It was not possible to study AGPs and PNG interaction because none of these compounds have fluorescence. No variation of the fluorescence intensity signal was verified for RG II-procyanidin B2 and procyanidin B2-AGPs interactions. On the other hand, PNG seem to cause a quenching effect on RG II fluorescence intensity, being this effect more pronounced in the absence of salt (low IS condition).

After these preliminary tests, fluorescence quenching conditions were adapted to study the different saliva samples (S and DS⁻ samples). So, the λ_{ex} was established ($\lambda_{ex}= 260$ nm) to avoid the maximum absorption wavelength of procyanidin B2 (282 nm) and at the same time not compromising the saliva fluorescence intensity signal.

The plots of relative fluorescence intensity for the interactions of S/DS⁻ samples and both tannins with increasing concentrations of polysaccharides (0.0-1.2 g.L⁻¹) are shown in Figure 55. The maximum fluorescence intensity of saliva in the absence of tannins corresponds to 100%. In the presence of PNG and procyanidin B2 (quenchers), SP fluorescence decreases about 25% for both tannins.

As it was previously referred, the influence of polysaccharides seems to be dependent of the saliva sample, which in turn, is related with the amount of salts. Figure 55 shows that in general, polysaccharides were more effective on the interactions between tannins and DS⁻ sample, which corresponds to saliva with lower amount of salts. More precisely, polysaccharides were able to decrease the quenching effect and, consequently, to increase the SP fluorescence intensity at least in five of the eight interactions studied by this technique. Concerning AGPs, this effect was observed for S-procyanidin B2, S-PNG and DS⁻-PNG interactions, being more pronounced for the two first interactions. On the

other hand, in the presence of RG II this effect was noted for DS-PNG and DS-procyanidin B2 interactions.

In general, RG II was more effective than AGPs, since it caused a higher recovery of fluorescence, especially for the interaction between DS⁻ with both tannins, which is in agreement with the HPLC results.

In all these cases, the increase of fluorescence intensity was concomitant with the increasing of polysaccharides concentrations, confirming this way that these compounds have the capacity to reduce the tannins' quenching ability toward SP.

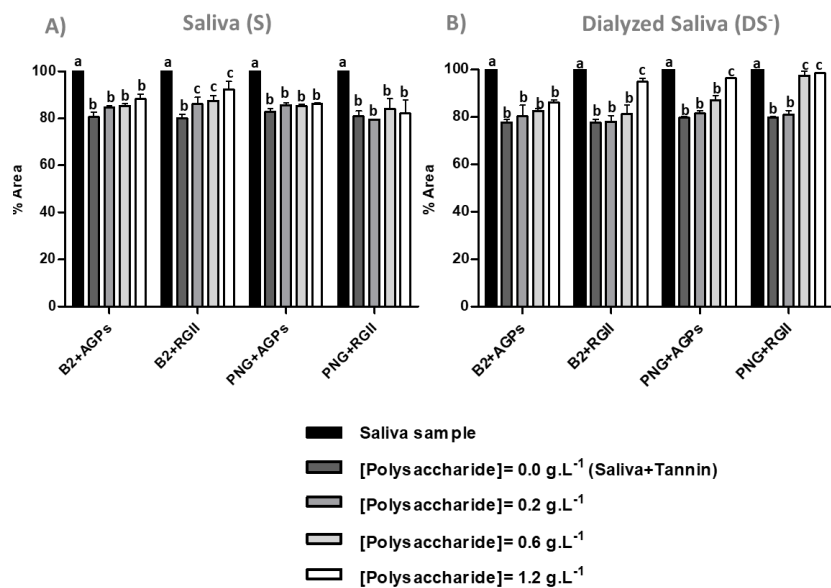


Figure 55 - Variation (%) in fluorescence intensity at 260 nm of two saliva samples (S and DS⁻) and PNG (4 μ M) and procyanidin B2 (40 μ M), with increasing concentrations of different polysaccharides – AGPs and RG II. These results represent the average of three independent experiments. Values with different letters within each column are significantly different ($P \leq 0.05$).

E3.4.3. Nephelometry measurements and SDS-PAGE experiments

It is well known that the interaction between proteins and tannins leads to an aggregation process. Thus, the inhibitory effect of polysaccharides, AGPs and RG II, against SP aggregation and further precipitation by tannins was evaluated by measuring the decrease of the aggregates in solution by nephelometry (Figure 56).

Firstly, control experiments with tannins or proteins and increasing polysaccharide concentrations were made to investigate if there is any aggregation between them. In general, for the control experiments between tannins and polysaccharides, the aggregation value increased with the increase of polysaccharide concentration. On the

other hand, the aggregation value of the interaction between proteins and polysaccharides remained practically constant as polysaccharide concentration increased. For this reason, the blank of polysaccharides and tannins was subtracted to the aggregation value obtained for each experiment. A relative aggregation value (%) was then calculated as the ratio between the scatter intensity of each sample and the control condition (SP with tannin in the absence of polysaccharide, 100%). Values lower than 100% indicate less scattered light, which may be due to smaller or less aggregates.

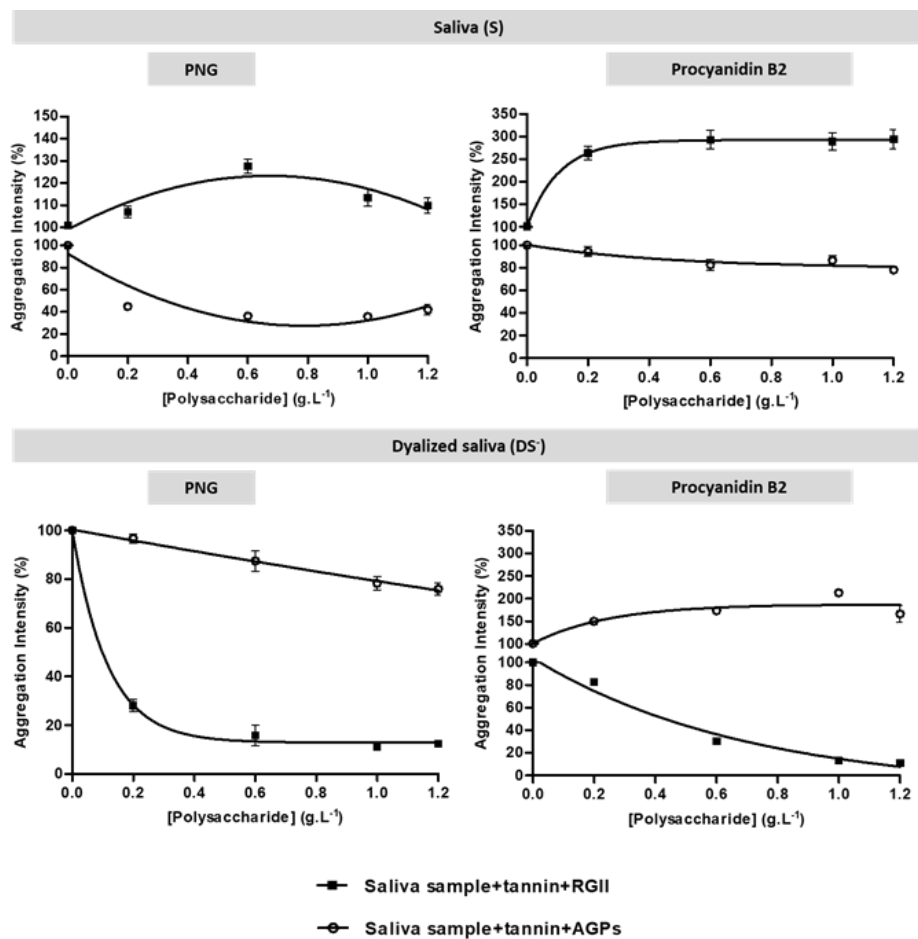


Figure 56 - Influence of AGPs and RG II concentration on aggregate formation (%) at 400 nm, between two saliva samples (Saliva, S and dialyzed saliva, DS-) and tannins, PNG (60 µM) and procyanidin B2 (540 µM).

Concerning the influence of polysaccharides on the interaction between S sample and tannins (PNG and procyanidin B2) it was possible to note that AGPs and RG II have different behaviors. For S-PNG interaction, RG II contributed to an increase of aggregation, being the aggregation value higher than the aggregation control value (100%, corresponding to saliva+PNG). However, in the presence of AGPs there was a higher decrease of aggregation. For S-procyanidin B2 interactions, RG II and AGPs exhibited a similar behavior as that one for the interaction S-PNG: an increase of

aggregation in the presence of RG II (higher than in the absence of RG II) and a slightly decrease of aggregation with AGPs.

In the case of RG II the results may be explained by the formation of bigger or more aggregates, which probably will culminate in precipitation. On the other hand, the decrease of aggregation in the presence of AGPs seems to suggest that there is less scattered light, which may be due to smaller or less aggregates.

Concerning DS⁻-sample, the presence of polysaccharides, RG II and AGPs, on the DS⁻-PNG interaction seems to inhibit or reduce the formation of insoluble aggregates due to a decrease of aggregation. For DS⁻-procyanidin B2 interactions, it is possible to observe a distinct behavior for each polysaccharide. When RG II is present, there is a decrease of aggregation, while in the presence of AGPs there is an increase of aggregation. For the interaction of DS⁻ sample with both tannins, the polysaccharide effect is more pronounced in the presence of RG II than in the presence of AGPs, which is in agreement with the results obtained by HPLC and fluorescence studies.

These results taken together allowed to suggest the underlying mechanism for most interactions (Table 17). RG II and AGPs seem to act by a competition mechanism on the interaction between DS⁻ sample and PNG. The same mechanism may be suggested for the effect of RG II on DS⁻ sample interaction with procyanidin B2 as well as for AGPs on S-PNG interaction. In these interactions, a decrease of the quenching effect (fluorescence studies), a decrease in aggregation (nephelometry) and a high recovery of the SP chromatographic peaks area (HPLC) point to a competition mechanism, in which SP and polysaccharides compete for tannin binding resulting in less tannin available to bind and to aggregate with SP. The higher ability of polysaccharides to inhibit or reduce SP precipitation by tannins in dialyzed saliva can be explained by the lower amount of salts which corresponds to a lower IS. RG II is a negatively charged polysaccharide being its effect affected by the presence of salts. For instance, at higher IS, the ions in solution, especially cations such as Na⁺, can be attracted by negative charges in the surface of polysaccharides and can neutralize them, thereby reducing their ionic character. For this reason, the acidic polysaccharides will have a similar behavior as the neutral ones, being less effective in preventing aggregation. This effect is more visible for RG II than for AGPs, because the latter has a more neutral character and, this way, it is not so affected by the presence of salts. Indeed, AGPs compete with SP from S sample to bind PNG, having more affinity for the tannin than for the SP. Since AGPs are not so affected by the presence of salts and they are a neutral, they have more

affinity for PNG which is a less polar tannin explaining why they can act by a competition mechanism in this interaction.

However, for some interactions such as S-PNG-RG II, S-procyanidin B2-RG II, S-procyanidin B2-AGPs and DS⁻-procyanidin B2-AGPs the results obtained were not able to elucidate by which mechanism RG II and AGPs can act. For this reason, the pellets that resulted from the S/ DS⁻ interaction with tannins in the absence and presence of the RG II or AGPs were analyzed by SDS-PAGE. So, to analyze these pellets, all precipitates were resolubilized by heating (90 °C) in 25 µL of electrophoresis sample buffer. Figure 57 displays the obtained protein bands after SDS-PAGE separation.

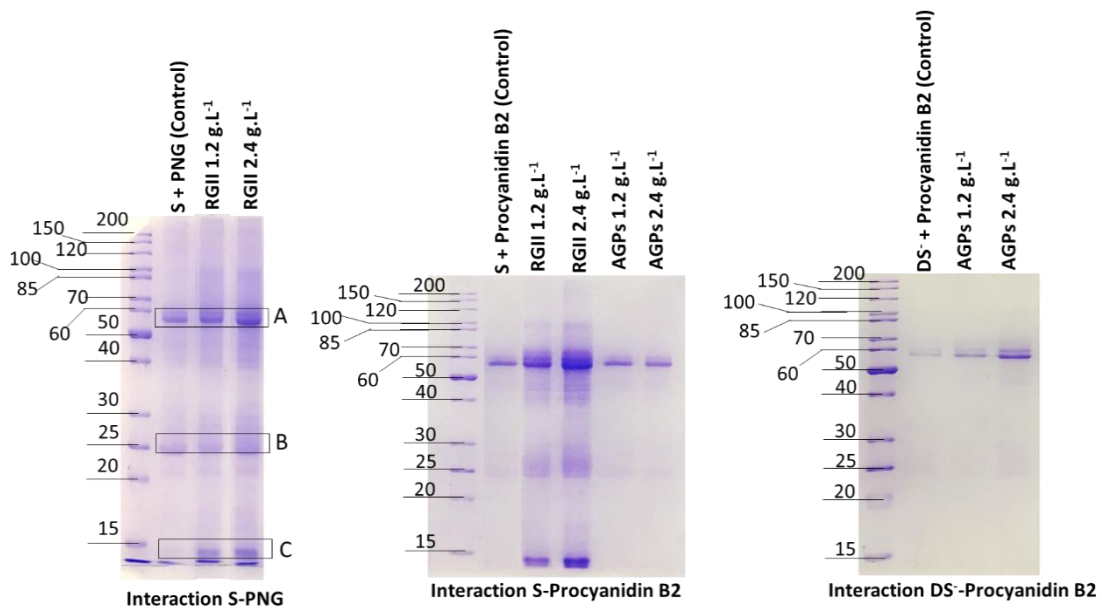


Figure 57 - SDS-PAGE of the pellets that resulted from the interaction between S/DS⁻ and tannins (PNG and procyanidin B2) in the absence (Control) and presence of the several polysaccharides (RG II and AGPs, 1.2 g. L⁻¹ and 2.4 g. L⁻¹). The molecular weight markers are identified, and the molecular mass marked on the left side is expressed in kDa. The gels were stained with Imperial Protein Stain, a Coomassie R-250 dye-based reagent.

Table 17 - Summary of the suggested mechanisms for the polysaccharides' effect on the interaction between SP and tannins used in this work.

	Tannin	Polysaccharide	HPLC results	Fluorescence quenching	Nephelometry measurements	SDS-PAGE	Mechanism of action
S sample	PNG	RG II	No recovery	No decrease of quenching effect	Increase aggregation	Higher precipitation	No effect
		AGPs	Recovery	Decrease of quenching effect	Decrease aggregation	-	Competition mechanism
	Procyandin B2	RG II	No recovery	No decrease of quenching effect	Increase aggregation	Higher precipitation	No effect
		AGPs	Recovery	Decrease of quenching effect	Decrease aggregation	Same precipitation	Ternary mechanism
DS- sample	PNG	RG II and AGPs	Recovery	Decrease of quenching effect	Decrease aggregation	-	Competition mechanism
	Procyandin B2	RG II	Recovery	Decrease of quenching effect	Decrease aggregation	-	Competition mechanism
		AGPs	No recovery	No decrease of quenching effect	Increase aggregation	Higher precipitation	No effect

The results obtained by SDS-PAGE taken together with the other results gave evidences about the effect of polysaccharides (RG II and AGPs) on these interactions. However, it is important to bear in mind that by SDS-PAGE are not present all SP families, giving only some insights about the general profile of interaction. This way, the protein bands with more relevant results are identified with letters A; B and C. According to the molecular weight of these protein bands and based on the results reported in the literature, it was possible to identify three SP families [129, 178]. This way, proteins A (~56 kDa), B (~24 kDa) and C (~14 kDa) seem to correspond to α -amylase, PRPs and cystatins, respectively. The SDS-PAGE results for the interaction between S sample with PNG and procyanidin B2 showed that the presence of RG II caused a high protein precipitation, especially for protein bands A and C, greater than the one observed in the control which is in the absence of this polysaccharide (Control, saliva+tannin). This evidence can be observed by more intense bands for some SP families. The same behavior was observed for AGPs on DS⁻ sample interaction with procyanidin B2, where the presence of this polysaccharide caused a higher precipitation than the one in its absence, and this time only for protein band A. Furthermore, for all these interactions, no decrease of the quenching effect (fluorescence studies), no recovery of the SP chromatographic peaks area (HPLC) and an increase in aggregation (nephelometry) were observed. All together these results point that RG II can form more aggregates or can form bigger aggregates with SP-tannin complexes, increasing the aggregation and, consequently, resulting in precipitation. Curiously, it seems that RG II in these cases can have a syneRG Ic effect with tannins contributing for a higher protein precipitation. The results observed can be explained once again by the presence of salts which compromises the ability of RG II in preventing SP precipitation. For AGPs, on the interaction between DS⁻ sample and procyanidin B2, it seems that this polysaccharide does not have the ability to bind procyanidin and, this way act by a competition mechanism. On the other hand, it also seems that AGPs do not have the ability to form a ternary complex with this SP-tannin aggregate.

The SDS-PAGE results for the effect of AGPs on the interaction between S sample with procyanidin B2 demonstrated that in the presence of this polysaccharide does not exist the reduction of protein precipitated, being the protein band similar to the protein band in the absence of AGPs (control, saliva+tannin). Moreover, for these interactions, it was observed a decrease of the quenching effect (fluorescence studies), a recovery of the SP chromatographic peaks area (HPLC) and a decrease in aggregation (nephelometry). Although the results obtained by these techniques could point for a competition mechanism, the observed changes were not so pronounced as the ones observed for

the interactions in which polysaccharides act by this mechanism. For this reason, the results seem to suggest that AGP act by a different mechanism on the S sample interaction with procyanidin B2 - a ternary mechanism. According to this mechanism, polysaccharides can form a ternary complex with SP-tannin aggregates enhancing its solubility which could be explained by the decrease of aggregation. In this case, the interaction between procyanidin B2 and SP from S sample seems to be stronger than the procyanidin B2 interaction with AGPs, probably due to the polarity of these two molecules. In this case, AGPs can then encapsulate this complex, forming a ternary complex.

The overall results indicate that, in general, most polysaccharides were able to highly reduce the interactions between SP and tannins. All the techniques together clearly showed that there is a non-aggregation or (re)solubilization of SP-tannin aggregates upon the addition of polysaccharides, throughout a competitive mechanism or by the formation of a ternary complex (protein-tannin-polysaccharide), respectively. From the presented results, it is possible to note that the influence of polysaccharides is dependent both on the saliva sample (the presence or absence of salts) as well as on the tannin and polysaccharide structures

In conclusion, RG II, an acidic polysaccharide, was more effective in the inhibition of precipitation of SP, especially for aPRPs and statherin/P-B peptide, than AGPs which is a neutral polysaccharide. This is in agreement with some works reporting the high ability of RG II to reduce protein-tannin interactions [268, 282, 283]. It is also important to take into account that besides the central role of the polysaccharide structure, protein and tannin structures are also important for the effect of those polysaccharides.

E4. Conclusions

Overall, the obtained results show that some polysaccharides commonly found in wine are able to inhibit the interaction and precipitation of SP with tannins. It is important to bear in mind that during food or beverages ingestion procyanidins and polysaccharides are present together in the food matrix and they will interact firstly between them, and after with SP present in saliva (competitive medium). Thus, this could be an important information, since it was already described the importance of polysaccharides on the mouthfeel properties of wines such as mellowess, fullness and roughness[169, 281]. Therefore, they could be used on astringency modulation of several tannin-rich beverages.

Considering that these polysaccharides are present in wine in considerable amounts, along with other polysaccharides as mannoproteins, they can probably lead to a decrease in astringency perception. This could mean that wines with high levels of these polysaccharides would present lower astringency, even if they have a high polyphenolic content. From a food sensorial perspective, this could be a valuable information for winemaking industry which can develop methods in order to use these polysaccharides during winemaking, and this way, to modulate astringency of tannin-rich products in order to make them more attractive for the consumers.

F. The effect of pectic polysaccharides from grape skin on salivary protein-tannin interactions

Abstract

Procyanidins (PC) interaction with macromolecules such as proteins and polysaccharides are of most importance in food chemistry, particularly related to astringency perception modulation. In this work, the potential of white grape (*Vitis Vinifera L.*) skins for the extraction of water-soluble and chelator soluble pectic polysaccharides was investigated. Furthermore, the impact of these pectic fractions on low polymerized grape seeds procyandins and salivary proteins (SP) interactions was studied by a combined approach, including High Performance Liquid Chromatography (HPLC) and Sodium Dodecylsulfate-Polyacrylamide Gel Electrophoresis (SDS-PAGE). Water (WSP) and chelate soluble fractions (CSP) were found to be composed by high uronic acids content (709 and 820 µg.mg⁻¹ dry matter) and very low neutral sugar content corresponding to 68 and 29 µg.mg⁻¹ dry matter. Both pectic polysaccharides have shown to reduce SP-procyandins interaction, resulting on a decrease on the amount of precipitated protein which was observed by HPLC and SDS-PAGE. Both pectic polysaccharides fractions seem to act by a competition in which they compete for procyandins binding. However, WSP was the most effective in inhibiting SP precipitation, especially for acidic proline-rich proteins (aPRPs).

F1. Introduction

Polyphenols associations with food macromolecules such as proteins and polysaccharides are fundamental factors affecting the organoleptic and nutritional attributes of polyphenol-rich food products, such as astringency, bitter taste and colour [197]. For instance, astringency is generally accepted to be due to specific interactions between salivary proteins SP and tannins. These interactions result in the formation of insoluble aggregates that precipitate, affecting palate lubrication and causing an unpleasant sensation of roughness, dryness and constriction [113, 127, 128].

On the other hand, polyphenol-polysaccharide interactions have also been shown to occur, affecting significantly not only polyphenols extractability but also their functional and nutritional properties [301, 302]. SP-tannin interactions have been extensively studied but much less information is available regarding the interactions between tannins

and cell wall polysaccharides, although polysaccharides have been shown to influence tannin-protein aggregation, possibly leading to a change in astringency perception [269, 271, 273].

PC are polyphenols which belong to the class of flavonoids and may differ by their degree of polymerization and by the type of interflavanic linkage [7]. Flavan-3-ol units are most frequently linked via B-type bonds, that is, C4-C8 and C4-C6 and they can also be esterified with gallic acid. Among cell wall polysaccharides, pectin which is a major constituent of most plant cell walls has been demonstrated to bind strongly to polyphenols in solution, particularly to tannins and anthocyanins [154, 303]. These associations are fast and spontaneous and usually involve weak non-covalent interactions such as hydrogen bonds and hydrophobic interactions. However, pectin is a very heterologous plant polymer with different structural regions, which will affect the interaction with polyphenols [271].

Pectin are predominantly constituted of 1→4 linked galacturonic acids (α -D-GalpA) that can be methyl esterified and/or acetylated ("smooth regions") and branched regions of rhamnogalacturonans (RG I and RG II). RG I is formed by repeating units →4)- α -D-GalpA-(1→2)- α -L-Rhap-(1→), with the rhamnose residues of the RG fractions being decorated by long side-chains composed mostly of galactose and arabinose. RG II presents a backbone of (1→4) linked α -D-GalpA with side chains containing rhamnose and a variety of rare monosaccharides [152, 153]. The affinity of pectin to PC depends on several factors like structure, composition and concentration of both polysaccharides and PC, which can modulate the interaction between these biomolecules.

Therefore, this work aimed to identify the type of cell-wall polysaccharides present in water (WSP) and chelator (CSP) extracts of white grape skin. This will allow to obtain new insights regarding polysaccharides structural features and the impact on low polymerized PC-SP interaction, providing useful information to the food and beverage industry. With this purpose, HPLC and SDS-Page were used to study these interactions.

F2. Materials and Methods

F2.1. Plant materials

White grapes (*Vitis vinifera* L.), kindly provided by Lavradores de Feitoria®, were collected from a vineyard located in Cima Corgo at the Douro Region. Grapes were brought to the laboratory and frozen at -20° C. Skins were separated from seeds and pulps, frozen and freeze-dried until further analysis.

F2.2. Isolation of procyanidins

PC fraction was isolated from a commercial grape seeds extract (*Vitis vinifera* L.) (Vitisol®) by low pressure Toyopearl HW-40 (s) gel column chromatography (100 mm x 10 mm i.d., 0.8 mL·min⁻¹) as described in the literature [181]. Briefly, 2 g of grounded grape seeds extract were dissolved in methanol and eluted with this same solvent at 295 nm, yielding four fractions. PC composition of each fraction was determined by direct analysis by Electrospray Ionization-Mass Spectrometry (ESI-MS) (Finnigan DECA XP PLUS). Fraction containing PC dimers and galloyl derivatives was chosen to perform the interaction studies.

F2.3. Isolation of human saliva

Saliva was collected from several healthy and nonsmoking volunteers and treated as previously described [70]. Briefly, trifluoroacetic acid (TFA) solution was added to 900 µL of collected saliva (0.1% final concentration), the solution was then centrifuged at 8000 g for 5 min and the supernatant was separated from the precipitate. Saliva collection was conducted according to the Declaration of Helsinki and was approved by the Ethics Committee of Medical School of University of Porto (EK84032011).

F2.4. Isolation of pectic polysaccharides

The alcohol-insoluble residue (AIR) was obtained from white grape skins according to an adaptation of the methodology described in the literature [304]. Grounded grape skins were suspended in boiling water for 5 min and after that were homogenized using an Ultra-Turrax® for 2 min. Absolute ethanol was added (70% ethanol final concentration) and the mixture was placed into an ultrasound bath for 15 min at room temperature and then into a water bath for 30 min at 40° C. The raw alcohol insoluble solids were

separated by centrifugation (2500 rpm, 15 min, room temperature) and extracted again using 70% ethanol solution. The washing procedure with fresh 70% ethanol was repeated several times until a clear extract was obtained. Finally, the AIR was washed twice with 96% ethanol, once with acetone and dried overnight.

F2.5. Consecutive fractional extraction of AIR

Consecutive fractional extraction of the AIR was performed as follows, according to the methodologies described by Slavov and colleagues [305, 306]: 1) Hot-water extraction: AIR (7.5 g) was extracted with hot water (150 mL distilled water) at 90° C for 1h with constant stirring. The residue was separated by centrifugation (15 minutes, 2500 rpm, room temperature) and subjected to another extraction with hot water. Then, the filtrates were combined and evaporated under vacuum to 1/3 of its initial volume. The concentrated liquid containing the polysaccharides was precipitated with 3 volumes of absolute ethanol and left for 24h at 4° C. In order to completely remove the ethanol, the precipitate obtained was centrifugated, re-dissolved in water and evaporated. Then, the concentrated solution was subjected to dialysis (Spectra/Por®, 6-8 KDa cut-off) for 48h against distilled water, freeze dried and denoted as water-soluble pectic polysaccharides (WSP). 2) Ammonium oxalate extraction: The residue resulted from the hot-water extraction was treated with 50 mM oxalate solution at 50° C for 1h (pH=5) with constant stirring. After centrifugation (2500 rpm, 15 min, room temperature), the residue was subjected to a second extraction. Both filtrates were combined and evaporated under vacum to 1/3 of its initial volume. Then the concentrated filtrate was treated as described above and denoted as chelate-soluble pectic polysaccharides (CSP).

F2.6. The influence of pectic polysaccharides on salivary protein-procyanidin interaction

SP and PC were analyzed by HPLC-DAD before and after SP interaction with PC, and pectic polysaccharides addition. The control condition was a mixture of saliva (110 µL) and distilled water (70 µL). For PC experiments in the absence of polysaccharides, a mixture of saliva (110 µL) and PC (3.0 g. L⁻¹) (final volume of 180 µL) was shaken, kept to react for 10 min and centrifuged (10500 rpm, 5 min). After centrifugation, the SP and PC present in the supernatant were analyzed by HPLC. For the ternary system involving SP, tannins and polysaccharides, tannins firstly react with increasing pectic polysaccharides concentrations (0.5, 0.8 and 1.2 g.L⁻¹) for 30 minutes. After

centrifugation (13400 rpm, 5 min), saliva (110 µL) was added to the supernatant and kept to react for more 10 minutes. The resulting solutions were centrifuged (10500 rpm, 5 min), and the SP and PC present in the supernatant were analyzed by HPLC. The SP analysis was performed according to an adaptation of the procedure described in the literature [103, 178] at 214 nm on a Vydac C8 column (150 × 2.1 mm; 5 µm). The HPLC solvents were 0.2% aqueous TFA (eluent A) and 0.2% TFA in ACN/water 80/20 (v/v) (eluent B). The initial conditions (15% eluent B) were maintained for 10 minutes and after that, the gradient applied was linear from 15 to 60% (eluent B) in 40 min, at a flow rate of 0.5 mL·min⁻¹. These conditions were maintained for another 5 minutes. After the program, the column was washed with 100% eluent B for 10 minutes in order to elute S-type cystatins and other late-eluting proteins. After washing, the column was stabilized with the initial conditions.

PC were analyzed by HPLC-DAD/ESI-MS at 280 nm on an Agilent Poroshell 120 EC-C18 column (150 × 4.6 mm i.d., 2.7 µm), according to literature [307]. The HPLC solvents were 0.5% aqueous formic acid (eluent A) and 0.5% formic acid in ACN (eluent B). The gradient applied was linear from 0 to 40% (eluent B) in 55 min, at a flow rate of 0.5 mL·min⁻¹. After the program, the column was washed with 100% eluent B to elute other PC and aggregates. After washing, the column was stabilized with the initial conditions. MS analysis was done on a Finnigan Surveyor series liquid chromatograph. Detection was carried out between 200 and 700 nm using a Finnigan Surveyor PDA Plus detector. The mass detection was carried out by a Finnigan LCQ DECA XP MAX (Finnigan Corp., San José, Calif., USA) mass detector with an API (Atmospheric Pressure Ionisation) source of ionisation and an ESI interface. The capillary voltage was 4 V and the capillary temperature 325 °C. Spectra were recorded in negative ion mode between m/z 0 and 2000. The mass spectrometer was programmed to do a series of three scans: a full mass, a zoom scan of the most intense ion in the first scan, and a MS–MS of the most intense ion using relative collision energy of 30 and 60 V.

F2.7. SDS-PAGE

The precipitates resulted from the interaction between SP and PC in the absence and presence of pectic polysaccharide fractions (WSP and CSP), as well as the saliva control were analyzed by SDS-PAGE. This method is based on a separation of proteins according to their sizes using a 16% acrylamide resolving gel. The precipitates were resolubilized in 50 µL of electrophoresis buffer (125 mM Tris-HCl pH 6.8, 20 % v/v

glycerol, 4 % SDS, 10 % v/v β -mercaptoethanol, and 0.004 % bromophenol blue) and heated at 90 °C for 20 min. The cathode buffer was 0.1 M Tris, 0.1 M tricine, and 0.1% SDS. The anode buffer was 0.2 M Tris-HCl, pH 8.9. The running buffer was 0.2 M Tris-HCl pH 8.3, 1.9 M glycine and 0.1 % SDS. Molecular weight markers were broad ranged (Precision Plues ProteinTM Unstained Standards, Bio-Rad). The separation was performed on a Bio-Rad MiniProtean Cell electrophoresis apparatus (Bio-Rad) at constant amperage (0.4 Å). After electrophoresis, the gels were stained with Imperial Protein Stain - a Coomassie R-250 dye-based reagent - for 30 min. The destaining step was done by washing the gels overnight with water:methanol:acetic acid (70:20:10 v/v/v).

F2.8. Analytical methods

F2.8.1. Total polyphenols determination

The total polyphenolic contents of each pectic fraction were determined with the Folin-Ciocalteu assay. Pectic fractions were dissolved in distilled water (1.0 mg.mL^{-1}) and an aliquot of these solutions was mixed with Folin-Ciocalteu reagente, water and sodium carbonate solution (20%). After 30 min incubation at room temperature, absorbance was measured at 750 nm in an UV/Vis spectrophotometer (PowerwaveXS Microplate Reader). Gallic acid (GA) was used as standard and the results were expressed as μg gallic acid equivalents (GAE) per mg dry matter in extracts. The measurements were performed in triplicate.

F2.8.2. Soluble proteins determination

Soluble protein content of each pectic fraction was determined by a dye binding assay according to Lin et al 2016. Briefly, pectic fractions were dissolved in distilled water (1.0 mg.mL^{-1}) and an aliquot of these solutions was mixed with Bradford reagent in a 96 well micropate, incubated for 10 min at room temperature and absorbance was measured at 595 nm. Protein content in each pectin sample was calculated relative to bovine serum albumin (BSA) standard and were expressed as μg bovine serum albumin equivalents (BSAE) per mg dry matter in extracts. The measurements were performed in triplicate.

F2.9. Polysaccharide analysis

Characterization of pectic polysaccharides was performed following the procedure described by Nunes *et al.*, 2008 [308]. Monosaccharides were released from cell wall polysaccharides by a pre-hydrolysis in 200 µL of H₂SO₄ (72%) for 3 hours at room temperature, followed by 2.5 hours hydrolysis in 1 M H₂SO₄ at 100° C. Neutral sugars composition were determined after conversion to their alditol acetates by Gas Chromatography (GC), using 2-deoxyglucose as internal standard according to the methodology described in the literature [308]. Results were expressed as µg sugar.mg⁻¹ dry sample.

Uronic acids (UA) determination in the cell wall material were determined by a modification of the 3-phenylphenol colourimetric method. Samples were prepared by hydrolysis in 200 µL of H₂SO₄ (72%) for 3 hours at room temperature followed by 1 h in 1 M H₂SO₄ at 100° C. A calibration curve was made with D-galacturonic acid. The hydrolysis of all samples was done in duplicate and each one was analyzed twice. UA content was expressed as µg galacturonic acid equivalent per mg cell wall.

F2.10. Statistical analysis

Analysis were performed with n > 3 and the values obtained was expressed as mean values and standard error of mean (SEM). Statistical significance was detected by analysis of variance (ANOVA), followed by the Bonferroni's test; Differences were considered to be statistically significant at P< 0.05. All statistical data were processed using GraphPad Prism version 5.0 for Windows.

F3. Results and Discussion

This work aimed to provide new informations regarding the relative affinity of dimeric PC and galloyl derivatives toward SP, together with the impact of pectic polysaccharides (WSP and CSP) on these interactions. This information was achieved by HPLC-DAD analysis of SP and PC in the absence and in the presence of pectic polysaccharides and by SDS-PAGE analysis of precipitated SP.

F3.1. Composition of the interaction species

F3.1.1. Pectic polysaccharides fractions

In order to clarify the binding between PC and pectic polysaccharides obtained from white grape skin and also the impact of these interactions on SP-PC interaction, a detailed analysis and characterization of these pectic fractions was performed. The raw plant material was initially treated with heated 70% ethanol, according to De Vries method [309], in order to remove the low-molecular substances, such as polyphenols, sugars and salts while obtaining the AIR.

This method was selected to obtain the AIR as it has been described as the appropriate cell-wall material isolation procedure in grapes, compared to other standard procedures [310]. This insoluble residue accounted for 17% of the freeze-dried skin tissue (w/w). Monosaccharide composition and total sugar content ($\mu\text{g}.\text{mg}^{-1}$ dry matter) of isolated WSP and CSP are shown in Tables 18 and 19. The two polysaccharide fractions were obtained with lower yields (4.1% and 2.3%) (Table 18). Higher value was obtained in a previous study where HEPES and buffer-soluble polysaccharides account for 13% of the skin tissues [311]. However, the plant material did not have exactly the same characteristics as the sample used in this work. These overall lower yields probably implied that the initial heating process with 70% ethanol for AIR obtainment resulted in the partial solubilization and consequently loss of some water-soluble pectic-type polysaccharides [305].

To obtain different polysaccharide fractions, the AIR was sequentially extracted with water and ammonium oxalate solution. For instance, while pectin with a high degree of esterification, mainly located in the middle lamella of the cell wall, is solubilized by water, low-esterified pectins disposing of abundant free carboxylic groups are usually extracted by chelating calcium ions [312]. Compositional analysis of the water and chelator fractions showed that their total sugar content was very similar, consisting respectively of 77% and 85% by weight of polysaccharides. Although polysaccharides were the main constituents of the cell-wall material, 9-12% of bound proteins and polyphenolic compounds were also found.

Table 18 shows the content in proteins (expressed as μg BSA equivalents. mg^{-1}) and the content in phenolic compounds (expressed as μg gallic acid equivalents. mg^{-1}) of the water and chelator fractions isolated from the AIR residue. The polyphenolic content of these fractions was shown to correspond to approximately 8 and 5% dry weight (WSP

and CSP, respectively), while soluble protein content was shown to be less than 4% for both fractions.

Polysaccharides analysis indicated that both fractions were characterized by high UA content (709 and 820 $\mu\text{g}.\text{mg}^{-1}$ dry matter) and very low neutral sugar content corresponding to 68 and 29 $\mu\text{g}.\text{mg}^{-1}$ dry matter. This indicates that these two fractions are rich in homogalacturonans (Tables 18 and 19) [154]. In fact, it is well known that polysaccharides extracted by chelate extractants are mostly pectic chains of homogalacturonan linked to each other through calcium bridges, which form the so called “egg-box” system in plants cell walls [155]. The degradation of these systems was accompanied by the release of part of homogalacturonan, resulting in higher UA content. However, according to other data published in the literature, the water-soluble fraction was expected to be comprised of higher amounts neutral sugars (ca. 60-72% arabinose and galactose) [313]. Our results seemed to indicate that probably some of the skin water soluble polysaccharides, particularly arabinose and galactose could have been lost during ethanol precipitation. Main neutral sugars present in WSP were arabinose (31 $\mu\text{g}.\text{mg}^{-1}$) and galactose (21 $\mu\text{g}.\text{mg}^{-1}$), followed by a small amount of rhamnose (4 $\mu\text{g}.\text{mg}^{-1}$) (Table 19). The CSP fraction showed a lower amount of neutral sugars compared to WSP fraction, with the most abundant being arabinose, followed by galactose (Table 19). The Ara/Gal ratio is characteristic of the PRAGs-like structures. This ratio was higher for CSP fraction (2.7) in comparison with the WSP fraction (1.5), which probably could indicate a higher release of arabinose or polysaccharides rich in arabinose arising from the pectic framework of this fraction [314, 315]. On the other hand, the ratio of (Ara+Gal) to Rhamnose was calculated to estimate the relative importance of the neutral side-chains to the RG backbone, since it is assumed that most of the arabinose and galactose are associated with pectin hairy regions. This ratio was lower for CSP fraction (7.3) than in WSP fraction (13.0), which could indicate that CSP fraction contains more structures from the hairy regions of pectins (RG-like structures) [276, 314, 315]. Besides, the (Ara + Gal)/Rha ratio of WSP indicates that the RG structures in this fraction carry more neutral lateral chains than CSP fraction [276]. Finally, the UA/(Ara+Gal) ratio was lower for WSP (13.6) compared to CSP (37.2). The relatively high proportion of Ara and Gal, as well as the presence of UA, suggests that WSP has a higher amount of branched pectic polysaccharides compared to CSP fraction [308].

Table 18 - Consecutive fractional extraction of AIR and chemical characteristics of the extracted polysaccharides fractions. $\mu\text{g. mg}^{-1}$ dry weight (UA, uronic acids; NS, neutral sugars; TS, total sugars; SP, soluble proteins; P, polyphenols).

	Yield* (%)	UA ($\mu\text{g. mg}^{-1}$)	NS ($\mu\text{g. mg}^{-1}$)	TS ($\mu\text{g. mg}^{-1}$)	SP ($\mu\text{g. mg}^{-1}$)	P ($\mu\text{g. mg}^{-1}$)
WSP	4.1	709	68	777	35.1 ± 0.2	84 ± 4
CSP	2.3	820	29	848	31 ± 1	49 ± 1

*Yield is expressed in mg of dry weight material per g of AIR obtained (7.5 g).

Table 19 - Neutral sugar composition of the extracted polysaccharide fractions ($\mu\text{g. mg}^{-1}$ dry weight).

	Rha	Fuc	Ara	Xyl	Man	Gal	Glc	(Ara+Gal)/Rha	Ara/Gal	UA/(Ara+Gal)
	($\mu\text{g. mg}^{-1}$)									
WSP	4	0	31	6	2	21	4	13.0	1.5	13.6
CSP	3	0	16	2	0	6	2	7.3	2.7	37.2

Rha – Rhamonse; Fuc – Fucose; Ara – Arabinose; Xyl – Xylose; Man – Mannose; Gal – Galactose; Glc – Glucose

F3.1.2. Procyanidins

A low polymerized PC fraction obtained after extraction and purification from grape seeds was selected for these interaction studies. This fraction was analyzed by HPLC-DAD/ESI-MS allowing the identification of several dimeric PC (B1, B3, B6, B4, B2, B7, B5 - major compounds, corresponding to about 90% of total PC content at 280 nm (λ_{max}) and galloyl derivatives (B2g and epicatechin gallate, ECG). Small amounts of a trimeric PC could also be detected on this fraction. PC identification was performed based on the retention time of standards compounds and according to the data described in the literature (Figure 58) [307].

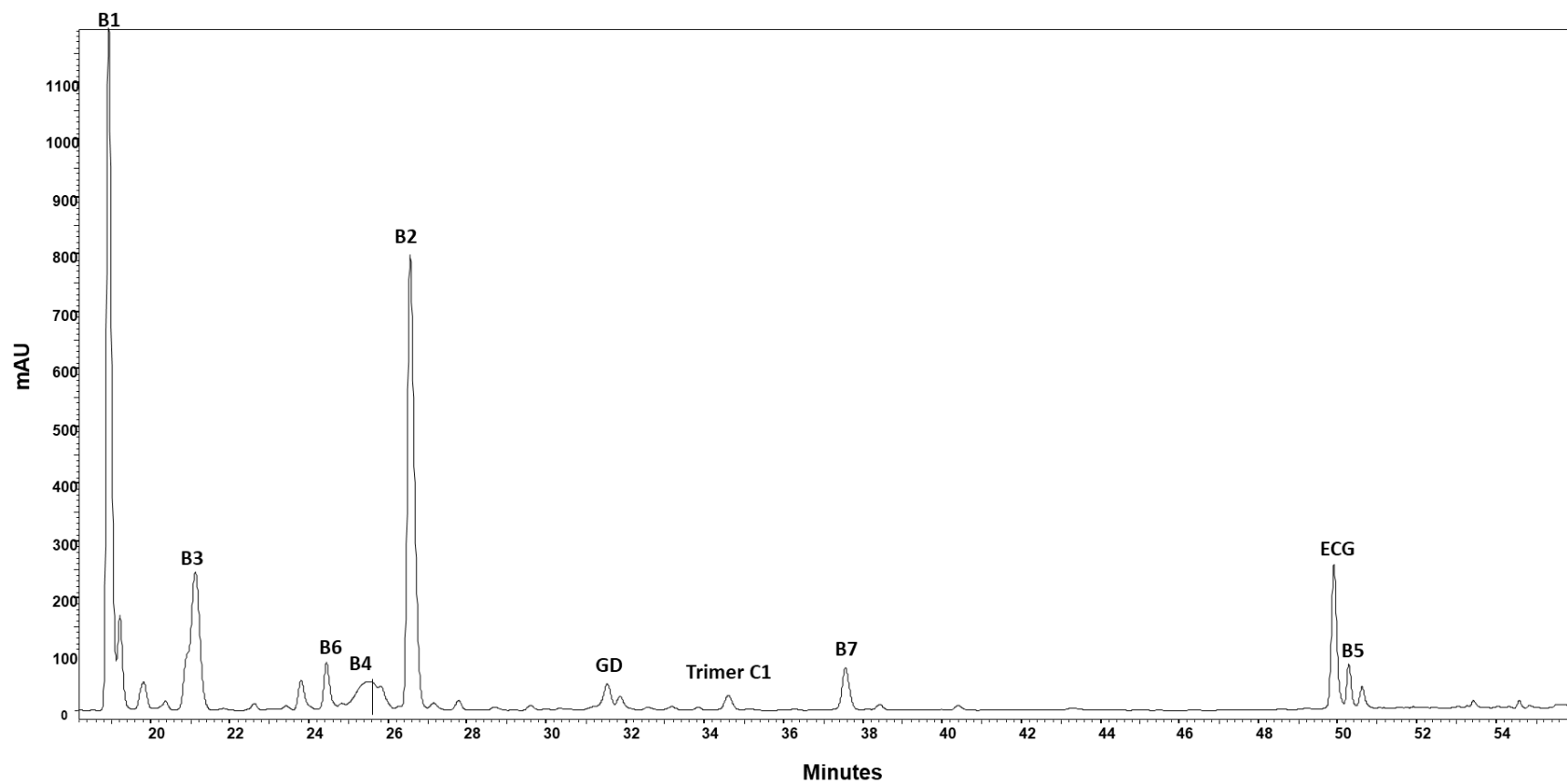


Figure 58 - HPLC-DAD chromatogram detected a 280 nm of the mixture of PC used in this work and respective identification. ECG - epicatechin gallate; GD – galloylated dimer.

F3.2. Salivary proteins-procyanidins interaction

The relative affinity of a low polymerized PC fraction toward specific SP was assessed by HPLC-DAD analysis, through the determination of both unbound tannins and non-complexed SP after tannin-proteins interaction and consequent precipitation. The percentage of insoluble complexes was determined by subtracting the area of each SP family (or PC) obtained in the HPLC analysis from the respective area of the control sample (saliva without PC or PC alone).

Preliminary experiments were made in order to determine the preferential tannin concentration that lead to a significant precipitation of the SP families (gPRPs, aPRPs, statherin/P-B peptide and cystatins). It can be seen on Figure 59 that the addition of 3.0 g.L⁻¹ of PC fraction practically depleted aPRPs (~95%) and statherin/P-B peptide (~85%), and reduce the amount of cystatins (~30). gPRPs were practically not affected by PC, evidencing a negligible interaction with these compounds (~5%). No information could be obtained regarding bPRPs, due to overlapping with PC chromatographic peaks. In previous works, the same relative affinity has already been observed with pure compounds (condensed and hydrolizable tannins) showing the higher affinity of aPRPs and P-B peptide [253, 265, 288].

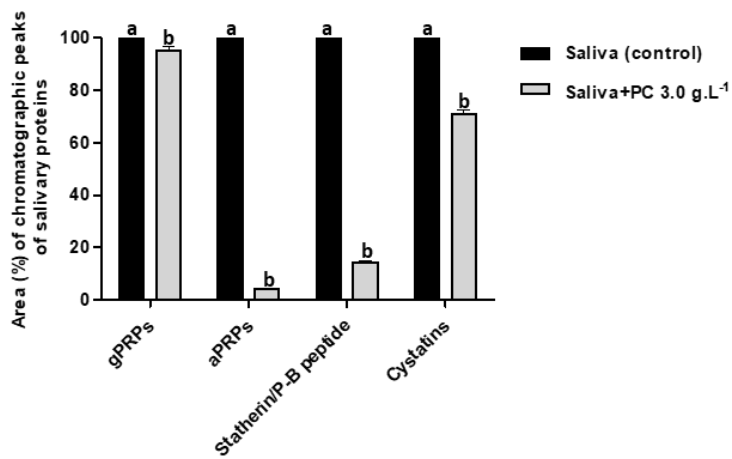


Figure 59 - Influence of PC fraction (3.0 g. L⁻¹) after interaction with several SP families (gPRPs, aPRPs, statherin/P-B peptide and cystatins) determined by HPLC at 214 nm. Values with different letters within each SP are significantly different ($P<0.05$).

In order to understand the specificity and the impact of tannin structure on SP-PC interaction, PC profile was also analyzed by HPLC-DAD before and after saliva interaction. Due to PC tendency to self-associate, at higher concentrations PC aggregates could be formed and be sedimented after centrifugation, leading to an over-

estimation of the amount of PC bound to proteins [109, 113, 316]. For this reason, it was necessary to centrifuge the control sample (PC alone) prior to HPLC-DAD analysis.

The HPLC profile of PC fraction after saliva interaction evidenced a slight decrease on PC content (Figure 60). However, a detailed analysis shown that galloyl derivatives (B2g and ECG) evidenced a higher affinity to these SP families resulting on a more notorious reduction of the amount of unbound galloyl derivatives. This could be observed particularly for the galloylated dimer (GD) (~44% bound PC) and to a smaller extension for the galloylated monomeric PC, ECG (~14%). Within dimeric PC, B4 showed the largest decrease (~14%), the same as for the galloylated monomer, while other dimeric PC showed similar amounts of bound tannins after protein interaction (~4-8%). The only exception was for PC B1 which did not show a significant decrease, evidencing a lower protein affinity. The trimeric PC also showed a slight decrease on the amount of free compound, suggesting a lower affinity for these SP. All together these results seem to indicate that PC structure affect their interaction with SP, particularly the presence of galloyl moieties. In fact, accordingly to what was already reported in the literature, increasing the degree of galloylation of proanthocyanidins also increases their ability to precipitate proteins [136, 316].

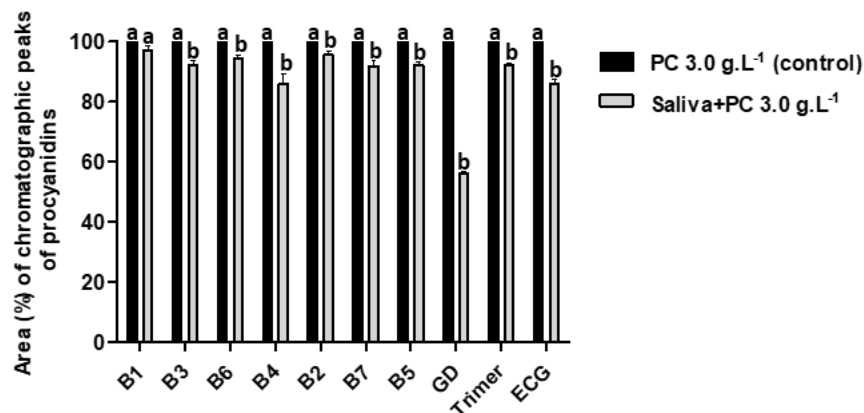


Figure 60 - PC fraction profile variation after interaction with SP determined by HPLC-DAD at 280 nm. Values with different letters within each procyanidin are significantly different ($P<0.05$).

F3.3. Effect of pectic polysaccharides on salivary proteins-procyanidins interactions

F3.3.1. HPLC analysis

In order to understand the impact of pectic polysaccharides on SP-PC interactions, polysaccharides and PC were mixed together and let to react prior to saliva addition. This experimental approach intended to mimic the natural occurring polyphenol-cell wall

polysaccharide interaction during fruit processing and beverages production. PC and polysaccharides fractions (WSP and CSP) were prepared at different polysaccharide concentration (0.5; 0.8; 1.2 and 1.5 g.L⁻¹) and left to react for 30 min. Only after polysaccharide-PC interaction and centrifugation, saliva was added and reacted for 10 min.

Both WSP and CSP fractions were able to reduce the interaction between SP and PC, showing a clear recovery of proteins chromatographic peaks, particularly those for aPRPs and statherin/P-B peptide. These results, evidence that probably a solubilization of proteins-PC complexes or a competition interaction between SP and polysaccharides for PC binding may occur.

Figure 61 shows the variation of the chromatographic peaks area of the major SP families with increasing concentrations of WSP and CSP, expressed relatively to the saliva control (saliva without PC and polysaccharides, 100%). In general, the presence of these polysaccharide fractions induced the recovery of the SP chromatographic peaks, although this recovery was not complete. Increasing polysaccharide concentration resulted on a higher protein recovery, except for the higher polysaccharide concentration (1.5 g.L⁻¹) which did not evidence significant difference compared to the previous concentration (1.2 g.L⁻¹). Indeed, it seems that there is a kind of stabilization at the polysaccharide concentration of 1.2 g.L⁻¹. The only exception is for aPRPs which was observed a recovery of this SP family with the highest WSP concentration. Concerning gPRPs, it was observed that they were not affected by the addition of pectic polysaccharides and did not show a significant difference for the control sample with increasing polysaccharide concentrations (for both WSP and CSP). A detailed analysis of the efficiency of each polysaccharide fraction seemed to indicate that it depends both on the SP but also on the polysaccharide type and concentration. For instance, WSP have more influence on aPRPs-tannins interaction than on other SP families, probably due to the differential affinity of this pectic polysaccharide fraction for PC and SP. Concerning aPRPs it was possible to observe that WSP was the most efficient polysaccharide in preventing protein precipitation. In fact, for the same WSP and CSP concentration, a highest recovery of aPRPs chromatographic peak area could be observed for WSP (~90%). For CSP, despite increasing polysaccharide concentration, protein recovery could only be achieved up to ~55%. This clearly seems to indicate that specific structural features of these polysaccharides' fractions could be inducing different affinities and simultaneously a change on proteins recovery efficiency. Statherin/P-B peptide were co-eluted under the chromatographic conditions tested wherein, showing

a decrease of approximately 86% of statherine/P-B peptide chromatographic area when compared to control sample, probably due to the higher P-B peptide affinity towards tannins as already reported in previous works [267, 288]. In the presence of WSP and CSP polysaccharides fractions, a maximum of protein recovery up to 66% could be noticed, despite polysaccharide concentration increase. Regarding cystatins, addition of WSP caused a significantly recovery of its chromatographic peak area compared to SP-PC interaction at 0.8 and 1.2 g.L⁻¹. Higher polysaccharide concentration did not induce an increase on protein recovery. Considering CSP, all concentrations tested evidenced a protein recovery, although there was no difference statistically significant at the higher concentration tested.

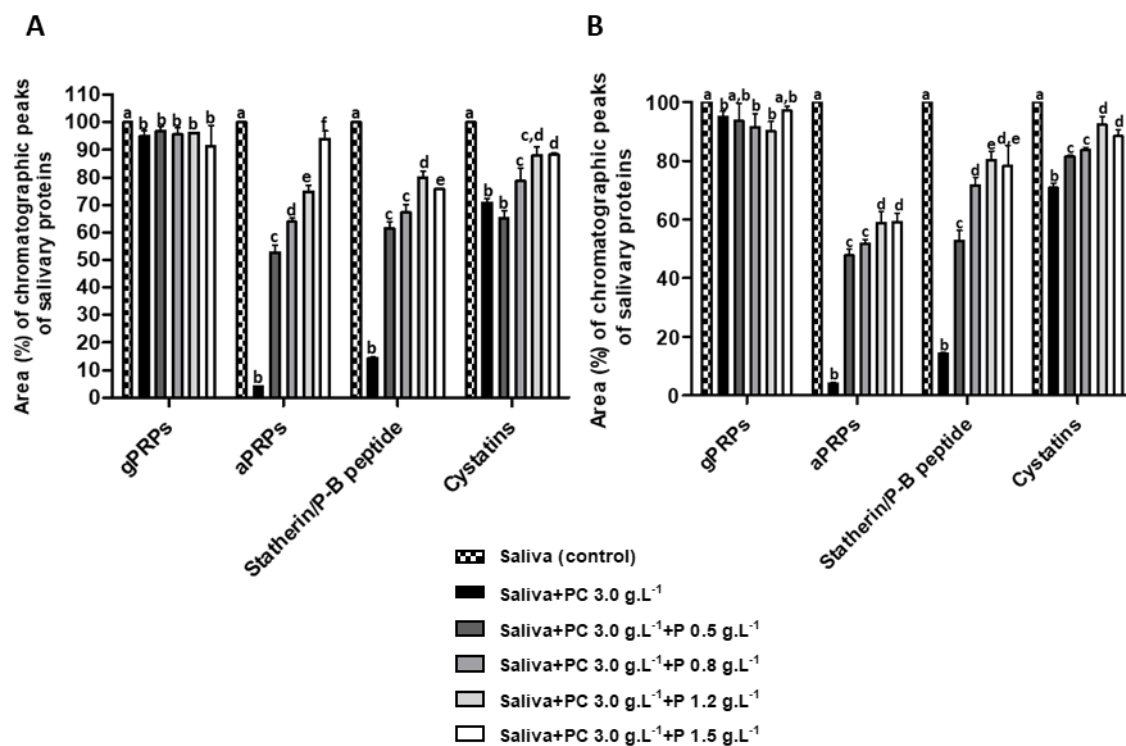


Figure 61 - Influence of increasing pectic polysaccharide concentration (A-WSP and B-CSP) on SP interaction with PC fraction (3.0 g.L⁻¹) determined by HPLC at 214 nm. Values with different letters within each SP family are significantly different ($P<0.05$).

PC profile after pectic polysaccharide and SP interaction was also evaluated (Figures 62 and 63). In this ternary system, a slight decrease on PC amount in the supernatants after centrifugation could be detected, compared to the control sample containing only PC.

For WSP, PC amount did not evidence a clearly difference compared to the SP-PC control sample. The only exception was for the GD which showed a clear recovery with the increase of polysaccharide concentration.

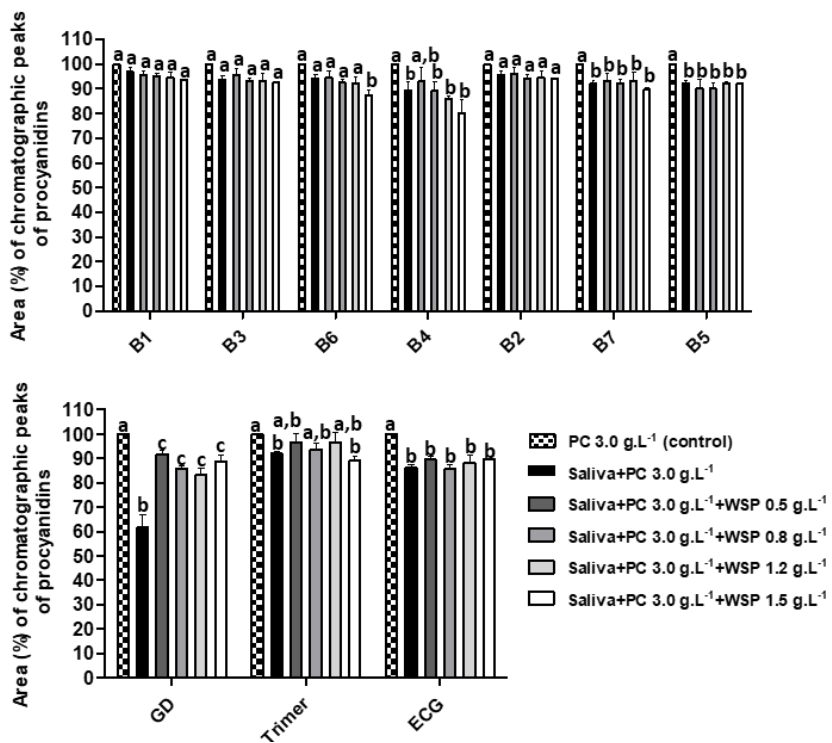


Figure 62 - Influence of SP and increasing pectic polysaccharide concentration (WSP) on 3.0 g.L⁻¹ of PC fraction determined by HPLC-DAD. Values with different letters within each procyanidin are significantly different ($P<0.05$).

However, the addition of increasing amounts of CSP caused some different behaviors in PC. For B1 no significant differences could be noticed in PC amount with increasing pectic polysaccharide concentrations (compared to SP-PC interaction control sample). For B4 and B7 a slight increase of PC amount in the supernatants could be noticed for higher CSP concentration. This same behavior could also be noticed for the GD, where in fact, increasing polysaccharide concentration from 0.5 g.L⁻¹ up to 1.5 g.L⁻¹ caused practically a 40% recuperation of PC amount compared to control sample (PC alone).

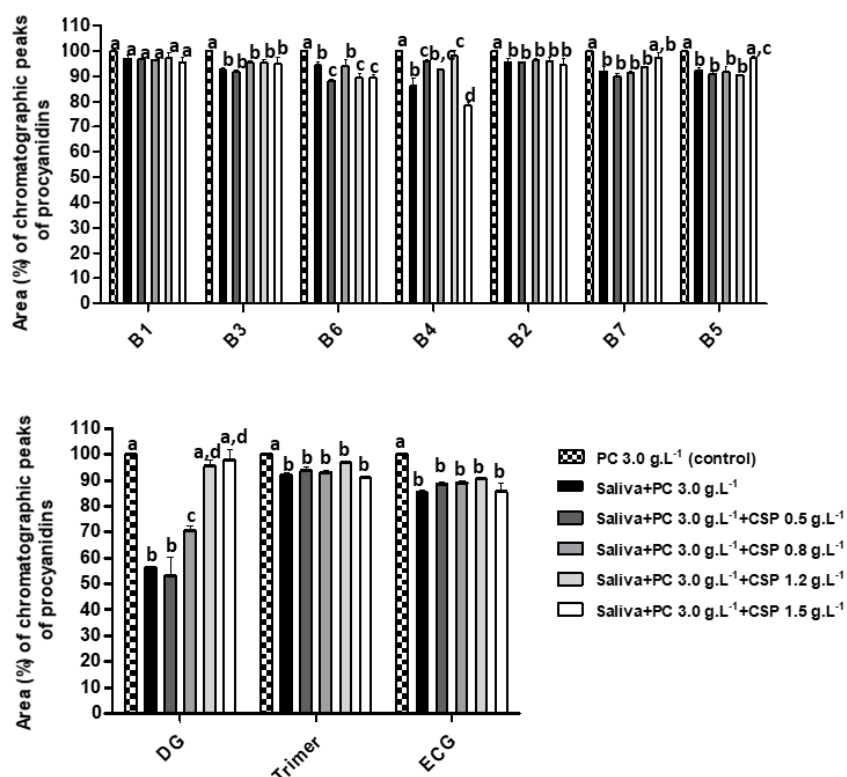


Figure 63 - Influence of SP and increasing pectic polysaccharide concentration (CSP) on 3.0 g.L⁻¹ of PC fraction determined by HPLC-DAD. Values with different letters within each procyanidin are significantly different ($P<0.05$).

F3.3.2. SDS-PAGE

Besides the HPLC analysis of the supernatant resulted from saliva interaction with PC fraction in the absence and presence of both pectic polysaccharides, the resulting precipitates were also analyzed by SDS-PAGE aiming to verify the efficiency of the selected pectic polysaccharides fractions in inhibiting SP-PC interactions (Figure 64).

The results obtained by SDS-PAGE analysis of the precipitates demonstrated that interaction with WSP and CSP decreases SP that were precipitated due to PC interaction. However, it is important to bear in mind that by SDS-PAGE are not present all SP families, giving only some insights about the general profile of interaction. This way, the protein band where polysaccharides had a higher effect corresponds to PRPs. PRPs band was identified based on its molecular weight and according to the literature [129, 178]. Thus, these polysaccharides are more effective toward PRPs-PC interactions, since this protein band is less intense in comparison with the control (saliva+PC), corresponding to a decrease of SP precipitation. This is particularly evident for WSP fraction. These results are in agreement with the HPLC results where it was

observed the highest recovery for the chromatographic peaks area of PRPs due to less SP precipitation.

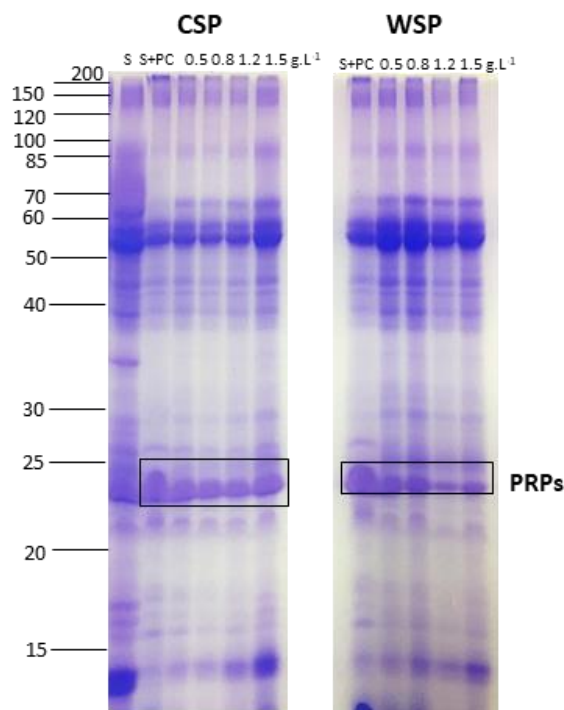


Figure 64 - SDS-PAGE of saliva (S) and of the precipitates that resulted from the interaction between SP and PC in the absence (S+PC, control) and presence of increasing concentrations of the polysaccharides fractions (CSP and WSP). The molecular weight markers were substituted by lines, and the molecular mass marked on the left side is expressed in kDa. The gel was stained with Imperial Protein Stain, a Coomassie R-250 dye-based reagent.

F3.4. Interaction between pectic polysaccharides and procyanidins

F3.4.1. HPLC-DAD analysis

To better understand the interactions between pectic polysaccharides and PC, PC and polysaccharides were subjected to the previous experimental approach and supernatants were analyzed by HPLC-DAD.

PC chromatographic profile alterations was also evaluated due to pectic polysaccharides interactions and the determination of the amount and nature of PC that remained in solution after pectic polysaccharides interaction was also performed. According to the cell wall-PC interaction data, presented on Figures 65 and 66, it could be observed that PC do not interact or interacted slightly with both polysaccharides' fractions. In general, it could be observed that cell-wall polysaccharides interaction with PC changed according to polysaccharide concentration. In fact, smaller polysaccharide concentrations (0.5 and 0.8 g.L^{-1}) resulted in a more efficient interaction with PC, while

higher concentrations did not evidenced significant changes compared to control sample (PC alone). This is particularly evident for the WSP fraction and for some PC, such as dimers B6, B4 and B7, GD, and ECG (Figure 65). However, the results obtained by HPLC did not allow to obtain much information about polysaccharides-PC interaction, probably because this technique is not the most suitable for this analysis. Ongoing research has the objective to obtain more information about polysaccharides-PC interactions, using Isothermal Titration Microcalorimetry (ITC).

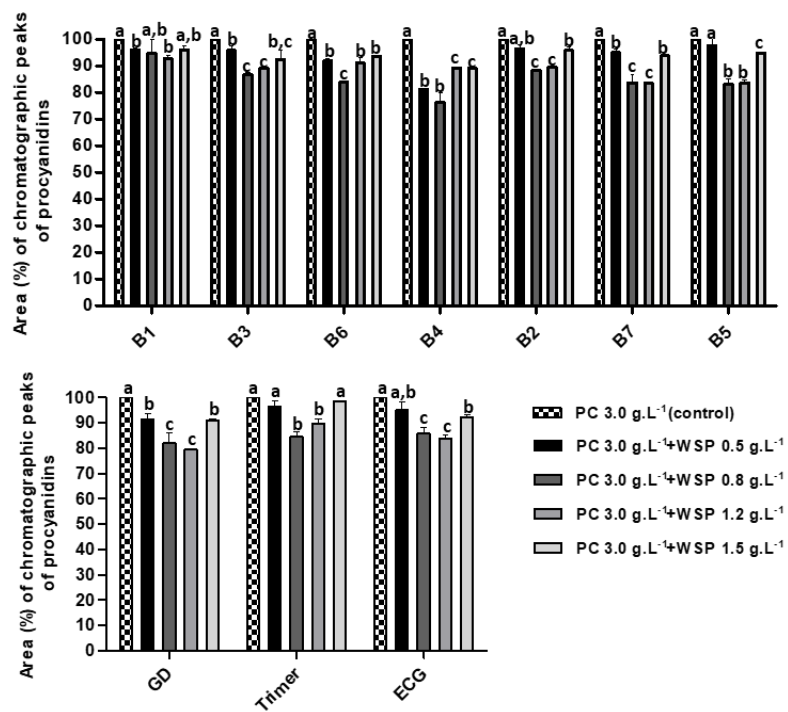


Figure 65 - PC fraction profile variation due to different polysaccharide concentration (WSP) determined by HPLC-DAD. Values with different letters within each proanthocyanidin are significantly different ($P<0.05$).

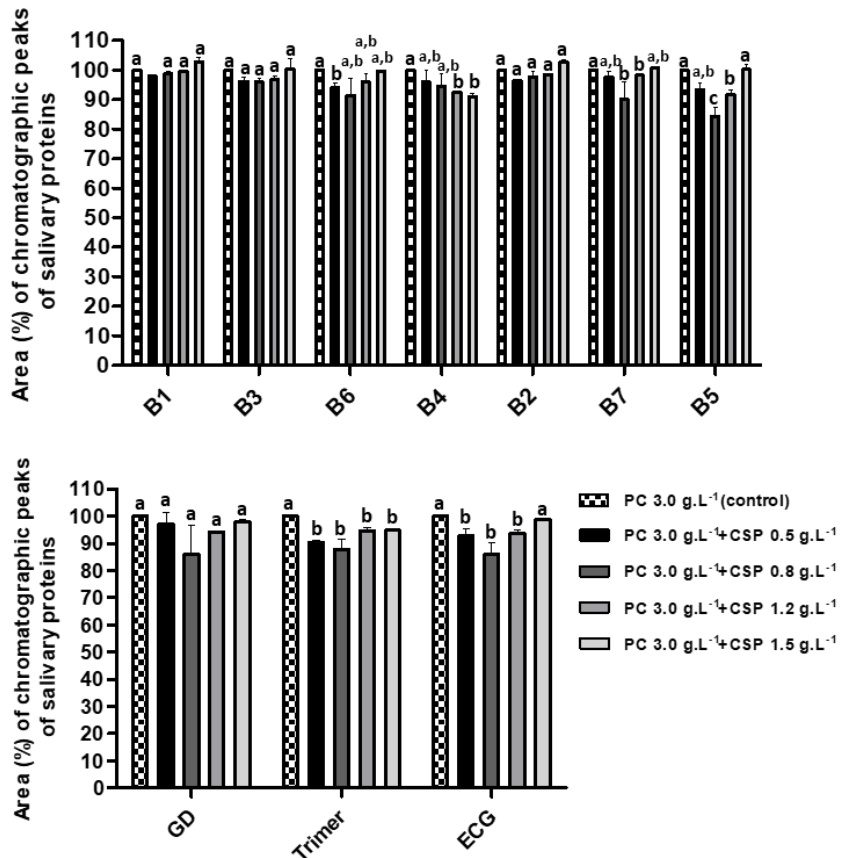


Figure 66 - PC fraction profile variation due to different polysaccharide concentration (CSP) determined by HPLC-DAD. Values with different letters within each procyanidin are significantly different ($P<0.05$).

Overall, the results suggest that these pectic polysaccharides were able to disrupt SP-PC interactions. The underlying mechanism of this effect seems to be the competition one, in which WSP and CSP compete with SP for PC binding. The SDS-PAGE results are in agreement with the HPLC ones, in which WSP fraction was the most efficient to reduce SP-PC interaction.

It was already described that acidic polysaccharides are more able to affect these interactions [282, 283]. Both pectic fractions have in general a high amount of UA, but curiously the UA content of WSP fraction is lower than the CSP fraction. Furthermore, the results suggest that WSP fraction has a higher amount of branched pectic polysaccharides, carrying more neutral side-chains compared to CSP. Although it was already reported that neutral side chains can limit interactions with PC [302, 317], in this work it seems that they can favor these interactions. However, it is important to take into account that in most of these studies the authors used PC with higher degree of polymerization ($n=9-30$), while herein it was used a PC mixture mainly composed by dimers. Furthermore, these pectic fractions have been not yet characterized in terms of

the methylation degree, which could give important informations in order to explain their different efficiency on the inhibition of SP-PC interactions. It was already reported the influence of the methylation degree on the interaction between polysaccharides and PC [154].

Moreover, there are some studies which refers that some pectic water soluble polysaccharides can inhibit protein-tannin aggregation due to the formation of tannin-polysaccharides complexes [268, 271, 273].

F4. Conclusions

A water-soluble (WSP) and chelator-soluble (CSP) pectic polysaccharide fractions were obtained from white grape skin as an attempt of a product development for beverages taste modulation, particularly related to astringency. This work gathered fundamental evidences that pectic polysaccharides could be used to inhibit SP-PC interactions. In summary, these results suggest that these polysaccharides fractions can disrupt SP-PC interaction by a competition mechanism. However, their effect is dependent of several features, especially polysaccharides and PC structure.

These results have a very important implication for the beverages industry which can optimize the potential use of these pectic polysaccharides for beverages taste modulation.

IV. Final Remarks and Future Work

This work was focused on the understanding of taste perception, particularly on astringency. As astringency influences the overall quality of red wine, the knowledge of the structure/activity relationship on the sensory properties as well as the underlying mechanisms of astringency development are important aspects of winemaking.

Bearing this, it was important to study the interaction between salivary proteins and tannins, regarding different aspects: 1) the presence of salivary proteins in a non-competitive assay (alone); 2) the class of the tannin used (condensed vs. hydrolyzable) as well as the respective structure; 3) the influence of other factors, such as pH and ionic strength. It was studied the interaction between a model of mucin protein, which is very important for its lubricating properties, with different condensed tannins. The results obtained showed that procyanidins are able to interact with mucin but is affected by their size and structural features. Although it was observed an increase of interaction for more polymerized procyanidins fractions, the same it was not observed for a pure compound such as procyanidin tetramer due probably to a lack of structural flexibility of this structure, contributing for steric constraints. Furthermore, mucin-tannin interactions were affected by pH and ionic strength, but also by the presence of solvents like EtOH and DMSO. When comparing the effect of solvents on the binding affinity, hydrogen bonds seem to be more relevant for mucin interaction with procyanidins fractions and procyanidin B4, than for mucin-tetramer interaction which have a similar contribution of these two types of bonds.

It was also studied the interaction of different salivary proteins families (PRPs and P-B peptide), in a non-competitive assay, with procyanidins. It was observed that P-B peptide was in the major part of the cases one of the salivary proteins with higher affinity for all procyanidins and, oppositely aPRPs, were the salivary proteins with less affinity to the studied procyanidins. In general, among procyanidins, the trimer showed the higher affinity toward salivary proteins. This study also allowed to assign the first epitopes of interaction for each procyanidin (rings B and E for procyanidin B2 and galloyl ring for procyanidin B2g).

Furthermore, the affinity of ellagitannins (hydrolyzable tannins) and procyanidins toward three families of salivary proteins were also evaluated. It was chosen three families of salivary proteins which were not PRPs (statherin, P-B peptide and cystatins). It was noted that ellagitannins interact better with the three salivary proteins families than procyanidins which is related to the ability to establish hydrophobic interactions, which are the main driving forces for protein-tannin interactions. Among ellagitannins, punicalagin

demonstrated the highest affinity to interact with salivary proteins, while regarding procyanidins, procyanidin B6 the highest affinity.

After studying protein-tannin interaction, it was analyzing the influence of polysaccharides on this interaction. Firstly, it was studied the effect of two wine polysaccharides, RG II and AGPs, on the interaction between tannins (condensed and hydrolyzable) and salivary proteins in a competitive and non-competitive assay. In general, both polysaccharides were able to inhibit or reduce salivary-protein tannin interactions. However, RG II, an acidic polysaccharide, was the most efficient. Polysaccharides' effect is also affected by the presence of salts which compromise the action of acidic polysaccharides like RG II. Polysaccharides can act by two different mechanisms: 1) they can encapsulate protein-tannin complexes, enhancing their solubility in aqueous solution; or 2) they can compete with salivary proteins for tannin binding, reducing the tannin available to interact with proteins. However, the mechanisms by which polysaccharides can act are dependent of several protein, tannin and polysaccharide features (e.g. tannin structure and salivary proteins alone or in saliva).

In the last part, it was studied the effect of two pectic polysaccharides fractions (WSP and CSP) from grape skin on protein-tannin interactions. In this study, it was used saliva and a mixture of dimeric procyanidins. In general, both fractions were able to reduce salivary protein-tannin interactions, being WSP more efficient than CSP. Curiously, WSP has less uronic acids than CSP, which are usually associated with higher ability to disrupt protein-tannin interactions.

Overall, the understanding of these aspects can enable growers and winemakers to have more control over the characteristics of the produced wine. Moreover, with this valuable information winemaking industry can develop methods in order to use these polysaccharides during winemaking, and this way, to modulate astringency of tannin-rich products in order to make them more attractive for the consumers.

Future work should address the influence of these polysaccharides on different food matrixes. The experimental approach should be the analysis of the salivary protein profile after sipping a modified beverage solution by the addition of polysaccharides (e.g. red wine and juice fruits). In addition to this, it would be also important to analyze these beverages in terms of polyphenol composition. Also, the influence of these polysaccharides should be also studied on mucin-procyanidin interaction, since mucin is responsible for the oral lubrication which is closely related to astringency.

It would be also interesting to study the influence of these polysaccharides on other models for protein-tannin interaction which have been also proposed to explain astringency sensation, such as with oral epithelial cells and mechanoreceptors.

Furthermore, the influence of polysaccharides with different composition obtained from other natural sources using, for example, by-products from food industry, could be also analyzed in future work.

References

1. El Gharris, H., *Polyphenols: food sources, properties and applications - a review*. International Journal of Food Science and Technology, 2009. **44**(12): p. 2512-2518.
2. Naczk, M. and F. Shahidi, *Phenolics in cereals, fruits and vegetables: Occurrence, extraction and analysis*. Journal of Pharmaceutical and Biomedical Analysis, 2006. **41**(5): p. 1523-1542.
3. Santos-Buelga, C. and A. Scalbert, *Proanthocyanidins and tannin-like compounds - nature, occurrence, dietary intake and effects on nutrition and health*. Journal of the Science of Food and Agriculture, 2000. **80**(7): p. 1094-1117.
4. Manach, C., et al., *Polyphenols: food sources and bioavailability*. American Journal of Clinical Nutrition, 2004. **79**(5): p. 727-747.
5. Krook, M.A. and A.E. Hagerman, *Stability of polyphenols epigallocatechin gallate and pentagalloyl glucose in a simulated digestive system*. Food Research International, 2012. **49**(1): p. 112-116.
6. de Freitas, V. and N. Mateus, *Protein/Polyphenol interactions: Past and present contributions. Mechanisms of astringency perception*. Current Organic Chemistry, 2012. **16**(6): p. 724-746.
7. Cheynier, V., *Polyphenols in foods are more complex than often thought*. American Journal of Clinical Nutrition, 2005. **81**(1): p. 223S-229S.
8. Scalbert, A., et al., *Dietary polyphenols and the prevention of diseases*. Critical Reviews in Food Science and Nutrition, 2005. **45**(4): p. 287-306.
9. Kähkönen, M.P., et al., *Berry anthocyanins: isolation, identification and antioxidant activities*. Journal of the Science of Food and Agriculture, 2003. **83**(14): p. 1403-1411.
10. Cavalcanti, R.N., D.T. Santos, and M.A.A. Meireles, *Non-thermal stabilization mechanisms of anthocyanins in model and food systems-An overview*. Food Research International, 2011. **44**(2): p. 499-509.
11. Goiffon, J.P., M. Brun, and M.J. Bourrier, *High-Performance Liquid-Chromatography of red fruit anthocyanins*. Journal of Chromatography, 1991. **537**(1-2): p. 101-121.
12. Castañeda-Ovando, A., et al., *Chemical studies of anthocyanins: A review*. Food Chemistry, 2009. **113**(4): p. 859-871.
13. Del Rio, D., G. Borges, and A. Crozier, *Berry flavonoids and phenolics: bioavailability and evidence of protective effects*. British Journal of Nutrition, 2010. **104**: p. S67-S90.
14. Faria, A., et al., *Antioxidant properties of prepared blueberry (*Vaccinium myrtillus*) extracts*. Journal of Agricultural and Food Chemistry, 2005. **53**(17): p. 6896-6902.
15. Visioli, F., et al., *Polyphenols and Human Health: A Prospectus*. Critical Reviews in Food Science and Nutrition, 2011. **51**(6): p. 524-546.
16. Garcia-Estevez, I., et al., *First evidences of interaction between pyranoanthocyanins and salivary proline-rich proteins*. Food Chemistry, 2017. **228**: p. 574-581.
17. Ferrer-Gallego, R., et al., *New Anthocyanin-Human Salivary Protein Complexes*. Langmuir, 2015. **31**(30): p. 8392-8401.
18. Hackman, R., J. Polagruto, et al, *Flavanols: Digestion, absorption and bioactivity*. Phytochemistry Reviews, 2008. **7**(1): p. 195-208.
19. Arts, I.C.W., B. van de Putte, and P.C.H. Hollman, *Catechin contents of foods commonly consumed in The Netherlands. 1. Fruits, vegetables, staple foods, and processed foods*. Journal of Agricultural and Food Chemistry, 2000. **48**(5): p. 1746-1751.
20. Arts, I.C.W., B. van de Putte, and P.C.H. Hollman, *Catechin contents of foods commonly consumed in The Netherlands. 2. Tea, wine, fruit juices, and chocolate milk*. Journal of Agricultural and Food Chemistry, 2000. **48**(5): p. 1752-1757.
21. Faria, A., et al., *Procyanidins as antioxidants and tumor cell growth modulators*. Journal of Agricultural and Food Chemistry, 2006. **54**(6): p. 2392-2397.
22. de la Iglesia, R., et al., *Healthy properties of proanthocyanidins*. Biofactors, 2010. **36**(3): p. 159-168.

23. Jin, Y.R., et al., *Antiplatelet activity of epigallocatechin gallate is mediated by the inhibition of PLC gamma 2 phosphorylation, elevation of PGD(2) production, and maintaining calcium-ATPase activity*. Journal of Cardiovascular Pharmacology, 2008. **51**(1): p. 45-54.
24. Bennick, A., *Interaction of plant polyphenols with salivary proteins*. Critical Reviews in Oral Biology & Medicine, 2002. **13**(2): p. 184-196.
25. Bate-Smith, E.e.S., T, *Comparative Biochemistry*. New York, Academic Press, 1962.
26. Halsam, E. and T.H. Lilley, *Natural astringency in foodstuffs—a molecular interpretation*. Critical reviews in food science and nutrition, 1988. **27**(1): p. 1-40.
27. Souquet, J.M., et al., *Polymeric proanthocyanidins from grape skins*. Phytochemistry, 1996. **43**(2): p. 509-512.
28. McRae, J.M. and J.A. Kennedy, *Wine and Grape Tannin Interactions with Salivary Proteins and Their Impact on Astringency: A Review of Current Research*. Molecules, 2011. **16**(3): p. 2348-2364.
29. Griffiths, D.W., *The inhibition of digestive enzymes by polyphenolic compounds*. Advances in experimental medicine and biology, 1986. **199**: p. 509-16.
30. Goncalves, R., et al., *Inhibition of trypsin by condensed tannins and wine*. Journal of Agricultural and Food Chemistry, 2007. **55**(18): p. 7596-7601.
31. Smeriglio, A., et al., *Proanthocyanidins and hydrolysable tannins: occurrence, dietary intake and pharmacological effects*. British Journal of Pharmacology, 2017. **174**(11): p. 1244-1262.
32. Beecher, G.R., *Proanthocyanidins: Biological activities associated with human health*. Pharmaceutical Biology, 2004. **42**: p. 2-20.
33. Bate-Smith, E.C., *Astringency in foods*. Food Chemistry, 1954. **23**: p. 124.
34. Haslam, E.C., *Practical polyphenolics: From structure to molecular recognition and physiological action*. Cambridge University Press, 1998.
35. Cheynier, V., *Phenolic compounds: from plants to foods*. Phytochemistry Reviews, 2012. **11**(2-3): p. 153-177.
36. Mueller-Harvey, I., *Analysis of hydrolysable tannins*. Animal Feed Science and Technology, 2001. **91**(1-2): p. 3-20.
37. Serrano, J., et al., *Tannins: Current knowledge of food sources, intake, bioavailability and biological effects*. Molecular Nutrition and Food Research, 2009. **53**(SUPPL. 2): p. 310-329.
38. Sarneckis, C.J., et al., *Quantification of condensed tannins by precipitation with methyl cellulose: development and validation of an optimised tool for grape and wine analysis*. Australian Journal of Grape and Wine Research, 2006. **12**(1): p. 39-49.
39. Haslam, E. and Y. Cai, *Plant polyphenols (vegetable tannins) - Gallic acid metabolism*. Natural Product Reports, 1994. **11**(1): p. 41-66.
40. Clifford, M.N. and A. Scalbert, *Ellagitannins - nature, occurrence and dietary burden*. Journal of the Science of Food and Agriculture, 2000. **80**(7): p. 1118-1125.
41. Quideau, S., et al., *Plant Polyphenols: Chemical Properties, Biological Activities, and Synthesis*. Angewandte Chemie-International Edition, 2011. **50**(3): p. 586-621.
42. Singleton, V.L.a.J.A.R., *Colorimetry of total phenolics with phosphomolybdic-phosphotungstic acid reagent*. Am J Enol Viti, 1965. **16**: p. 144–158.
43. de Freitas, V.A.P., et al., *A review of the current knowledge of red wine colour*. Oeno One, 2017. **51**(1): p. 15.
44. Siebert, K.J., *Haze formation in beverages*. Lwt-Food Science and Technology, 2006. **39**(9): p. 987-994.
45. Scalbert, A. and G. Williamson, *Dietary intake and bioavailability of polyphenols*. Journal of Nutrition, 2000. **130**(8): p. 2073S-2085S.
46. Macheix, J.-J., A. Fleuriet, et al., *Les composés phénoliques des végétaux*. Presses Polytechniques et Universitaires Romandes, 2005.

47. Dinnella, C., et al., *Individual astringency responsiveness affects the acceptance of phenol-rich foods*. Appetite, 2011. **56**(3): p. 633-642.
48. Gu, L.W., et al., *Concentrations of proanthocyanidins in common foods and estimations of normal consumption*. Journal of Nutrition, 2004. **134**(3): p. 613-617.
49. Morley, N., Clifford, T., Salter, L., Campbell, S., Gould, D. e Curnow, A., *The Green Tea Polyphenol (-)-Epigallocatechin Gallate and Green Tea Can Protect Human Cellular DNA from Ultraviolet and Visible Radiation-Induced Damage*. Photodermatology, Photoimmunology & Photomedicine, 2005. **21**(1): p. 15-22.
50. Azevedo, J., et al., *Antioxidant properties of anthocyanidins, anthocyanidin-3-glucosides and respective portisins*. Food Chemistry, 2010. **119**(2): p. 518-523.
51. Wolfe, K.L., et al., *Cellular antioxidant activity of common fruits*. Journal of Agricultural and Food Chemistry, 2008. **56**(18): p. 8418-8426.
52. Singh, A., S. Holvoet, and A. Mercenier, *Dietary polyphenols in the prevention and treatment of allergic diseases*. Clinical and Experimental Allergy, 2011. **41**(10): p. 1346-1359.
53. Funatogawa, K., et al., *Antibacterial activity of hydrolyzable tannins derived from medicinal plants against Helicobacter pylori*. Microbiology and Immunology, 2004. **48**(4): p. 251-261.
54. Taguri, T., T. Tanaka, and I. Kouno, *Antimicrobial activity of 10 different plant polyphenols against bacteria causing food-borne disease*. Biological & Pharmaceutical Bulletin, 2004. **27**(12): p. 1965-1969.
55. Halliwell, B., R. Aeschbach, et al, *The characterization of antioxidants*. Food Chem. Toxicol., 1995. **33**: p. 601-617.
56. da Silva Porto, P.A.L., J.A.N. Laranjinha, and V.A.P. de Freitas, *Antioxidant protection of low density lipoprotein by procyanidins: structure/activity relationships*. Biochemical pharmacology, 2003. **66**(6): p. 947-54.
57. Orgogozo, J.M., et al., *Wine consumption and dementia in the elderly: A prospective community study in the Bordeaux area*. Revue Neurologique, 1997. **153**(3): p. 185-192.
58. Renaud, S. and M. Delorgeril, *Wine, alcohol, platelets, and the French Paradox for Coronary Heart-Disease*. Lancet, 1992. **339**(8808): p. 1523-1526.
59. Oliveira, H., et al., *Experimental and Theoretical Data on the Mechanism by Which Red Wine Anthocyanins Are Transported through a Human MKN-28 Gastric Cell Model*. Journal of Agricultural and Food Chemistry, 2015. **63**(35): p. 7685-7692.
60. Mullen, W., C.A. Edwards, and A. Crozier, *Absorption, excretion and metabolite profiling of methyl-, glucuronyl-, glucosyl- and sulpho-conjugates of quercetin in human plasma and urine after ingestion of onions*. British Journal of Nutrition, 2006. **96**(1): p. 107-116.
61. Donovan, J.L., et al., *Catechin is metabolized by both the small intestine and liver of rats*. Journal of Nutrition, 2001. **131**(6): p. 1753-1757.
62. Baba, S., et al., *Absorption and urinary excretion of (-)-epicatechin after administration of different levels of cocoa powder or (-)-epicatechin in rats*. Journal of Agricultural and Food Chemistry, 2001. **49**(12): p. 6050-6056.
63. Gonthier, M.P., et al., *Metabolism of dietary procyanidins in rats*. Free Radical Biology and Medicine, 2003. **35**(8): p. 837-844.
64. Carpenter, G.H., *The Secretion, Components, and Properties of Saliva*, in *Annual Review of Food Science and Technology*, Vol 4, M.P. Doyle and T.R. Klaenhammer, Editors. 2013. p. 267-276.
65. Humphrey, S.P. and R.T. Williamson, *A review of saliva: Normal composition, flow, and function*. Journal of Prosthetic Dentistry, 2001. **85**(2): p. 162-169.
66. Gibbins, H.L. and G.H. Carpenter, *Alternative Mechanisms of Astringency - What is the role of saliva?* Journal of Texture Studies, 2013. **44**(5): p. 364-375.

67. Dodds, M.W.J., D.A. Johnson, and C.K. Yeh, *Health benefits of saliva: a review*. Journal of Dentistry, 2005. **33**(3): p. 223-233.
68. Ekström, J., et al., *Dysphagia: Diagnosis and Treatment*, O. Ekberg, Editor. 2012, Springer-Verlag Berlin Heidelberg p. 19-47.
69. Dinnella, C., et al., *Saliva Characteristics and Individual Sensitivity to Phenolic Astringent Stimuli*. Chemical Senses, 2009. **34**(4): p. 295-304.
70. Brandao, E., et al., *Human saliva protein profile: Influence of food ingestion*. Food Research International, 2014. **64**: p. 508-513.
71. Dawes, C., A.M. O'Connor, and J.M. Aspen, *The effect on human salivary flow rate of the temperature of a gustatory stimulus*. Archives of Oral Biology, 2000. **45**(11): p. 957-961.
72. Mese, H. and R. Matsuo, *Salivary secretion, taste and hyposalivation*. Journal of Oral Rehabilitation, 2007. **34**(10): p. 711-723.
73. Mandel, I.D., *Relation of saliva and plaque to caries*. Journal of Dental Research, 1974. **53**(2): p. 246-266.
74. Dawes, C., *Circadian-rhythms in human salivary flow-rate and composition*. Journal of Physiology, 1972. **220**(3): p. 529-545.
75. Dawes, C., *Circadian-rhythms in flow-rate and composition of unstimulated and stimulated human submandibular saliva* Journal of Physiology-London, 1975. **244**(2): p. 535-548.
76. Zheng, L., et al., *Clock Genes Show Circadian Rhythms in Salivary Glands*. Journal of Dental Research, 2012. **91**(8): p. 783-788.
77. Ferguson, D.B. and C.A. Botchway, *A comparison of circadian variation in the flow-rate and composition of stimulated human-parotid, sub-mandibular and whole salivas from the same individuals*. Archives of Oral Biology, 1980. **25**(8-9): p. 559-568.
78. Bennick, A., *Chemical and physical characteristics of a phosphoprotein from human parotid saliva*. Biochemical Journal, 1975. **145**(3): p. 557-567.
79. Boze, H., et al., *Proline-Rich Salivary Proteins Have Extended Conformations*. Biophysical Journal, 2010. **99**(2): p. 656-665.
80. Lu, Y. and A. Bennick, *Interaction of tannin with human salivary proline-rich proteins*. Archives of Oral Biology, 1998. **43**(9): p. 717-728.
81. Mamula, P.W., et al., *Localization of the human salivary protein complex (SPC) to chromosome band 12p13.2*. Cytogenetics and Cell Genetics, 1985. **39**(4): p. 279-284.
82. Stubbs, M., et al., *Encoding of human basic and glycosylated proline-rich proteins by the PRE gene complex and proteolytic processing of their precursor proteins*. Archives of Oral Biology, 1998. **43**(10): p. 753-770.
83. Messana, I., et al., *Facts and artifacts in proteomics of body fluids. What proteomics of saliva is telling us?* Journal of Separation Science, 2008. **31**(11): p. 1948-1963.
84. Mehansho, H., L.G. Butler, and D.M. Carlson, *Dietary tannins and salivary proline-rich proteins - Interactions, induction, and defense-mechanisms* Annual Review of Nutrition, 1987. **7**: p. 423-440.
85. Robinovitch, M.R., et al., *Parotid salivary basic proline-rich proteins inhibit HIV-I infectivity*. Oral Diseases, 2001. **7**(2): p. 86-93.
86. Vitorino, R., et al., *Towards defining the whole salivary peptidome*. Proteomics Clinical Applications, 2009. **3**(5): p. 528-540.
87. Hatton, M.N., et al., *Masticatory lubrication - The role of carbohydrate in the lubricating property of a salivary glycoprotein albumin complex*. Biochemical Journal, 1985. **230**(3): p. 817-820.
88. McArthur, C., G.D. Sanson, and A.M. Beal, *SALIVARY PROLINE-RICH PROTEINS IN MAMMALS - ROLES IN ORAL HOMEOSTASIS AND COUNTERACTING DIETARY TANNIN*. Journal of Chemical Ecology, 1995. **21**(6): p. 663-691.

89. Oppenheim, F.G., G.D. Offner, and R.F. Troxler, *Amino-acid sequence of a proline-rich phosphoglycoprotein from parotid secretion of the subhuman primate macaca-fascicularis*. Journal of Biological Chemistry, 1985. **260**(19): p. 671-679.
90. Carpenter, G.H. and G.B. Proctor, *O-Linked glycosylation occurs on basic parotid salivary proline-rich proteins*. Oral Microbiology and Immunology, 1999. **14**(5): p. 309-315.
91. Vitorino, R., et al., *Finding new posttranslational modifications in salivary proline-rich proteins*. Proteomics, 2010. **10**(20): p. 3732-3742.
92. Bennick, A., M. Cannon, and G. Madapallimattam, *Factors affecting the adsorption of salivary acidic proline-rich proteins to hydroxyapatite*. Caries Research, 1981. **15**(1): p. 9-20.
93. Bennick, A., D. Kells, and G. Madapallimattam, *Interaction of calcium-ions and salivary acidic proline-rich proteins with hydroxyapatite - a possible aspect of inhibition of hydroxyapatite formation*. Biochemical Journal, 1983. **213**(1): p. 11-20.
94. Hay, D.I., et al., *Inhibition of calcium-phosphate precipitation by human salivary acidic proline-rich proteins - structure-activity-relationships*. Calcified Tissue International, 1987. **40**(3): p. 126-132.
95. Oppenheim, F.G., et al., *Salivary proteome and its genetic polymorphisms*, in *Oral-Based Diagnostics*, D. Malamud and R.S. Niedbala, Editors. 2007, Blackwell Publishing: Oxford. p. 22-50.
96. Schlesinger, D.H., D.I. Hay, and M.J. Levine, *Complete primary structure of statherin, a potent inhibitor of calcium-phosphate precipitation, from the saliva of the monkey, macaca-arctoides*. International Journal of Peptide and Protein Research, 1989. **34**(5): p. 374-380.
97. Sabatini, L.M., et al., *cDNA cloning and chromosomal localization (4q 11-13) of a gene for statherin, a regulator of calcium in saliva*. American Journal of Human Genetics, 1987. **41**(6): p. 1048-1060.
98. Hay, D.I., Smith, D. J., Schluckebier, S. K. e Moreno, E. C., *Basic Biological Sciences Relationship between Concentration of Human Salivary Statherin and Inhibition of Calcium Phosphate Precipitation in Stimulated Human Parotid Saliva*. Journal of Dental Research, 1984. **63**(6): p. 857-863.
99. Gibbons, R.J. and D.I. Hay, *Human salivary acidic proline-rich proteins and statherin promote the attachment of actinomyces-viscosus LY7 to apatitic surfaces*. Infection and Immunity, 1988. **56**(2): p. 439-445.
100. Douglas, W.H., et al., *Statherin - a major boundary lubricant of human saliva*. Biochemical and Biophysical Research Communications, 1991. **180**(1): p. 91-97.
101. Raj, P.A., et al., *Salivary statherin - Dependence on sequence, charge, hydrogen-bonding potency, and helical conformation for adsorption to hydroxyapatite and inhibition of mineralization*. Journal of Biological Chemistry, 1992. **267**(9): p. 5968-5976.
102. Inzitari, R., et al., *Detection in human saliva of different statherin and P-B fragments and derivatives*. Proteomics, 2006. **6**(23): p. 6370-6379.
103. Messana, I., et al., *Characterization of the human salivary basic proline-rich protein complex by a proteomic approach*. Journal of Proteome Research, 2004. **3**(4): p. 792-800.
104. Bansil, R. and B.S. Turner, *Mucin structure, aggregation, physiological functions and biomedical applications*. Current Opinion in Colloid & Interface Science, 2006. **11**(2-3): p. 164-170.
105. Davies, H.S., et al., *Reorganisation of the salivary mucin network by dietary components: insights from green tea polyphenols*. PloS one, 2014. **9**(9): p. e108372.
106. Castagnola, M., et al., *A cascade of 24 histatins (histatin 3 fragments) in human saliva - Suggestions for a pre-secretory sequential cleavage pathway*. Journal of Biological Chemistry, 2004. **279**(40): p. 41436-41443.

107. Oppenheim, F.G., et al., *Histatins, a novel family of histidine-rich proteins in human-parotid secretion - isolation, characterization, primary structure, and fungistatic effects on candida-albicans*. Journal of Biological Chemistry, 1988. **263**(16): p. 7472-7477.
108. Gusman, H., et al., *Salivary histatin 5 is an inhibitor of both host and bacterial enzymes implicated in periodontal disease*. Infection and Immunity, 2001. **69**(3): p. 1402-1408.
109. Wroblewski, K., et al., *The molecular interaction of human salivary histatins with polyphenolic compounds*. European Journal of Biochemistry, 2001. **268**(16): p. 4384-4397.
110. Hagerman, A.E. and L.G. Butler, *The specificity of proanthocyanidin-protein interactions*. Journal of Biological Chemistry, 1981. **256**(9): p. 4494-4497.
111. Kalyanaraman, B., P.I. Premovic, and R.C. Sealy, *Semiquinone anion radicals from addition of amino-acids, peptides, and proteins to quinones derived from oxidation of catechols and catecholamines - an electron-spin-resonance spin stabilization study*. Journal of Biological Chemistry, 1987. **262**(23): p. 11080-11087.
112. Oh, H.I., et al., *Hydrophobic interaction in tannin-protein complexes*. Journal of Agricultural and Food Chemistry, 1980. **28**(2): p. 394-398.
113. Baxter, N.J., et al., *Multiple interactions between polyphenols and a salivary proline-rich protein repeat result in complexation and precipitation*. Biochemistry, 1997. **36**(18): p. 5566-5577.
114. Hagerman, A.E. and K.M. Klucher, *Tannin-protein interactions*. Progress in clinical and biological research, 1986. **213**: p. 67-76.
115. Haslam, E., *Symmetry and promiscuity in procyanidin biochemistry*. Phytochemistry, 1977. **16**(11): p. 1625-1640.
116. Charlton, A.J., et al., *Tannin interactions with a full-length human salivary proline-rich protein display a stronger affinity than with single proline-rich repeats*. Febs Letters, 1996. **382**(3): p. 289-292.
117. Canon, F., et al., *Ability of a salivary intrinsically unstructured protein to bind different tannin targets revealed by mass spectrometry*. Analytical and Bioanalytical Chemistry, 2010. **398**(2): p. 815-822.
118. Haslam, E., *Natural polyphenols (vegetable tannins) as drugs: Possible modes of action*. Journal of Natural Products, 1996. **59**(2): p. 205-215.
119. Hagerman, A.E., M.E. Rice, and N.T. Richardson, *Mechanisms of protein precipitation for two tannins, pentagalloyl glucose and epicatechin(16) (4 → 8) catechin (procyanidin)*. Journal of Agricultural and Food Chemistry, 1998. **46**(7): p. 2590-2595.
120. Charlton, A.J., et al., *Polyphenol/peptide binding and precipitation*. Journal of Agricultural and Food Chemistry, 2002. **50**(6): p. 1593-1601.
121. Siebert, K.J., N.V. Troukhanova, and P.Y. Lynn, *Nature of polyphenol-protein interactions*. Journal of Agricultural and Food Chemistry, 1996. **44**(1): p. 80-85.
122. Jobstl, E., et al., *Molecular model for astringency produced by polyphenol/protein interactions*. Biomacromolecules, 2004. **5**(3): p. 942-949.
123. Hagerman, A.E. and C.T. Robbins, *Implications of soluble tannin-protein complexes for tannin analysis and plant defense-mechanisms*. Journal of Chemical Ecology, 1987. **13**(5): p. 1243-1259.
124. Luck, G., et al., *Polyphenols, astringency and proline-rich proteins*. Phytochemistry, 1994. **37**(2): p. 357-371.
125. Lee, C.B. and H.T. Lawless, *Time-course of astringent sensations*. Chemical Senses, 1991. **16**(3): p. 225-238.
126. Lesschaeve, I. and A.C. Noble, *Polyphenols: factors influencing their sensory properties and their effects on food and beverage preferences*. American Journal of Clinical Nutrition, 2005. **81**(1): p. 330S-335S.
127. Soares, S., et al., *Sensorial properties of red wine polyphenols: Astringency and bitterness*. Critical Reviews in Food Science and Nutrition, 2017. **57**(5): p. 937-948.

128. Ma, W., et al., *A review on astringency and bitterness perception of tannins in wine*. Trends in Food Science & Technology, 2014. **40**(1): p. 6-19.
129. Delius, J., et al., *Effect of Astringent Stimuli on Salivary Protein Interactions Elucidated by Complementary Proteomics Approaches*. Journal of Agricultural and Food Chemistry, 2017. **65**(10): p. 2147-2154.
130. Biegler, M., et al., *Cationic astringents alter the tribological and rheological properties of human saliva and salivary mucin solutions*. Biotribology, 2016. **6**: p. 12-20.
131. Lee, C.A., B. Ismail, and Z.M. Vickers, *The Role of Salivary Proteins in the Mechanism of Astringency*. Journal of Food Science, 2012. **77**(4): p. C381-C387.
132. Dinnella, C., et al., *Temporary modification of salivary protein profile and individual responses to repeated phenolic astringent stimuli*. Chemical Senses, 2010. **35**(1): p. 75-85.
133. Schobel, N., et al., *Astringency Is a Trigeminal Sensation That Involves the Activation of G Protein-Coupled Signaling by Phenolic Compounds*. Chemical Senses, 2014. **39**(6): p. 471-487.
134. Payne, C., et al., *Interaction of astringent grape seed procyanidins with oral epithelial cells*. Food Chemistry, 2009. **115**(2): p. 551-557.
135. Ployon, S., et al., *Mechanisms of astringency: Structural alteration of the oral mucosal pellicle by dietary tannins and protective effect of bPRPs*. Food Chemistry, 2018. **253**: p. 79-87.
136. de Freitas, V. and N. Mateus, *Structural features of procyanidin interactions with salivary proteins*. Journal of Agricultural and Food Chemistry, 2001. **49**(2): p. 940-945.
137. Okuda, T., K. Mori, and T. Hatano, *Effects of the interaction of tannins with coexisting substances .4. Relationship of the structures of tannins to the binding activities with hemoglobin and methylene-blue*. Chemical & Pharmaceutical Bulletin, 1985. **33**(4): p. 1424-1433.
138. Kawamoto, H., F. Nakatsubo, and K. Murakami, *Quantitative-determination of tannin and protein in the precipitates by High-Performance Liquid Chromatography*. Phytochemistry, 1995. **40**(5): p. 1503-1505.
139. Ricardo-Da-Silva, J.M., et al., *Interaction of grape seed procyanidins with various proteins in relation to wine fining*. Journal of the Science of Food and Agriculture, 1991. **57**(1): p. 111-125.
140. Pascal, C., et al., *Interactions between a non glycosylated human proline-rich protein and flavan-3-ols are affected by protein concentration and polyphenol/protein ratio*. Journal of Agricultural and Food Chemistry, 2007. **55**(12): p. 4895-4901.
141. Sarni-Manchado, P., V. Cheynier, and M. Moutounet, *Interactions of grape seed tannins with salivary proteins*. Journal of Agricultural and Food Chemistry, 1999. **47**(1): p. 42-47.
142. Pianet, I., et al., *Modeling procyanidin self-association processes and understanding their micellar organization: A study by diffusion NMR and molecular mechanics*. Langmuir, 2008. **24**(19): p. 11027-11035.
143. Cala, O., et al., *NMR and molecular modeling of wine tannins binding to saliva proteins: revisiting astringency from molecular and colloidal prospects*. Faseb Journal, 2010. **24**(11): p. 4281-4290.
144. Bacon, J.R. and M.J.C. Rhodes, *Development of a competition assay for the evaluation of the binding of human parotid salivary proteins to dietary complex phenols and tannins using a peroxidase-labeled tannin*. Journal of Agricultural and Food Chemistry, 1998. **46**(12): p. 5083-5088.
145. Obreque-Slier, E., et al., *Tannin-protein interaction is more closely associated with astringency than tannin-protein precipitation: experience with two oenological tannins and a gelatin*. International Journal of Food Science and Technology, 2010. **45**(12): p. 2629-2636.

146. Deaville, E.R., et al., *Hydrolyzable tannin structures influence relative globular and random coil protein binding strengths*. Journal of Agricultural and Food Chemistry, 2007. **55**(11): p. 4554-4561.
147. Sarni-Manchado, P., et al., *Influence of the glycosylation of human salivary proline-rich proteins on their interactions with condensed tannins*. Journal of Agricultural and Food Chemistry, 2008. **56**(20): p. 9563-9569.
148. Wakabayashi, K., *Changes in cell wall polysaccharides during fruit ripening*. Journal of Plant Research, 2000. **113**(1111): p. 231-237.
149. Goldstein, J.L. and T. Swain, *Changes in tannins in ripening fruits*. Phytochemistry, 1963. **2**(4): p. 371-383.
150. Mateus, N., et al., *Proanthocyanidin composition of red Vitis vinifera varieties from the Douro valley during ripening: Influence of cultivation altitude*. American Journal of Enology and Viticulture, 2001. **52**(2): p. 115-121.
151. Vincken, J.P., et al., *If homogalacturonan were a side chain of rhamnogalacturonan I. Implications for cell wall architecture*. Plant Physiology, 2003. **132**(4): p. 1781-1789.
152. Perez, S., K. Mazeau, and C.H. du Penhoat, *The three-dimensional structures of the pectic polysaccharides*. Plant Physiology and Biochemistry, 2000. **38**(1-2): p. 37-55.
153. Ochoa-Villarreal, M., et al., *Plant Cell Wall Polymers: Function, Structure and Biological Activity of Their Derivatives, in Polymerization*. 2012.
154. Watrelot, A.A., et al., *Interactions between Pectic Compounds and Procyandins are Influenced by Methylation Degree and Chain Length*. Biomacromolecules, 2013. **14**(3): p. 709-718.
155. Voragen, A.G.J., et al., *Pectin, a versatile polysaccharide present in plant cell walls*. Structural Chemistry, 2009. **20**(2): p. 263-275.
156. Pérez, S., M.A. Rodríguez-Carvajal, and T. Doco, *A complex plant cell wall polysaccharide: rhamnogalacturonan II. A structure in quest of a function*. Biochimie, 2003. **85**(1): p. 109-121.
157. Ozawa, T., T.H. Lilley, and E. Haslam, *Polyphenol interactions. 3. Polyphenol interactions - Astringency and the loss of astringency in ripening fruit*. Phytochemistry, 1987. **26**(11): p. 2937-2942.
158. Haslam, E.L., T. H.; Warminski, E.; Liao, H.; Cai, Y.; Martin, R.; Gaffney, and P.N.L. S. H.; Goulding, G., *Polyphenol complexation – A study in molecular recognition. In Phenolic Compounds in Food and Their Effects on Health I*. American Chemical Society: Washington, DC, 1992: p. 8-50.
159. Pellerin, P., et al., *Structural characterization of red wine rhamnogalacturonan II*. Carbohydrate Research, 1996. **290**(2): p. 183-197.
160. Vidal, S., et al., *The polysaccharides of red wine: total fractionation and characterization*. Carbohydrate Polymers, 2003. **54**(4): p. 439-447.
161. Apolinar-Valiente, R., et al., *Polysaccharide Composition of Monastrell Red Wines from Four Different Spanish Terroirs: Effect of Wine-Making Techniques*. Journal of Agricultural and Food Chemistry, 2013. **61**(10): p. 2538-2547.
162. Ayestaran, B., Z. Guadalupe, and D. Leon, *Quantification of major grape polysaccharides (Tempranillo v.) released by maceration enzymes during the fermentation process*. Analytica Chimica Acta, 2004. **513**(1): p. 29-39.
163. Waters, E.J., P. Pellerin, and J.M. Brillouet, *A saccharomyces mannoprotein that protects wine from protein haze*. Carbohydrate Polymers, 1994. **23**(3): p. 185-191.
164. Pellerin, P., et al., *Characterization of five type II arabinogalactan-protein fractions from red wine of increasing uronic acid content*. Carbohydrate Research, 1995. **277**(1): p. 135-143.
165. Doco, T., et al., *Polysaccharide patterns during the aging of Carignan noir red wines*. American Journal of Enology and Viticulture, 1999. **50**(1): p. 25-32.

166. Doco, T., et al., *Structural modification of wine arabinogalactans during aging on lees*. American Journal of Enology and Viticulture, 2003. **54**(3): p. 150-157.
167. Escot, S., et al., *Release of polysaccharides by yeasts and the influence of released polysaccharides on colour stability and wine astringency*. Australian Journal of Grape and Wine Research, 2001. **7**(3): p. 153-159.
168. Goncalves, F., et al., *Characterization of white wine mannoproteins*. Journal of Agricultural and Food Chemistry, 2002. **50**(21): p. 6097-6101.
169. Vidal, S., et al., *The mouth-feel properties of polysaccharides and anthocyanins in a wine like medium*. Food Chemistry, 2004. **85**(4): p. 519-525.
170. Carvalho, E., et al., *Application of flow nephelometry to the analysis of the influence of carbohydrates on protein-tannin interactions*. Journal of the Science of Food and Agriculture, 2006. **86**(6): p. 891-896.
171. Rawel, H.A., K. Meidtner, and J. Kroll, *Binding of selected phenolic compounds to proteins*. Journal of Agricultural and Food Chemistry, 2005. **53**(10): p. 4228-4235.
172. Yan, Q.Y. and A. Bennick, *Identification of Histatins as Tannin-Binding Proteins in Human Saliva*. Biochemical Journal, 1995. **311**: p. 341-347.
173. Serafini, M., G. Maiani, and A. FerroLuzzi, *Effect of ethanol on red wine tannin-protein (BSA) interactions*. Journal of Agricultural and Food Chemistry, 1997. **45**(8): p. 3148-3151.
174. Bajec, M.R. and G.J. Pickering, *Astringency: Mechanisms and perception*. Critical Reviews in Food Science and Nutrition, 2008. **48**(9): p. 858-875.
175. Kallithraka, S., J. Bakker, and M.N. Clifford, *Evidence that salivary proteins are involved in astringency*. Journal of Sensory Studies, 1998. **13**(1): p. 29-43.
176. Quijada-Morin, N., et al., *Effect of the addition of flavan-3-ols on the HPLC-DAD salivary-protein profile*. Food Chemistry, 2016. **207**: p. 272-278.
177. Monteleone, E., et al., *Prediction of perceived astringency induced by phenolic compounds*. Food Quality and Preference, 2004. **15**(7-8): p. 761-769.
178. Soares, S., et al., *Reactivity of human salivary proteins families toward food polyphenols*. Journal of Agricultural and Food Chemistry, 2011. **59**(10): p. 5535-5547.
179. Asquith, T.N., et al., *Binding of condensed tannins to salivary proline-rich glycoproteins - the role of carbohydrate*. Journal of Agricultural and Food Chemistry, 1987. **35**(3): p. 331-334.
180. Vincenzi, S., et al., *Grape seed proteins: a new fining agent for astringency reduction in red wine*. Australian Journal of Grape and Wine Research, 2013. **19**(2): p. 153-160.
181. de Freitas, V.A.P., et al., *Characterisation of oligomeric and polymeric procyanidins from grape seeds by liquid secondary ion mass spectrometry*. Phytochemistry, 1998. **49**(5): p. 1435-1441.
182. Soares, S., et al., *Interaction between red wine procyanidins and salivary proteins: effect of stomach digestion on the resulting complexes*. Rsc Advances, 2015. **5**(17): p. 12664-12670.
183. Gonzalez-Manzano, S., et al., *Influence of the degree of polymerisation in the ability of catechins to act as anthocyanin copigments*. European Food Research and Technology, 2008. **227**(1): p. 83-92.
184. Delcour, J.A., D. Ferreira, and D.G. Roux, *Synthesis of Condensed Tannins .9. The Condensation Sequence of Leucocyanidin with (+)-Catechin and with the Resultant Procyanidins*. Journal of the Chemical Society-Perkin Transactions 1, 1983(8): p. 1711-1717.
185. Geissman, T.A. and N.N. Yoshimur, *Synthetic Proanthocyanidin*. Tetrahedron Letters, 1966(24): p. 2669-2673.

186. Puskas, I., et al., *Aspects of determining the molecular weight of cyclodextrin polymers and oligomers by static light scattering*. Carbohydrate Polymers, 2013. **94**(1): p. 124-128.
187. Papadopoulou, A., R.J. Green, and R.A. Frazier, *Interaction of flavonoids with bovine serum albumin: A fluorescence quenching study*. Journal of Agricultural and Food Chemistry, 2005. **53**(1): p. 158-163.
188. Soares, S., N. Mateus, and V. De Freitas, *Interaction of different polyphenols with bovine serum albumin (BSA) and human salivary alpha-amylase (HSA) by fluorescence quenching*. Journal of Agricultural and Food Chemistry, 2007. **55**(16): p. 6726-6735.
189. Dias, R., et al., *The interaction between tannins and gliadin derived peptides in a celiac disease perspective*. Rsc Advances, 2015. **5**(41): p. 32151-32158.
190. Lakowicz, J.R., *Principles of fluorescence spectroscopy*. 2nd ed ed. 1999, New York: Kluwer Academic/Plenum Publishers.
191. Ferreira, M. and P. Gameiro, *Ciprofloxacin Metalloantibiotic: An Effective Antibiotic with an Influx Route Strongly Dependent on Lipid Interaction?* Journal of Membrane Biology, 2015. **248**(1): p. 125-136.
192. Goncalves, R., et al., *Mechanisms of Tannin-Induced Trypsin Inhibition: A Molecular Approach*. Langmuir, 2011. **27**(21): p. 13122-13129.
193. Viegas, A., et al., *Saturation-Transfer Difference (STD) NMR: A Simple and Fast Method for Ligand Screening and Characterization of Protein Binding*. Journal of Chemical Education, 2011. **88**(7): p. 990-994.
194. Piotto, M., V. Saudek, and V. Sklenar, *Gradient-Tailored Excitation for Single-Quantum NMR-Spectroscopy of Aqueous-Solutions*. Journal of Biomolecular Nmr, 1992. **2**(6): p. 661-665.
195. Abe, Y., et al., *Structural characterization of a procyanidin tetramer and pentamer from the apple by low-temperature NMR analysis*. Tetrahedron Letters, 2008. **49**(45): p. 6413-6418.
196. Le Bourvellec, C., S. Guyot, and C. Renard, *Non-covalent interaction between procyanidins and apple cell wall material Part I. Effect of some environmental parameters*. Biochimica Et Biophysica Acta-General Subjects, 2004. **1672**(3): p. 192-202.
197. Le Bourvellec, C. and C. Renard, *Interactions between Polyphenols and Macromolecules: Quantification Methods and Mechanisms*. Critical Reviews in Food Science and Nutrition, 2012. **52**(1-3): p. 213-248.
198. Rasoulzadeh, F., et al., *Fluorescence quenching study of quercetin interaction with bovine milk xanthine oxidase*. Spectrochimica Acta Part a-Molecular and Biomolecular Spectroscopy, 2009. **72**(1): p. 190-193.
199. Goncalves, R., N. Mateus, and V. De Freitas, *Study of the Interaction of Pancreatic Lipase with Procyanidins by Optical and Enzymatic Methods*. Journal of Agricultural and Food Chemistry, 2010. **58**(22): p. 11901-11906.
200. Frazier, R.A., et al., *Interactions of tea tannins and condensed tannins with proteins*. Journal of Pharmaceutical and Biomedical Analysis, 2010. **51**(2): p. 490-495.
201. Streiff, J.H., et al., *Saturation transfer difference nuclear magnetic resonance spectroscopy as a method for screening proteins for anesthetic binding*. Molecular Pharmacology, 2004. **66**(4): p. 929-935.
202. Haselhorst, T., A.-C. Lamerz, and M.v. Itzstein, *Saturation transfer difference NMR spectroscopy as a technique to investigate protein-carbohydrate interactions in solution*. Methods in molecular biology (Clifton, N.J.), 2009. **534**: p. 375-86.
203. de la Iglesia, R., et al., *Healthy properties of proanthocyanidins*. BioFactors, 2010. **36**(3): p. 159-168.
204. Soares, S., et al., *Sensorial Properties of Red Wine Polyphenols: Astringency and Bitterness*. Critical Reviews in Food Science and Nutrition, 2015: p. 00-00.

205. ASTM, *Standard Terminology to Sensory Evaluation of Materials and Products*. Annual Book of ASTM Standards. Vol. 15.07. 1989, Philadelphia, PA: American Society of Testing and Materials.
206. Manconi, B., et al., *The intriguing heterogeneity of human salivary proline-rich proteins: Short title: Salivary proline-rich protein species*. Journal of Proteomics, 2016. **134**: p. 47-56.
207. Vitorino, R., et al., *Finding new posttranslational modifications in salivary proline-rich proteins*. PROTEOMICS – Clinical Applications, 2011. **5**(3-4): p. 197-197.
208. Lu, Y. and A. Bennick, *Interaction of tannin with human salivary proline-rich proteins*. Arch. Oral Biol., 1998. **43**: p. 717-728.
209. Quijada-Morín, N., et al., *Effect of the addition of flavan-3-ols on the HPLC-DAD salivary-protein profile*. Food Chemistry, 2016. **207**: p. 272-278.
210. Brandão, E., et al., *In Vivo Interactions between Procyanidins and Human Saliva Proteins: Effect of Repeated Exposures to Procyanidins Solution*. Journal of Agricultural and Food Chemistry, 2014. **62**(39): p. a9562-9568.
211. Rothwell, J.A., et al., *Phenol-Explorer 3.0: a major update of the Phenol-Explorer database to incorporate data on the effects of food processing on polyphenol content*. Database, 2013. **2013**.
212. Soares, S., et al., *Effect of condensed tannins addition on the astringency of red wines*. Chemical Senses, 2011. **37**: p. 191-198.
213. Puskás, I., et al., *Aspects of determining the molecular weight of cyclodextrin polymers and oligomers by static light scattering*. Carbohydrate Polymers, 2013. **94**(1): p. 124-128.
214. Teixeira, N., et al., *Structural Features of Copigmentation of Oenin with Different Polyphenol Copigments*. Journal of Agricultural and Food Chemistry, 2013. **61**(28): p. 6942-6948.
215. Gonçalves, R., et al., *Mechanisms of Tannin-Induced Trypsin Inhibition: A Molecular Approach*. Langmuir, 2011. **27**(21): p. 13122-13129.
216. Tarascou, I., et al., *A 3D structural and conformational study of procyanidin dimers in water and hydro-alcoholic media as viewed by NMR and molecular modeling*. Magnetic Resonance in Chemistry, 2006. **44**(9): p. 868-880.
217. Izaguirre, J.A., et al., *Langevin stabilization of molecular dynamics*. The Journal of Chemical Physics, 2001. **114**(5): p. 2090-2098.
218. Case DA, et al., *Amber 12*. 2012, University of California, San Francisco.
219. Cala, O., et al., *NMR and molecular modeling of wine tannins binding to saliva proteins: revisiting astringency from molecular and colloidal prospects*. The FASEB Journal, 2010. **24**(11): p. 4281-4290.
220. Ferrer-Gallego, R., et al., *Characterization of Sensory Properties of Flavanols—A Molecular Dynamic Approach*. Chemical Senses, 2015. **40**(6): p. 381-390.
221. Cala, O., et al., *The colloidal state of tannins impacts the nature of their interaction with proteins: The case of salivary proline-rich protein/procyanidins binding*. Langmuir, 2012. **28**(50): p. 17410-17418.
222. Zhang, Z. and A.G. Marshall, *A universal algorithm for fast and automated charge state deconvolution of electrospray mass-to-charge ratio spectra*. Journal of the American Society for Mass Spectrometry, 1998. **9**(3): p. 225-233.
223. Tarascou, I., et al., *Structural and conformational analysis of two native procyanidin trimers*. Magnetic Resonance in Chemistry, 2007. **45**(2): p. 157-166.
224. Gyémánt, G., et al., *Evidence for pentagalloyl glucose binding to human salivary α -amylase through aromatic amino acid residues*. Biochimica et Biophysica Acta (BBA) - Proteins & Proteomics, 2009. **1794**(2): p. 291-296.

225. Mayer, M. and B. Meyer, *Characterization of ligand binding by saturation transfer difference NMR spectroscopy*. Angewandte Chemie International Edition, 1999. **38**(12): p. 1784-1788.
226. Watrelot, A.A., C.M.G.C. Renard, and C. Le Bourvellec, *Comparison of microcalorimetry and haze formation to quantify the association of B-type procyanidins to poly-l-proline and bovine serum albumin*. LWT - Food Science and Technology, 2015. **63**(1): p. 376-382.
227. Deaville, E.R., et al., *Hydrolyzable tannin structures influence relative globular and random coil protein binding strengths*. J. Agric. Food Chem., 2007. **55**(11): p. 4554-4561.
228. Tarascou, I., et al., *A 3D structural and conformational study of procyanidin dimers in water and hydro-alcoholic media as viewed by NMR and molecular modeling*. Magnetic Resonance in Chemistry, 2006. **44**(9): p. 868-880.
229. Cala, O., et al., *Towards a Molecular Interpretation of Astringency: Synthesis, 3D Structure, Colloidal State, and Human Saliva Protein Recognition of Procyanidins*. Planta Med, 2011. **77**(EFirst): p. 1116,1122.
230. Jauregi, P., et al., *Astringency reduction in red wine by whey proteins*. Food Chemistry, 2016. **199**: p. 547-555.
231. Canon, F., et al., *Ability of a salivary intrinsically unstructured protein to bind different tannin targets revealed by mass spectrometry*. Analytical and Bioanalytical Chemistry, 2010. **398**(2): p. 815-822.
232. Canon, F., et al., *Binding site of different tannins on a human salivary proline-rich protein evidenced by dissociative photoionization tandem mass spectrometry*. Tetrahedron, 2015. **71**(20): p. 3039-3044.
233. Tarascou, I., et al., *Structural and conformational analysis of two native procyanidin trimers*. Magnetic Resonance in Chemistry, 2007. **45**(2): p. 157-166.
234. McRae, J.M., R.J. Falconer, and J.A. Kennedy, *Thermodynamics of Grape and Wine Tannin Interaction with Polyproline: Implications for Red Wine Astringency*. Journal of Agricultural and Food Chemistry, 2010. **58**(23): p. 12510-12518.
235. Frazier, R.A., et al., *Probing protein-tannin interactions by isothermal titration microcalorimetry*. J. Agric. Food Chem., 2003. **51**(18): p. 5189-5195.
236. Hagerman, A.E., M.E. Rice, and N.T. Ritchard, *Mechanisms of protein precipitation for two tannins, pentagalloyl glucose and epicatechin₁₆(4-8) catechin (procyanidin)*. J. Agric. Food Chem., 1998. **46**(7): p. 2590-2595.
237. Charlton, A.J., et al., *Tannin interactions with a full-length human salivary proline-rich protein display a stronger affinity than with single proline-rich repeats*. FEBS Lett., 1996. **382**(3): p. 289-292.
238. Canon, F., et al., *Folding of a Salivary Intrinsically Disordered Protein upon Binding to Tannins*. Journal of the American Chemical Society, 2011. **133**(20): p. 7847-7852.
239. Simon, C., et al., *Three-dimensional structure and dynamics of wine tannin-saliva protein complexes. A multitechnique approach*. Biochemistry, 2003. **42**(35): p. 10385-10395.
240. Soares, S., et al., *Reactivity of human salivary proteins families toward food polyphenols*. Journal of Agricultural and Food Chemistry, 2011. **59**(10): p. 5535-5547.
241. Santos-Buelga, C. and A. Scalbert, *Proanthocyanidins and tannin-like compounds – nature, occurrence, dietary intake and effects on nutrition and health*. Journal of the Science of Food and Agriculture, 2000. **80**(7): p. 1094-1117.
242. Zillich, O.V., et al., *Polyphenols as active ingredients for cosmetic products*. Int J Cosmet Sci, 2015. **37**(5): p. 455-64.
243. Garcia-Estevez, I., et al., *Development of a fractionation method for the detection and identification of oak ellagitannins in red wines*. Analytica Chimica Acta, 2010. **660**(1-2): p. 171-176.
244. Chira, K. and P.L. Teissedre, *Relation between volatile composition, ellagitannin content and sensory perception of oak wood chips representing different toasting processes*. European Food Research and Technology, 2013. **236**(4): p. 735-746.

245. Vivas, N., et al., *Conformational Interpretation of Vescalagin and Castalagin Physicochemical Properties*. Journal of Agricultural and Food Chemistry, 2004. **52**(7): p. 2073-2078.
246. Esatbeyoglu, T., V. Wray, and P. Winterhalter, *Dimeric procyanidins: screening for B1 to B8 and semisynthetic preparation of B3, B4, B6, And B8 from a polymeric procyanidin fraction of white willow bark (*Salix alba*)*. J Agric Food Chem, 2010. **58**(13): p. 7820-30.
247. Balas, L. and J. Vercauteren, *Extensive high-resolution reverse 2D NMR analysis for the structural elucidation of procyanidin oligomers*. Magnetic Resonance in Chemistry, 1994. **32**(7): p. 386-393.
248. Schlesinger, D.H., D.I. Hay, and M.J. Levine, *Complete primary structure of statherin, a potent inhibitor of calcium phosphate precipitation, from the saliva of the monkey, *Macaca arctoides**. Int J Pept Protein Res, 1989. **34**(5): p. 374-80.
249. Helmerhorst, E.J., et al., *Mass Spectrometric Identification of Key Proteolytic Cleavage Sites in Statherin Affecting Mineral Homeostasis and Bacterial Binding Domains*. J Proteome Res, 2010. **9**(10): p. 5413-21.
250. Isemura, S. and E. Saitoh, *Nucleotide sequence of gene PBI encoding a protein homologous to salivary proline-rich protein P-B*. J Biochem, 1997. **121**(6): p. 1025-30.
251. Henskens, Y.M.C., et al., *Cystatins S and C in Human Whole Saliva and in Glandular Salivas in Periodontal Health and Disease*. Journal of Dental Research, 1994. **73**(10): p. 1606-1614.
252. Obreque-Slier, E., et al., *Tannin–protein interaction is more closely associated with astringency than tannin–protein precipitation: experience with two oenological tannins and a gelatin*. International Journal of Food Science & Technology, 2010. **45**(12): p. 2629-2636.
253. Soares, S., N. Mateus, and V. de Freitas, *Interaction of different classes of salivary proteins with food tannins*. Food Research International, 2012. **49**(2): p. 807-813.
254. Hofmann, T., et al., *Protein binding and astringent taste of a polymeric procyanidin, 1,2,3,4,6-penta-O-galloyl-beta-D-glucopyranose, castalagin, and grandinin*. Journal of Agricultural and Food Chemistry, 2006. **54**(25): p. 9503-9509.
255. Soares, S., et al., *Reactivity of human salivary proteins families toward food polyphenols*. J Agric Food Chem, 2011. **59**(10): p. 5535-47.
256. Lu, J., K. Ding, and Q. Yuan, *Determination of Punicalagin Isomers in Pomegranate Husk*. Chromatographia, 2008. **68**(3): p. 303-306.
257. Bras, N.F., et al., *Understanding the Binding of Procyanidins to Pancreatic Elastase by Experimental and Computational Methods*. Biochemistry, 2010. **49**(25): p. 5097-5108.
258. Lakowicz, J.R., *Principles of Fluorescence Spectroscopy* Vol. 3rd Edition. 2006: Springer US.
259. Viegas, A., et al., *Saturation-Transfer Difference (STD) NMR: A Simple and Fast Method for Ligand Screening and Characterization of Protein Binding*. Journal of Chemical Education, 2011. **88**: p. 990-994.
260. Dupenhoat, C., et al., *Structural elucidation of new dimeric ellagitannins from Quercus-Robur L. roburins A-E*. Journal of the Chemical Society-Perkin Transactions 1, 1991(7): p. 1653-1660.
261. Kraszni, M., A. Marosi, and C.K. Larive, *NMR assignments and the acid-base characterization of the pomegranate ellagitannin punicalagin in the acidic pH-range*. Analytical and Bioanalytical Chemistry, 2013. **405**(17): p. 5807-5816.
262. Glabasnia, A. and T. Hofmann, *Sensory-directed identification of taste-active ellagitannins in American (*Quercus alba* L.) and European oak wood (*Quercus robur* L.) and quantitative analysis in bourbon whiskey and oak-matured red wines*. Journal of Agricultural and Food Chemistry, 2006. **54**(9): p. 3380-3390.

263. Glabasnia, A. and T. Hofmann, *Identification and sensory evaluation of dehydro- and deoxy-ellagitannins formed upon toasting of oak wood (Quercus alba L.)*. Journal of Agricultural and Food Chemistry, 2007. **55**(10): p. 4109-4118.
264. Lipinska, L., E. Klewicka, and M. Sojka, *Structure, occurrence and biological activity of ellagitannins: a general review*. Acta Sci Pol Technol Aliment, 2014. **13**(3): p. 289-99.
265. Branda, E., et al., *In Vivo Interactions between Procyanidins and Human Saliva Proteins: Effect of Repeated Exposures to Procyanidins Solution*. Journal of Agricultural and Food Chemistry, 2014. **62**(39): p. 9562-9568.
266. Manconi, B., et al., *The intriguing heterogeneity of human salivary proline-rich proteins Short title: Salivary proline-rich protein species*. Journal of Proteomics, 2016. **134**: p. 47-56.
267. Soares, S., et al., *Contribution of Human Oral Cells to Astringency by Binding Salivary Protein/Tannin Complexes*. Journal of Agricultural and Food Chemistry, 2016. **64**(41): p. 7823-7828.
268. Carvalho, E., et al., *Influence of wine pectic polysaccharides on the interactions between condensed tannins and salivary proteins*. Journal of Agricultural and Food Chemistry, 2006. **54**(23): p. 8936-8944.
269. Soares, S., N. Mateus, and V. de Freitas, *Carbohydrates inhibit salivary proteins precipitation by condensed tannins*. Journal of Agricultural and Food Chemistry, 2012. **60**(15): p. 3966-3972.
270. de Freitas, V., E. Carvalho, and N. Mateus, *Study of carbohydrate influence on protein-tannin aggregation by nephelometry*. Food Chemistry, 2003. **81**(4): p. 503-509.
271. Watrelot, A.A., D.L. Schulz, and J.A. Kennedy, *Wine polysaccharides influence tannin-protein interactions*. Food Hydrocolloids, 2017. **63**: p. 571-579.
272. Mateus, N., et al., *Influence of the tannin structure on the disruption effect of carbohydrates on protein-tannin aggregates*. Analytica Chimica Acta, 2004. **513**(1): p. 135-140.
273. Riou, V., et al., *Aggregation of grape seed tannins in model wine - effect of wine polysaccharides*. Food Hydrocolloids, 2002. **16**(1): p. 17-23.
274. Lu, J.J., K. Ding, and Q.P. Yuan, *Determination of punicalagin isomers in pomegranate husk*. Chromatographia, 2008. **68**(3-4): p. 303-306.
275. Pellerin, P., et al., *Complexation du plomb dans les vins par les dimères de rhamnogalacturonane II, un polysaccharide pectique du raisin*. Journal International Science Vigne Vin, 1997. **31**: p. 33-41.
276. Ducasse, M.A., et al., *Isolation of Carignan and Merlot red wine oligosaccharides and their characterization by ESI-MS*. Carbohydrate Polymers, 2010. **79**(3): p. 747-754.
277. Doco, T., M.A. O'Neill, and P. Pellerin, *Determination of the neutral and acidic glycosyl-residue compositions of plant polysaccharides by GC-EI-MS analysis of the trimethylsilyl methyl glycoside derivatives*. Carbohydrate Polymers, 2001. **46**(3): p. 249-259.
278. Soares, S.I., et al., *Mechanistic Approach by Which Polysaccharides Inhibit alpha-Amylase/Procyanidin Aggregation*. Journal of Agricultural and Food Chemistry, 2009. **57**(10): p. 4352-4358.
279. Vidal, S., et al., *Structural characterization of the pectic polysaccharide rhamnogalacturonan II: evidence for the backbone location of the aceric acid-containing oligoglycosyl side chain*. Carbohydrate Research, 2000. **326**(4): p. 277-294.
280. Goncalves, R., N. Mateus, and V. De Freitas, *Influence of Carbohydrates on the Interaction of Procyanidin B3 with Trypsin*. Journal of Agricultural and Food Chemistry, 2011. **59**(21): p. 11794-11802.
281. Vidal, S., et al., *The mouth-feel properties of grape and apple proanthocyanidins in a wine-like medium*. Journal of the Science of Food and Agriculture, 2003. **83**(6): p. 564-573.

282. Vidal, S., et al., *Use of an experimental design approach for evaluation of key wine components on mouth-feel perception*. Food Quality and Preference, 2004. **15**(3): p. 209-217.
283. Boulet, J.C., et al., *Models based on ultraviolet spectroscopy, polyphenols, oligosaccharides and polysaccharides for prediction of wine astringency*. Food Chemistry, 2016. **190**: p. 357-363.
284. Gawel, R., A. Oberholster, and I. Leigh Francis, *A 'Mouth-feel Wheel': terminology for communicating the mouth-feel characteristics of red wine*. Australian Journal of Grape and Wine Research, 2000. **6**(3): p. 203-207.
285. Laguna, L., B. Bartolome, and M.V. Moreno-Arribas, *Mouthfeel perception of wine: Oral physiology, components and instrumental characterization*. Trends in Food Science & Technology, 2017. **59**: p. 49-59.
286. Guadalupe, Z., et al., *Quantitative determination of wine polysaccharides by gas chromatography-mass spectrometry (GC-MS) and size exclusion chromatography (SEC)*. Food Chemistry, 2012. **131**(1): p. 367-374.
287. Rinaldi, A., A. Gambuti, and L. Moio, *Application of the SPI (Saliva Precipitation Index) to the evaluation of red wine astringency*. Food Chemistry, 2012. **135**(4): p. 2498-2504.
288. Silva, M., et al., *Molecular Interaction Between Salivary Proteins and Food Tannins*. Journal of Agricultural and Food Chemistry, 2017. **65**(31): p. 6415-6424.
289. Neyraud, E., et al., *Variability of human saliva composition: Possible relationships with fat perception and liking*. Archives of Oral Biology, 2012. **57**(5): p. 556-566.
290. Helmerhorst, E.J. and F.G. Oppenheim, *Saliva: a dynamic proteome*. Journal of Dental Research, 2007. **86**(8): p. 680-693.
291. Pascal, C., et al., *Aggregation of a proline-rich protein induced by epigallocatechin gallate and condensed tannins: Effect of protein glycosylation*. Journal of Agricultural and Food Chemistry, 2008. **56**(15): p. 6724-6732.
292. Lee, C.A. and Z.M. Vickers, *Astringency of Foods May Not be Directly Related to Salivary Lubricity*. Journal of Food Science, 2012. **77**(9): p. S302-S306.
293. Nayak, A. and G.H. Carpenter, *A physiological model of tea-induced astringency*. Physiology & Behavior, 2008. **95**(3): p. 290-294.
294. Guadalupe, Z., et al., *Determination of Must and Wine Polysaccharides by Gas Chromatography-Mass Spectrometry (GC-MS) and Size-Exclusion Chromatography (SEC)*, in *Polysaccharides: Bioactivity and Biotechnology*, K.G. Ramawat and J.-M. Mérillon, Editors. 2014, Springer International Publishing: Cham. p. 1-28.
295. Vidal, S., et al., *Taste and mouth-feel properties of different types of tannin-like polyphenolic compounds and anthocyanins in wine*. Analytica Chimica Acta, 2004. **513**(1): p. 57-65.
296. Quijada-Morin, N., et al., *Polyphenolic, polysaccharide and oligosaccharide composition of Tempranillo red wines and their relationship with the perceived astringency*. Food Chemistry, 2014. **154**: p. 44-51.
297. Gaffney, S.H., et al., *The association of polyphenols with caffeine and alpha-cyclodextrin and beta-cyclodextrin in aqueous-media*. Journal of the Chemical Society-Chemical Communications, 1986(2): p. 107-109.
298. Brandão, E., et al., *The role of wine polysaccharides on salivary protein-tannin interaction: A molecular approach*. Carbohydrate Polymers, 2017. **177**(Supplement C): p. 77-85.
299. Soares, S., et al., *Study of human salivary proline-rich proteins interaction with food tannins*. Food Chemistry, 2018. **243**: p. 175-185.
300. Larsen, M.J. and E.I.F. Pearce, *Saturation of human saliva with respect to calcium salts*. Archives of Oral Biology, 2003. **48**(4): p. 317-322.

301. Renard, C., A.A. Watrelot, and C. Le Bourvellec, *Interactions between polyphenols and polysaccharides: Mechanisms and consequences in food processing and digestion*. Trends in Food Science & Technology, 2017. **60**: p. 43-51.
302. Zhu, F., *Interactions between cell wall polysaccharides and polyphenols*. Critical Reviews in Food Science and Nutrition, 2018. **58**(11): p. 1808-1831.
303. Padayachee, A., et al., *Binding of polyphenols to plant cell wall analogues - Part 1: Anthocyanins*. Food Chemistry, 2012. **134**(1): p. 155-161.
304. Hernandez-Hierro, J.M., et al., *Relationship between skin cell wall composition and anthocyanin extractability of Vitis vinifera L. cv. Tempranillo at different grape ripeness degree*. Food Chemistry, 2014. **146**: p. 41-47.
305. Slavov, A., et al., *Combined recovery of polysaccharides and polyphenols from Rosa damascena wastes*. Industrial Crops and Products, 2017. **100**: p. 85-94.
306. Slavov, A., et al., *Physico-chemical characterization of water-soluble pectic extracts from Rosa damascena, Calendula officinalis and Matricaria chamomilla wastes*. Food Hydrocolloids, 2016. **61**: p. 469-476.
307. Garcia-Estevez, I., C. Alcalde-Eon, and M.T. Escribano-Bailon, *Flavanol Quantification of Grapes via Multiple Reaction Monitoring Mass Spectrometry: Application to Differentiation among Clones of Vitis vinifera L. cv. Rufete Grapes*. Journal of Agricultural and Food Chemistry, 2017. **65**(31): p. 6359-6368.
308. Nunes, C., J.A. Saraiva, and M.A. Coimbra, *Effect of candying on cell wall polysaccharides of plums (Prunus domestica L.) and influence of cell wall enzymes*. Food Chemistry, 2008. **111**(3): p. 538-548.
309. De Vries, J.A., et al., *Extraction and purification of pectins from Alcohol Insoluble Solids from ripe and unripe apples*. Carbohydrate Polymers, 1981. **1**(2): p. 117-127.
310. Apolinar-Valiente, R., et al., *Application and comparison of four selected procedures for the isolation of cell-wall material from the skin of grapes cv. Monastrell*. Analytica Chimica Acta, 2010. **660**(1-2): p. 206-210.
311. Vidal, S., et al., *Polysaccharides from grape berry cell walls. Part I: tissue distribution and structural characterization of the pectic polysaccharides*. Carbohydrate Polymers, 2001. **45**(4): p. 315-323.
312. Fugel, R., R. Carle, and A. Schieber, *A novel approach to quality and authenticity control of fruit products using fractionation and characterisation of cell wall polysaccharides*. Food Chemistry, 2004. **87**(1): p. 141-150.
313. Vicens, A., et al., *Changes in Polysaccharide and Protein Composition of Cell Walls in Grape Berry Skin (Cv. Shiraz) during Ripening and Over-Ripening*. Journal of Agricultural and Food Chemistry, 2009. **57**(7): p. 2955-2960.
314. Apolinar-Valiente, R., et al., *Oligosaccharides of Cabernet Sauvignon, Syrah and Monastrell red wines*. Food Chemistry, 2015. **179**: p. 311-317.
315. Apolinar-Valiente, R., et al., *Effect of enzyme additions on the oligosaccharide composition of Monastrell red wines from four different wine-growing origins in Spain*. Food Chemistry, 2014. **156**: p. 151-159.
316. Sarni-Manchado, P. and V. Cheynier, *Study of non-covalent complexation between catechin derivatives and peptides by electrospray ionization mass spectrometry*. Journal of Mass Spectrometry, 2002. **37**(6): p. 609-616.
317. Watrelot, A.A., et al., *Neutral sugar side chains of pectins limit interactions with procyanidins*. Carbohydrate Polymers, 2014. **99**: p. 527-536.

Supplementary Information

EXPERIMENTAL SECTION

Molecular Dynamics Simulations (MD)

The X-ray structures of the different peptides (PRP1, PRP3, IB-8b and P-B) were obtained by homology modeling technique using the program MODELLER [1]. The structures of B2 and B2g molecules were optimized with the HF/6-31G(d) level of theory and using the Gaussian 09 suite of program [2]. The RESP algorithm was used to recalculate the atomic charges [3]. These calculations were further used for the parameterization of these molecules using the antechamber tool. The force fields GAFF [4] and parm99 [5] were used to characterize the B2 and B2g molecules and the peptides, respectively, during geometry optimization and Molecular Dynamics (MD) simulations.

Three different simulations were performed for each system: 1) with one peptide; 2) with one peptide and one molecule of B2 or B2g; and 3) with four B2 or B2g molecules randomly positioned near the peptide (to reproduce the experimental conditions). The system geometries were optimized in two stages, followed by MD simulations of 100 ps at NVT ensemble, and considering periodic boundaries conditions. Further, 50 ns of MD simulation with an isothermal-isobaric NPT ensemble were run. The SHAKE and the Verlet leapfrog algorithms were used to constrain the hydrogen bonds, and to integrate the equations of motion with a time step of 2 fs [6]. A cut-off of 10 Å was used to truncate the non-bonded interactions, whilst the Particle-Mesh Ewald method [7] was employed to include long-range interactions.

Table S1. Thermodynamic parameters (ΔH , ΔG and $-T\Delta S$) of interactions between procyanidins dimer B2, B2g and trimer and salivary proteins (bPRPs, gPRPs, aPRPs and P-B).

Set	B2			B2g			Trimer			
	ΔH [cal.mol $^{-1}$]	ΔG [kcal.mol $^{-1}$]	$-T\Delta S$ [kcal.mol $^{-1}$]	ΔH [cal.mol $^{-1}$]	ΔG [kcal.mol $^{-1}$]	$-T\Delta S$ [kcal.mol $^{-1}$]	ΔH [cal.mol $^{-1}$]	ΔG [kcal.mol $^{-1}$]	$-T\Delta S$ [kcal.mol $^{-1}$]	
bPRP	n(1,2)	78.5 ± 38.2	-8.1 ± 1.7	-8.2 ± 1.6	258 ± 12.4	-9.7 ± 1.9	-9.9 ± 1.9	-386 ± 110.0	-9.1 ± 1.8	-8.7 ± 1.7
	n(2,2)	-350.4 ± 12.4	-6.7 ± 1	-6.3 ± 1	-82.6 ± 6.0	-8.1 ± 1.6	-7.97 ± 1.6	-3900 ± 1110.0	-5.9 ± 1.1	-2.0 ± 0.1
gPRP	n(1,2)	-1.45 ± 0.6	-8.4 ± 1.6	-8.3 ± 1.6	735.5 ± 9.6	-9.6 ± 1.9	-10.4 ± 1.9	151.8 ± 1.2	-8.5 ± 1.5	-8.6 ± 1.4
	n(2,2)	-392.2 ± 10.9	-5.9 ± 0.8	-5.5 ± 0.8	-399.6 ± 24.8	-7.4 ± 1.3	-7.0 ± 1.2	-514.5 ± 12.9	-6.1 ± 0.9	-5.6 ± 0.8
aPRP	n(1,2)	-635.0 ± 179.0	-6.5 ± 1.2	-5.9 ± 1	-413.2 ± 0.7	-8.4 ± 1.3	-8.0 ± 1.3	-380.2 ± 24.8	-8.3 ± 1.6	-8.0 ± 1.5
	n(2,2)	-3920.3 ± 258.2	-5.4 ± 0.9	-1.5 ± 0.6	-8070.1 ± 13.1	-5.9 ± 0.8	2.2 ± 0.8	-6472.3 ± 175.8	-5.5 ± 0.9	1.0 ± 0.7
P-B	n(1,2)	-2672.1 ± 11.4	-8.1 ± 1.3	-5.5 ± 1.3	-3055.6 ± 26.6	-10.8 ± 2	-7.8 ± 2	-2680.6 ± 10.9	-7.4 ± 1.2	-4.7 ± 1.2
	n(2,2)	-874.9 ± 0.3	-7.1 ± 1.2	-6.2 ± 1.2	2.3 ± 1.4	-8.4 ± 1.6	-8.4 ± 1.5	-453.7 ± 0.09	-7.6 ± 1.4	-7.2 ± 1.4

ΔH - enthalpy, ΔG – free Gibbs energy, ΔS – entropy, T – temperature

Table S2. Hydrogen bonds present during more than 20% of each MD simulation in the simulations with B2. Distances in Angstrom.

B2	Atom 1	Atom 2	Atom 3	% Simulation	Distance (1-3)	Angle (1-2-3)
PRP1	B_2_152@O60	GLY_128@H	GLY_128@N	0.5754	2.8805	158.7911
	PRO_125@O	B_2_152@H55	B_2_152@O54	0.5295	2.7026	154.5148
	ASP_50@O	B_2_154@H55	B_2_154@O54	0.3516	2.7308	153.8974
	GLN_41@OE1	B_2_154@H61	B_2_154@O60	0.3443	2.7268	157.5947
	PRO_135@O	B_2_152@H44	B_2_152@O43	0.2893	2.7009	161.5554
	SER_40@O	B_2_153@H57	B_2_153@O56	0.2844	2.6705	164.0013
	GLN_49@OE1	B_2_153@H61	B_2_153@O60	0.2623	2.7360	153.1841
	GLN_38@O	B_2_153@H61	B_2_153@O60	0.2361	2.7126	156.7334
	ASP_50@OD1	B_2_154@H40	B_2_154@O39	0.2254	2.6404	162.4404
PRP3	ASP_50@OD1	B_2_109@H38	B_2_109@O37	0.6424	2.5913	167.2498
	ASP_2@OD2	B_2_110@H38	B_2_110@O37	0.6392	2.5912	165.8994
	ASP_50@OD1	B_2_109@H36	B_2_109@O35	0.6260	2.5813	167.2910
	GLN_54@O	B_2_110@H40	B_2_110@O39	0.5584	2.7047	160.4732
	PRO_95@O	B_2_108@H44	B_2_108@O43	0.5500	2.7063	160.0934
	GLN_55@O	B_2_110@H55	B_2_110@O54	0.4028	2.7420	161.3579
	GLN_93@OE1	B_2_107@H61	B_2_107@O60	0.4028	2.7528	160.4181
	ASP_50@OD2	B_2_109@H38	B_2_109@O37	0.3352	2.5869	167.8157
	ASP_50@OD2	B_2_109@H36	B_2_109@O35	0.3308	2.5814	167.5070
	PRO_78@O	B_2_108@H68	B_2_108@O63	0.2776	2.6878	162.6885
	GLN_97@OE1	B_2_108@H61	B_2_108@O60	0.2584	2.7422	151.9554
	GLN_80@O	B_2_107@H59	B_2_107@O58	0.2176	2.7035	164.0510
	ASP_2@OD2	B_2_110@H36	B_2_110@O35	0.2168	2.5959	167.3794
	PRO_95@O	B_2_108@H57	B_2_108@O56	0.2060	2.6863	160.9406
IB-8b	PRO_20@O	B_2_45@H57	B_2_45@O56	0.4830	2.6853	164.7157
	PRO_19@O	B_2_45@H44	B_2_45@O43	0.4722	2.7386	163.5831
	GLN_25@O	B_2_45@H59	B_2_45@O58	0.4147	2.7500	154.2331
	GLN_41@O	B_2_47@H57	B_2_47@O56	0.2577	2.7314	147.9792
	GLY_11@O	B_2_46@H40	B_2_46@O39	0.2457	2.7038	159.0332
	B_2_48@O60	GLY_11@H	GLY_11@N	0.2225	2.8836	159.7453
	HIE_12@O	B_2_48@H36	B_2_48@O35	0.2173	2.7032	164.3180
	PRO_16@O	B_2_45@H36	B_2_45@O35	0.2097	2.6986	161.7717
P-B	PRO_40@O	B_2_59@H38	B_2_59@O37	0.3485	2.6794	161.9355
	PRO_42@O	B_2_59@H44	B_2_59@O43	0.2890	2.6974	160.3943
	PRO_54@O	B_2_61@H38	B_2_61@O37	0.2122	2.6976	150.7403

Table S3. Hydrogen bonds present during more than 20% of each MD simulation in the simulations with B2-3'-O-gallate. Distances in Angstrom.

B2-3'-O-gallate	Atom 1	Atom 2	Atom 3	% Simulation	Distance (1-3)	Angle (1-2-3)
PRP1	GLU_28@OE1	B2G_154@H77	B2G_154@O76	0.7484	2.5826	167.6574
	GLU_28@OE1	B2G_154@H75	B2G_154@O74	0.7212	2.5909	167.0051
	ASP_27@O	B2G_153@H36	B2G_153@O35	0.5648	2.7231	159.3626
	PHE_25@O	B2G_153@H38	B2G_153@O37	0.5616	2.7444	149.2263
	GLU_23@O	B2G_154@H55	B2G_154@O54	0.4924	2.6712	161.4736
	GLU_23@OE2	B2G_153@H40	B2G_153@O39	0.4380	2.6288	165.0753
	B2G_151@O43	GLN_120@HE22	GLN_120@NE2	0.3740	2.8737	160.0282
	GLY_83@O	B2G_151@H75	B2G_151@O74	0.3724	2.8102	147.7727
	GLU_23@OE1	B2G_154@H40	B2G_154@O39	0.3672	2.6468	161.3849
	ILE_26@O	B2G_154@H79	B2G_154@O78	0.3136	2.7912	147.9667
	HIE_84@ND1	B2G_151@H77	B2G_151@O76	0.2796	2.8419	149.0123
	PRO_75@O	B2G_107@H40	B2G_107@O39	0.9152	2.6645	160.2007
PRP3	PRO_78@O	B2G_107@H42	B2G_107@O41	0.7324	2.6910	160.0504
	ASP_2@OD2	B2G_110@H42	B2G_110@O41	0.4796	2.6044	165.1279
	PRO_79@O	B2G_107@H75	B2G_107@O74	0.4584	2.7533	152.5442
	GLN_81@O	B2G_107@H77	B2G_107@O76	0.2868	2.7647	150.6299
	ASP_2@OD1	B2G_110@H42	B2G_110@O41	0.2788	2.6165	164.6303
	ASP_2@OD2	B2G_110@H75	B2G_110@O74	0.2628	2.6239	161.6118
	B2G_110@O60	GLY_62@H	GLY_62@N	0.2576	2.8798	158.5434
	ASP_2@OD1	B2G_110@H75	B2G_110@O74	0.2328	2.6256	161.7471
	LEU_3@O	B2G_110@H40	B2G_110@O39	0.2092	2.7324	157.8135
	B2G_107@O58	ARG_91@HH21	ARG_91@NH2	0.2068	2.8534	155.7567
	PRO_42@O	B2G_109@H42	B2G_109@O41	0.2060	2.6209	154.9167
IB-8b	GLN_44@OXT	B2G_45@H77	B2G_45@O76	0.6213	2.5672	167.6192
	GLN_44@OXT	B2G_45@H79	B2G_45@O78	0.6186	2.5939	167.6631
	PRO_34@O	B2G_47@H55	B2G_47@O54	0.4219	2.7062	163.0776
	SER_42@O	B2G_47@H55	B2G_47@O54	0.3360	2.6854	159.7698
	PRO_34@O	B2G_47@H40	B2G_47@O39	0.3146	2.7091	159.8850
	B2G_46@O60	ARG_2@HH12	ARG_2@NH1	0.2968	2.8438	156.2669
	GLY_32@O	B2G_45@H75	B2G_45@O74	0.2733	2.7495	147.7946
	PRO_28@O	B2G_45@H44	B2G_45@O43	0.2648	2.7013	156.0078
	PRO_3@O	B2G_48@H44	B2G_48@O43	0.2474	2.7259	159.8201
	GLY_31@O	B2G_45@H75	B2G_45@O74	0.2101	2.8010	151.5741
	GLN_44@O	B2G_45@H77	B2G_45@O76	0.2092	2.5715	167.7750
	GLN_44@O	B2G_45@H79	B2G_45@O78	0.2087	2.6050	167.2161
P-B	B2G_47@O60	ARG_33@HE	ARG_33@NE	0.2003	2.8392	154.2084
	GLY_6@O	B2G_60@H38	B2G_60@O37	0.7026	2.6901	162.6348
	PRO_47@O	B2G_61@H79	B2G_61@O78	0.5104	2.6753	161.3824
	TYR_45@O	B2G_61@H44	B2G_61@O43	0.5060	2.6831	161.6395
	PRO_53@O	B2G_59@H44	B2G_59@O43	0.4576	2.7112	163.0071

	B2G_60@O60	ARG_5@HH11	ARG_5@NH1	0.3909	2.8572	159.0935
	GLY_3@O	B2G_60@H57	B2G_60@O56	0.3541	2.7314	151.0167
	PRO_44@O	B2G_61@H75	B2G_61@O74	0.3405	2.7676	150.0668
	TYR_45@O	B2G_61@H75	B2G_61@O74	0.2086	2.7128	154.0445

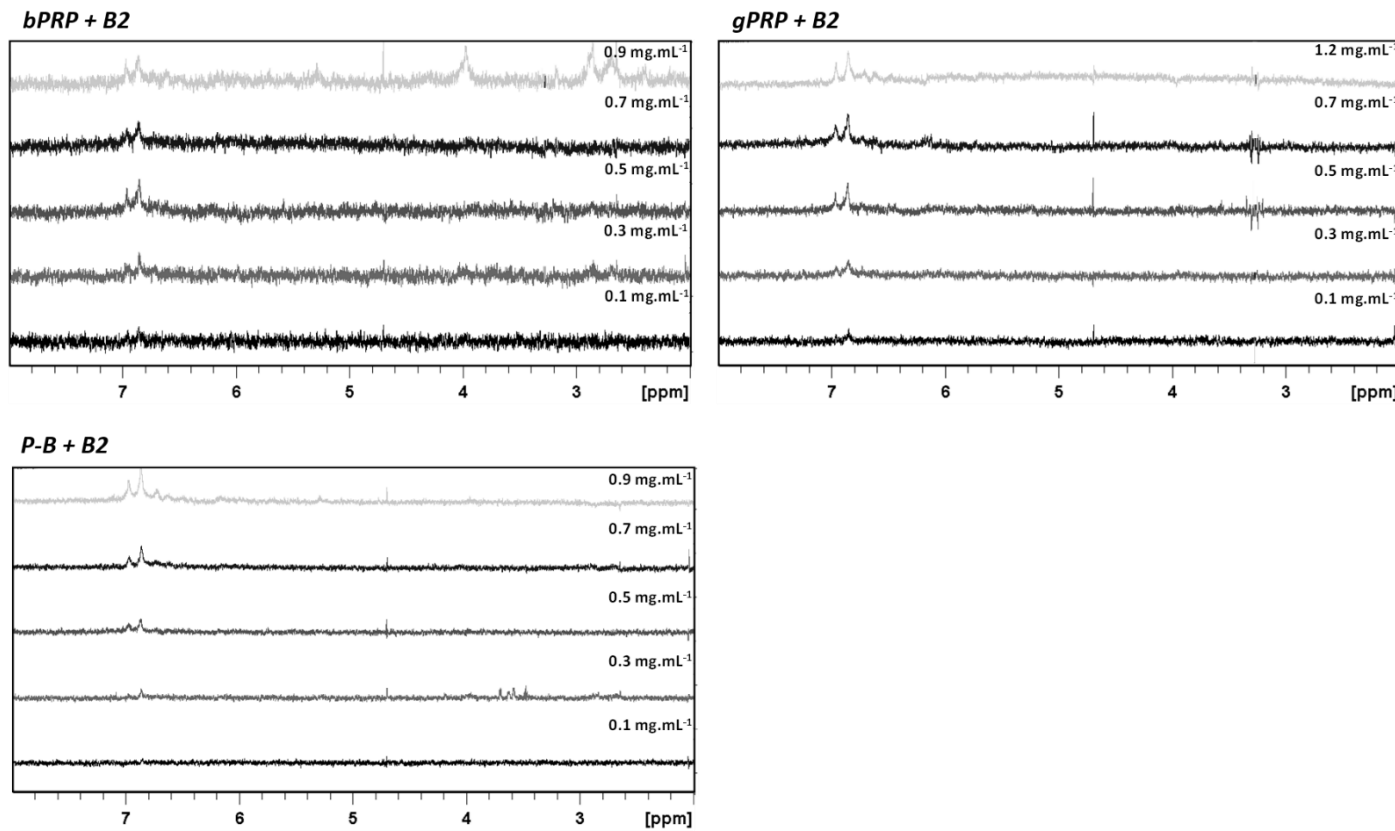


Figure S1. STD-NMR spectra for the interaction between the different PRPs (3.0 μ M) and procyanidin dimer B2 at increasing procyanidin concentration showing the 8.0-2.0 ppm region where most protons resonate. Spectra were recorded at 600 MHz and 300 K in deuterium oxide (D_2O).

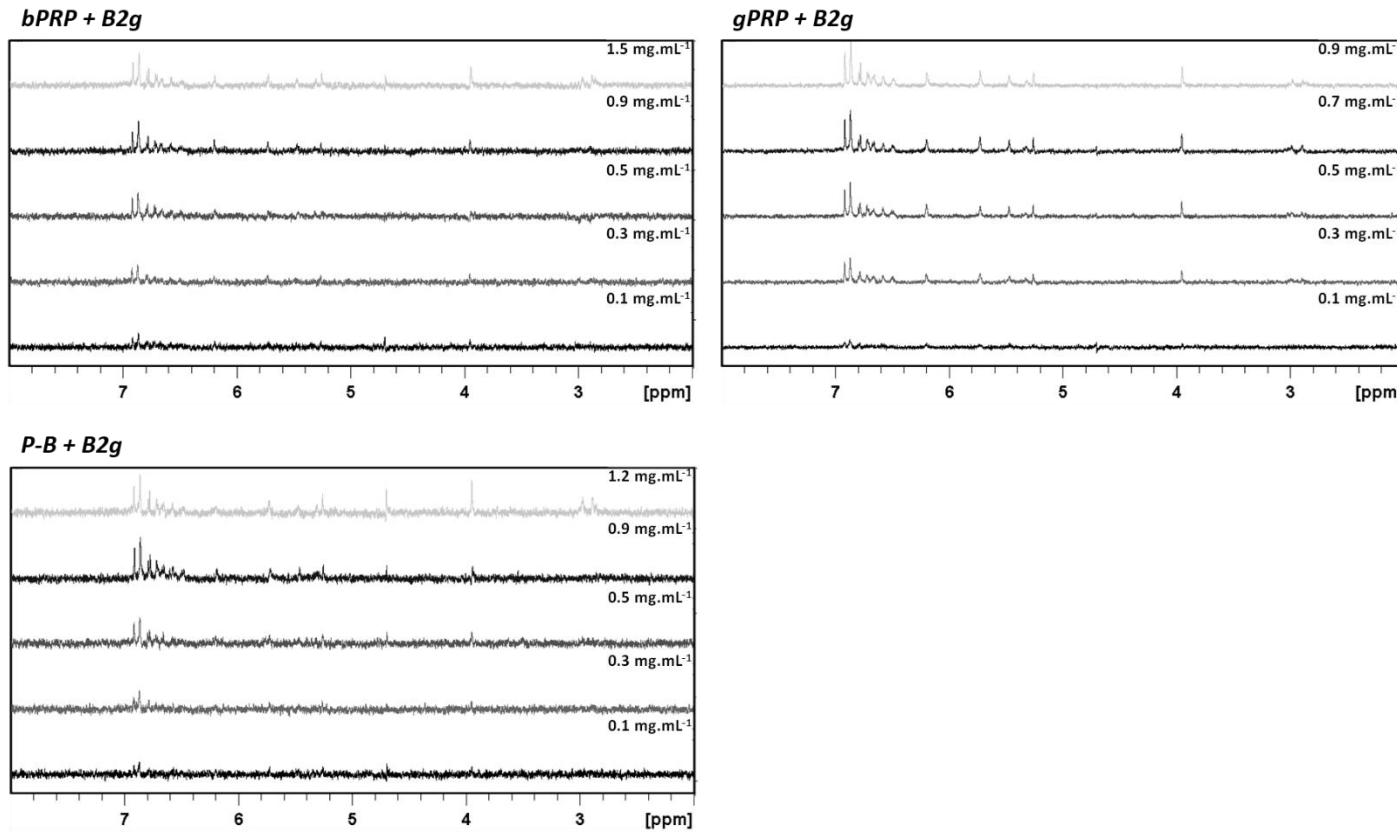


Figure S2. STD-NMR spectra for the interaction between the different PRPs (3.0 μ M) and procyanidin dimer B2 -3O'-gallate (B2g) at increasing procyanidin concentration showing the 8.0-2.0 ppm region where most protons resonate. Spectra were recorded at 600 MHz and 300 K in deuterium oxide (D_2O).

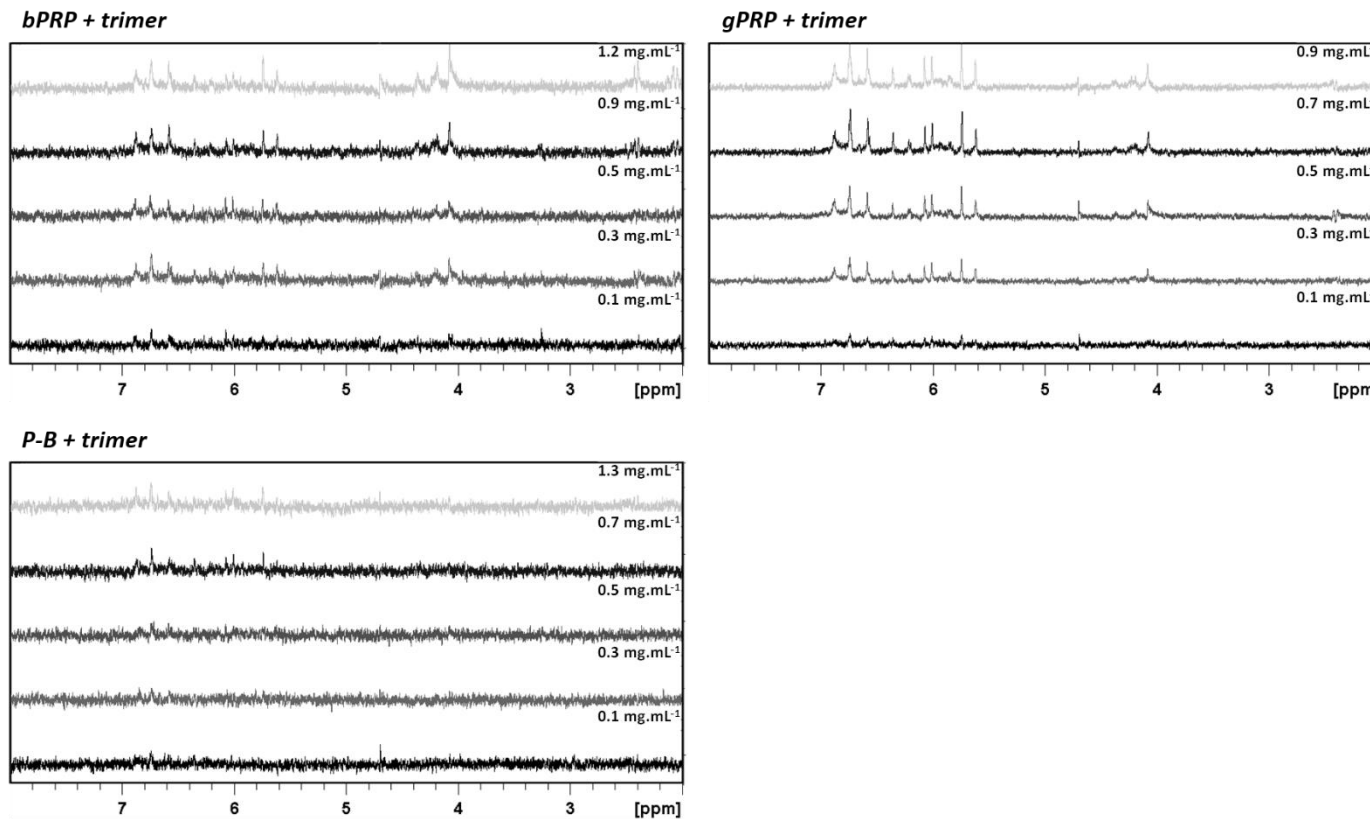


Figure S3. STD-NMR spectra for the interaction between the different PRPs (3.0 μ M) and procyanidin trimer at increasing procyanidin concentration showing the 8.0-2.0 ppm region where most protons resonate. Spectra were recorded at 600 MHz and 300 K in deuterium oxide (D_2O).

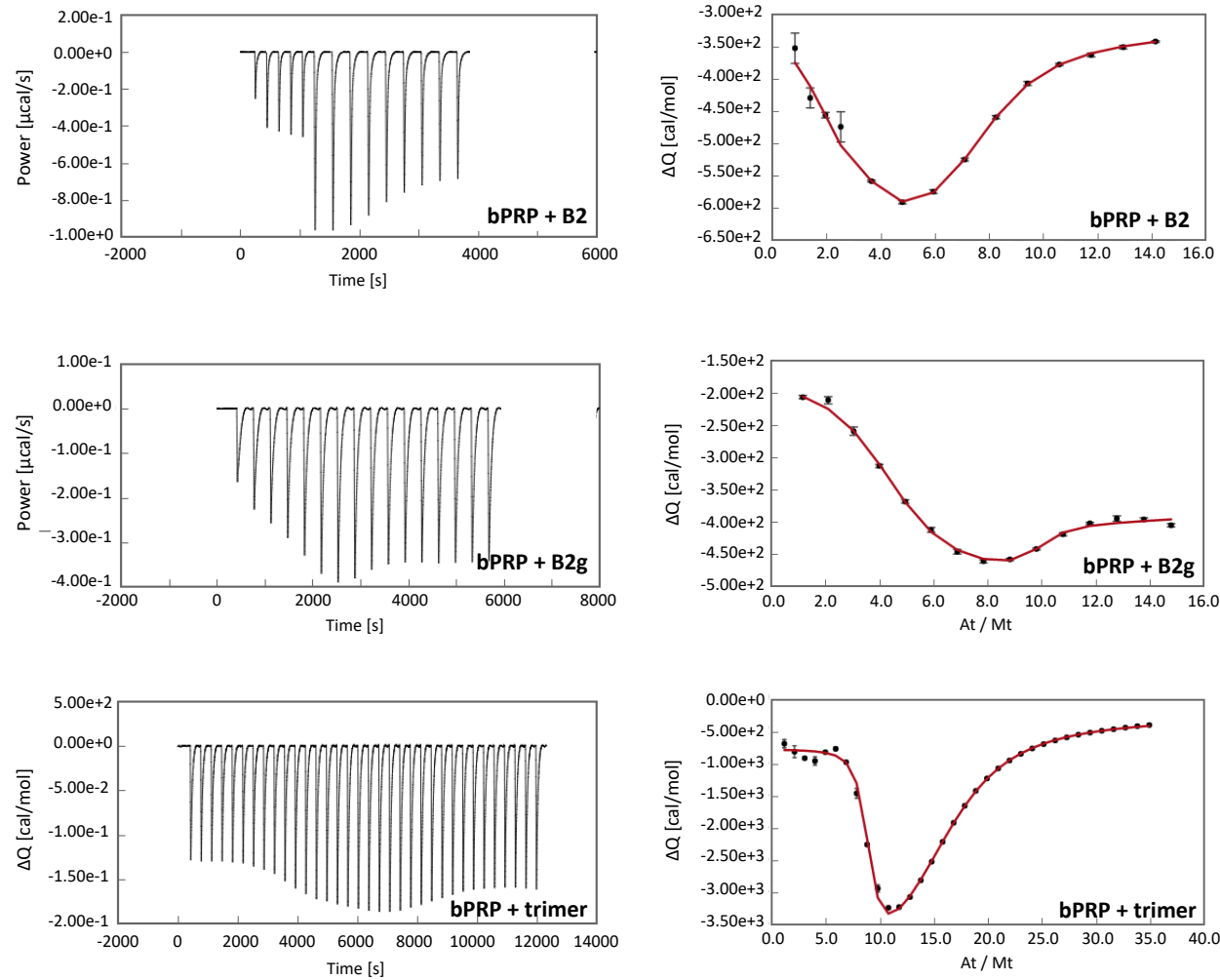


Figure S4. ITC interaction of bPRP (30.0 μ M) with procyanidin B2, procyanidin B2g and procyanidin trimer: thermogram (left side) and binding isotherm (points) and fitting curve (line) (right side).

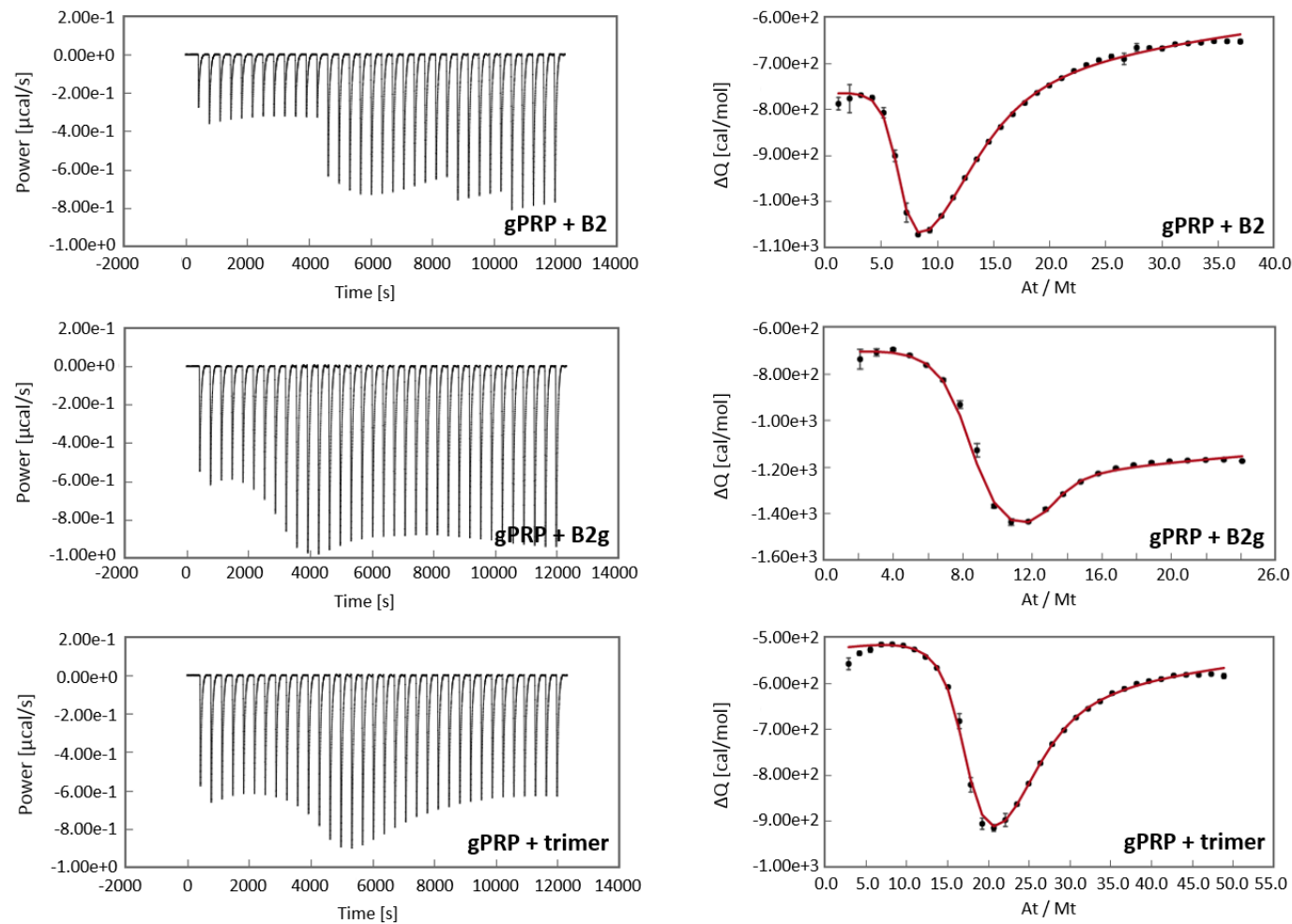


Figure S5. ITC interaction of gPRP (30.0 μM) with procyanidin B2, procyanidin B2g and procyanidin trimer: thermogram (left side) and binding isotherm (points) and fitting curve (line) (right side).

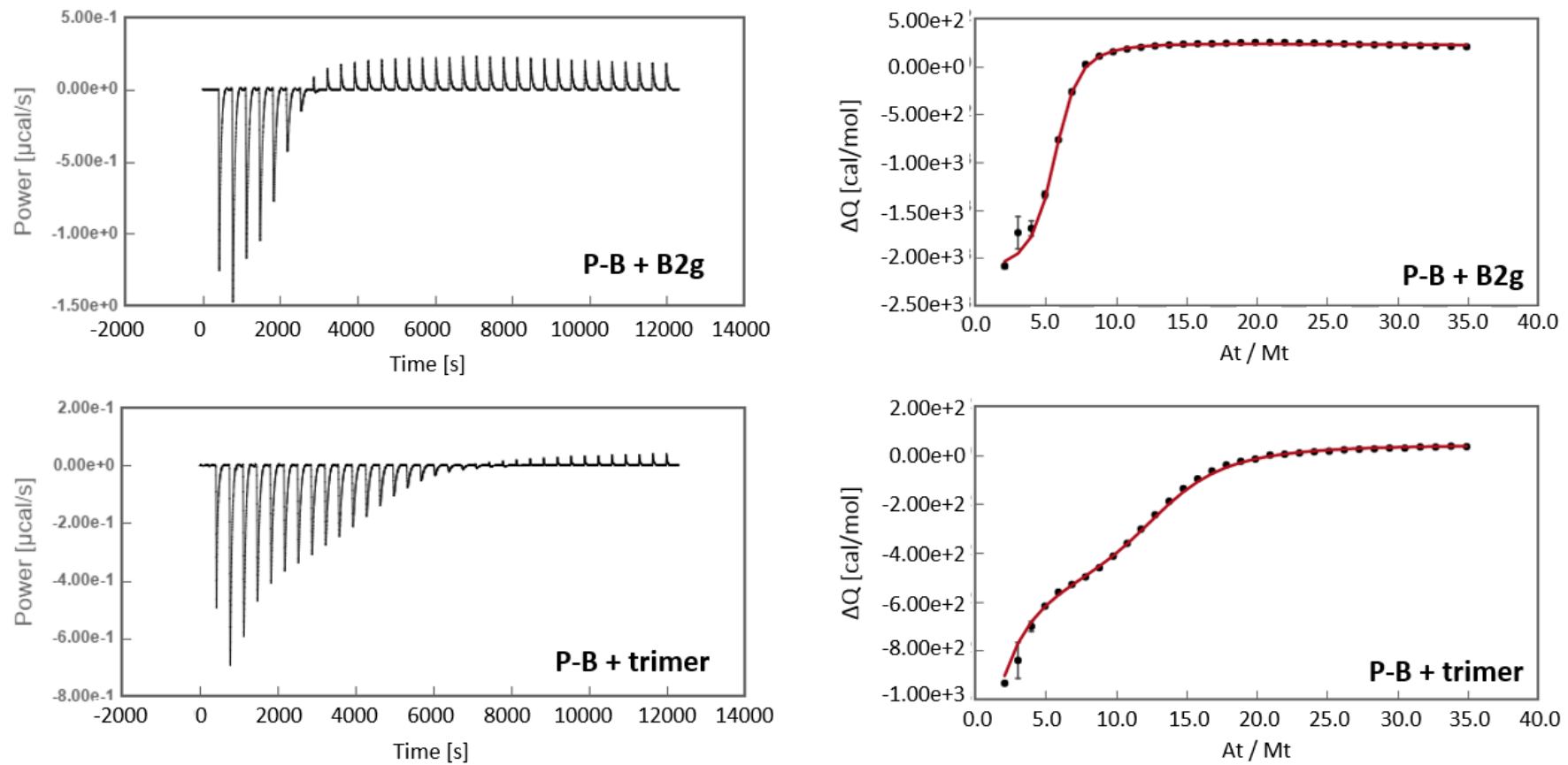


Figure S6. ITC interaction of P-B (30.0 μM) with procyanidin B2, procyanidin B2g and procyanidin trimer: thermogram (left side) and binding isotherm (points) and fitting curve (line) (right side).